14q32 Noncoding RNAs in vascular remodelling

Goossens, E.A.C.

14q32 noncoding RNAs in vascular remodelling

Eveline A.C. Goossens

Cover: aquarel painting of arterial vascular remodelling processes by Bettina Goossens on a background of 14q32 microRNA sequences and (post-)transcriptional 14q32 regulators' gene sequences described in this thesis.

Printing: Ridderprint | www.ridderprint.nl
ISBN: 978-94-6375-835-2

14q32 noncoding RNAs in vascular remodelling

Proefschrift

ter verkrijging van
de graad van Doctor aan de Universiteit Leiden,
op gezag van Rector Magnificus prof. mr. C.J.J.M. Stolker,
volgens besluit van het College voor Promoties
te verdedigen op donderdag 9 april 2020
klokke 15.00 uur

door

Eveline Albertine Cornelia Goossens

geboren te Leiderdorp in 1993

Promotor:	Prof. dr. P.H.A. Quax
Copromotor:	Dr. A.Y. Nossent
Leden promotiecommissie:	Prof. dr. J.F. Hamming
	Prof. dr. J.W. Jukema
	Prof. dr. M.J.T.H. Goumans
	Dr. E.E.J.M. Creemers (Amsterdam UMC)
	Dr. S.C.A. de Jager (UMC Utrecht)

Table of Contents

Chapter 1

General Introduction

General introduction

Cardiovascular disease

Cardiovascular disease is the collective term for multiple diseases of both the heart and blood vessels. It is among the most frequently occurring diseases in the world with high morbidity and mortality rates, especially in the western world[1]. These rates increase with increasing welfare of countries due to risk factors that are more common in a modern lifestyle. Examples of risk factors for cardiovascular disease are intake of too much salt and fat, a sedentary lifestyle and a lack of physical activity. This results in hypertension, hypercholesterolemia, obesity and diabetes and could lead to cardiovascular diseases like peripheral arterial disease and myocardial infarction. Eventually, end stage peripheral arterial disease could lead to severely ischemic lower limbs that need to be amputated in a final stage to save the patient's life. After myocardial infarction, the ischemic heart tissue is not able to contract properly. This leads to heart failure, defined by the inability of the heart to pump sufficient blood through the whole body to supply all organs with enough oxygen and nutrients. To avoid end stage peripheral arterial disease and heart failure, therapeutic interventions are present, but nowadays still insufficient to completely save patients from suffering. Therefore, new therapeutic options are needed to decrease the burden of cardiovascular diseases.

A common factor in the various types of cardiovascular disease is that some form of vascular remodelling occurs. Vascular remodelling processes can be divided into negative and positive vascular remodelling. Negative remodelling processes include atherosclerosis, restenosis, aneurysm formation and remodelling after arteriovenous fistula formation, all disadvantageous for vascular health. Positive remodelling processes comprise angiogenesis and arteriogenesis, together called neovascularization and are beneficial adaptive processes.

Negative vascular remodelling

Atherosclerosis is the complex process of vessel wall thickening. In fact, it is the thickening of the intimal layer of the arterial wall. Atheroma formation starts with lipid accumulating cells that extravasate and form a fatty streak[2]. Among the extravasating cells, macrophages (foam cells) and T cells are the most common cell types[3]. Over time, cells accumulate in the intimal layer and smooth muscle cells will migrate from the medial layer to the intimal layer to form a large extracellular matrix and fibrous cap[4]. When the atheroma grows, the inner part can become necrotic and the fibrous cap loses stability. Such a plaque is called instable and, when an instable atherosclerotic plaque ruptures, a thrombus can attach to it in the lumen causing a partial or complete occlusion of the artery. The initial vessel wall thickening already

decreases lumen area and causes a reduced blood flow to downstream tissues. This results in deprivation of oxygen and nutrients to the tissues and in peripheral arterial disease a ruptured atherosclerotic plaque with arterial occlusion causes clinical features of pain, pallor, pulselessness, paresthesia, poikilothermia and paralysis (the six Ps). A ruptured atherosclerotic plaque in the carotid artery can lead to ischemic stroke as parts of the carotid thrombus can release from it and can obstruct the flow in the smaller downstream branching intracranial vessels. In the coronary artery, a thrombus leads to myocardial infarction. Ischemic myocardium results in dying myocardial cells with subsequent inability to contract and pump sufficient blood through the body. This lack of reaching adequate cardiac output is called heart failure and, more specifically, ischemic heart failure in case of myocardial infarction.

These acute clinical situations should be treated immediately to save ischemic tissues. Current invasive revascularization treatment options for peripheral arterial disease and coronary artery disease comprise endovascular interventions or bypass surgery. Endovascular therapies include balloon angioplasty with or without stent placement. This treatment is effective, however, the disadvantage of this therapy is the high risk of restenosis[5]. The second treatment option, bypass surgery, is less favorable in the acute situation, but recommended when endovascular therapies are not possible, not successful or the vessel shows recurrent occlusions. Bypasses can be made from the patients own arterial or venous vessels. The latter is more common and more easily available, but tends to show higher graft occlusion rates. This is called vein graft disease, the formation of an atheromatous plaque in the grafted vein[6].

During restenosis, previously stenosed arteries that were treated by an angioplasty procedure with or without stenting, are narrowed again. This secondary stenosis is triggered by manipulation of the occluded vessel. The response to this manipulation consists of two cellular components, namely an inflammatory cell reaction and a reaction by vascular smooth muscle cells (VSMCs). Inflammatory cells adhere to the injured vessel wall and cause an inflammatory reaction. Macrophages, like in atherosclerosis, are the most common cell type that invade into the vessel wall and even further increase the inflammatory reaction. VSMCs are the second cell type that is triggered by the manipulation of the occluded vessel wall. VSMCs start to proliferate and migrate from the medial layer into the intimal layer, where they form a neointimal layer. Furthermore, extracellular matrix remodelling accompanies these reactions, resulting in thickened vessel walls.

Positive vascular remodelling

Positive vascular remodelling comprise processes that are beneficial during vascular disease and includes angiogenesis and arteriogenesis, together called neovascularization. Angiogenesis is the formation of new capillary blood vessels into tissues where no existing blood vessels are located and is driven by hypoxia[7]. Arteriogenesis is the process of blood vessel maturation out of small pre-existing vessels by increased shear stress[8]. Both neovascularization processes are needed to restore blood flow to ischemic tissues in atherosclerosis or restenosis. Under physiological conditions neovascularization occurs, however, this is not sufficient to fully restore blood flow to downstream tissues and should be reinforced to form fully functional new blood vessels that function as bypass. Neovascularization is not always regarded as a positive vascular remodelling process. In the field of oncology, neovascularization to supply blood to the neoplasm is an undesirable process and possible therapeutic targets should be investigated for not affecting this neovascularization. This thesis will focus on neovascularization as treatment strategy for cardiovascular disease and thus as a positive remodelling process.

Taken together, new treatment options are needed for cardiovascular diseases either to stimulate the body to improve positive remodelling processes or to inhibit negative vascular remodelling processes. Since current interventional treatment options for cardiovascular disease are not completely optimal, the aim of research is to find new therapeutic options with higher efficacy. Genetic components of cardiovascular disease have been studied widely over the last decades. One of these genetic components is the field of noncoding RNAs (ncRNAs) and what is known, is yet far from complete.

Noncoding RNAs

Only a small proportion of the genome encodes for mRNA leading to protein production. The majority of the genome (>95%) is not protein-coding[9] and therefore called noncoding. Before the role of ncRNAs was discovered, this was called junk-DNA. NcRNAs are RNAs that are transcribed from DNA, but not further translated into proteins. However, as RNA it regulates other RNAs, like messenger RNA (mRNA), transfer RNA (tRNA) or ribosomal RNA (rRNA). Thereby, ncRNAs can affect ongoing cellular processes. All ncRNAs can be divided into small ncRNAs, including microRNAs and small nucleolar RNAs (snoRNAs), and long noncoding RNAs, based on their length in nucleotides. This thesis will focus on microRNAs and snoRNAs.

MicroRNAs

MicroRNAs are small ncRNAs of approximately 22 nucleotides in length and were first described in 2001[10-13]. They are transcribed by RNA polymerase II to primary microRNAs and subsequently processed by Drosha, a processing complex, into precursor microRNAs. These are transported from the nucleus to the cytosol and there the precursor microRNAs are cleaved into two mature microRNA strands by the enzyme Dicer[14, 15]. Mature microRNAs are loaded onto the RNA Induced Silencing Complex (RISC) and in this form able to bind complementary to the 3'-untranslated region of their target mRNA. By binding to a target mRNA, translation is inhibited. Therefore, microRNAs are called post-transcriptional regulators of gene expression. One microRNA can have up to several hundreds of target genes. If the target genes act in common physiological or pathophysiological processes and are targeted by one single microRNA, entire processes can be regulated. This has previously been shown for several non-cardiovascular[16, 17] and cardiovascular diseases[18, 19]. MicroRNAs tend to occur in clusters and have already shown tissue specific expression patterns[20].

Small nucleolar RNAs

As well as microRNAs, small nucleolar RNAs (snoRNAs) belong to the group of small ncRNAs, although they are longer than microRNAs with an average length of 60-200 nucleotides[21]. SnoRNAs can be divided into C/D-box snoRNAs and H/ACA-box snoRNAs based on their mechanism of action. C/D-box snoRNAs modulate target ncRNAs via 2'O-ribose-methylation, whereas H/ACA-box snoRNAs modulate other ncRNAs via pseudouridylation. Some snoRNAs have known cellular functions like in cholesterol trafficking[22] and in metabolic stress[23], but they also target other regulators like rRNAs[24] or regulate alternative splicing of mRNAs[25]. However, many snoRNAs do not have known target RNAs and are presumed to have non-canonical targets. Moreover, the role of snoRNAs in cardiovascular disease has not been elucidated and needs to be investigated in depth.

DNA methylation

DNA methylation is an epigenetic feature that is characterized by the addition of a methyl group to a cytosine nucleotide to form a 5-methylcytosine. DNA methylation is subject to mutagenic loss, but is conserved in CpG-islands that mainly are located in promotor regions of genes[26]. DNA methylation occurs under the influence of DNA methyltransferases (DNMTs).

DNMTs can be divided into de novo DNMTs DNMT3A and 3B[27, 28], that methylate unmethylated DNA, and maintenance DNMT DNTM1[29], that methylates hemi-methylated DNA or preserve preexisting methylation patterns during replication. DNA methylation is variable between individuals and that is why CpG-rich regions are called Differentially Methylated Regions (DMRs). DNA methylation status can change under the influence of pathophysiological conditions, like in cancer[30-34], but also in cardiovascular disease[35, 36]. DNA methylation acts mostly by inhibiting gene expression through prevention of transcription, but is also known to affect alternative splicing[37].

14q32 noncoding RNA cluster

NcRNAs and DNA methylation appear throughout the whole genome and are factors that influence and regulate gene expression. Previously published Reverse Target Prediction analysis[38, 39] analyzed genes that were known to act in cardiovascular disease, for microRNAs by which they were targeted. The result of this was that many microRNAs were located closely to each other. In fact, they were located in a large conserved gene cluster on the 14th chromosome in humans (14q32 locus)[40]. Besides 54 microRNAs, the human 14q32 locus contains 41 snoRNAs, 3 DMRs, 3 long noncoding RNAs, and 3 coding genes[38, 41]. The locus is shown in Figure 1. The human 14q32 locus is also known as DIO3-DLK1 locus, called after two coding genes located along this locus. The murine equivalent of this locus is located on the 12F1 location[40] and contains 61 microRNAs[38].

MicroRNAs of this cluster have been studied extensively in several experimental murine models. Our group has found that inhibition of miR-494 inhibits atherosclerotic plaque development and increases plaque stability[39], but inhibition of miR-495 decreases post-interventional restenosis in mice[42]. Furthermore, inhibition of miR-329, miR-487b, miR-494 and miR-495 also increases post-ischemic neovascularization in mice[38] and miR-487b plays a role in angiotensin II-induced aneurysm formation in rats[43]. Moreover, other groups also found that the 14q32 microRNA cluster is involved in many different vascular remodelling processes[41, 44, 45].

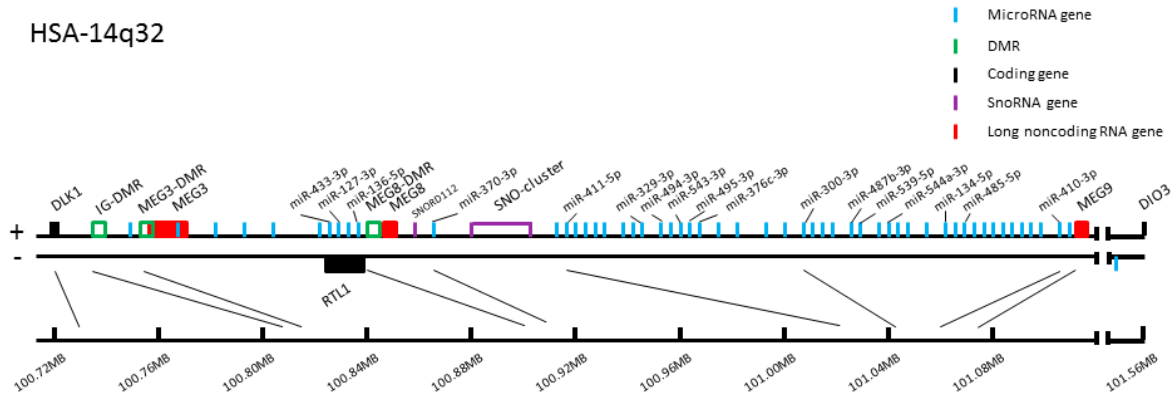

Figure 1 Schematic presentation of the human 14q32 locus. Protein coding genes are depicted in black, long noncoding RNA genes in red, microRNA genes important in vascular remodelling in blue, DMRs in green and snoRNA genes in purple.

NcRNAs of the 14q32 locus have functions in cardiovascular disease or vascular remodelling, but it is unknown whether all ncRNAs are located in all vessels, healthy or not, or that ncRNAs are vessel-specific and actually have their own "fingerprint". We know that parts of the human vasculature are more prone to different types of cardiovascular disease than others. Atherosclerosis occurs predominantly in larger arterial walls where disturbed flow is present[46], while arterial aneurysms occur in the aortic wall or intracranial artery walls[47, 48]. As we know that these processes can be regulated by different 14q32 ncRNAs, it is interesting to investigate whether 14q32 ncRNA expression is vascular location specific or even cell layer specific, like has been shown for non-14q32 microRNAs miR-126[49] and miR-145[19, 50].

Expression regulators of 14q32 microRNAs – (post-)transcriptional regulators

Previous studies have shown that microRNAs of the 14q32 cluster have multiple functions in vascular remodelling processes and that inhibiting them is beneficial, i.e. negative remodelling is inhibited and/or positive remodelling is stimulated. It is possible to directly interfere with microRNA expression by administrating microRNA-inhibiting antisense oligonucleotides[38, 39, 42] or microRNA mimics. However, it would be interesting to find factors by which 14q32 microRNA expression is regulated naturally and, thereby, finding targets to regulate complete physiological processes instantly. Myocyte Enhancer Factor 2A (MEF2A), Cold-Inducible RNA-Binding Protein (CIRBP) and Hydroxyacyl-Coenzyme A Dehydrogenase Trifunctional Multienzyme Complex Subunit Beta (HADHB) have already been shown to bind 14q32 microRNAs post-transcriptionally[51, 52] and more in-depth knowledge about the mechanism of action of RNA-binding proteins and possible transcriptional factors is needed.

DNA methylation

DNA methylation is one of the mechanisms that is known to regulate transcription. The three DMRs located along the human 14q32 locus are called Intergenic-DMR (IG-DMR), Maternally Expressed Gene 3-DMR (MEG3-DMR) and Maternally Expressed Gene 8-DMR (MEG8-DMR). IG-DMR is located between the DLK1-gene and the DIO3-gene, but upstream from all ncRNAs. MEG3-DMR is partially overlapping the beginning of the lncRNA MEG3-gene and MEG8-DMR is located just upstream of the lncRNA MEG8-gene. The murine DMRs are called Dlk1-DMR, IG-DMR and Glt2-DMR. DNA methylation of the 14q32 locus is known to change in several pathophysiological conditions[30, 32, 33, 53] and was also found to be changed in cardiovascular disease[54]. 14q32 DNA methylation has been described to associate with microRNA expression[31, 54] and it has to be assessed whether individual microRNAs also correlate with DNA methylation status within the DMRs. Furthermore, like microRNA expression, DNA methylation is disease specific and vascular diseases occur in different locations throughout the human vasculature. It could be hypothesized that DNA methylation is altered in a vascular location-specific and disease-specific manner.

Myostatin

Myostatin, also known as Growth Differentiation Factor-8 (GDF-8), is a member of the Transforming Growth Factor beta (TGF-β) superfamily and it is a protein that negatively regulates skeletal muscle cell proliferation and differentiation. Myostatin knockout in mice results in excessive skeletal muscle growth[55]. It is known that myostatin affects microRNA expression of the 14q32 locus, also called the callipyge locus. In fact, mutations in the myostatin gene or in the callipyge locus, that result in the inability of myostatin to bind to the locus, cause the typical callipyge phenotype. This phenotype is characterized by excessive muscle mass and that explains the origination of the name “callipyge”. In ancient Greek the word καλλος means beautiful and πυγη means buttocks. This phenotype is favorable in cattle. In mice, myostatin knockdown resulted in increased muscle mass and 14q32 microRNA upregulation[56], whereas myostatin addition led to muscle atrophy[57]. However, myostatin not only acts in skeletal muscle cells, but also in vascular smooth muscle cells (VSMCs)[58]. Exactly this is the cell type to target in restenosis and, more specifically, of which proliferation and hyperplasia has to be inhibited. Taken together, it could be hypothesized that myostatin administration causes 14q32 microRNA downregulation and, subsequently, restenosis is decreased. Together with the fact that a previous study showed that direct inhibition of 14q32 microRNA miR-495 caused decreased restenosis[42], this makes myostatin an even more promising target to inhibit restenosis via downregulation of the 14q32 locus in experimental restenosis. The effect of myostatin on macrophages has to be investigated, as this previous

study already found that miR-495 inhibition decreased influx of macrophages into the vessel wall in experimental restenosis.

Cold-Inducible RNA-Binding Protein

Cold-Inducible RNA-Binding Protein (CIRBP) is another 14q32 microRNA expression regulator and belongs to the post-transcriptional regulators. RNA-binding proteins (RBPs), as the name suggests, are proteins that are able to bind RNAs during post-transcriptional processing[59]. They do not only bind mRNAs, but also microRNAs[60]. CIRBP was shown to bind to two 14q32 precursor microRNAs, namely miR-329 and miR-495. By doing this, CIRBP induces processing into mature microRNAs[51]. As already described in 2014 by Welten et al[38], these microRNAs have an effect on post-ischemic neovascularization. By direct inhibition of these microRNAs with antisense oligonucleotides, translation of pro-angiogenic mRNAs is no longer inhibited, and therefore post-ischemic neovascularization is promoted upon microRNA inhibition. CIRBP is also known to be regulated under hypothermic conditions[61-65]. Exactly the symptom of cold extremities is one of the clinical features of peripheral arterial disease due to insufficient blood supply to peripheral tissues. In this situation neovascularization is needed and CIRBP has to be investigated as a potential target in promoting post-ischemic neovascularization.

Thesis outline

The aim of this thesis is to investigate the expression of 14q32 noncoding RNAs in the vasculature and to identify possible regulators of 14q32 microRNA expression in vascular remodelling.

The first part of this thesis focusses on the role of 14q32 microRNAs, snoRNAs and DNA methylation in cardiovascular diseases and their presence in the human vasculature.

Chapter 2 reviews individual microRNAs and microRNA clusters and families that act in various forms of cardiovascular disease. It highlights the multifactorial nature of vascular remodelling processes in which microRNAs are acting and regulating their targets.

Chapter 3 is the first study that describes the importance of 14q32 snoRNAs in cardiovascular disease. In this chapter we show in a GWAS that single nucleotide polymorphisms (SNPs) in the snoRNA cluster were significantly associated with heart failure independently of other SNPs along the cluster. This indicates an independent role of the 14q32 snoRNA cluster in cardiovascular disease. Furthermore, 14q32 snoRNA expression varied widely throughout the human vasculature and expression seemed to be highly vessel location specific. In failing human coronary bypasses compared to naïve equivalents, snoRNA expression differed and 14q32 snoRNA expression was upregulated in plasma samples of ST-Elevation Myocardial Infarction patients. Potential mechanisms of action of 14q32 snoRNAs had not been uncovered, but in this study an attempt was made to find snoRNA target regulators.

In **chapter 4** the findings on intervascular and vascular disease specific 14q32 microRNA expression and DNA methylation were reported. We found vessel- and disease specific microRNA expression and, even within a vessel wall, different cell layers varied in microRNA expression. 14q32 microRNA expression did not associate with 14q32 DNA methylation or DNMTs. However, we observed highly vascular disease specific DNA methylation patterns suggesting that DNA methylation of the 14q32 locus does not directly affect individual microRNA expression, but acts as independent regulator of vascular remodelling. We confirmed these findings in a murine model for vein-graft disease and in a tissue ischemia mouse model.

The second part of this thesis zooms in on the regulatory mechanisms of 14q32 microRNA expression in vascular remodelling.

Chapter 5 focusses on myostatin as negative regulator of muscle cell proliferation and possible transcriptional regulator of 14q32 microRNA expression in restenosis. In this chapter, we report that addition of myostatin both *in vitro* and *in vivo* downregulated 14q32 microRNA expression and decreased proliferation marker expression. However, it did not affect post-interventional restenosis in a murine model, as myostatin did not clearly affect macrophages inflammatory properties and its 14q32 microRNA expression. This highlights the importance of targeting both the vascular smooth muscle cell proliferation and the macrophage induced inflammation in the process of restenosis inhibition.

In **chapter 6** we describe cold-inducible RNA binding protein (CIRBP) as post-transcriptional regulator of 14q32 microRNAs miR-329 and miR-495 in *in vitro* angiogenesis. CIRBP was known to inhibit precursor to mature microRNA processing and by downregulating the mature microRNA by knockdown of CIRBP, both scratch wound healing and tube formation were increased. Moreover, during cold-stress, which is a main feature of peripheral tissue in peripheral arterial disease, CIRBP was upregulated, but microRNA expression did not alter. Moreover, specifically splice variant 1 changed during siRNA mediated knockdown of CIRBP and hypothermia, whereas the other splice variants were not shown to be affected. The antisense strand of CIRBP contains a long noncoding RNA, CIRBP-AS1, with a yet unknown function and this RNA was also shown to be affected similarly by CIRPB knockdown and hypothermia. Knockdown of CIRBP-AS1 led to CIRBP downregulation and increased scratch wound healing as well. Although the exact pathophysiological mechanisms are not completely understood yet, this provides new possible targets for improving neovascularization in peripheral arterial disease.

All results of the described studies in this thesis are summarized and discussed in **chapter 7.** This chapter also provides future perspectives of the research described in this thesis.

References

1. WHO webpage http://www.who.int/mediacentre/factsheets/fs317/en/. 2019.
2. Stary HC, Chandler AB, Glagov S, Guyton JR, Insull W, Jr., Rosenfeld ME, Schaffer SA, Schwartz CJ, Wagner WD, Wissler RW. A definition of initial, fatty streak, and intermediate lesions of atherosclerosis. A report from the Committee on Vascular Lesions of the Council on Arteriosclerosis, American Heart Association. Circulation 1994;89:2462-2478.
3. Hansson GK. Inflammation, atherosclerosis, and coronary artery disease. The New England journal of medicine 2005;352:1685-1695.
4. Stary HC, Chandler AB, Dinsmore RE, Fuster V, Glagov S, Insull W, Jr., Rosenfeld ME, Schwartz CJ, Wagner WD, Wissler RW. A definition of advanced types of atherosclerotic lesions and a histological classification of atherosclerosis. A report from the Committee on Vascular Lesions of the Council on Arteriosclerosis, American Heart Association. Circulation 1995;92:1355-1374.
5. Nasr B, Kaladji A, Vent PA, Chaillou P, Costargent A, Quillard T, Goueffic Y. Long-Term Outcomes of Common Femoral Artery Stenting. Annals of vascular surgery 2017;40:10-18.
6. de Vries MR, Simons KH, Jukema JW, Braun J, Quax PH. Vein graft failure: from pathophysiology to clinical outcomes. Nature reviews Cardiology 2016;13:451-470.
7. Risau W. Mechanisms of angiogenesis. Nature 1997;386:671-674.
8. van Oostrom MC, van Oostrom O, Quax PH, Verhaar MC, Hoefer IE. Insights into mechanisms behind arteriogenesis: what does the future hold? Journal of leukocyte biology 2008;84:1379-1391.
9. Uchida S, Dimmeler S. Long noncoding RNAs in cardiovascular diseases. Circulation research 2015;116:737-750.
10. Pasquinelli AE, Reinhart BJ, Slack F, Martindale MQ, Kuroda MI, Maller B, Hayward DC, Ball EE, Degnan B, Muller P, Spring J, Srinivasan A, Fishman M, Finnerty J, Corbo J, Levine M, Leahy P, Davidson E, Ruvkun G. Conservation of the sequence and temporal expression of let-7 heterochronic regulatory RNA. Nature 2000;408:86-89.
11. Lagos-Quintana M, Rauhut R, Lendeckel W, Tuschl T. Identification of novel genes coding for small expressed RNAs. Science 2001;294:853-858.
12. Lau NC, Lim LP, Weinstein EG, Bartel DP. An abundant class of tiny RNAs with probable regulatory roles in Caenorhabditis elegans. Science 2001;294:858-862.
13. Lee RC, Ambros V. An extensive class of small RNAs in Caenorhabditis elegans. Science 2001;294:862-864.
14. Bernstein E, Caudy AA, Hammond SM, Hannon GJ. Role for a bidentate ribonuclease in the initiation step of RNA interference. Nature 2001;409:363-366.
15. Lee Y, Jeon K, Lee JT, Kim S, Kim VN. MicroRNA maturation: stepwise processing and subcellular localization. Embo j 2002;21:4663-4670.
16. Hebert SS, De Strooper B. Alterations of the microRNA network cause neurodegenerative disease. Trends in neurosciences 2009;32:199-206.
17. Croce CM. Causes and consequences of microRNA dysregulation in cancer. Nature reviews Genetics 2009;10:704-714.
18. van Rooij E, Olson EN. MicroRNA therapeutics for cardiovascular disease: opportunities and obstacles. Nat Rev Drug Discov 2012;11:860-872.
19. Wei Y, Nazari-Jahantigh M, Neth P, Weber C, Schober A. MicroRNA-126, -145, and -155: a therapeutic triad in atherosclerosis? Arterioscler Thromb Vasc Biol 2013;33:449-454.
20. Wienholds E, Kloosterman WP, Miska E, Alvarez-Saavedra E, Berezikov E, de Bruijn E, Horvitz HR, Kauppinen S, Plasterk RH. MicroRNA expression in zebrafish embryonic development. Science 2005;309:310-311.
21. Jorjani H, Kehr S, Jedlinski DJ, Gumienny R, Hertel J, Stadler PF, Zavolan M, Gruber AR. An updated human snoRNAome. Nucleic Acids Res 2016;44:5068-5082.

22. Brandis KA, Gale S, Jinn S, Langmade SJ, Dudley-Rucker N, Jiang H, Sidhu R, Ren A, Goldberg A, Schaffer JE, Ory DS. Box C/D small nucleolar RNA (snoRNA) U60 regulates intracellular cholesterol trafficking. The Journal of biological chemistry 2013;288:35703-35713.
23. Michel CI, Holley CL, Scruggs BS, Sidhu R, Brookheart RT, Listenberger LL, Behlke MA, Ory DS, Schaffer JE. Small nucleolar RNAs U32a, U33, and U35a are critical mediators of metabolic stress. Cell metabolism 2011;14:33-44.
24. McMahon M, Contreras A, Ruggero D. Small RNAs with big implications: new insights into H/ACA snoRNA function and their role in human disease. Wiley interdisciplinary reviews RNA 2015;6:173-189.
25. Scott MS, Ono M, Yamada K, Endo A, Barton GJ, Lamond AI. Human box C/D snoRNA processing conservation across multiple cell types. Nucleic Acids Res 2012;40:3676-3688.
26. Jeltsch A, Jurkowska RZ. New concepts in DNA methylation. Trends in biochemical sciences 2014;39:310-318.
27. Hsieh CL. In vivo activity of murine de novo methyltransferases, Dnmt3a and Dnmt3b. Molecular and cellular biology 1999;19:8211-8218.
28. Okano M, Xie S, Li E. Cloning and characterization of a family of novel mammalian DNA (cytosine-5) methyltransferases. Nature genetics 1998;19:219-220.
29. Leonhardt H, Bestor TH. Structure, function and regulation of mammalian DNA methyltransferase. Exs 1993;64:109-119.
30. Gonzalez-Vallinas M, Rodriguez-Paredes M, Albrecht M, Sticht C, Stichel D, Gutekunst J, Pitea A, Sass S, Sanchez-Rivera FJ, Lorenzo-Bermejo J, Schmitt J, De La Torre C, Warth A, Theis FJ, Muller NS, Gretz N, Muley T, Meister M, Tschaharganeh DF, Schirmacher P, Matthaus F, Breuhahn K. Epigenetically Regulated Chromosome 14q32 miRNA Cluster Induces Metastasis and Predicts Poor Prognosis in Lung Adenocarcinoma Patients. Molecular cancer research : MCR 2018;16:390-402.
31. Guo W, Dong Z, Liu S, Qiao Y, Kuang G, Guo Y, Shen S, Liang J. Promoter hypermethylation-mediated downregulation of miR-770 and its host gene MEG3, a long non-coding RNA, in the development of gastric cardia adenocarcinoma. Molecular carcinogenesis 2017;56:1924-1934.
32. Moradi S, Sharifi-Zarchi A, Ahmadi A, Mollamohammadi S, Stubenvoll A, Gunther S, Salekdeh GH, Asgari S, Braun T, Baharvand H. Small RNA Sequencing Reveals Dlk1-Dio3 Locus-Embedded MicroRNAs as Major Drivers of Ground-State Pluripotency. Stem cell reports 2017;9:2081-2096.
33. Oshima G, Poli EC, Bolt MJ, Chlenski A, Forde M, Jutzy JMS, Biyani N, Posner MC, Pitroda SP, Weichselbaum RR, Khodarev NN. DNA Methylation Controls Metastasis-Suppressive 14q32-Encoded miRNAs. Cancer Res 2019;79:650-662.
34. Xi S, Xu H, Shan J, Tao Y, Hong JA, Inchauste S, Zhang M, Kunst TF, Mercedes L, Schrump DS. Cigarette smoke mediates epigenetic repression of miR-487b during pulmonary carcinogenesis. The Journal of clinical investigation 2013;123:1241-1261.
35. Zaina S, Heyn H, Carmona FJ, Varol N, Sayols S, Condom E, Ramirez-Ruz J, Gomez A, Goncalves I, Moran S, Esteller M. DNA methylation map of human atherosclerosis. Circulation Cardiovascular genetics 2014;7:692-700.
36. Stratton MS, Farina FM, Elia L. Epigenetics and vascular diseases. Journal of molecular and cellular cardiology 2019;133:148-163.
37. Shayevitch R, Askayo D, Keydar I, Ast G. The importance of DNA methylation of exons on alternative splicing. RNA (New York, NY) 2018;24:1351-1362.
38. Welten SM, Bastiaansen AJ, de Jong RC, de Vries MR, Peters EA, Boonstra MC, Sheikh SP, Monica NL, Kandimalla ER, Quax PH, Nossent AY. Inhibition of 14q32 MicroRNAs miR-329, miR-487b, miR-494, and miR-495 increases neovascularization and blood flow recovery after ischemia. Circ Res 2014;115:696-708.

39. Wezel A, Welten SM, Razawy W, Lagraauw HM, de Vries MR, Goossens EA, Boonstra MC, Hamming JF, Kandimalla ER, Kuiper J, Quax PH, Nossent AY, Bot I. Inhibition of MicroRNA-494 Reduces Carotid Artery Atherosclerotic Lesion Development and Increases Plaque Stability. Annals of surgery 2015;262:841-847; discussion 847-848.
40. Seitz H, Royo H, Bortolin ML, Lin SP, Ferguson-Smith AC, Cavaille J. A large imprinted microRNA gene cluster at the mouse Dlk1-Gtl2 domain. Genome Res 2004;14:1741-1748.
41. Benetatos L, Hatzimichael E, Londin E, Vartholomatos G, Loher P, Rigoutsos I, Briasoulis E. The microRNAs within the DLK1-DIO3 genomic region: involvement in disease pathogenesis. Cellular and molecular life sciences : CMLS 2013;70:795-814.
42. Welten SMJ, de Jong RCM, Wezel A, de Vries MR, Boonstra MC, Parma L, Jukema JW, van der Sluis TC, Arens R, Bot I, Agrawal S, Quax PHA, Nossent AY. Inhibition of 14q32 microRNA miR-495 reduces lesion formation, intimal hyperplasia and plasma cholesterol levels in experimental restenosis. Atherosclerosis 2017;261:26-36.
43. Nossent AY, Eskildsen TV, Andersen LB, Bie P, Bronnum H, Schneider M, Andersen DC, Welten SM, Jeppesen PL, Hamming JF, Hansen JL, Quax PH, Sheikh SP. The 14q32 MicroRNA-487b Targets the Antiapoptotic Insulin Receptor Substrate 1 in Hypertension-Induced Remodeling of the Aorta. Ann Surg 2013;258:743-753.
44. Martinez-Micaelo N, Beltran-Debon R, Aragones G, Faiges M, Alegret JM. MicroRNAs Clustered within the 14q32 Locus Are Associated with Endothelial Damage and Microparticle Secretion in Bicuspid Aortic Valve Disease. Front Physiol 2017;8:648.
45. Dimmeler S, Yla-Herttuala S. 14q32 miRNA cluster takes center stage in neovascularization. Circ Res 2014;115:680-682.
46. Cunningham KS, Gotlieb AI. The role of shear stress in the pathogenesis of atherosclerosis. Laboratory investigation; a journal of technical methods and pathology 2005;85:9-23.
47. Fan XJ, Zhao HD, Yu G, Zhong XL, Yao H, Yang QD. Role of inflammatory responses in the pathogenesis of human cerebral aneurysm. Genetics and molecular research : GMR 2015;14:9062-9070.
48. Golledge J, Muller J, Daugherty A, Norman P. Abdominal aortic aneurysm: pathogenesis and implications for management. Arteriosclerosis, thrombosis, and vascular biology 2006;26:2605-2613.
49. van Solingen C, Seghers L, Bijkerk R, Duijs JM, Roeten MK, van Oeveren-Rietdijk AM, Baelde HJ, Monge M, Vos JB, de Boer HC, Quax PH, Rabelink TJ, van Zonneveld AJ. Antagomir-mediated silencing of endothelial cell specific microRNA-126 impairs ischemia-induced angiogenesis. J Cell Mol Med 2009;13:1577-1585.
50. Cheng Y, Liu X, Yang J, Lin Y, Xu DZ, Lu Q, Deitch EA, Huo Y, Delphin ES, Zhang C. MicroRNA-145, a novel smooth muscle cell phenotypic marker and modulator, controls vascular neointimal lesion formation. Circ Res 2009;105:158-166.
51. Downie Ruiz Velasco A, Welten SMJ, Goossens EAC, Quax PHA, Rappsilber J, Michlewski G, Nossent AY. Posttranscriptional Regulation of 14q32 MicroRNAs by the CIRBP and HADHB during Vascular Regeneration after Ischemia. Molecular therapy Nucleic acids 2019;14:329-338.
52. Welten SMJ, de Vries MR, Peters EAB, Agrawal S, Quax PHA, Nossent AY. Inhibition of Mef2a Enhances Neovascularization via Post-transcriptional Regulation of 14q32 MicroRNAs miR-329 and miR-494. Molecular therapy Nucleic acids 2017;7:61-70.
53. Dai R, Lu R, Ahmed SA. The Upregulation of Genomic Imprinted DLK1-Dio3 miRNAs in Murine Lupus Is Associated with Global DNA Hypomethylation. PloS one 2016;11:e0153509.
54. Aavik E, Lumivuori H, Leppanen O, Wirth T, Hakkinen SK, Brasen JH, Beschorner U, Zeller T, Braspenning M, van CW, Makinen K, Yla-Herttuala S. Global DNA methylation analysis of human atherosclerotic plaques reveals extensive genomic hypomethylation and reactivation at imprinted locus 14q32 involving induction of a miRNA cluster. Eur Heart J 2015;36:993-1000.

55. McPherron AC, Lawler AM, Lee SJ. Regulation of skeletal muscle mass in mice by a new TGF-beta superfamily member. Nature 1997;387:83-90.
56. Hitachi K, Tsuchida K. Myostatin-deficiency in mice increases global gene expression at the Dlk1-Dio3 locus in the skeletal muscle. Oncotarget 2017;8:5943-5953.
57. Zimmers TA, Davies MV, Koniaris LG, Haynes P, Esquela AF, Tomkinson KN, McPherron AC, Wolfman NM, Lee SJ. Induction of cachexia in mice by systemically administered myostatin. Science 2002;296:1486-1488.
58. Verzola D, Milanesi S, Bertolotto M, Garibaldi S, Villaggio B, Brunelli C, Balbi M, Ameri P, Montecucco F, Palombo D, Ghigliotti G, Garibotto G, Lindeman JH, Barisione C. Myostatin mediates abdominal aortic atherosclerosis progression by inducing vascular smooth muscle cell dysfunction and monocyte recruitment. Scientific reports 2017;7:46362.
59. Zhu X, Buhrer C, Wellmann S. Cold-inducible proteins CIRP and RBM3, a unique couple with activities far beyond the cold. Cellular and molecular life sciences : CMLS 2016;73:3839-3859.
60. Treiber T, Treiber N, Plessmann U, Harlander S, Daiss JL, Eichner N, Lehmann G, Schall K, Urlaub H, Meister G. A Compendium of RNA-Binding Proteins that Regulate MicroRNA Biogenesis. Molecular cell 2017;66:270-284.e213.
61. Al-Fageeh MB, Smales CM. Cold-inducible RNA binding protein (CIRP) expression is modulated by alternative mRNAs. RNA (New York, NY) 2009;15:1164-1176.
62. Fujita J. Cold shock response in mammalian cells. Journal of molecular microbiology and biotechnology 1999;1:243-255.
63. Liao Y, Tong L, Tang L, Wu S. The role of cold-inducible RNA binding protein in cell stress response. International journal of cancer 2017;141:2164-2173.
64. Liu A, Zhang Z, Li A, Xue J. Effects of hypothermia and cerebral ischemia on cold-inducible RNA-binding protein mRNA expression in rat brain. Brain research 2010;1347:104-110.
65. Lleonart ME. A new generation of proto-oncogenes: cold-inducible RNA binding proteins. Biochimica et biophysica acta 2010;1805:43-52.

Part I

Chapter 2

The multifactorial nature of microRNAs in vascular remodelling

Cardiovascular Research 2016 May 1;110(1):6-22

EAC Goossens[1,2] *
SMJ Welten[1,2] *
PHA Quax[1,2] ^
AY Nossent[1,2] ^

* Authors contributed equally to this work
^ Authors contributed equally to this work

[1]Department of Surgery and [2]Einthoven Laboratory for Experimental Vascular Medicine, Leiden University Medical Center, Leiden, The Netherlands

Abstract

Vascular remodelling is a multifactorial process that involves both adaptive and maladaptive changes of the vessel wall through, among others, cell proliferation and migration, but also apoptosis and necrosis of the various cell types in the vessel wall. Vascular remodelling can be beneficial, e.g. during neovascularization after ischaemia, as well as pathological, e.g. during atherosclerosis and aneurysm formation. In recent years, it has become clear that microRNAs are able to target many genes that are involved in vascular remodelling processes and either can promote or inhibit structural changes of the vessel wall. Since many different processes of vascular remodelling are regulated by similar mechanisms and factors, both positive and negative vascular remodelling can be affected by the same microRNAs. A large number of microRNAs has been linked to various aspects of vascular remodelling and indeed, several of these microRNAs regulate multiple vascular remodelling processes, including both the adaptive processes angiogenesis and arteriogenesis as well as maladaptive processes of atherosclerosis, restenosis and aneurysm formation. Here, we discuss the multifactorial role of microRNAs and microRNA clusters that were reported to play a role in multiple forms of vascular remodelling and are clearly linked to cardiovascular disease (CVD). The microRNAs reviewed are miR-126, miR-155 and the microRNA gene clusters 17-92, 23/24/27, 143/145 and 14q32. Understanding the contribution of these microRNAs to the entire spectrum of vascular remodelling processes is important, especially as these microRNAs may have great potential as therapeutic targets for treatment of various CVDs.

Introduction

MicroRNAs

MicroRNAs are a class of endogenous noncoding RNA molecules of approximately 22 nucleotides in length. MicroRNAs inhibit translation of mRNAs into proteins by binding to specific sites in the 3'-untranslated region (3'UTR) of their target mRNAs. Rather than completely silencing their target gene, binding of a microRNA leads to modest target downregulation. However, a single microRNA is able to downregulate the expression of numerous target genes, and by doing so, that single microRNA can regulate complex, multifactorial physiological processes[1]. MicroRNAs have been shown to play an important role in human diseases, including cardiovascular disease (CVD). In this review, we describe the multifactorial nature of microRNAs in the regulation of vascular remodelling, by discussing the different target genes and regulatory mechanisms that have been described for these microRNAs. Although many microRNAs play a role in some aspects of vascular remodelling, we focused on those microRNAs that play a role in multiple forms of vascular remodelling and are clearly linked to CVD. The individual microRNAs miR-126 and miR-155, the microRNA gene clusters 17-92, 23/24/27, 143/145, and the largest known microRNA gene cluster 14q32, all met these criteria (Figure 1). An overview of confirmed target genes for these microRNAs is given in Tables 1 and 2.

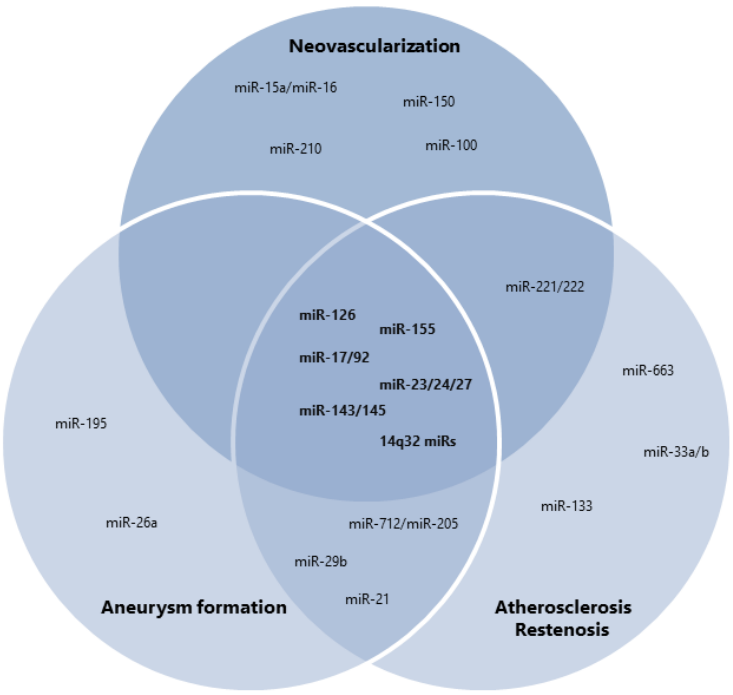

Figure 1 The top microRNAs reported to play a role in each of the following vascular remodelling processes, atherosclerosis and restenosis formation, aneurysm formation, and neovascularization are shown. MicroRNAs that were reported to play a role in multiple forms of these processes were selected for this review and shown here in bold.

Non-standard abbreviations and acronyms	
3'UTR	3'-untranslated region
AAA	Abdominal aortic aneurysm
AAV	Adeno-associated virus
AngII	Angiotensin II
CAD	Coronary artery disease
CVD	Cardiovascular disease
EC	Endothelial cell
HDL	High-density lipoprotein
IA	Intracranial aneurysm
LNA	Locked nucleic acid
miR	MicroRNA
MO	Morpholino
MP/MV	Microparticle/Microvesicle
MSC	Mesenchymal stem cell
oxLDL	Oxidized low-density lipoprotein
PBMC	Peripheral blood mononuclear cell
siRNA	Small-interfering RNA
TLR	Toll-like receptor
(V)LDL	(very) low-density lipoprotein
(V)SMC	(vascular) smooth muscle cell
Abbreviations of NCBI-annotated target genes	
ABCA1	ATP-binding cassette transporter A1
ACAT1	Acyl-CoA cholesterol acyltransferase-1
ACE	Angiotensin-converting enzyme
ANGPTL3	Angiopoietin-like 3
ARF6	ADP ribosylation factor 6
AT1R	Angiotensin II type 1 receptor
BCL2/6	B-cell lymphoma 2/6
bFGF	Basic fibroblast growth factor
BIC	B-cell integration cluster
BMP4	Bone morphogenetic protein 4
CCL2/MCP1	Monocyte chemoattractant protein 1
CD146	Cluster of differentiation 146 (melanoma cell adhesion molecule)
CDK4	Cyclin-dependent kinase 4
CPT1α	Carnitine palmitoyl transferase 1α
CXCL12/SDF1	Stromal derived factor-1
CXCR4	Chemokine (C-X-C motif) receptor 4
DGAT2	Diacylglycerol O-acyltransferase 2
DLK1	NOTCH1 inhibitor delta-like 1 homolog
E2F1	E2F transcription factor 1
EFNB2	Ephrin B2
eNOS	Endothelial nitric oxide synthase
ERK1/2	Extracellular signal-related kinase 1/2
ETS-1	V-ets avian erythroblastosis virus E26 oncogene homolog 1
FGFGR2	Fibroblast growth factor receptor 2
FLT1	VEGF receptor fms-related tyrosine kinase 1
FOXO3/4	Forkhead box O 3/4
FSR2	Fibroblast growth factor receptor substrate 2
FZD4	Frizzled class receptor 4
GATA2	GATA binding protein 2
GPAM	Glycerol-3-phosphate acyltransferase 1 mitochondrial
HIF1α/HIF2α	Hypoxia inducible factor 1/2, alpha subunit
HKII	Hexokinase II

HMGB1	HMG box-transcription protein 1
HMOX1	Heme oxygenase 1
ICAM1	Intracellular cell adhesion molecule 1
IGF1	Insulin-like growth factor 1
IL33	Interleukin 33
INSIG1	Insulin-induced gene 1
IRS1/2	Insulin receptor substrate 1/2
ITGβ8	Integrin β 8
JAK1	Janus kinase 1
KLF2/4/5	Krüppel-like factor 2/4/5
LPL	Lipoprotein lipase
LRP6	LDL receptor-related protein 6
MCP1/CCL2	Monocyte chemoattractant protein 1
MEF2a	Myocyte enhancer factor 2
MEG3	Maternally expressed gene 3
MIF	Macrophage migration inhibitory factor
MKK4	Mitogen-activated protein kinase kinase 4
MMP1/3	Matrix metalloproteinase 1/3
MRTFA	Myocardin-related transcription factor A
Myd88	Myeloid differentiation primary response gene
PAK4	p21-activated kinase 4
PIK3R2	Phosphoinositide-3-kinase, regulatory subunit 2
PPARγ	Proliferator-activator receptor gamma
PPP2R2A	Protein phosphatase 2 regulatory subunit B, alpha
RGS16	Regulator of G protein signalling 16
SDF1/CXCL12	Stromal derived factor-1
SEMA6A/6D/3B	Semaphorin 6A/6D/3B
SMAD3	SMAD family member 3
SOCS1/5	Suppressor of cytokine signalling 1/5
SPRED1	Sprouty-related, EVH1 domain containing 1
SREBPs	Sterol regulatory element-binding proteins
SRF	Serum response factor
TAB2	TGF-β activated kinase1/MAP3K7 binding protein 2
TGF-β(2)	Transforming growth factor β (2)
TGF-βR2	TGF-β receptor 2
TIMP3	Tissue inhibitor of metalloproteinase 3
TLR4	Toll-like receptor 4
TNF-α	Tumour necrosis factor alpha
TRIF	TIR-domain-containing adapter-inducing interferon-b
uPA	urokinase-type plasminogen activator
VCAM1	Vascular cell adhesion molecule 1
VE-cadherin	Vascular endothelial cadherin
VEGF	Vascular endothelial growth factor

Table 1 Non-standard abbreviations and acronyms

MicroRNA	Confirmed targets	Biological process affected
miR-126	VCAM1[2], SPRED1, and PIK3R2[3–5]	Angiogenesis, vascular integrity
	SDF1/CXCL12[6,7]	Migration of CD34+ progenitor cells
	RGS16[6]	Recruitment of Sca-1+ endothelial progenitor cells, atherosclerosis
	FOXO3, BCL2, and IRS1[8]	VSMC turnover
	DLK1 (miR-126-5p)[9]	Endothelial repair, atherosclerosis

miR-155		SOCS1[10]	Pro-inflammatory signalling
		TAB2[11]	Anti-inflammatory signalling
		PU.1[12]	Monocyte/macrophage infiltration, T lymphocyte activation
		AT1R[13], ETS-1[14]	HUVEC activation and migration
		AT1R[15], SOCS1[15]	Angiogenesis, Arteriogenesis
		BCL6, CCL2[16]	Atherosclerosis
		HMGB1[17]	Foam cell formation
		MMP1 and MMP3[18]	Matrix degradation
miR-23-24-27	miR-23 and miR-27	SEMA6A, SEMA6D, SPROUTY2[19]	EC sprouting, angiogenesis
	miR-23b	E2F1[20]	Rb phosphorylation, EC growth arrest
		uPA, SMAD3, FOXO4[21]	VSMC phenotypic switching
	miR-24	GATA2, PAK4[22]	Vascularity, cardiac function, and infarct size after myocardial infarction
		NDST1[23]	HSPG sulfation and affinity of HSPGs for VEGF, endothelial cell responsiveness to VEGFA
		HMOX1[24]	SMC apoptosis and proliferation
		INSIG1[25]	Lipid accumulation and plasma triglyceride levels
		CHI3L1[26]	Inflammation, AAA formation
	miR-27a	VE-cadherin[27]	Vascular leakage
	miR-27b	ABCA1, LPL, ACAT1[28]	Cholesterol efflux, lipid uptake and cholesteryl-ester formation
miR-17-92	miR-17-92	TSP1, CTGF[29]	Tumour angiogenesis
	miR-17/20	JAK1[30]	Angiogenesis
	miR-19a	CyclinD1[31]	EC proliferation
		FZD4 and LRP6[32]	WNT signalling, arteriogenesis
	miR-92a	KLF2, KLF4, SOCS5[33]	Endothelial homeostasis, atherosclerosis
		ITGA5[34]	Blood flow recovery after ischaemia and LV function after myocardial infarction
		KLF4 and MKK[35]	EC proliferation and migration
miR-143/145	miR-143/145	HKII, ITGβ8[36]	Angiogenesis, vessel stability
		ACE[37]	Atherosclerosis
	miR-143	ELK1[38]	VSMC proliferation
		AKT[39]	Angiogenesis, tumourigenesis
	miR-145	IGF-I, IRS1[40,41]	Tumour angiogenesis
		HIF2α[42]	Angiogenesis
		KLF5[43]	Transdifferentiation of fibroblasts to myofibroblasts, neointima formation
		KLF4[44]	VSMC differentiation
		JAMA1[45]	Leukocyte recruitment
		ABCA1[46]	Cholesterol efflux
14q32 miRs	miR-329	MEF2a[47], CD146[48]	Angiogenesis, arteriogenesis, EC proliferation
	miR-494	VEGFA, EFNB2, FGFR2[47]	Angiogenesis, arteriogenesis, myofibroblast proliferation
		TIMP3, TGFB2, IL33[49]	Atherosclerosis
	miR-376b-5p	HIF1α/VEGF signalling pathway[50]	Angiogenesis
	miR-377	VEGFA[51]	Angiogenesis
	miR-136	PPP2R2A[52]	VSMC proliferation
	miR-758	ABCA1[53]	Cholesterol efflux
	miR-370	CPT1α[54]	Fatty acid β oxidation
	miR-487b	IRS1[55]	Outward remodelling of the aorta

Table 2 Overview of confirmed target genes for microRNAs discussed

Vascular remodelling

Vascular remodelling comprises beneficial adaptive responses of the vessel wall to changes in haemodynamic forces, vasoactive stimuli or growth factors, but also maladaptive responses that can lead to CVD[56]. Thus, vascular remodelling can be divided into adaptive and maladaptive processes regarding vessel wall structure and blood supply towards downstream tissues[57]. For this review, we focused on neovascularization on the one hand and on atherosclerosis, postinterventional restenosis and aneurysm formation on the other. All of these processes are orchestrated by microRNAs[57].

When studying the role of microRNAs in these processes, there are several microRNAs that have been very well described. For example, one of the most promising microRNAs as therapeutic target for the treatment of atherosclerotic disease is miR-33a/b (discussed below), as it controls cholesterol metabolism, a crucial mechanism in CVD. The phenotype of smooth muscle cells (SMCs), either contractile or proliferative, is also imperative for vascular remodelling and neointima formation. Several microRNAs, including miR-133, miR-125b, miR-26a, miR-663, and miR-1, have been shown to control SMC phenotype and function[58–62]. In aneurysm formation, the miR-29 family has been shown to play a major role by targeting genes that are involved in extracellular matrix homeostasis. Inhibition of miR-29b in two murine abdominal aortic aneurysm (AAA) models increased expression of genes encoding for collagen and elastin and reduced expression of matrix metalloproteinases, resulting in decreased aneurysm progression in these mice[63]. Similarly, miR-21 regulated AAA expansion through targeting of PTEN[64].

Therapeutic potential of microRNAs

Several microRNAs that gave promising results as therapeutic targets in murine models of CVD are now being studied in larger animal models. A relevant example is the miR-33 family, consisting of miR-33a and miR-33b. Both miR-33a and miR-33b regulate the expression of cholesterol transporter ABCA1, which mediates the efflux of cholesterol[65]. Inhibition or deficiency of miR-33a reduced progression of plaques and raised HDL levels in atherosclerotic mouse models[65 – 67]. Since rodents lack miR-33b, extrapolation of these results to a human situation was not straightforward. Systemic inhibition of miR-33a/b in African green monkeys, which do express miR-33b, led to increased expression of ABCA1 in the liver of treated animals and increased plasma HDL levels[68]. The authors also observed the regulation of other genes involved in fatty acid oxidation and fatty acid synthesis, leading to a decrease in plasma VLDL levels, an effect that was not observed in mice[68]. Moreover, no overt toxicity was observed in animals treated with anti-miRs, supporting the development of anti-miR-33 therapeutics for treatment of atherosclerosis.

Janus phenomenon

However, caution is wanted when intervening in individual processes of vascular remodelling. This is best illustrated by the Janus phenomenon, named after the two-faced Roman deity Janus. The Janus phenomenon was first described by Epstein et al., who noticed that interventions used to stimulate arteriogenesis also increased atherosclerosis and vice versa[69]. The phenomenon is explained by the fact that there is a strong overlap in the mechanisms that underlie the various forms of vascular remodelling. One of the important mechanisms shared in vascular remodelling are the inflammatory responses. Since microRNAs can target numerous genes that may be involved in many processes, modulation of one microRNA could influence more than one form of vascular remodelling. This could be positive, for example when targeting a single microRNA inhibits various forms of maladaptive remodelling simultaneously. However, an unwanted effect could be that anti-atherogenic microRNAs also have anti-arteriogenic effects due to common pathways in atherosclerosis and arteriogenesis. The Janus phenomenon is a major drawback for many novel therapeutics designed to modulate vascular remodelling and must also be taken into account when exploring the therapeutic potential of microRNAs.

Therefore, we chose to discuss those microRNAs, miR-126, miR-155, and microRNA gene clusters 17-92, 23/24/27, 143/145, and 14q32, that play a confirmed role in multiple forms of vascular remodelling and are clearly linked to CVD.

miR-126

MiR-126 is one of the most abundantly expressed microRNAs in endothelial cells (ECs)[70]. The miR-126 gene is located on human chromosome 9 and gives rise to two mature microRNAs, miR-126-3p and miR-126-5p. Generally, the role of miR-126 in vascular remodelling as described in the literature corresponds to miR-126-3p (Figure 2). MiR-126 is also abundantly expressed in platelets, suggesting a role for miR-126 in vascular homeostasis and inflammation[71]. Platelets are a major source of circulating miR-126[72]. Consequently, levels of circulating miR-126 are influenced by the use of platelet inhibitors, such as aspirin[72]. The delivery of miR-126 by platelet microparticles (MPs) to primary human macrophages was reported recently, and miR-126 derived from these platelet MPs influences macrophage gene expression and function[69]. Levels of miR-126 are differentially expressed in plasma samples of patients with coronary artery disease (CAD)[74].

Neovascularization

The first studies from 2008 that investigated the role of miR-126 in EC function demonstrated that miR-126 targets VCAM1[2]. Increased expression of adhesion molecules such as VCAM1

and increased leukocyte adherence to ECs are necessary for the initiation of angiogenesis. Both mechanisms are stimulated by inhibition of miR-126[2]. In HUVECs, inhibition of miR-126 led to increased proliferation and migration[3]. Furthermore, injection of miR-126 inhibitors into zebrafish embryos affected blood vessel integrity, as was demonstrated by collapsed lumens and compromised endothelial tube organization[3]. Studies in mice showed that inhibition of miR-126 decreased recovery after myocardial infarction and impaired angiogenic capacity in a hindlimb ischaemia model[4,5,75]. These effects were partially mediated via inhibitors of VEGF signalling, namely SPRED1 and PIK3R2[3–5]. Both Spred1 and Pik3r2 are upregulated in the absence of miR-126, causing an increase in vascular permeability and leakage[3,5]. MiR-126 was also shown to target CXCL12[6]. Silencing miR-126 induced CXCL12 expression that enhanced migration of CD34+ progenitor cells *in vitro* and increased the number of circulating bone marrow-derived progenitor cells after hindlimb ischaemia *in vivo*[6,7].

In addition, exosomes from human CD34+ cells, which are rich in miR-126, have great angiogenic capacity both *in vitro* and *in vivo*[76]. Mocharla et al. showed that CD34+ peripheral blood mononuclear cells (PBMCs) secrete microvesicles and exosomes that are enriched with miR-126[77]. These microvesicles and exosomes are taken up by ECs and facilitate the pro-angiogenic effects of miR-126[77].

Atherosclerosis

Atherosclerotic plaque progression is often accompanied by apoptosis of (vascular) cells in the plaque[78]. During apoptosis, ECs release microvesicles that are enriched with miR-126[6]. Delivery of miR-126 to recipient vascular cells inhibits the progression of atherosclerosis, presumably via suppression of RGS16, which is a negative regulator of CXCR4. Subsequent upregulation of CXCR4 led to the production of CXCL12. This reduced lesion formation by decreasing the number of macrophages and apoptotic cells in the plaque and increasing the recruitment of endothelial progenitor cells for repair in a mouse model for atherosclerosis[6]. Vesicle-independent transfer of miR-126 from ECs to SMCs was also reported, increasing miR-126 levels in SMCs (Figure 2). Decreased expression of miR-126 target genes FOXO3, BCL2, and IRS1 led to increased proliferation of SMCs[8]. Subjecting ECs to laminar shear stress or miR-126 inhibition abolished these effects. In miR-126$^{-/-}$ mice, neointima formation was attenuated compared with wild-type mice after ligation of the left common carotid artery[8]. Recently, the contribution of miR-126-5p to atherosclerosis formation was demonstrated by Schober et al[9]. Hypercholesterolaemic miR-126$^{-/-}$ApoE$^{-/-}$ and miR-126$^{+/+}$ApoE$^{-/-}$ mice were subjected to endothelial denudation. After 14 and 28 days, lesion area was increased in miR-126$^{-/-}$ApoE$^{-/-}$ mice compared with control animals[9]. Moreover, endothelial recovery of the

carotid lumen was impaired in miR-126$^{-/-}$ApoE$^{-/-}$ animals due to reduced EC proliferation[9]. In these animals, expression of multiple miR-126-5p predicted target genes was increased, whereas expression of known miR-126-3p targets was not[9]. The authors confirmed targeting of DLK1 by miR-126-5p and demonstrated that inhibition of miR-126-5p increased Dlk1 expression and reduced EC proliferation[9]. To identify the specific role of miR-126-3p and miR-126-5p in endothelial repair, denuded arteries of ApoE$^{-/-}$ mice were treated with miR-126-3p-, miR-126-5p-, or control-miR inhibitors. Treatment with anti-miR-126-5p, but not anti-miR-126-3p, significantly increased the lesion area and impaired endothelial recovery and EC proliferation[9].

In untreated ApoE$^{-/-}$ mice, disturbed flow led to decreased miR-126-5p levels and increased Dlk1 mRNA and protein levels in the carotid artery, whereas miR-126-3p levels were unaltered[9]. The authors proposed that miR-126-5p plays a role in regulating EC proliferation at non-predilection sites, whereas miR-126-3p presumably regulates the replicative capacity of ECs at predilection sites[9]. Finally, in human atherosclerotic lesions, miR-126-5p levels were found to inversely correlate with DLK1 expression and the number of lesional macrophages and positively correlated with EC proliferation, suggesting an atheroprotective effect of increased miR-126-5p levels in humans[9].

Aneurysm

Although miR-126 is upregulated in AAA and upregulation correlated with decreased TNF-α expression, the exact function of miR-126 in AAA pathogenesis is still unknown[79]. In plasma of patients with AAA, miR-126 was significantly downregulated compared with plasma of healthy volunteers, but not compared to patients with CAD[79].

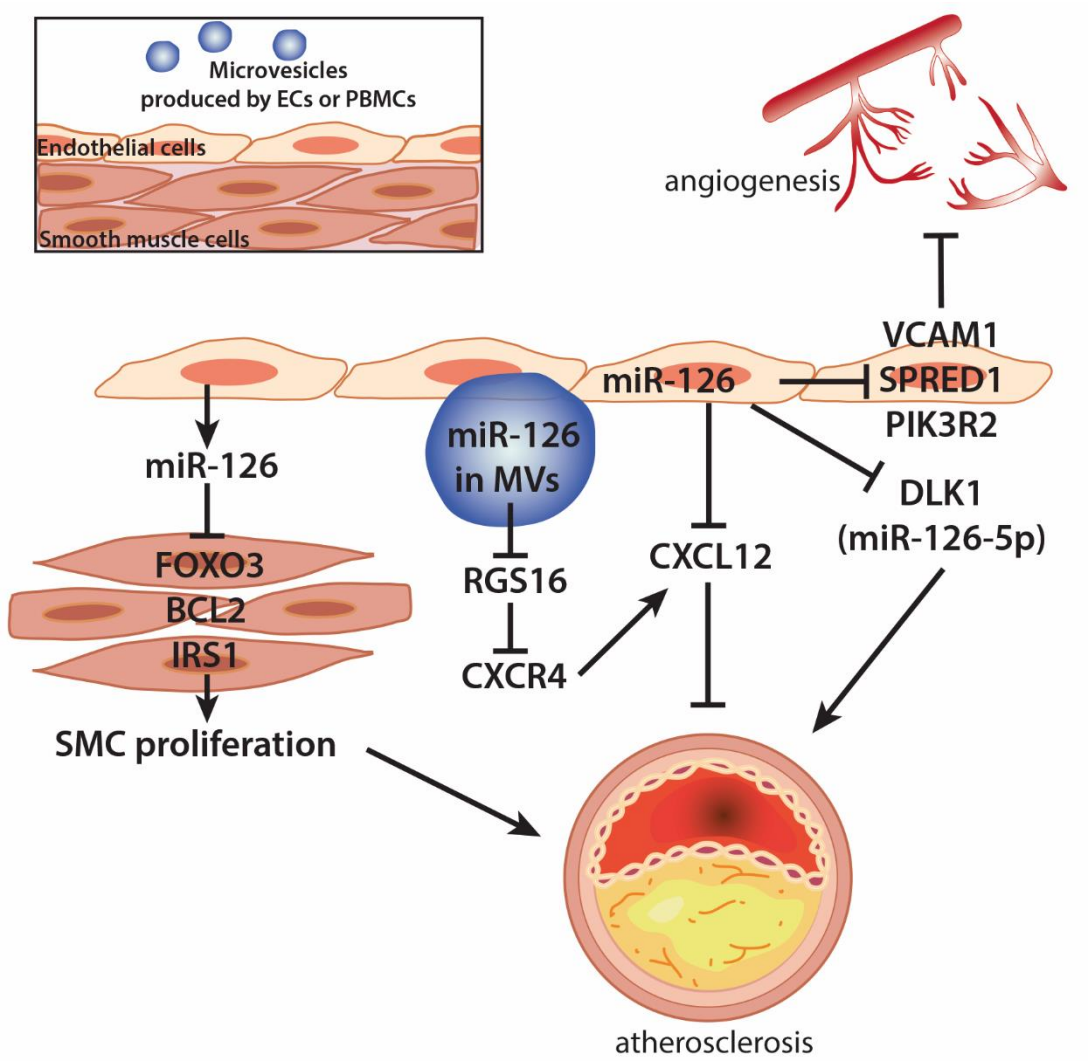

Figure 2 The role of endothelial miR-126 in vascular remodelling. MiR-126 regulates angiogenesis and vascular integrity via targeting of VCAM1 and targeting the inhibitors of VEGF signalling; SPRED1 and PIK3R2. Via microvesicle-mediated delivery from ECs to neighbouring vascular cells, miR-126 inhibits RGS16, an inhibitor of CXCR4, resulting in the expression of CXCL12 and reducing atherosclerosis. Paracrine secretion of miR-126 from ECs to SMCs leads to inhibition of FOXO3, BCL2, and IRS1 target genes and increases proliferation of SMCs, which contributes to the atherogenic actions of miR-126. In addition, miR-126-5p suppresses the NOTCH1 inhibitor DLK1, thereby limiting atherosclerosis. Arrows indicate upregulation. Capped lines indicate inhibition. MV, microvesicle; EC, endothelial cell; SMC, smooth muscle cell; PBMCs, peripheral blood mononuclear cells. For full target gene names, see Table 1.

miR-155

The miR-155 gene is located within an exon of the noncoding RNA BIC on human chromosome 21. MiR-155 is highly expressed by activated B and T cells, but also by monocytes and macrophages[80,81]. In addition, miR-155 is expressed in ECs and SMCs[14].

MiR-155 is upregulated in macrophages via TLR ligands, such as LPS[81]. MiR-155 exerts pro-inflammatory effects via targeting of the anti-inflammatory SOCS1[10]. In contrast, anti-

inflammatory effects of miR-155 signalling have also been described via targeting of TAB2[11] (Figure 3).

In 2012, Corsten et al.[12] described a role for miR-155 in CVD, demonstrating upregulation of miR-155 during the acute inflammatory phase of viral myocarditis. Systemic inhibition of miR-155 reduced cardiac monocyte/macrophage infiltration, decreased T-lymphocyte activation, and reduced myocardial damage in a mouse model of acute viral myocarditis[12].

Neovascularization

MiR-155 is co-expressed with AT1R in HUVECs and SMCs, where it represses AT1R expression[13]. Interestingly, a single nucleotide polymorphism (+1166 A/C), which is associated with CVD, was found to disrupt a miR-155 target site in the 3'UTR of AT1R[13]. Overexpression of miR-155 reduced migration of HUVECs in response to Angiotensin II (AngII) via targeting of the AT1R.

ETS-1 has two potential binding sites for miR-155 in its 3'UTR and is another target of miR-155 in HUVECs[14]. ETS-1 and its downstream target genes VCAM1, MCP1, and FLT1 were induced in HUVECs upon stimulation with AngII. Overexpression of miR-155 abrogated this effect[14].

Recent work by Pankratz et al.[15] demonstrated that miR-155 exerts both anti-angiogenic and pro-arteriogenic functions after induction of hindlimb ischaemia in mice[82]. MiR-155 was upregulated 7 days after femoral artery ligation in mice. Inhibition of miR-155 in HUVECs resulted in increased EC proliferation and tube formation[15]. These results were confirmed in aortic ring assays, as well as in *in vivo* Matrigel plug assays using miR-155$^{-/-}$ mice. In miR-155$^{-/-}$ ECs, expression of AT1R was increased. AT1R expression could be manipulated by overexpression or inhibition of miR-155 in both human and murine ECs. The authors concluded that the antiangiogenic properties of miR-155 are mediated via AT1R[15] (Figure 2). Despite the anti-angiogenic properties of miR-155, blood flow recovery after hindlimb ischaemia was impaired in miR-155$^{-/-}$ mice. MiR-155 deficiency decreased migration of bone marrow-derived macrophages. MiR-155$^{-/-}$ macrophages showed significantly reduced expression levels of pro-arteriogenic cytokines and chemokines upon LPS stimulation, compared with wild-type cells. SOCS1 was identified as a potential mediator, as this was the most upregulated target gene in miR-155$^{-/-}$ BMDMs. Knockdown of SOCS1 indeed reversed the effects of miR-155 deficiency on pro-arteriogenic cytokine production[15].

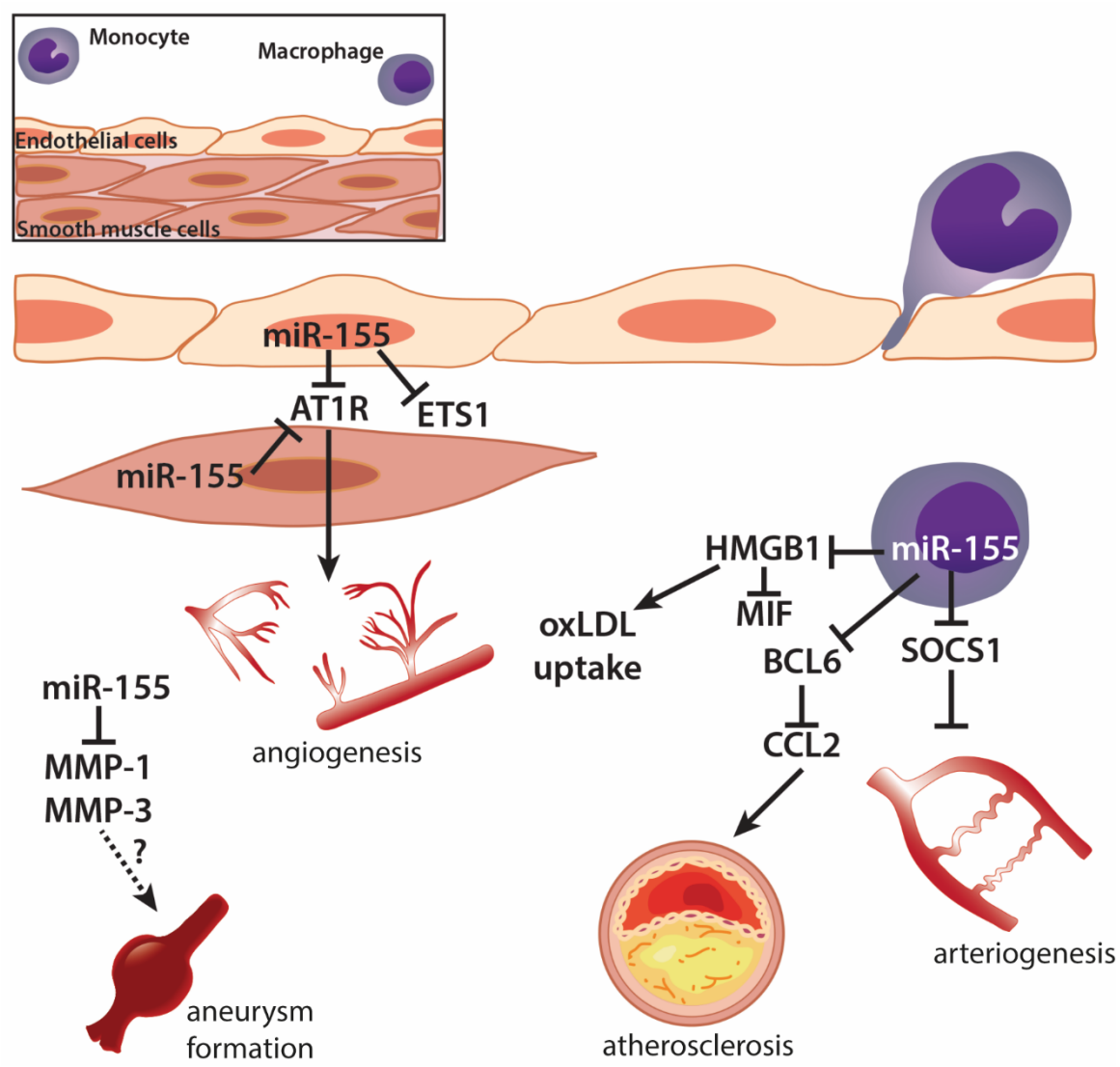

Figure 3 The inflammatory miR-155 in vascular remodelling. MiR-155 is co-expressed with AT1R in HUVECs and SMCs and inhibits expression of AT1R in these cells. ETS1 transcription factor is also targeted by miR-155 in HUVECs. Via these targets, miR-155 affects angiogenesis. In addition, miR-155 has been demonstrated to affect arteriogenesis. This effect is mediated by inhibition of SOCS1 in macrophages, resulting in upregulation of pro-arteriogenic cytokines. MiR-155 in atherosclerotic plaques is predominantly expressed in (pro-inflammatory) macrophages, where it suppresses the transcription factor BCL6. In addition, miR-155 targets HMGB1, increasing oxLDL uptake by macrophages. MiR-155 reduces matrix metalloproteinases MMP-1 and MMP-3, which could reduce matrix degradation and progression of aneurysm formation. Arrows indicate upregulation. Capped lines indicate inhibition. The dashed line indicates possible interactions that have not been confirmed yet. (HUV)EC, (human umbilical venous) endothelial cell; SMC, smooth muscle cell. For full target gene names, see Table 1.

Atherosclerosis

Expression of miR-155 was upregulated in human atherosclerotic plaques, predominantly in pro-inflammatory macrophages[16,83]. However, circulating levels of miR-155 were significantly lower in patients with CAD compared with healthy volunteers[74]. In several studies, treatment

of macrophages with oxidized LDL and IFN-γ led to upregulation of miR-155, whereas suppression of miR-155 by oxLDL treatment has also been reported[16,84 – 86]. Nazari-Jahantigh et al. demonstrated that miR-155 targets BCL6, a transcription factor that attenuates pro-inflammatory NF-kB signalling and directly represses CCL2. Leukocyte-specific deletion of miR-155 decreased Ccl2 signalling and reduced atherosclerotic plaque formation in ApoE$^{-/-}$ mice[16]. Recently, Tian et al.[17] showed that miR-155 targets HMGB1, which suppresses MIF and increases uptake of oxLDL by macrophages. Elevated miR-155 levels enhanced oxLDL-induced foam cell formation by targeting HMGB1. Systemic inhibition of miR-155 in ApoE$^{-/-}$ mice resulted in smaller atherosclerotic plaques that contained less lipid-laden macrophages[17]. However, opposite findings on the role of miR-155 in atherosclerosis have also been reported. LDL-R$^{-/-}$ mice transplanted with miR-155$^{-/-}$ bone marrow developed larger lesions compared with mice transplanted with wild-type bone marrow[87]. Increased numbers of macrophages and neutrophils were present in these lesions as well as increased numbers of granulocytes and inflammatory monocytes in the circulation[87]. Apparently, miR-155 can have opposite effects in macrophages, being either pro- or anti-inflammatory (Figure 3).

Aneurysm

MiR-155 is significantly upregulated in AAA tissue[79]. However, expression of miR-155 was lower in plasma of patients with AAA compared with plasma levels of healthy controls and of patients with CAD[79]. In models for rheumatoid arthritis, overexpression of miR-155 led to downregulation of MMP1 and MMP3[18]. This suggests that overexpression of miR-155 in AAA may function as an endogenous rescue mechanism that inhibits matrix degradation and progression of aneurysm formation[18].

miR-17-92 cluster

The miR-17-92 gene cluster is located within intron 3 of the C13orf25 gene on human chromosome 13 and encodes six individual microRNAs, namely miR-17, miR-18a, miR-19a, miR-20a, miR-19b-1, and miR-92a[88] (Figure 4). Recently, it was shown that expression of the miR-17-92 cluster in ECs is stimulated by VEGF, via activation of the Erk/Elk1 pathway[89]. Upon stimulation, expression of miR-17-92 contributed to endothelial proliferation and angiogenic sprouting *in vitro* and physiological angiogenesis *in vivo*[89].

Neovascularization

In 2009, Bonauer et al. showed that miR-92a is highly expressed in human ECs and overexpression of miR-92a in ECs blocked sprouting in a three-dimensional angiogenesis

model. *In vivo* inhibition of miR-92a increased the number of perfused vessels in Matrigel plugs and improved blood flow recovery after hindlimb ischaemia[34]. ITGA5 was identified as a direct target of miR-92a[34]. To elucidate the specific function of the other members of the miR-17-92 cluster in angiogenesis, Doebele et al.[30] overexpressed or blocked individual members of the cluster both *in vitro* and *in vivo*. *In vitro* inhibition of all miR-17-92 members, except miR-19, resulted in increased sprouting of EC spheroids[30]. Combined inhibition of miR-17 and miR-20a was shown to promote angiogenesis in Matrigel plugs *in vivo*, whereas inhibition of other members showed trends but no significant effects on angiogenesis[30]. Expression of JAK1 was reduced at mRNA and protein level upon miR-17 overexpression and inhibition of JAK1 using siRNAs was shown to reduce *in vitro* angiogenesis. Using luciferase assays, JAK1 was confirmed as a direct target of miR-17[30].

The contribution of the miR-17-92 cluster to physiological and pathological arteriogenesis was studied by Landskroner-Eiger et al[32]. Endothelial specific knockout of miR-17-92 in mice showed that these animals had more pre-existent collateral arterioles. Consequently, these animals showed improved blood flow recovery after ischaemia. MiR-19a targets components of WNT signalling, namely FZD4 and LRP6. Inhibition of miR-19a improved post-ischaemic blood flow recovery[32].

Expression of the miR-17-92 cluster is repressed by HDAC9 in ECs[90]. Inhibition of HDAC9 reduced neovascularization *in vitro* and *in vivo*. Inhibition of HDAC9, using either a broad spectrum HDAC inhibitor or siRNAs against HDAC9, increased expression of the miR-17-92 cluster, suggesting that the anti-angiogenic effects of HDAC9 inhibition are mediated through the miR-17-92 cluster. Indeed, inhibition of miR-17-20a combined, but not of miR-17 alone, completely rescued the reduced sprouting and network formation in HDAC9-deficient ECs[90].

Atherosclerosis

Several studies showed that miR-17-92 cluster members are regulated by changes in shear stress[20,31]. Upregulation of miR-19a by laminar shear stress has an anti-proliferative effect on ECs via targeting of Cyclin D1[31]. MiR-92a expression was reduced in HUVECs that were subjected to atheroprotective laminar shear stress, leading to upregulation of KLF2[91]. Expression of KLF2 targets eNOS and thrombomodulin were decreased upon miR-92a overexpression[91].

MicroRNA expression profiling in HUVECs revealed upregulation of miR-92a upon low shear stress conditions and the presence of oxLDL[33]. Accordingly, miR-92a expression was higher in the vasculature of both mice and humans in atheroprone regions with low shear stress[33]. MiR-92a inhibition reduced atherosclerosis formation in hypercholesterolaemic $LDLR^{-/-}$ mice. Expression of target genes Klf2 and Klf4 was increased upon anti-miR-92a treatment. The

authors identified SOCS5 as a novel target of miR-92a, which is involved in the regulation of endothelial inflammation[33]. Furthermore, circulating ICAM-1 levels were reduced in anti-miR-92a-treated animals. These results suggest that upregulation of miR-92a by oxLDL in atheroprone regions promotes endothelial dysfunction and atherosclerosis formation[33]. Interestingly, inhibition of miR-92a in rats reduced neointima formation in carotid arteries after vascular injury[35]. MiR-92a inhibition increased EC proliferation and migration, improving reendothelialization after balloon injury or arterial stenting. Expression of KLF4 and MKK was upregulated by miR-92a inhibition[35]. MiR-92a is a promising therapeutic target to reduce atherosclerosis development and postinterventional restenosis.

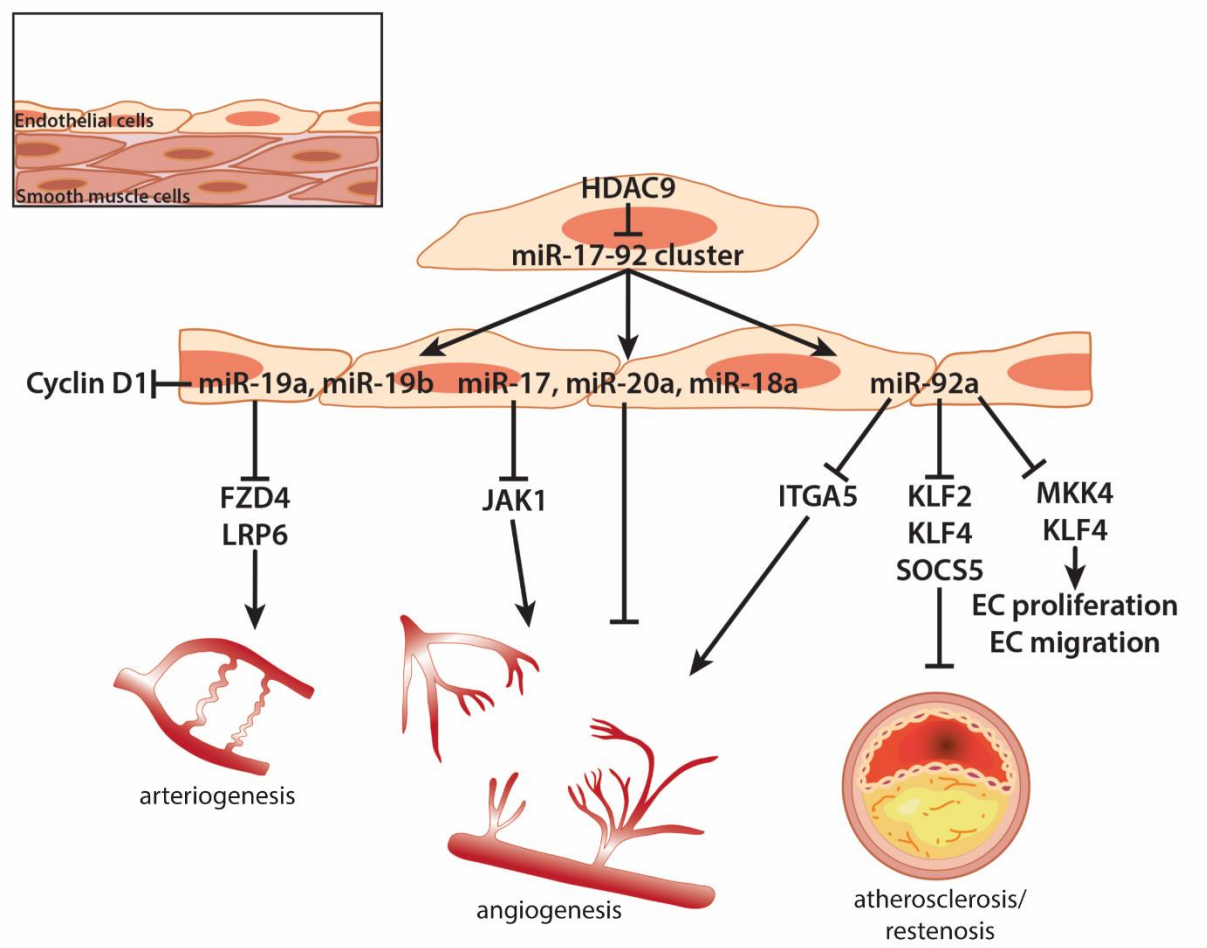

Figure 4 The role of the miR-17-92 cluster in vascular remodelling. MiR-17-92 cluster members regulate angiogenesis via suppression of several target genes. MiR-17 reduces expression of JAK1. ITGA5 is targeted by miR-92a. In addition, miR-92a targets KLF2, KLF4, and SOCS5, promoting atherosclerosis formation. Proliferation and migration of endothelial cells are regulated by targeting of MKK4 and KLF4 by miR-92a. MiR-19a has an anti-proliferative effect in ECs via suppression of Cyclin D1. Other target genes of miR-19a include FZD4 and LRP6, regulators of WNT signalling. Targeting of these genes by miR-19a affects collateral artery formation and blood flow recovery after ischaemia. Arrows indicate upregulation. Capped lines indicate inhibition. EC, endothelial cell. For full target gene names, see Table 1.

Aneurysm

Two members of the 17-92 cluster, miR-20a and miR-92a, were significantly upregulated in ECs of AAA tissue, but a causative role has yet to be confirmed[79].

miR-23/24/27 family

The miR-23/24/27 family consists of two separate microRNA gene clusters. The mouse intergenic miR-23a-27a-24-2 cluster lies on chromosome 8; in humans this cluster is located on chromosome 19. The miR-23b-27b-24-1 cluster has an intronic location on mouse chromosome 13, chromosome 9 in humans[19,92]. Members of the miR-23/24/27 family are highly expressed in vascularized tissues and ECs[93] (Figure 5). Laminar flow and unidirectional shear stress increase the expression of miR-23b, miR-27a/b, and miR-24 in ECs[20,94,95]. Increased expression of miR-23b and miR-27b by pulsatile shear flow was found to correlate with EC growth arrest. The expression of cell cycle gene E2F1 was downregulated by miR-23b and miR-27b[20]. Moreover, phosphorylation of the Rb protein was blocked by miR-23b. Decreased Rb-phosphorylation reduces EC proliferation and inhibits cell cycle progression[20]. Anti-miR-23b, but not antimiR-27, treatment of HUVECs resulted in partial reversal of shear stress-induced growth arrest[90].

Neovascularization

Knockdown of miR-23a/b and miR-27a/b decreased *in vitro* EC sprouting and *ex vivo* aortic ring sprouting[19]. Anti-angiogenic genes SEMA6A, SEMA6D, and SPROUTY2 are targeted by miR-23a/b and miR-27a/b, as shown by luciferase gene reporter assays[19]. Urbich et al. showed that *in vivo* angiogenesis was also affected upon inhibition of miR-27a/b. Anti-miR-27a/b treatment decreased the number of perfused vessels in Matrigel plugs[96]. Moreover, inhibition of miR-27a/b impaired vasculogenesis in zebrafish embryos. *In vitro* experiments showed additional targeting of SEMA3B but *in vivo*, only SEMA6A was a target of miR-27 a/b[96]. Young et al.[27] showed that miR-27a also targets VE-cadherin, both *in vitro* and *in vivo*.

MiR-24 is expressed in cardiac ECs[22]. The expression of miR-24 is induced upon hypoxia and miR-24 is enriched in cardiac ECs compared with other cardiac cells after cardiac ischaemia[22,24]. Overexpression of miR-24 in HUVECs increased apoptosis and impaired tube formation, sprouting, migration, and proliferation[22]. The endothelium-enriched transcription factors GATA2 and PAK4 were validated as targets of miR-24. Inhibition of miR-24 increased vascularity and decreased myocardial infarct size in mice[22]. Another confirmed target gene for miR-24 in ECs is NDST1. Inhibition of NDST1 by miR-24 decreased sulfation of HSPGs and subsequently the binding affinity of HSPGs for VEGFA. MiR-24-mediated suppression of NDST1 lowered VEGFR2 levels and reduced EC responsiveness to VEGFA[23]. Via these

mechanisms, miR-24 affects EC responsiveness to VEGFA. MiR-24 also affected apoptosis, proliferation and function of SMCs, partially through HMOX1[24].

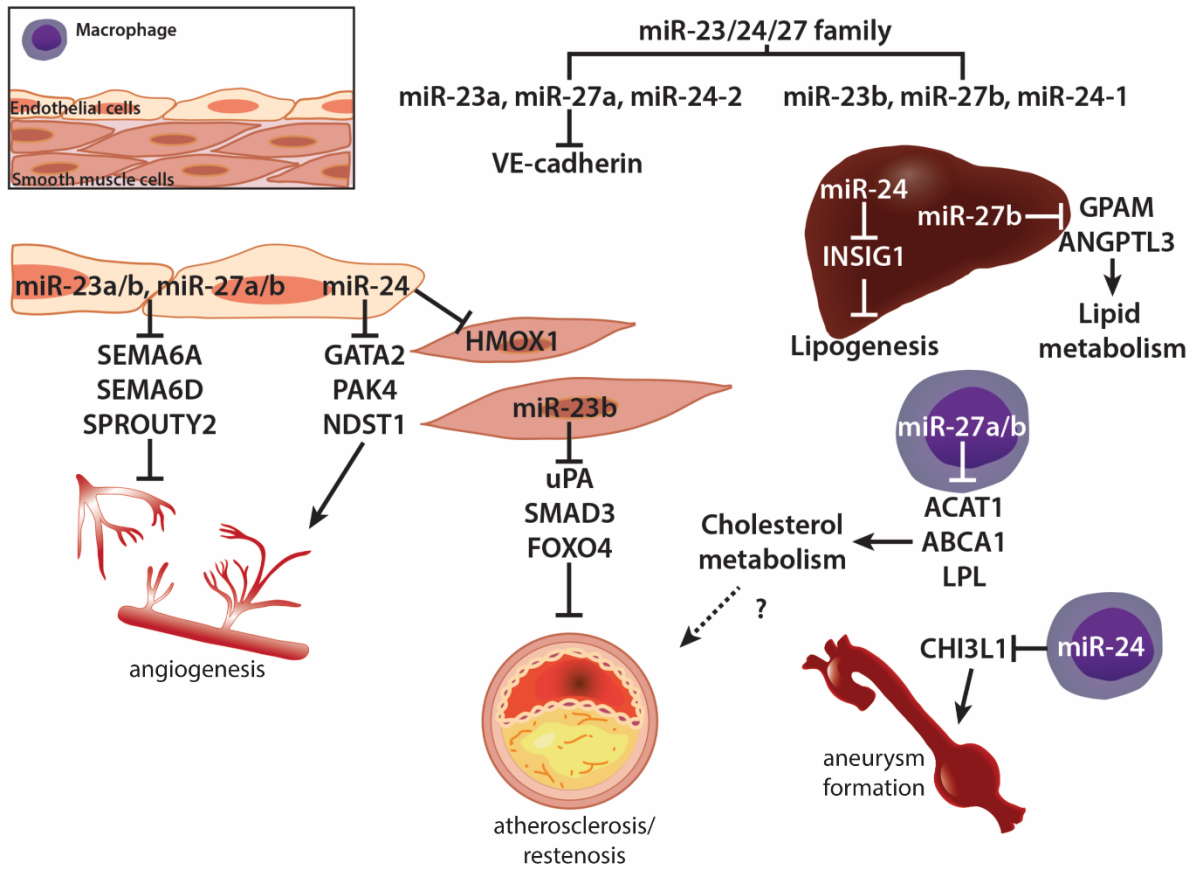

Figure 5 Different roles in vascular remodelling for microRNAs of the miR-23/24/27 family. The miR-23/24/27 family consists of two miR clusters, namely the miR-23a-27a-24-2 cluster and the miR-23b-27b-24-1 cluster. MiR-23a/b and miR-27a/b target the anti-angiogenic genes SEMA6A, SEMA6D, and SPROUTY2. In addition, miR-27a inhibits expression of VE-cadherin. MiR-24 inhibits proliferation, migration, and sprouting of HUVECs via the endothelium-enriched transcription factor GATA2, PAK4, and NDST1. Moreover, miR-24 affects SMC apoptosis, proliferation, and function via HMOX1. Expression of miR-23b in SMCs was found to target uPA, SMAD3, and FOXO4, which results in decreased proliferation and migration of SMCs. Overexpression of miR-23b decreases neointima formation upon balloon injury in rats. Members of the miR-23/24/27 family also play an important role in lipid metabolism. Cholesterol metabolism is affected by miR-27a/b through suppression of ACAT1, ABCA1, and LPL in macrophages. In the liver, miR-27b targets the lipogenic genes GPAM and ANGPTL3, whereas miR-24 suppresses expression of INSIG1. Of the miR-23/24/27 family members, only miR-24 has been described to affect AAA formation. MiR-24 is expressed in macrophages in the adventitia of murine aneurysmal tissue, where it is co-localized with and inhibits expression of the CHI3L1 gene. Arrows indicate up-regulation. Capped lines indicate inhibition. The dashed lines indicate an interaction that has not been confirmed yet. (HUV)EC, (human umbilical venous) endothelial cell; SMC, smooth muscle cell. For full target gene names, see Table 1.

Atherosclerosis, restenosis and lipid metabolism

The effects of miR-24 and 27b as described here are predominantly on lipid metabolism, which will ultimately also influence atherosclerosis[25,28,97]. MiR-24 and miR-27b are upregulated in livers of high-fat diet (HFD)-fed mice[25,97]. Inhibition of miR-24 in HFD-fed mice reduced plasma triglyceride levels and lipid accumulation in the liver, but did not affect plasma cholesterol levels. This effect was mediated via increased expression of INSIG1 in the liver and subsequent decreased expression of SREBPs and other lipogenic genes[25].

MiR-27b targets several additional lipogenic genes, including PPARγ, ANGPTL3, and GPAM. However, direct binding of miR-27b to the 3'UTR of the mRNAs of these genes was not demonstrated[97]. Upregulation of hepatic miR-27b was observed in HFD ApoE$^{-/-}$ mice, and expression of miR-27b target genes Angptl3 and Gpam was reduced[97]. Experiments performed in the THP-1 human monocyte cell line showed that miR-27a/b regulates cholesterol homeostasis[28]. MiR-27a/b targeting of ABCA1 affected apoA1-mediated cholesterol efflux in macrophages[28]. Lipid uptake was also affected by miR-27a/b, as was shown by reduced oxLDL binding to macrophages after miR-27a/b overexpression. This was mediated by miR-27a/b target gene LPL. Finally, cholesteryl-ester formation was reduced by miR-27a/b via targeting of ACAT1[28].

The contribution of miR-23b to SMC phenotypic switching upon vascular injury was recently reported by Iaconetti et al[21]. Expression of miR-23b was reduced after carotid injury in rats. Increased proliferation and migration of SMCs was observed upon miR-23b inhibition, whereas overexpression of miR-23b led to reduced proliferation and migration[21]. Overexpression of miR-23b resulted in decreased neointima formation in rat carotid arteries after balloon angioplasty and target genes uPA, SMAD3, and FOXO4 were downregulated in these animals[21].

Aneurysm

MicroRNA expression profiling revealed decreased expression of the miR-23b/miR-24-1 cluster, in human intracranial aneurysmal (IA) samples[98,99]. In murine AAA models, the miR-23b-27b-24 cluster is also downregulated. MiR-24 was most significantly downregulated, leading to upregulation of the inflammatory target gene CHI3L1[26]. In situ hybridization showed localization of miR-24 in adventitial macrophages of aneurysmal aortic mouse tissue. MiR-24 co-localized with CHI3L1 in activated macrophages, where CHI3L1 drives inflammatory gene expression[26]. Modulation of miR-24 levels in murine AAA models using either pre-miR-24 or anti-miR-24 led to reduced and increased AAA formation, respectively[26]. In summary, miR-23b-24-27b family members are downregulated in human IA samples and murine AAA models and modulation of miR-24 influences aortic inflammation, thereby

contributing to AAA development[26,98,99]. This renders the miR-23-24-27 family a potentially interesting therapeutic target for AAA treatment.

miR-143/145 cluster

The miR-143/145 gene cluster contains two highly conserved microRNAs, which are located on human chromosome 5. In 2007, these microRNAs were first described as downregulated in rat carotid arteries after induction of balloon injury[100]. Restoration of miR-143 and miR-145 expression levels using an adenoviral vector reduced neointima formation upon balloon injury in rat carotids[101,102]. MiR-145 is the most abundantly expressed microRNA in healthy rat carotid arteries, where it is predominantly localized in SMCs[103]. During SMC differentiation from multipotent stem cells, high transcript levels of miR-143 and miR-145 are observed[44]. Upregulation of these microRNAs allows for SMC differentiation, whereas their expression is downregulated upon proliferation[44]. Together, these microRNAs play an important role in the differentiation and proliferation of SMCs. Differentiation of SMCs is induced via SRF, myocardin and myocardin-related transcription factors, but can also be induced via the Jag-1/Notch signaling pathway[38,104]. These factors also regulate the transcription of the miR-143/145 cluster, further promoting differentiation of SMCs[38,104] (Figure 6, upper panel). Expression of contractile genes is mediated via (among other factors) KLF4, which is directly targeted by miR-145[44]. Inhibition of KLF4 by miR-145 increases expression of SMC markers[44]. MiR-143 can directly inhibit proliferation of SMCs via targeting of ELK1[38].

In accordance with these findings, Boettger et al.[37] described that miR-143/145-deficient mice have a thinner arterial medial layer and a decreased blood pressure. In general, the miR-143/145 cluster has proven essential for SMC function and controls the phenotypic switch of contractile SMCs towards synthetic VSMCs[37,44,101,103] (Figure 6, upper panel).

Neovascularization

MiR-145 inhibits tumour angiogenesis via targeting of IGF1, the IRS1 pathway, and its downstream genes N-RAS and VEGFA[40,41]. MiR-143 was found to inactivate AKT, which is a downstream signalling molecule in the IGF1 receptor pathway and thereby regulates angiogenesis and tumourigenesis[39]. Inactivation of AKT by miR-143 resulted in decreased protein levels of HIF-1α and reduced VEGFA expression[39]. In neuroblastoma samples, miR-145 expression was also downregulated, which was inversely correlated with HIF-2α expression[42]. The authors showed that miR-145 can directly target HIF-2α and suppress angiogenesis, which was demonstrated by tube formation of neuroblastoma cells[42].

Although these findings relate mainly to pathological angiogenesis, many fundamental mechanisms are shared with physiological angiogenesis, such as receptor signalling cascades

(e.g. HIF-1α), proliferation, and migration of vascular cells and tube formation[105]. Indeed, Wang et al.[43] found that miR-145 was transiently downregulated *in vivo* following coronary artery occlusion in mice and *in vitro* upon hypoxia treatment of cardiac fibroblasts. Inhibition of miR-145 increased infarct scar size at 7 and 28 days after myocardial infarction in mice. However, reduced differentiation of cardiac fibroblasts towards myofibroblasts, and not decreased angiogenesis, most likely mediated these effects[43]. The authors demonstrated that transfection with miR-145 increased the number of α-SMA positive cells in fibroblast cultures, thus inducing transdifferentiation of fibroblasts into myofibroblasts. KLF5 is a direct target of miR-145. Transfection with miR-145 decreased expression of KLF5 and increased myocardin expression. These data suggest that miR-145 mediates differentiation of cardiac fibroblasts to myofibroblasts through the KLF5-myocardin pathway[43].

Work by Climent et al.[36] suggests that miR-143 and miR-145 are transferred from SMCs to ECs via membrane protrusions. TGF-β induces the transfer of miR-143/145, as inhibition of either the TGF-β pathway or TGF-βR2 reduced miR-143/145 transfer towards ECs[36]. Overexpression of miR-143 and miR-145 in ECs reduced proliferation and the ability to form capillary-like structures on Matrigel[36]. The authors identified HKII and ITGβ8 as direct targets of miR-143/145 that modulate the angiogenic potential of ECs[36] (Figure 6).

Atherosclerosis and restenosis

MiR-143/145$^{-/-}$ mice develop spontaneous neointimal lesions in the femoral arteries at older age[37]. Angiotensin-converting enzyme (ACE) was identified as a target for miR-143/145. Increased expression of ACE in miR-143/145$^{-/-}$ mice resulted in increased AngII levels, which subsequently contributed to the synthetic phenotype of miR-143/145$^{-/-}$ SMCs[37]. ApoE$^{-/-}$ mice treated with SMC-specific lentiviral miR-145 showed a reduction in plaque size and an increase in atherosclerotic plaque stability[106]. This is in line with the finding that overexpression of miR-145 decreased neointima formation in balloon injured arteries by modulation of KLF5 expression[102]. However, reduced neointima formation after carotid artery ligation in miR-143/145$^{-/-}$ mice has also been reported[107]. The authors explained this by the fact that the SMCs in their knockout model were already deficient in miR-145 at the onset of injury, whereas in the overexpression model, miR-145 expression was normal at the onset of the experiment[107].

In humans, miR-145 levels were significantly lower in plaques than in atherosclerosis-free regions[106]. Cholesterol loading of mouse aortic SMCs resulted in downregulation of SMC markers, whereas expression of macrophage markers was increased[108]. Expression of miR-143 and miR-145, as well as the expression of SRF and myocardin, was downregulated[108]. Cholesterol loading, via downregulation of the miR-143/145/SRF/Myocardin axis, causes

reprogramming of SMCs towards a macrophage-like phenotype[108]. Moreover, statin treatment, which is the most common form of anti-atherosclerotic therapy today, increases expression of miR-143/145 in ECs[109].

In addition to intercellular transfer of miR-143/145 from SMCS to ECs, transport of miR-143/145 in the opposite direction has also been described[36]. Increases in laminar shear stress lead to upregulation of KLF2, which subsequently induces transcription of the miR-143/145 cluster in ECs[109]. Upregulation of miR-145 in ECs was shown to repress JAM-A, which reduces leukocyte recruitment and infiltration and thus atherosclerosis formation[45]. KLF2 also triggered release of EC-derived MVs, which transfer miR-143/145 from ECs to SMCs. Injection of MVs that are rich in miR-143/145 in HFD-fed mice led to a reduction of plaque formation[109]. In contrast, miR-143/145$^{-/-}$ mice developed smaller atherosclerotic lesions compared with LDLR$^{-/-}$ controls[46]. Plaques of miR-143/145$^{-/-}$ mice contained less macrophages and analysis of plasma cholesterol levels revealed decreased VLDL and LDL fractions. ABCA1 was confirmed as miR-145 target in this study, but this was not reflected by increased HDL levels in miR-143/145$^{-/-}$ mice[46].

Aneurysm

MiR-145 was downregulated in IA tissues[98]. Elia et al.[101] demonstrated that both miR-143 and miR-145 were reduced in human thoracic aorta aneurysms, which correlated with SMC function[110]. In AAA however, expression levels of miR-145 and miR-143 were similar to those in normal abdominal aortic tissues[79]. Homozygous miR-143/145$^{-/-}$ mice showed structural defects in the SMC layer of the aorta[21]. Additionally, the SMCs in the media of aortas from miR-143/145$^{-/-}$ mice had a dedifferentiated phenotype, demonstrated by increased migration and proliferation and an increased protein synthesis[21].

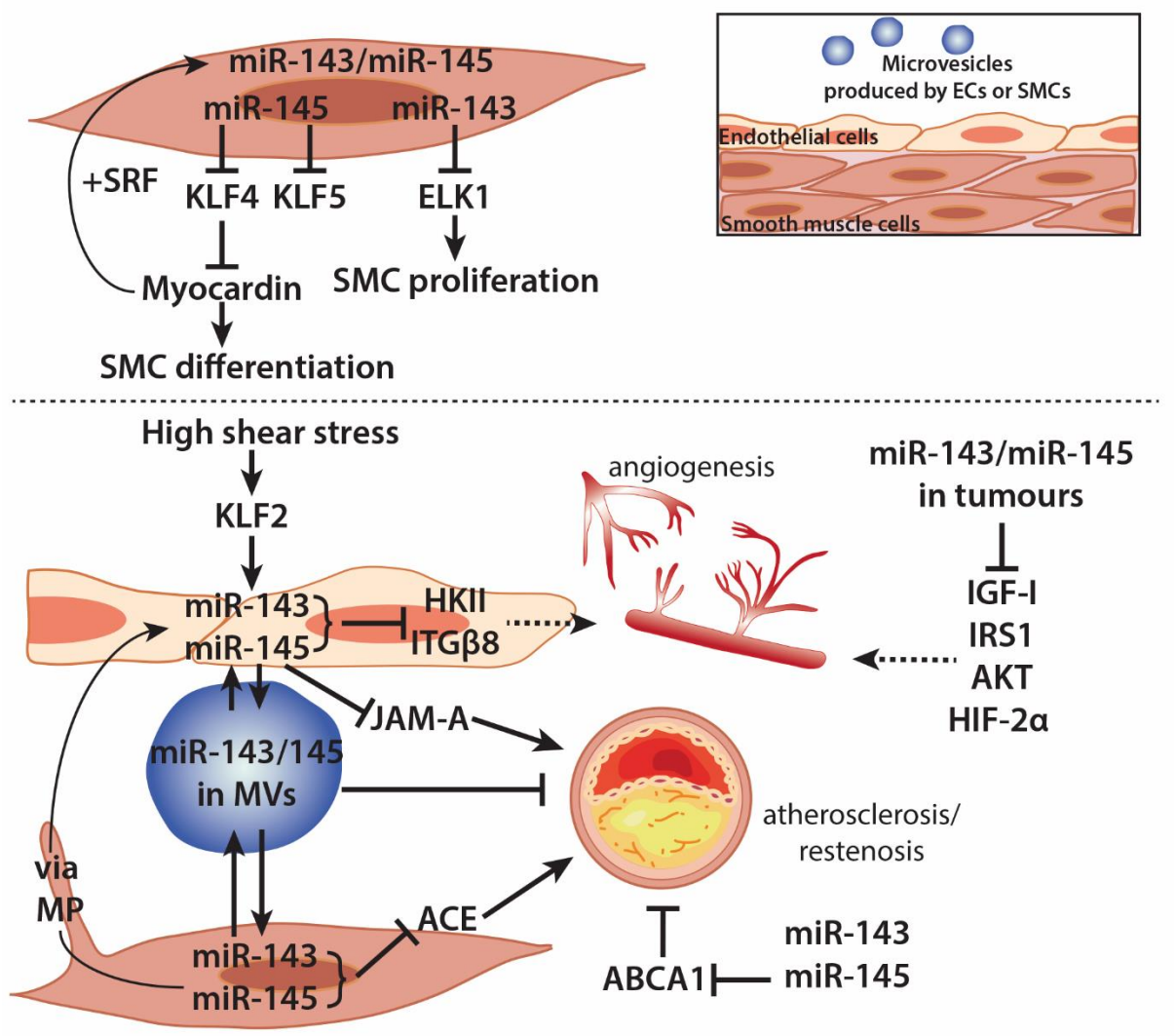

Figure 6 The miR-143/145 cluster in vascular remodelling. MiR-143 and miR-145 control SMC phenotype. Differentiation of SMCs is regulated by SRF, Myocardin and myocardin-related transcription factors (MRTFs). Via a feedback loop, these factors also regulate expression of the miR-143/miR-145 cluster itself (upper panel). Inhibition of KLF4 and KLF5 by miR-145 results, via Myocardin, in SMC differentiation and myofibroblast transdifferentiation, whereas targeting of ELK1 by miR-143 inhibits proliferation of SMCs. TGF-β and BMP4 are also able to activate expression of the miR-143/miR-145 cluster (not shown here). In addition, high shear stress, via KLF2, increases expression of miR-143/miR-145 in ECs (Figure 6, lower panel). In tumours, miR-145 suppresses IGF1 and the IRS1 pathway, affecting angiogenesis. In addition, miR-145 targets HIF2α and suppresses angiogenesis. MiR-143 targets AKT, thereby decreasing HIF1α and VEGFA expression. Transfer of miR-143/145 from VSMCs to ECs via membrane protrusions (MP) decreases the expression of HKII and ITGβ8 and via this mechanism presumably modulates angiogenesis. Intercellular transfer of miR-143/145 via MVs has also been described. MVs rich in miR-143/145 inhibit atherosclerotic plaque formation. ACE is another target of miR-143/145 which affects atherosclerosis. Arrows indicate upregulation. Capped lines indicate inhibition. The dashed lines indicate interactions that have not been confirmed yet. MP, membrane protrusion; MV, microvesicle; EC, endothelial cell; SMC, smooth muscle cell. For full target gene names, see Table 1.

14q32 microRNA gene cluster

The 14q32 microRNA cluster is the largest known mammalian microRNA gene cluster, located on human chromosome 14 and mouse chromosome 12. The cluster consists of 54 microRNAs in humans and 61 in mice[47,111] (Figure 7). It is assumed that transcription of the 14q32 microRNA gene cluster is controlled by the long noncoding RNA MEG3, also located on human chromosome 14, as deletion of MEG3 leads to downregulation of 14q32 microRNAs, as was shown in MEG3$^{-/-}$ mice[112]. MEG3$^{-/-}$ embryos have increased expression of VEGF pathway genes and increased cortical microvessel density[112] .

Neovascularization

Using a reverse target prediction analysis, where we looked for putative microRNA binding sites in the 3'UTRs of a set of nearly 200 neovascularization genes, our research group observed enrichment of binding sites for 14q32 microRNAs in the 3'UTRs of these genes. Microarray analyses performed on adductor muscle tissue of mice that underwent single ligation of the femoral artery as a model for effective neovascularization showed upregulation of 14q32 microRNAs following three different expression patterns[47]. We observed so-called early responders, microRNAs whose expression was upregulated 24 h after induction of ischaemia, late responders whose expression was upregulated from 72 h after ischaemia induction and non-responders. Inhibition of early responders miR-487b, miR-494, late responder miR-329, and non-responder miR-495 led to increased neovascularization and an improved blood flow recovery after hindlimb ischaemia in mice. Inhibition of miR-329, miR-487b, and miR-495 increased proliferation of human umbilical arterial ECs[47]. *In vivo*, inhibition of miR-329 led to upregulation of target genes TLR4, VEGFA, FGFR2, and MEF2A, whereas TLR4, VEGFA, ARF6, EFNB2, and FGFR2 were upregulated upon inhibition of miR-494. Using dual luciferase reporter gene assays, direct binding of miR-494 to the 3'UTRs of VEGFA, EFNB2, and FGFR2 was demonstrated. MiR-329 directly targets MEF2a and although VEGFA was regulated by miR-329, this was an indirect effect[47]. MiR-495 directly targets the 3'UTR of CCL2 and via this mechanism, proliferation, and apoptosis of HUVECs is affected[113]. Inhibition of miR-329, miR-487b, miR-494, and miR-495 also increased sprouting in aortic ring assays[47]. Wang et al. showed that miR-329 is a negative regulator of angiogenesis by targeting CD146, which functions as co-receptor for VEGFR2. Inhibition of miR-329 increased angiogenesis in this study, both *in vitro* and *in vivo*[48].

In a model for cerebral ischaemia, 14q32 miR-376b-5p also regulates angiogenesis. Expression of miR-376b-5p was decreased following middle cerebral artery occlusion (MCAO) in rats and miR-376b-5p inhibited angiogenesis *in vivo*, as well as in HUVEC cultures, via targeting of the HIF-1α-mediated VEGFA/Notch-1 signalling pathway[50]. In another study, 14q32 microRNA

miR-377 was identified as the most significantly downregulated microRNA in hypoxia-treated mesenchymal stem cells (MSCs) in rats[51]. Knockdown of miR-377 in HUVECs promoted angiogenesis *in vitro*, via direct targeting of VEGFA. To elucidate whether hypoxia-associated miR-377-regulated MSC induced myocardial angiogenesis in ischaemic hearts, the authors transduced rat MSCs with lentiviral vectors to overexpress or suppress miR-377 expression. MSCs with lentiviral miR-377, anti-miR-377, or empty vector were then injected into ischaemic rat hearts after ligation of the left anterior descending coronary artery. Inhibition of miR-377 in MSCs enhanced angiogenesis, decreased the area of fibrosis, and improved cardiac function of these animals[51].

Atherosclerosis

MicroRNA expression profiling in symptomatic vs. asymptomatic human atherosclerotic plaques showed upregulated expression of 14q32 microRNA miR-127[114]. Our group also investigated expression of 14q32 microRNAs in stable vs. unstable plaques of patients who underwent carotid endarterectomy surgery. We observed upregulation of 14q32 miR-494 in unstable atherosclerotic plaques. Inhibition of miR-494 led to reduced plaque formation in mice, while plaque stability was increased[49]. Moreover, total plasma cholesterol and VLDL fractions were decreased in these animals. Inhibition of miR-494 led to upregulation of target genes TGFB2, TIMP3, and IL33.

In addition, 14q32 microRNA miR-136 was upregulated in human atherosclerotic plaques. This microRNA is also highly expressed in synthetic SMCs *in vitro*[52]. MiR-136 targets PPP2R2A, resulting in increased ERK1/2 phosphorylation and increased proliferation of SMCs. The authors proposed that via this mechanism, miR-136 contributes to abnormal proliferation of SMCs, which is often observed in atherosclerosis[52].

In a study performed by Ramirez et al., the 14q32 microRNA miR-758 regulated ABCA1 in macrophages. Transfection of J774-macrophages with miR-758 reduced cholesterol efflux[53]. MiR-758 levels were furthermore regulated by dietary cholesterol *in vivo*. High dietary fat repressed miR-758 expression in the liver as well as in peritoneal macrophages, whereas ABCA1 levels were increased[53]. In another study, miR-758 levels were upregulated in hypercholesterolaemic human plaques compared with normocholesterolaemic plaques[115]. ABCA1 mRNA levels were also increased in hypercholesterolaemic patients, whereas protein levels were similar to normocholesterolaemic patients, suggesting strong posttranscriptional regulation of ABCA1 by miR-758. These human data suggest a role for miR-758 as ABCA1 modulator in human atherosclerotis[115].

A role for the 14q32 microRNA miR-370 in lipid metabolism and atherosclerosis was first described by Iloupoulos et al., mainly via direct targeting of CPT1α, an important enzyme in

fatty acid β-oxidation[54]. Other lipogenic genes such as SREBP-1c and DGAT2 were also regulated by miR-370. Using transfection experiments with sense and antisense miR-370, this regulation was mediated indirectly via miR-122[54].

Finally, extensive hypomethylation of the 14q32 locus was observed in human atherosclerotic plaques, which resulted in upregulation of several 14q32 microRNAs[116]. These findings suggest a role for epigenetic modulation of the 14q32 microRNA cluster in atherosclerosis[116].

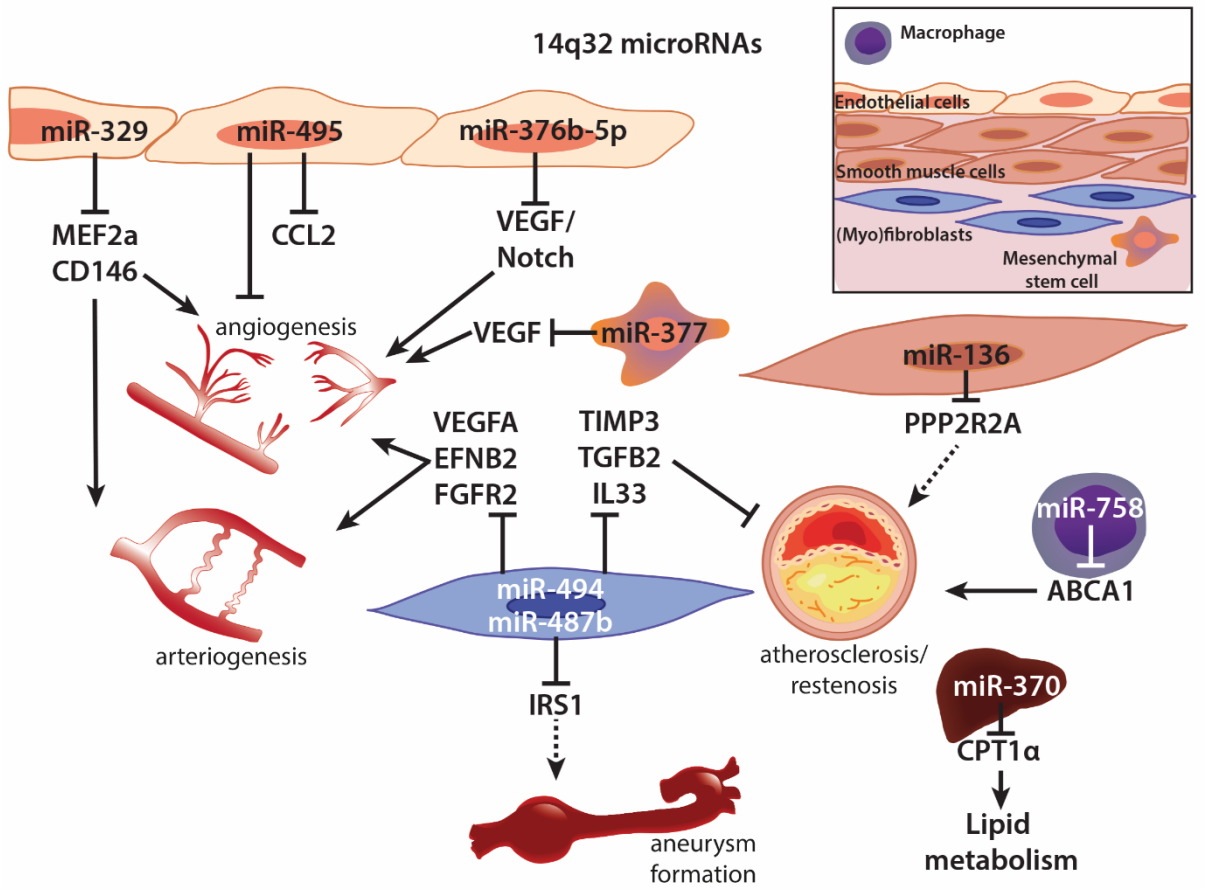

Figure 7 Roles for 14q32 miRs in vascular remodelling. MiR-329 inhibits angiogenesis and arteriogenesis via targeting of the co-receptor for VEGFR2, CD136, and MEF2a. Arteriogenesis and angiogenesis are also inhibited by miR-494, which suppresses VEGFA, EFNB2, and FGFR2. MiR-495 inhibits both arteriogenesis and angiogenesis. Proliferation and migration of HUVECs are affected by miR-495, via targeting of CCL2. VEGF signalling is further influenced through targeting of the HIF1α-mediated VEGF/Notch signalling pathway by miR-376-5p and via direct targeting of VEGF by miR-377. MiR-494 also influences atherosclerosis, through the inhibition of several target genes namely TIMP3, TGF-β2, and IL33. MiR-136 is up-regulated in human atherosclerotic plaques, where it targets PPP2R2A. Furthermore, cholesterol metabolism is affected by miR-758 through suppression of ABCA1 and by miR-370 via direct targeting of CPT1α. MiR-487b is highly expressed in the adventitia of rat aortae during chronic hypertension. Here, miR-487b targets IRS1, where it is thought to contribute to outward remodelling of the aorta. Arrows indicate up-regulation. Capped lines indicate inhibition. (HUV)EC, (human umbilical venous) endothelial cell. For full target names, see Table 1.

Aneurysm

MiR-487b is involved in hypertension-induced outward remodelling of the aorta. Chronic hypertension induced via AngII infusion led to significant upregulation of miR-487b in the aortae of rats[55]. MiR-487b was predominantly expressed in the adventitia and co-localized with the vasoactive IRS1. Using luciferase reporter gene assays, miR-487b was shown to directly target the IRS1 3'UTR, both in rats and in humans. MiR-487b downregulated expression of IRS1 in aortae of hypertensive rats, both at mRNA and at protein level[55].

Although further research into this extraordinarily large microRNA cluster is necessary, it is clear that the 14q32 microRNAs play important but diverse roles in the multiple processes of vascular remodelling, opening up new possibilities for prevention, detection, and treatment of CVD[117] (Figure 7).

Circulating microRNAs

Several of the microRNAs discussed in this review are also expressed in the circulation and could be used as biomarkers for vascular remodelling and CVD. For example, circulating miR-155 was expressed at significantly lower levels in CAD patients compared with healthy volunteers[73]. Likewise, circulating levels of miR-126, miR-17, and miR-92a were decreased in these patients[73,117]. Several miRs, including miR-126, were significantly increased in plasma of patients with insufficient collateral artery function[118]. Furthermore, circulating levels of several 14q32 microRNAs, including miR-134, miR-328, miR-370, miR-487a ,and miR-480 may have a diagnostic value for acute myocardial infarction, CAD, and cardiac death[119–123]. 14q32 miR-487b was increased in circulating leukocytes of patients with acute ischaemic stroke[124]. Other 14q32 microRNAs, including miR-665 and miR-541, have been reported to play a role in heart failure and cardiac hypertrophy, respectively[125,126]. Nevertheless, these findings need to be confirmed in large prospective cohort studies to determine the potential use of these microRNAs as biomarkers for CVD.

Future perspectives

In this review, we have described the multifactorial nature of microRNAs in vascular remodelling, as demonstrated by their role in multiple remodelling processes. Adaptive remodelling, such as arteriogenesis and angiogenesis, is stimulated by miR-126 and by the miR-23/24/27 family. Correspondingly, these microRNAs inhibit pathological remodelling, including atherosclerosis and restenosis. MiR-17/92, the 14q32 miRs, and miR-143/145 induce pathological remodelling, while they inhibit adaptive remodelling (except miR-143/145, for which different effects on pathological remodelling have been described).

MiR-155 was found to inhibit angiogenesis but stimulated arteriogenesis and was also reported to play contradicting roles in atherosclerosis formation.

The role of these microRNAs in the molecular mechanisms leading to aneurysm formation however is still poorly described; except for miR-24 and miR-487b, the microRNAs discussed here were only described to be differentially regulated in aneurysms, and a causative role has yet to be elucidated (Figure 8). As mentioned in the introduction, a single microRNA is able to target numerous genes and can regulate complex (patho)physiological processes. Often in literature, a single target gene is validated to explain the observed *in vivo* and *in vitro* effects upon microRNA modulation. However, it is far more plausible that the observed effects are caused by modulation of many genes involved in these (patho)physiological processes rather than one gene. Since microRNAs only modestly downregulate the expression of their target genes, it can be difficult to confirm significant changes in target gene expression. Nevertheless, the multifactorial nature of microRNAs in both adaptive and maladaptive vascular remodelling offers great opportunities for development of future therapeutics for treatment and prevention of CVD. In conclusion, the multifactorial effects on vascular remodelling observed for the microRNAs discussed here will hopefully stimulate the continued efforts to explore the potential of microRNAs as therapeutic target.

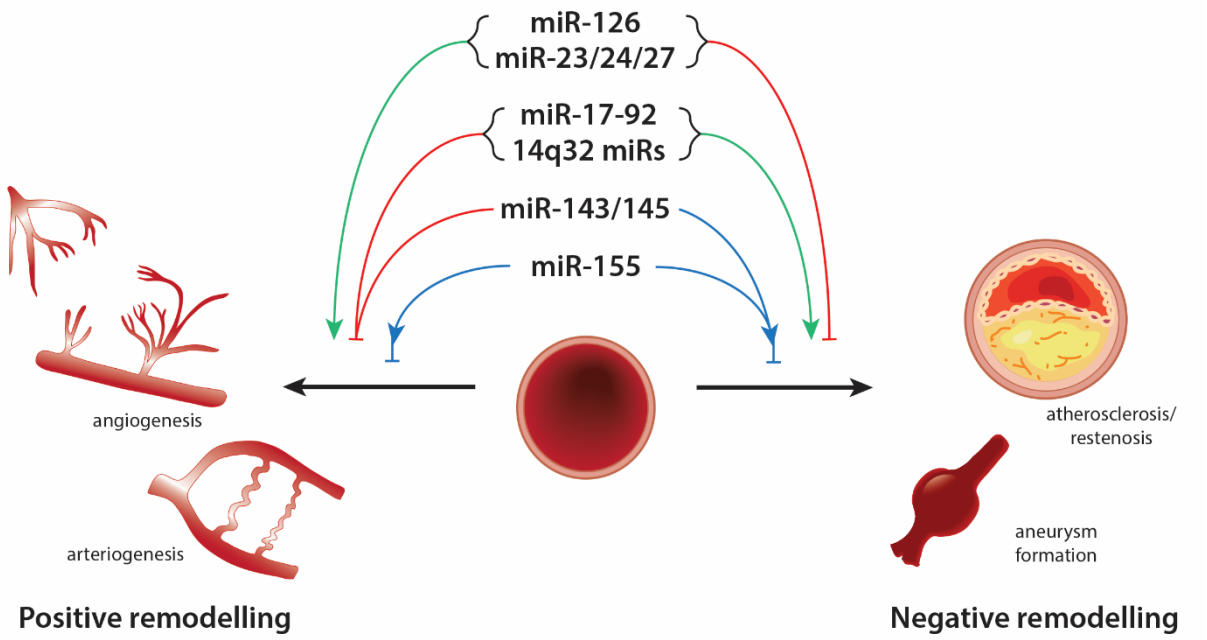

Figure 8 Graphical abstract. Several vascular microRNAs can influence multiple processes of vascular remodelling. MiR-126 is both pro-angiogenic as well as anti-atherosclerotic, like the miR-23-24-27 family. On the other hand, the 17-92 microRNA cluster and 14q32 miRs are anti-angiogenic, but pro-atherosclerotic. For miR-155 and miR-143/145, both pro- and anti-angiogenic functions have been reported, as well as pro- and anti-atherosclerotic roles. Green arrows indicate a stimulatory function, whereas red arrows represent an inhibitory function. Blue arrows are used when both stimulatory as well as inhibitory roles have been reported.

References

1. Rajewsky N. microRNA target predictions in animals. Nat Genet 2006;38 Suppl: S8–13.
2. Harris TA, Yamakuchi M, Ferlito M, Mendell JT, Lowenstein CJ. MicroRNA-126 regulates endothelial expression of vascular cell adhesion molecule 1. Proc Natl Acad Sci U S A 2008;105:1516–1521.
3. Fish JE, Santoro MM, Morton SU, Yu S, Yeh RF,Wythe JD, Ivey KN, Bruneau BG, Stainier DY, Srivastava D. miR-126 regulates angiogenic signaling and vascular integrity. Dev Cell 2008;15:272–284.
4. van Solingen C, Seghers L, Bijkerk R, Duijs JM, Roeten MK, van Oeveren-Rietdijk AM, Baelde HJ, Monge M, Vos JB, de Boer HC, Quax PH, Rabelink TJ, van Zonneveld AJ. Antagomir-mediated silencing of endothelial cell specific microRNA-126 impairs ischemia-induced angiogenesis. J Cell Mol Med 2009;13:1577–1585.
5. Wang S, Aurora AB, Johnson BA, Qi X, McAnally J, Hill JA, Richardson JA, Bassel-Duby R, Olson EN. The endothelial-specific microRNA miR-126 governs vascular integrity and angiogenesis. Dev Cell 2008;15:261–271.
6. Zernecke A, Bidzhekov K, Noels H, Shagdarsuren E, Gan L, Denecke B, Hristov M, Koppel T, Jahantigh MN, Lutgens E, Wang S, Olson EN, Schober A,Weber C. Delivery of microRNA-126 by apoptotic bodies induces CXCL12-dependent vascular protection. Sci Signal 2009;2:ra81.
7. van Solingen C., de Boer HC, Bijkerk R, Monge M, van Oeveren-Rietdijk AM, Seghers L, de Vries MR, van der Veer EP, Quax PH, Rabelink TJ, van Zonneveld AJ. MicroRNA-126 modulates endothelial SDF-1 expression and mobilization of Sca-1(+)/Lin(-) progenitor cells in ischaemia. Cardiovasc Res 2011;92:449–455.
8. Zhou J, Li YS, Nguyen P, Wang KC, Weiss A, Kuo YC, Chiu JJ, Shyy JY, Chien S. Regulation of vascular smooth muscle cell turnover by endothelial cell-secreted microRNA-126: role of shear stress. Circ Res 2013;113:40–51.
9. Schober A, Nazari-Jahantigh M, Wei Y, Bidzhekov K, Gremse F, Grommes J, Megens RT, Heyll K, Noels H, Hristov M, Wang S, Kiessling F, Olson EN, Weber C. MicroRNA-126-5p promotes endothelial proliferation and limits atherosclerosis by suppressing Dlk1. Nat Med 2014;20:368–376.
10. Lu LF, Thai TH, Calado DP, Chaudhry A, Kubo M, Tanaka K, Loeb GB, Lee H, Yoshimura A, Rajewsky K, Rudensky AY. Foxp3-dependent microRNA155 confers competitive fitness to regulatory T cells by targeting SOCS1 protein. Immunity 2009;30:80–91.
11. Ceppi M, Pereira PM, Dunand-Sauthier I, Barras E, Reith W, Santos MA, Pierre P. MicroRNA-155 modulates the interleukin-1 signaling pathway in activated human monocyte-derived dendritic cells. Proc Natl Acad Sci U S A 2009;106:2735–2740.
12. Corsten MF, Papageorgiou A, Verhesen W, Carai P, Lindow M, Obad S, Summer G, Coort SL, Hazebroek M, van LR, Gijbels MJ, Wijnands E, Biessen EA, de Winther MP, Stassen FR, Carmeliet P, Kauppinen S, Schroen B, Heymans S. MicroRNA profiling identifies microRNA-155 as an adverse mediator of cardiac injury and dysfunction during acute viral myocarditis. Circ Res 2012;111:415–425.
13. Sethupathy P, Borel C, Gagnebin M, Grant GR, Deutsch S, Elton TS, Hatzigeorgiou AG, Antonarakis SE. Human microRNA-155 on chromosome 21 differentially interacts with its polymorphic target in the AGTR1 3' untranslated region: a mechanism for functional single-nucleotide polymorphisms related to phenotypes. Am J Hum Genet 2007;81:405–413.
14. Zhu N, Zhang D, Chen S, Liu X, Lin L, Huang X, Guo Z, Liu J,Wang Y, YuanW, Qin Y. Endothelial enriched microRNAs regulate angiotensin II-induced endothelial inflammation and migration. Atherosclerosis 2011;215:286–293.
15. Pankratz F, Bemtgen X, Zeiser R, Leonhardt F, Kreuzaler S, Hilgendorf I, Smolka C, Helbing T, Hoefer I, Esser JS, Kustermann M, Moser M, Bode C, Grundmann S. Micro-RNA-155 Exerts Cell-Specific Antiangiogenic but Proarteriogenic Effects During Adaptive Neovascularization. Circulation 2015;131:1575–1589.

16. Nazari-Jahantigh M, Wei Y, Noels H, Akhtar S, Zhou Z, Koenen RR, Heyll K, Gremse F, Kiessling F, Grommes J, Weber C, Schober A. MicroRNA-155 promotes atherosclerosis by repressing Bcl6 in macrophages. J Clin Invest 2012;122:4190–4202.
17. Tian FJ, An LN, Wang GK, Zhu JQ, Li Q, Zhang YY, Zeng A, Zou J, Zhu RF, Han XS, Shen N, Yang HT, Zhao XX, Huang S, Qin YW, Jing Q. Elevated microRNA-155 promotes foam cell formation by targeting HBP1 in atherogenesis. Cardiovasc Res 2014; 103:100–110.
18. Stanczyk J, Pedrioli DM, Brentano F, Sanchez-Pernaute O, Kolling C, Gay RE, Detmar M, Gay S, Kyburz D. Altered expression of MicroRNA in synovial fibroblasts and synovial tissue in rheumatoid arthritis. Arthritis Rheum 2008;58:1001–1009.
19. Zhou Q, Gallagher R, Ufret-Vincenty R, Li X, Olson EN,Wang S. Regulation of angiogenesis and choroidal neovascularization by members of microRNA-23/27/24 clusters. Proc Natl Acad Sci U S A 2011;108:8287–8292.
20. Wang KC, Garmire LX, Young A, Nguyen P, Trinh A, Subramaniam S, Wang N, Shyy JY, Li YS, Chien S. Role of microRNA-23b in flow-regulation of Rb phosphorylation and endothelial cell growth. Proc Natl Acad Sci U S A 2010;107:3234–3239.
21. Iaconetti C, De Rosa S, Polimeni A, Sorrentino S, Gareri C, Carino A, Sabatino J, Colangelo M, Curcio A, Indolfi C. Down-regulation of miR-23b induces phenotypic switching of vascular smooth muscle cells in vitro and in vivo. Cardiovasc Res 2015; 107:522–533.
22. Fiedler J, Jazbutyte V, Kirchmaier BC, Gupta SK, Lorenzen J, Hartmann D, Galuppo P, Kneitz S, Pena JT, Sohn-Lee C, Loyer X, Soutschek J, Brand T, Tuschl T, Heineke J, Martin U, Schulte-Merker S, Ertl G, Engelhardt S, Bauersachs J, Thum T. MicroRNA-24 regulates vascularity after myocardial infarction. Circulation 2011;124: 720–730.
23. Kasza Z, Fredlund FP, Tamm C, Eriksson AS, O'Callaghan P, Heindryckx F, Spillmann D, Larsson E, Le JS, Eriksson I, Gerwins P, Kjellen L, Kreuger J. MicroRNA-24 suppression of N-deacetylase/N-sulfotransferase-1 (NDST1) reduces endothelial cell responsiveness to vascular endothelial growth factor A (VEGFA). J Biol Chem 2013;288:25956–25963.
24. Fiedler J, Stohr A, Gupta SK, Hartmann D, Holzmann A, Just A, Hansen A, Hilfiker-Kleiner D, Eschenhagen T, Thum T. Functional MicroRNA Library Screening Identifies the HypoxaMiR MiR-24 as a Potent Regulator of Smooth Muscle Cell Proliferation and Vascularization. Antioxid Redox Signal 2013;21:1167–1176.
25. Ng R, Wu H, Xiao H, Chen X, Willenbring H, Steer CJ, Song G. Inhibition of micro-RNA-24 expression in liver prevents hepatic lipid accumulation and hyperlipidemia. Hepatology 2014;60:554–564.
26. Maegdefessel L, Spin JM, Raaz U, Eken SM, Toh R, Azuma J, Adam M, Nagakami F, Heymann HM, Chernugobova E, Jin H, Roy J, Hultgren R, Caidahl K, Schrepfer S, Hamsten A, Eriksson P, McConnell MV, Dalman RL, Tsao PS. miR-24 limits aortic vascular inflammation and murine abdominal aneurysm development. Nat Commun 2014;5:5214.
27. Young JA, Ting KK, Li J, Moller T, Dunn L, Lu Y, Moses J, Prado-Lourenco L, Khachigian LM, Ng M, Gregory PA, Goodall GJ, Tsykin A, Lichtenstein I, Hahn CN, Tran N, ShackelN, Kench JG, McCaughan G, Vadas MA, Gamble JR. Regulation of vascular leak and recovery from ischemic injury by general and VE-cadherin-restricted miRNA antagonists of miR-27. Blood 2013;122:2911–2919.
28. Zhang M, Wu JF, Chen WJ, Tang SL, Mo ZC, Tang YY, Li Y, Wang JL, Liu XY, Peng J, Chen K, He PP, Lv YC, Ouyang XP, Yao F, Tang DP, Cayabyab FS, Zhang DW, Zheng XL, Tian GP, Tang CK. MicroRNA-27a/b regulates cellular cholesterol efflux, influx and esterification/hydrolysis in THP-1 macrophages. Atherosclerosis 2014;234:54–64.
29. Dews M, Homayouni A, Yu D, Murphy D, Sevignani C,Wentzel E, Furth EE, Lee WM, Enders GH, Mendell JT, Thomas-Tikhonenko A. Augmentation of tumor angiogenesis by a Myc-activated microRNA cluster. Nat Genet 2006;38:1060–1065.

30. Doebele C, Bonauer A, Fischer A, Scholz A, Reiss Y, Urbich C, Hofmann WK, Zeiher AM, Dimmeler S. Members of the microRNA-17-92 cluster exhibit a cellintrinsic antiangiogenic function in endothelial cells. Blood 2010;115:4944–4950.
31. Qin X,Wang X,Wang Y, Tang Z, Cui Q, Xi J, Li YS, Chien S,Wang N. MicroRNA-19a mediates the suppressive effect of laminar flow on cyclin D1 expression in human umbilical vein endothelial cells. Proc Natl Acad Sci U S A 2010;107:3240–3244.
32. Landskroner-Eiger S, Qiu C, Perrotta P, Siragusa M, Lee MY, Ulrich V, Luciano AK, Zhuang ZW, Corti F, Simons M, Montgomery RL, Wu D, Yu J, Sessa WC. Endothelial miR-17 approximately 92 cluster negatively regulates arteriogenesis via miRNA-19 repression of WNT signaling. Proc Natl Acad Sci 2015;112:12812–12817.
33. Loyer X, Potteaux S, Vion AC, Guerin CL, Boulkroun S, Rautou PE, Ramkhelawon B, Esposito B, Dalloz M, Paul JL, Julia P, Maccario J, Boulanger CM, Mallat Z, Tedgui A. Inhibition of microRNA-92a prevents endothelial dysfunction and atherosclerosis in mice. Circ Res 2014;114:434–443.
34. Bonauer A, Carmona G, Iwasaki M, Mione M, Koyanagi M, Fischer A, Burchfield J, Fox H, Doebele C, Ohtani K, Chavakis E, Potente M, Tjwa M, Urbich C, Zeiher AM, Dimmeler S. MicroRNA-92a controls angiogenesis and functional recovery of ischemic tissues in mice. Science 2009;324:1710–1713.
35. Iaconetti C, Polimeni A, Sorrentino S, Sabatino J, Pironti G, Esposito G, Curcio A, Indolfi C. Inhibition of miR-92a increases endothelial proliferation and migration in vitro as well as reduces neointimal proliferation in vivo after vascular injury. Basic Res Cardiol 2012;107:296.
36. Climent M, Quintavalle M, Miragoli M, Chen J, Condorelli G, Elia L. TGFbeta Triggers miR-143/145 Transfer From Smooth Muscle Cells to Endothelial Cells, Thereby Modulating Vessel Stabilization. Circ Res 2015;116:1753–1764.
37. Boettger T, Beetz N, Kostin S, Schneider J, Kruger M, Hein L, Braun T. Acquisition of the contractile phenotype by murine arterial smooth muscle cells depends on the Mir143/145 gene cluster. J Clin Invest 2009;119:2634–2647.
38. Davis-Dusenbery BN, Chan MC, Reno KE,Weisman AS, Layne MD, Lagna G, Hata A. Down-regulation of Kruppel-like factor-4 (KLF4) by microRNA-143/145 is critical for modulation of vascular smooth muscle cell phenotype by transforming growth factor-beta and bone morphogenetic protein 4. J Biol Chem 2011;286:28097–28110.
39. Qian X, Yu J, Yin Y, He J,Wang L, Li Q, Zhang LQ, Li CY, Shi ZM, Xu Q, LiW, Lai LH, Liu LZ, Jiang BH. MicroRNA-143 inhibits tumor growth and angiogenesis and sensitizes chemosensitivity to oxaliplatin in colorectal cancers. Cell Cycle 2013;12: 1385–1394.
40. Zou C, Xu Q, Mao F, Li D, Bian C, Liu LZ, Jiang Y, Chen X, Qi Y, Zhang X, Wang X, Sun Q, Kung HF, Lin MC, Dress A, Wardle F, Jiang BH, Lai L. MiR-145 inhibits tumor angiogenesis and growth by N-RAS and VEGF. Cell Cycle 2012;11:2137–2145.
41. La Rocca G., Shi B, Badin M, De Angelis T., Sepp-Lorenzino L, Baserga R. Growth inhibition by microRNAs that target the insulin receptor substrate-1. Cell Cycle 2009;8:2255–2259.
42. Zhang H, Pu J, Qi T, Qi M, Yang C, Li S, Huang K, Zheng L, Tong Q. MicroRNA-145 inhibits the growth, invasion, metastasis and angiogenesis of neuroblastoma cells through targeting hypoxia-inducible factor 2 alpha. Oncogene 2014;33:387–397.
43. Wang YS, Li SH, Guo J, Mihic A, Wu J, Sun L, Davis K, Weisel RD, Li RK. Role of miR-145 in cardiac myofibroblast differentiation. J Mol Cell Cardiol 2014;66:94–105.
44. Cordes KR, Sheehy NT, White MP, Berry EC, Morton SU, Muth AN, Lee TH, Miano JM, Ivey KN, Srivastava D. miR-145 and miR-143 regulate smooth muscle cell fate and plasticity. Nature 2009;460:705–710.
45. Schmitt MM, Megens RT, Zernecke A, Bidzhekov K, van den Akker NM, Rademakers T, van Zandvoort MA, Hackeng TM, Koenen RR, Weber C. Endothelial junctional adhesion molecule-a guides monocytes into flow-dependent predilection sites of atherosclerosis. Circulation 2014;129:66–76.

46. Sala F, Aranda JF, Rotllan N, Ramirez CM, Aryal B, Elia L, Condorelli G, Catapano AL, Fernandez-Hernando C, Norata GD. MiR-143/145 deficiency attenuates the progression of atherosclerosis in Ldlr-/-mice. Thromb Haemost 2014;112:796–802.
47. Welten SM, Bastiaansen AJ, de Jong RC, de Vries MR, Peters EA, Boonstra MC, Sheikh SP, Monica NL, Kandimalla ER, Quax PH, Nossent AY. Inhibition of 14q32 MicroRNAs miR-329, miR-487b, miR-494, and miR-495 increases neovascularization and blood flow recovery after ischemia. Circ Res 2014;115:696–708.
48. Wang P, Luo Y, Duan H, Xing S, Zhang J, Lu D, Feng J, Yang D, Song L, Yan X. MicroRNA 329 suppresses angiogenesis by targeting CD146. Mol Cell Biol 2013;33:3689–3699.
49. Wezel A, Welten SM, Razaway W, Lagraauw, de Vries MR, Goossens E.A.C., Boonstra MC, Kandimalla ER, Kuiper J, Quax PH, Bot I, Nossent AY. Inhibition of microRNA-494 reduces atherosclerotic lesion development and increases plaque stability. Ann Surg 2015;262:841–847.
50. Li LJ, Huang Q, Zhang N, Wang GB, Liu YH. miR-376b-5p regulates angiogenesis in cerebral ischemia. Mol Med Rep 2014;10:527–535.
51. Wen Z, Huang W, Feng Y, Cai W, Wang Y, Wang X, Liang J, Wani M, Chen J, Zhu P, Chen JM, Millard RW, Fan GC, Wang Y. MicroRNA-377 regulates mesenchymal stem cell-induced angiogenesis in ischemic hearts by targeting VEGF. PLoS One 2014;9:e104666.
52. Zhang CF, Kang K, Li XM, Xie BD. MicroRNA-136 Promotes Vascular Muscle Cell Proliferation Through the ERK1/2 Pathway by Targeting PPP2R2A in Atherosclerosis. Curr Vasc Pharmacol 2014;13:405–412.
53. Ramirez CM, Davalos A, Goedeke L, Salerno AG, Warrier N, Cirera-Salinas D, Suarez Y, Fernandez-Hernando C. MicroRNA-758 regulates cholesterol efflux through posttranscriptional repression of ATP-binding cassette transporter A1. Arterioscler Thromb Vasc Biol 2011;31:2707–2714.
54. Iliopoulos D, Drosatos K, Hiyama Y, Goldberg IJ, Zannis VI. MicroRNA-370 controls the expression of microRNA-122 and Cpt1alpha and affects lipid metabolism. J Lipid Res 2010;51:1513–1523.
55. Nossent AY, Eskildsen TV, Andersen LB, Bie P, Bronnum H, Schneider M, Andersen DC, Welten SM, Jeppesen PL, Hamming JF, Hansen JL, Quax PH, Sheikh SP. The 14q32 MicroRNA-487b Targets the Antiapoptotic Insulin Receptor Substrate 1 in Hypertension-Induced Remodeling of the Aorta. Ann Surg 2013;258:743–753.
56. Gibbons GH, Dzau VJ. The emerging concept of vascular remodeling. N Engl J Med 1994;330:1431–1438.
57. Wei Y, Schober A, Weber C. Pathogenic arterial remodeling: the good and bad of microRNAs. Am J Physiol Heart Circ Physiol 2013;304:H1050–H1059.
58. Torella D, Iaconetti C, Catalucci D, Ellison GM, Leone A, Waring CD, Bochicchio A, Vicinanza C, Aquila I, Curcio A, Condorelli G, Indolfi C. MicroRNA-133 controls vascular smooth muscle cell phenotypic switch in vitro and vascular remodeling in vivo. Circ Res 2011;109:880–893.
59. Villeneuve LM, Kato M, Reddy MA,Wang M, Lanting L, Natarajan R. Enhanced levels of microRNA-125b in vascular smooth muscle cells of diabetic db/db mice lead to increased inflammatory gene expression by targeting the histone methyltransferase Suv39h1. Diabetes 2010;59:2904–2915.
60. Leeper NJ, Raiesdana A, Kojima Y, Chun HJ, Azuma J, Maegdefessel L, Kundu RK, Quertermous T, Tsao PS, Spin JM. MicroRNA-26a is a novel regulator of vascular smooth muscle cell function. J Cell Physiol 2011;226:1035–1043.
61. Liu K, Ying Z, Qi X, Shi Y, Tang Q. MicroRNA-1 regulates the proliferation of vascular smooth muscle cells by targeting insulin-like growth factor 1. Int J Mol Med 2015;36: 817–824.
62. Li P, Zhu N, Yi B, Wang N, Chen M, You X, Zhao X, Solomides CC, Qin Y, Sun J. MicroRNA-663 regulates human vascular smooth muscle cell phenotypic switch and vascular neointimal formation. Circ Res 2013;113:1117–1127.

63. Maegdefessel L, Azuma J, Toh R, Merk DR, Deng A, Chin JT, Raaz U, Schoelmerich AM, Raiesdana A, Leeper NJ, McConnell MV, Dalman RL, Spin JM, Tsao PS. Inhibition of microRNA-29b reduces murine abdominal aortic aneurysm development. J Clin Invest 2012;122:497–506.
64. Maegdefessel L, Azuma J, Toh R, Deng A, Merk DR, Raiesdana A, Leeper NJ, Raaz U, Schoelmerich AM, McConnell MV, Dalman RL, Spin JM, Tsao PS. MicroRNA-21 blocks abdominal aortic aneurysm development and nicotine-augmented expansion. Sci Transl Med 2012;4:122ra22.
65. Najafi-Shoushtari SH, Kristo F, Li Y, Shioda T, Cohen DE, Gerszten RE, Naar AM. MicroRNA-33 and the SREBP host genes cooperate to control cholesterol homeostasis. Science 2010;328:1566–1569.
66. Rayner KJ, Sheedy FJ, Esau CC, Hussain FN, Temel RE, Parathath S, van Gils JM, Rayner AJ, Chang AN, Suarez Y, Fernandez-Hernando C, Fisher EA, Moore KJ. Antagonism of miR-33 in mice promotes reverse cholesterol transport and regression of atherosclerosis. J Clin Invest 2011;121:2921–2931.
67. Rayner KJ, Suarez Y, Davalos A, Parathath S, Fitzgerald ML, Tamehiro N, Fisher EA, Moore KJ, Fernandez-Hernando C. MiR-33 contributes to the regulation of cholesterol homeostasis. Science 2010;328:1570–1573.
68. Rayner KJ, Esau CC, Hussain FN, McDaniel AL, Marshall SM, van Gils JM, Ray TD, Sheedy FJ, Goedeke L, Liu X, Khatsenko OG, Kaimal V, Lees CJ, Fernandez-Hernando C, Fisher EA, Temel RE, Moore KJ. Inhibition of miR-33a/b in non-human primates raises plasma HDL and lowers VLDL triglycerides. Nature 2011;478:404–407.
69. Epstein SE, Stabile E, Kinnaird T, Lee CW, Clavijo L, Burnett MS. Janus phenomenon: the interrelated tradeoffs inherent in therapies designed to enhance collateral formation and those designed to inhibit atherogenesis. Circulation 2004;109:2826–2831.
70. Kuehbacher A, Urbich C, Zeiher AM, Dimmeler S. Role of Dicer and Drosha for endothelial microRNA expression and angiogenesis. Circ Res 2007;101:59–68.
71. Gatsiou A, Boeckel JN, Randriamboavonjy V, Stellos K. MicroRNAs in platelet biogenesis and function: implications in vascular homeostasis and inflammation. Curr Vasc Pharmacol 2012;10:524–531.
72. de Boer HC, van Solingen C, Prins J, Duijs JM, Huisman MV, Rabelink TJ, van Zonneveld AJ. Aspirin treatment hampers the use of plasma microRNA-126 as a biomarker for the progression of vascular disease. Eur Heart J 2013;34:3451–3457.
73. Laffont B, Corduan A, Rousseau M, Duchez AC, Lee CH, Boilard E, Provost P. Platelet microparticles reprogram macrophage gene expression and function. Thromb Haemost 2016;115:311–323.
74. Fichtlscherer S, De Rosa S, Fox H, Schwietz T, Fischer A, Liebetrau C, Weber M, Hamm CW, Roxe T, Muller-Ardogan M, Bonauer A, Zeiher AM, Dimmeler S. Circulating microRNAs in patients with coronary artery disease. Circ Res 2010;107:677–684.
75. Katare R, Rawal S, Munasinghe PE, Tsuchimochi H, Inagaki T, Fujii Y, Dixit P, Umetani K, Kangawa K, Shirai M, Schwenke DO. Ghrelin Promotes Functional Angiogenesis in a Mouse Model of Critical Limb Ischemia Through Activation of Proangiogenic MicroRNAs. Endocrinology 2016;157:432–445.
76. Sahoo S, Klychko E, Thorne T, Misener S, Schultz KM, Millay M, Ito A, Liu T, Kamide C, Agrawal H, Perlman H, Qin G, Kishore R, Losordo DW. Exosomes from human CD34(+) stem cells mediate their proangiogenic paracrine activity. Circ Res 2011;109:724–728.
77. Mocharla P, Briand S, Giannotti G, Dorries C, Jakob P, Paneni F, Luscher T, Landmesser U. AngiomiR-126 expression and secretion from circulating CD34(+) and CD14(+) PBMCs: role for proangiogenic effects and alterations in type 2 diabetics. Blood 2013;121:226–236.
78. Stoneman VE, Bennett MR. Role of apoptosis in atherosclerosis and its therapeutic implications. Clin Sci (Lond) 2004;107:343–354.

79. Kin K, Miyagawa S, Fukushima S, Shirakawa Y, Torikai K, Shimamura K, Daimon T, Kawahara Y, Kuratani T, Sawa Y. Tissue- and plasma-specific MicroRNA signatures for atherosclerotic abdominal aortic aneurysm. J Am Heart Assoc 2012;1:e000745.
80. Turner M, Vigorito E. Regulation of B- and T-cell differentiation by a single microRNA. Biochem Soc Trans 2008;36:531–533.
81. O'Connell RM, Taganov KD, Boldin MP, Cheng G, Baltimore D. MicroRNA-155 is induced during the macrophage inflammatory response. Proc Natl Acad Sci U S A 2007;104:1604–1609.
82. Welten SM, Quax PH, Nossent AY. Letter Regarding Article, "MicroRNA-155 Exerts Cell-Specific Antiangiogenic but Proarteriogenic Effects During Adaptive Neovascularization". Circulation 2015;132:e375.
83. Raitoharju E, Lyytikainen LP, Levula M, Oksala N, Mennander A, Tarkka M, Klopp N, Illig T, Kahonen M, Karhunen PJ, Laaksonen R, Lehtimaki T. miR-21, miR-210, miR-34a, and miR-146a/b are up-regulated in human atherosclerotic plaques in the Tampere Vascular Study. Atherosclerosis 2011;219:211–217.
84. Huang RS, Hu GQ, Lin B, Lin ZY, Sun CC. MicroRNA-155 silencing enhances inflammatory response and lipid uptake in oxidized low-density lipoprotein-stimulated human THP-1 macrophages. J Investig Med 2010;58:961–967.
85. Zhu GF, Yang LX, Guo RW, Liu H, Shi YK,Wang H, Ye JS, Yang ZH, Liang X. miR-155 inhibits oxidized low-density lipoprotein-induced apoptosis of RAW264.7 cells. Mol Cell Biochem 2013;382:253–261.
86. Yang K, He YS, Wang XQ, Lu L, Chen QJ, Liu J, Sun Z, Shen WF. MiR-146a inhibits oxidized low-density lipoprotein-induced lipid accumulation and inflammatory response via targeting toll-like receptor 4. FEBS Lett 2011;585:854–860.
87. Donners MM, Wolfs IM, Stoger LJ, van der Vorst EP, Pottgens CC, Heymans S, Schroen B, Gijbels MJ, de Winther MP. Hematopoietic miR155 deficiency enhances atherosclerosis and decreases plaque stability in hyperlipidemic mice. PLoS One 2012;7:e35877.
88. Concepcion CP, Bonetti C, Ventura A. The microRNA-17-92 family of microRNA clusters in development and disease. Cancer J 2012;18:262–267.
89. Chamorro-Jorganes A, Lee MY, Araldi E, Landskroner-Eiger S, Fernandez-Fuertes M, Sahraei M, Quiles Del RM, van Solingen C, Yu J, Fernandez-Hernando C, Sessa WC, Suarez Y. VEGF-Induced Expression of miR-1792 Cluster in Endothelial Cells is Mediated by ERK/ELK1 Activation and Regulates Angiogenesis. Circ Res 2016;118:38–47.
90. Kaluza D, Kroll J, Gesierich S, Manavski Y, Boeckel JN, Doebele C, Zelent A, Rossig L, Zeiher AM, Augustin HG, Urbich C, Dimmeler S. Histone deacetylase 9 promotes angiogenesis by targeting the antiangiogenic microRNA-17-92 cluster in endothelial cells. Arterioscler Thromb Vasc Biol 2013;33:533–543.
91. Wu W, Xiao H, Laguna-Fernandez A, Villarreal G Jr.,Wang KC, Geary GG, Zhang Y, Wang WC, Huang HD, Zhou J, Li YS, Chien S, Garcia-Cardena G, Shyy JY. Flow-Dependent Regulation of Kruppel-Like Factor 2 Is Mediated by MicroRNA-92a. Circulation 2011;124:633–641.
92. Bang C, Fiedler J, Thum T. Cardiovascular importance of the microRNA-23/27/24 family. Microcirculation 2012;19:208–214.
93. Neth P, Nazari-Jahantigh M, Schober A,Weber C. MicroRNAs in flow-dependent vascular remodelling. Cardiovasc Res 2013;99:294–303.
94. Weber M, Baker MB, Moore JP, Searles CD. MiR-21 is induced in endothelial cells byshear stress and modulates apoptosis and eNOS activity. Biochem Biophys Res Commun 2010;393:643–648.
95. Ni CW, Qiu H, Jo H. MicroRNA-663 upregulated by oscillatory shear stress plays a role in inflammatory response of endothelial cells. Am J Physiol Heart Circ Physiol 2011;300:H1762-H1769.
96. Urbich C, Kaluza D, Fromel T, Knau A, Bennewitz K, Boon RA, Bonauer A, Doebele C, Boeckel JN, Hergenreider E, Zeiher AM, Kroll J, Fleming I, Dimmeler S. MicroRNA-27a/b controls

endothelial cell repulsion and angiogenesis by targeting semaphoring 6A. Blood 2012;119:1607–1616.
97. Vickers KC, Shoucri BM, Levin MG, Wu H, Pearson DS, Osei-Hwedieh D, Collins FS, Remaley AT, Sethupathy P. MicroRNA-27b is a regulatory hub in lipid metabolism and is altered in dyslipidemia. Hepatology 2013;57:533–542.
98. Jiang Y, Zhang M, He H, Chen J, Zeng H, Li J, Duan R. MicroRNA/mRNA profiling and regulatory network of intracranial aneurysm. BMC Med Genomics 2013;6:36.
99. Liu D, Han L, Wu X, Yang X, Zhang Q, Jiang F. Genome-wide microRNA changes in human intracranial aneurysms. BMC Neurol 2014;14:188.
100. Ji R, Cheng Y, Yue J, Yang J, Liu X, Chen H, Dean DB, Zhang C. MicroRNA expression signature and antisense-mediated depletion reveal an essential role of MicroRNA in vascular neointimal lesion formation. Circ Res 2007;100:1579–1588.
101. Elia L, Quintavalle M, Zhang J, Contu R, Cossu L, Latronico MV, Peterson KL, Indolfi C, Catalucci D, Chen J, Courtneidge SA, Condorelli G. The knockout of miR-143 and -145 alters smooth muscle cell maintenance and vascular homeostasis in mice: correlates with human disease. Cell Death Differ 2009;16:1590–1598.
102. Cheng Y, Liu X, Yang J, Lin Y, Xu DZ, Lu Q, Deitch EA, Huo Y, Delphin ES, Zhang C. MicroRNA-145, a novel smooth muscle cell phenotypic marker and modulator, controls vascular neointimal lesion formation. Circ Res 2009;105:158–166.
103. Zhang C. MicroRNA-145 in vascular smooth muscle cell biology: a new therapeutic target for vascular disease. Cell Cycle 2009;8:3469–3473.
104. Boucher JM, Peterson SM, Urs S, Zhang C, Liaw L. The miR-143/145 cluster is a novel transcriptional target of Jagged-1/Notch signaling in vascular smooth muscle cells. J Biol Chem 2011;286:28312–28321.
105. Anand S, Cheresh DA. Emerging Role of Micro-RNAs in the Regulation of Angiogenesis. Genes Cancer 2011;2:1134–1138.
106. Lovren F, Pan Y, Quan A, Singh KK, Shukla PC, Gupta N, Steer BM, Ingram AJ, Gupta M, Al-Omran M, Teoh H, Marsden PA, Verma S. MicroRNA-145 targeted therapy reduces atherosclerosis. Circulation 2012;126:S81–S90.
107. Xin M, Small EM, Sutherland LB, Qi X, McAnally J, Plato CF, Richardson JA, Bassel-Duby R, Olson EN. MicroRNAs miR-143 and miR-145 modulate cytoskeletal dynamics and responsiveness of smooth muscle cells to injury. Genes Dev 2009;23:2166–2178.
108. Vengrenyuk Y, Nishi H, Long X, Ouimet M, Savji N, Martinez FO, Cassella CP, Moore KJ, Ramsey SA, Miano JM, Fisher EA. Cholesterol loading reprograms the microRNA-143/145-myocardin axis to convert aortic smooth muscle cells to a dysfunctional macrophage-like phenotype. Arterioscler Thromb Vasc Biol 2015;35:535–546.
109. Hergenreider E, Heydt S, Treguer K, Boettger T, Horrevoets AJ, Zeiher AM, Scheffer MP, Frangakis AS, Yin X, Mayr M, Braun T, Urbich C, Boon RA, Dimmeler S. Atheroprotective communication between endothelial cells and smooth muscle cells through miRNAs. Nat Cell Biol 2012;14:249–256.
110. Boon RA, Dimmeler S. MicroRNAs and aneurysm formation. Trends Cardiovasc Med 2011;21:172–177.
111. Benetatos L, Hatzimichael E, Londin E, Vartholomatos G, Loher P, Rigoutsos I, Briasoulis E. The microRNAs within the DLK1-DIO3 genomic region: involvement in disease pathogenesis. Cell Mol Life Sci 2013;70:795–814.
112. Gordon FE, Nutt CL, Cheunsuchon P, Nakayama Y, Provencher KA, Rice KA, Zhou Y, Zhang X, Klibanski A. Increased expression of angiogenic genes in the brains of mouse meg3-null embryos. Endocrinology 2010;151:2443–2452.
113. Liu D, Zhang XL, Yan CH, Li Y, Tian XX, Zhu N, Rong JJ, Peng CF, Han YL. MicroRNA-495 regulates the proliferation and apoptosis of human umbilical vein endothelial cells by targeting chemokine CCL2. Thromb Res 2015;135:146–154.

114. Cipollone F, Felicioni L, Sarzani R, Ucchino S, Spigonardo F, Mandolini C, Malatesta S, Bucci M, Mammarella C, Santovito D, de LF, Marchetti A, Mezzetti A, Buttitta F. A unique microRNA signature associated with plaque instability in humans. Stroke 2011;42:2556–2563.
115. Mandolini C, Santovito D, Marcantonio P, Buttitta F, Bucci M, Ucchino S, Mezzetti A, Cipollone F. Identification of microRNAs 758 and 33b as potential modulators of ABCA1 expression in human atherosclerotic plaques. Nutr Metab Cardiovasc Dis 2015;25:202–209.
116. Aavik E, Lumivuori H, Leppanen O, Wirth T, Hakkinen SK, Brasen JH, Beschorner U, Zeller T, Braspenning M, van CW, Makinen K, Yla-Herttuala S. Global DNA methylation analysis of human atherosclerotic plaques reveals extensive genomic hypomethylation and reactivation at imprinted locus 14q32 involving induction of a miRNA cluster. Eur Heart J 2015;36:993–1000.
117. Dimmeler S, Yla-Herttuala S. 14q32 miRNA cluster takes center stage in neovascularization. Circ Res 2014;115:680–682.
118. Hakimzadeh N, Nossent AY, van der Laan AM, Schirmer SH, de Ronde MW, Pinto-Sietsma SJ, van RN, Quax PH, Hoefer IE, Piek JJ. Circulating MicroRNAs Characterizing Patients with Insufficient Coronary Collateral Artery Function. PLoS One 2015;10:e0137035.
119. He F, Lv P, Zhao X, Wang X, Ma X, Meng W, Meng X, Dong S. Predictive value of circulating miR-328 and miR-134 for acute myocardial infarction. Mol Cell Biochem 2014;394:137–144.
120. Hoekstra M, van der Lans CA, Halvorsen B, Gullestad L, Kuiper J, Aukrust P, van Berkel TJ, Biessen EA. The peripheral blood mononuclear cell microRNA signature of coronary artery disease. Biochem Biophys Res Commun 2010;394:792–797.
121. Li C, Fang Z, Jiang T, Zhang Q, Liu C, Zhang C, Xiang Y. Serum microRNAs profile from genome-wide serves as a fingerprint for diagnosis of acute myocardial infarction and angina pectoris. BMC Med Genomics 2013;6:16.
122. Matsumoto S, Sakata Y, Nakatani D, Suna S, Mizuno H, Shimizu M, Usami M, Sasaki T, Sato H, Kawahara Y, Hamasaki T, Nanto S, Hori M, Komuro I. A subset of circulating microRNAs are predictive for cardiac death after discharge for acute myocardial infarction. Biochem Biophys Res Commun 2012;427:280–284.
123. Wang J, Pei Y, Zhong Y, Jiang S, Shao J, Gong J. Altered serum microRNAs as novel diagnostic biomarkers for atypical coronary artery disease. PLoS One 2014;9:e107012.
124. Jickling GC, Ander BP, Zhan X, Noblett D, Stamova B, Liu D. microRNA expression in peripheral blood cells following acute ischemic stroke and their predicted gene targets. PLoS One 2014;9:e99283.
125. Mohnle P, Schutz SV, Schmidt M, Hinske C, Hubner M, Heyn J, Beiras-Fernandez A, Kreth S. MicroRNA-665 is involved in the regulation of the expression of the cardioprotective cannabinoid receptor CB2 in patients with severe heart failure. Biochem Biophys Res Commun 2014;451:516–521.
126. Liu F, Li N, Long B, Fan YY, Liu CY, Zhou QY, Murtaza I, Wang K, Li PF. Cardiac hypertrophy is negatively regulated by miR-541. Cell Death Dis 2014;5:e1171.

Chapter 3

Genetic associations and regulation of expression indicate an independent role for 14q32 snoRNAs in human cardiovascular disease

Cardiovascular Research 2019 Aug 1;115(10):1519-1532

EAC Goossens[1,2] *
KEJ Hakansson[1,2] *
S Trompet[3,4] *
E van Ingen[1,2]
MR de Vries[1,2]
RVCT van der Kwast[1,2]
RS Ripa[5]
J Kastrup[5]
PJ Hohensinner[6]
C Kaun[6]
J Wojta[6]
S Böhringer[7]
S Le Cessie[7,8]
JW Jukema[3]
PHA Quax[1,2]
AY Nossent[1,2,9]

* Authors contributed equally to this work

[1]Department of Surgery and [2]Einthoven Laboratory for Experimental Vascular Medicine, Leiden University Medical Center, Leiden, The Netherlands; [3]Department of Cardiology, Leiden University Medical Center, Leiden, the Netherlands; [4]Department of Gerontology and Geriatrics, Leiden University Medical Center, Leiden, the Netherlands; [5]Department of Cardiology, Rigshospitalet University of Copenhagen, Copenhagen, Denmark; [6]Department of Internal Medicine II, Medical University of Vienna, Vienna, Austria; [7]Department of Biomedical Data Sciences, Leiden University Medical Center, Leiden, the Netherlands; [8]Department of Clinical Epidemiology, Leiden University Medical Center, Leiden, the Netherlands; and [9]Ludwig Boltzmann Cluster for Cardiovascular Research, Vienna, Austria

Abstract

Aims: We have shown that 14q32 microRNAs are highly involved in vascular remodelling and cardiovascular disease. However, the 14q32 locus also encodes 41 'orphan' small nucleolar RNAs (snoRNAs). We aimed to gather evidence for an independent role for 14q32 snoRNAs in human cardiovascular disease.

Methods and results: We performed a lookup of the 14q32 region within the dataset of a genome wide association scan in 5244 participants of the PROspective Study of Pravastatin in the Elderly at Risk (PROSPER). Single nucleotide polymorphisms (SNPs) in the snoRNA-cluster were significantly associated with heart failure. These snoRNA-cluster SNPs were not linked to SNPs in the microRNA-cluster or in MEG3, indicating that snoRNAs modify the risk of cardiovascular disease independently. We looked at expression of 14q32 snoRNAs throughout the human cardio-vasculature. Expression profiles of the 14q32 snoRNAs appeared highly vessel specific. When we compared expression levels of 14q32 snoRNAs in human vena saphena magna (VSM) with those in failed VSM-coronary bypasses, we found that 14q32 snoRNAs were up-regulated. SNORD113.2, which showed a 17-fold up-regulation in failed bypasses, was also up-regulated two-fold in plasma samples drawn from patients with ST-elevation myocardial infarction directly after hospitalization compared with 30 days after start of treatment. However, fitting with the genomic associations, 14q32 snoRNA expression was highest in failing human hearts. *In vitro* studies show that the 14q32 snoRNAs bind predominantly to methyl-transferase Fibrillarin, indicating that they act through canonical mechanisms, but on non-canonical RNA targets. The canonical C/D-box snoRNA seed sequences were highly conserved between humans and mice.

Conclusions: 14q32 snoRNAs appear to play an independent role in cardiovascular pathology. 14q32 snoRNAs are specifically regulated throughout the human vasculature and their expression is up-regulated during cardiovascular disease. Our data demonstrate that snoRNAs merit increased effort and attention in future basic and clinical cardiovascular research.

Introduction

Noncoding RNAs (ncRNAs) are a booming topic of research. Formerly seen as 'junk RNA', ncRNAs have been shown to be important regulators of gene expression. Of all ncRNAs, microRNAs have been studied most extensively over the past decade. MicroRNAs bind the 3'UTR of their target messenger RNA (mRNA) to inhibit translation[1]. The fact that microRNAs can fine-tune expression levels of large sets of target genes, up to several hundred genes per microRNA, makes them attractive therapeutic targets for multifactorial pathophysiological processes, including cardiovascular disease. We have recently discovered that a large gene cluster of 54 microRNAs transcribed from the long arm of human chromosome 14 (14q32) is highly involved in cardiovascular pathology[2,3]. Inhibition of individual 14q32 microRNAs led to increases in post-ischaemic blood flow recovery and tissue perfusion in mice via increased neovascularization[4]. At the same time, inhibition of these microRNAs also decreased plasma cholesterol and atherosclerotic lesion formation, whereas increasing plaque stability in atherosclerosis-prone mice[5].

Besides 54 microRNAs, the human 14q32 locus also encodes genes for two other types of ncRNAs, namely three long noncoding RNAs (lncRNAs) and 41 small nucleolar RNAs (snoRNAs). Interestingly, one of these lncRNAs, MEG3, was found to be up-regulated in activated endothelial cells under hypoxia[6] and play a role in angiogenesis[7]. LncRNAs have caught the attention of many research groups. Even though their mechanisms-of-action are still poorly understood, the number of publications on lncRNAs in cardiovascular disease is increasing exponentially[8–19]. SnoRNAs on the other hand are still relatively unknown and understudied. Like microRNAs, snoRNAs are a class of highly conserved small ncRNA molecules[20]. SnoRNAs are typically between 60 nucleotides and 300 nucleotides long and can be divided into two subtypes. 'H/ACA box' snoRNAs modulate other ncRNAs via pseudouridylation. 'C/D box' snoRNAs modulate ncRNAs via 2'O-ribose-methylation. However, snoRNAs have also been found to act via non-canonical pathways. SnoRNAs influence metabolic stress, lipotoxicity, and intracellular cholesterol trafficking, independent of their canonical function[21,22]. Moreover, there are snoRNAs that have no known RNA targets at all. These snoRNAs most likely have mostly non-canonical functions and are referred to as 'orphan snoRNAs'. All 14q32 snoRNAs are orphan snoRNAs of the C/D box subtype[23]. With the increasing research attention for lncRNAs, we aimed to investigate whether orphan snoRNAs merit similar attention. First, we found significant associations of genetic variations specifically in the snoRNA region of the 14q32 locus with human cardiovascular disease. Second, we observed differential expression of 14q32 snoRNA levels throughout the human vasculature. And third, we demonstrate that snoRNA expression is regulated during cardiovascular disease, both in vascular tissue samples and in plasma, as

well in a murine model for vein graft disease. Overall, our data demonstrate that snoRNAs indeed merit similar effort and attention in future basic and clinical cardiovascular research as microRNAs and lncRNAs do.

Methods

PROspective study of pravastatin in the elderly at risk

PROspective study of pravastatin in the elderly at risk (PROSPER) was a prospective multicentre randomized placebo-controlled trial to assess whether treatment with pravastatin diminishes the risk of major vascular events in elderly[24]. Between December 1997 and May 1999, we screened and enrolled subjects in Scotland (Glasgow), Ireland (Cork), and the Netherlands (Leiden). Men and women aged 70–82 years were recruited if they had pre-existing vascular disease or increased risk of such disease because of smoking, hypertension, or diabetes. A total number of 5804 subjects were randomly assigned to pravastatin or placebo. The protocol meets the criteria of the Declaration of Helsinki and was approved by the medical ethics committees of each participating institution. Written informed consent was obtained from all participating subjects. All data have been anonymized.

The primary endpoint in the study was the combined endpoint of death from coronary heart disease, non-fatal myocardial infarction (MI), and occurrence of clinical stroke, either fatal or non-fatal. When death occurred following a non-fatal stroke within a period of 28 days, it was regarded as a fatal stroke. Secondary endpoints were the separate coronary and cerebrovascular components of the primary endpoint. Heart failure hospitalization was a tertiary endpoint. All endpoints were adjudicated by the study endpoint committee. More details about the diagnosis of the cerebrovascular and coronary events within the PROSPER study has been published elsewhere[25]. A whole genome wide screening had been performed in the sequential PHASE project[26]. Of 5763 subjects, DNA was available for genotyping. Genotyping was performed with the Illumina 660K beadchip, after QC (call rate <95%) 5244 subjects and 557 192 single nucleotide polymorphism (SNPs) were left for analysis. These SNPs were imputed to 2.5 million SNPs based on the HAPMAP build 36withMACH imputation software. For this study, we performed a candidate gene study. We extracted all SNPs within the genomic region of the 14q32 cluster from the 2.5 million SNP database with use of the PLINK software (http://pngu.mgh.harvard.edu/~purcell/plink/download.shtml#download).

As confirmation of our findings, data on associations between 14q32 SNPs and coronary artery disease/MI have been contributed by CARDIoGRAMplusC4D investigators and have been downloaded from http://www.cardiogramplusc4d.org.

Collection of human vascular tissues

Human vascular tissue samples, including vena saphena magna (VSM) samples, were collected during general surgery for various implications. Only surplus material, discarded after surgery, was collected and stored at -80°C. Failed coronary bypasses were collected during autopsy, formalin-fixed, and paraffin-embedded.

All samples were anonymized and no data were recorded that trace back to an individual's identity. Collection, storage, and processing of the samples were performed in compliance with the Medical Treatment Contracts Act (WGBO, 1995) and the Code of Conduct for Health Research using Body Material (Good Practice Code, Dutch Federation of Biomedical Scientific Societies, 2002) and the Dutch Personal Data Protection Act (WBP, 2001).

Human plasma samples

From a Danish cohort study on G-CSF treatment in ST-elevation myocardial infarction (STEMI) patients[27], 23 placebo-treated STEMI patients (21 men, two women) aged 54 ± 8 years (mean ± standard deviation) who had been treated successfully with primary percutaneous coronary intervention within 12 h after symptom onset were included in our study. STEMI was diagnosed from typical angina for more than 30min, the presence of ST-elevations >0.4mV in at least two contiguous leads on a standard 12-lead ECG and a significant rise in MI serum markers. Further inclusion criteria included age between 20 years to 70 years, a proximal lesion in a coronary artery branch and either serum creatine kinase-MB above 100IL/L or significant Q-wave development. Patients were excluded if they had a prior MI, significant non-culprit stenosis, ventricular arrhythmia after percutaneous coronary intervention, pregnancy, diagnosed, or suspected cancer, New York Heart Association class 3–4 heart failure symptoms or severe claustrophobia.

Blood samples were drawn from the antecubital vein using EDTA-coated tubes. Samples were kept on ice and processed within 30min after collection. Plasma was obtained from the samples by centrifugation at 3000g for 10min, with the plasma closest to the buffy coat being discarded. After centrifugation, the plasma samples were aliquoted and stored at -80°C until analysis.

The study was approved by the ethics committee at Rigshospitalet, Copenhagen, Denmark (KF 01-239/02). All patients received oral and written information about the study, and written informed consent was obtained before inclusion in the study, which conformed to the Declaration of Helsinki.

Collection of human heart failure tissues

Biopsies were collected from explanted end-stage failing human hearts, caused by dilatory cardiomyopathy (N= 9), ischaemic cardiomyopathy (N= 6), right ventricular dysplasia (N= 1), or congenital heart disease (N= 2). Samples were collected from both the apex and the affected ventricle. As we found no differences, average expression levels from the apex and ventricles were used for each patient in further analyses. All human material was obtained and processed according to the recommendations of the hospital's ethics committee and security board, including informed consent and in accordance with the Declaration of Helsinki. RNA was isolated from heart tissue using an automated Maxwell System with the respective mRNA tissue kit (Promega, WI, USA). cDNA was generated from equal amounts of RNA per experiment using a Promega GoScript reverse transcription system (Promega).

Murine vein graft model

All animal experiments have been approved by the Leiden University Medical Center animal ethics committee (Dier Ethische Commissie) and all animal procedures were performed conform to the guidelines from Directive 2010/63/EU of the European Parliament on the protection of animals used for scientific purposes. Male ApoE3*Leiden mice, aged 10weeks to 20weeks were housed with water and chow ad libitum. Mice were fed a western-type diet (ABdiets), which resulted in plasma cholesterol levels between 12mmol/L and 24mmol/L, as determined before surgery and after surgery (Roche Diagnostics).

Vein graft surgery was performed by donor caval vein interpositioning (caval vein of ~2mm length) in the carotid artery of recipient mice[28]. Before surgery, mice were anaesthetized with midazolam (5mg/kg, Roche Diagnostics), medetomidine (0.5mg/kg, Orion), and fentanyl (0.05mg/kg, Janssen Pharmaceutical). The adequacy of the anaesthesia was monitored by keeping track of the breathing frequency and the response to toe pinching of the mice. After the procedure, the mice were antagonized with atipamezol (2.5mg/kg, Orion) and fluminasenil (0.5mg/kg Fresenius Kabi). Buprenorphine (0.1mg/kg, MSD Animal Health) was given after surgery to relieve pain. Mice were sacrificed after 3 days, 7 days, 14 days, or 28 days (four mice per time point) by exsanguination under anaesthesia; 12 untransplanted caval veins were collected as time point 0; three caval veins were pooled yielding four samples. The vein grafts and caval veins were removed and snap frozen.

RNA isolation and rt/qPCR

Fresh-frozen human vascular tissue samples and murine vein graft/caval vein were submerged in liquid nitrogen and homogenized by use of pestle and mortar. After complete evaporation of the liquid nitrogen, total RNA was isolated by standard TRIzol-chloroform

extraction. From cells, the medium was removed and cells were washed in PBS, after which the cells were lysed in TRIzol and RNA isolated by standard TRIzol-chloroform extraction. From paraffin embedded human coronary bypasses, total RNA was isolated using the RNeasy FFPE Kit according to manufacturer's protocol (Qiagen). From human plasma samples, total RNA from 100µL of plasma was extracted using the miRCURY RNA Isolation Kit—Biofluids (Exiqon) according to manufacturer's protocol, including rDNase treatment to prevent DNA contamination. RNA quantity and purity were checked using nanodrop (Nanodrop® Technologies).

RNA was reverse transcribed using 'high-capacity RNA to cDNA kit' (ThermoFisher) and quantified by qPCR using SybrGreen reagents (Qiagen) on the VIIa7 (ThermoFisher). SnoRNA expression was normalized against U6 alone or U6 and GAPDH together, to warrant reference gene stability over samples, using the 2^{-dCt} method. Human snoRNA primer sequences were taken from a study by Valleron et al[29]. Although the snoRNAs and U6 could be reliably and reproducibly measured in RNA isolated from paraffin-embedded human failed coronary bypass tissues, longer RNAs, including MEG3, MEG8, could not, most likely due to degradation of longer RNAs by RNases. Shorter RNAs are protected from RNase digestion, as they are in complex with RNA Binding Proteins[30]. All qPCR primers used are given in Supplementary data, Table S5.

Isolation of human umbilical venous and arterial endothelial cells, arterial smooth muscle cells, and arterial fibroblasts

Umbilical cords were collected from full-term pregnancies and stored in sterile PBS at 4°C and subsequently used for cell isolation within 7 days. For human umbilical venous endothelial cell/human umbilical arterial endothelial cell (HUVEC/HUAEC) isolation, a cannula was inserted in the umbilical vein or in one of the umbilical arteries and flushed with sterile PBS. The vessels were infused with 0.075% collagenase Type II (Worthington, Lakewood, NJ, USA) and incubated at 37°C for 20min. The collagenase solution was collected and the vessels were flushed with PBS in order to collect all detached endothelial cells. The cell suspensions were centrifuged at 400g for 5min, and the pellet was resuspended in HUVEC/HUAEC culture medium [M199 (PAA, Pasching, Austria), 10% heat inactivated human serum (PAA), 10% heat inactivated newborn calf serum (PAA), 1% penicillin/streptomycin (MP Biomedicals, Solon, OH, USA), 150mg/mL endothelial cell growth factor (kindly provided by Dr Koolwijk, VU Medical Center, Amsterdam, the Netherlands), and 0.1% heparin (LEO Pharma, Ballerup Danmark)]. HUAECs were cultured in plates coated with 1% gelatin.

The second artery was removed and cleaned from remaining connective tissue. Endothelial cells were removed by gently rolling the artery over a blunted needle. The tunica adventitia and tunica media were separated using surgical forceps. After overnight incubation in human umbilical arterial smooth muscle cell/human umbilical arterial fibroblast (HUASMC/HUAF) culture medium [DMEM GlutaMAX™ (Invitrogen, GIBCO, Auckland, New Zealand), 10% heat inactivated foetal bovine serum (PAA), 10% heat inactivated human serum, 1% penicillin/streptomycin, and 1% non-essential amino acids (PAA)], both tunicae were incubated separately in a 2mg/mL collagenase Type II solution (Worthington) at 37°C. Cell suspensions were filtered over a 70 mm cell strainer and centrifuged at 400 g for 10min. Cell pellets were resuspended and plated in culture medium. Cells isolated from the tunica adventitia were washed with culture medium after 90 min to remove slow-adhering non-fibroblast cells.

Primary cell culture

Cells were cultured at 37°C in a humidified 5% CO_2 environment. Culture medium was refreshed every 2–3 days. Cells were passed using trypsin-EDTA (Sigma, Steinheim, Germany) at 90–100% (HUVECs, HUAECs, and HUASMCs) or 70–80% confluency (HUAFs). HUVECs, HUASMCs, and HUAFs were used up to passage six and HUAECs up to passage three. Stock solutions of isolated HUVECs, HUASMCs, and HUAFs up to passage four, and HUAECs up to passage two were stored at -180°C in DMEM GlutaMAX™ containing 20% FBS and 10% DMSO (Sigma).

3T3 cell culture

3T3 cells were cultured at 37°C under 5% CO_2. Cells were grown in DMEM (PAA) with high glucose and stable L-glutamine, supplemented with 10% foetal calf serum and penicillin/streptomycin.

Primary mouse fibroblasts culture

Murine primary fibroblasts were isolated from ear-clippings of 3-week old C57BL/6 mice. Ear clippings were cut into small pieces, which were embedded in 0.2% gelatin in 10 cm2 plates and covered in DMEM supplemented with 20% FCSi and 1% NEAA for approximately 7 days, cells were expanded to passage 3 and frozen down in liquid nitrogen for later use. Fibroblasts from P4 were trypsinized and passed into 12-wells plates for scratch-wound healing assays. Cells were used up to passage P5–P7.

RBP-immunoprecipitation

For RNA binding protein (RBP)-immunoprecipitation (RIP), either HUAFs or 3T3 cells were grown to 70–80% confluence in T-175 culture flasks, one flask per RBP-pull-down, in normal culture medium. We used the EZ-Magna RIP RNA-Binding Protein Immunoprecipitation Kit (Merck-Millipore) for cell lysis, sample preparation and RBP-pull-down, according to manufacturer's protocol. We used antibodies against SNRP70 (provided with EZ-Magna RIP kit), Dicer, AGO1, Fibrillarin, and a negative control IgG (all by Abcam) for RBP-pull-down. RNA was isolated using standard TRIzol-chloroform extraction and snoRNA expression was measured by rt/qPCR as described above. Expression was normalized to expression in a 10% input sample, using the 2^{-dCt} method; after cell lysis, but before RBP-pull-down, 10% (100 mL) of each lysate was collected and used for RNA extraction directly.

SnoRNA upregulation in vitro and scratch-wound healing assay

Primary murine fibroblasts were seeded in 12-well plates at 50 000 cells per well in normal culture medium. The next day, cells were incubated with 10ng/mL 3rd generation antisense molecules (3GAs) in medium with 0.5% foetal calf serum for 24 h. Sequences of all 3GAs used are given in Supplementary data, Table S4. After 24 h, medium was aspirated and a scratch-wound was made across the diameter of each well using a p200 pipet tip. Next, cells were washed with PBS, and fresh low serum medium containing 3GAs was added. In order to monitor wound closure, live phase-contrast microscopy (Axiovert 40C, Carl Zeiss) was used for taking pictures immediately after (0 h) and 12 h after introducing the scratch-wound. Pictures were taken at two different locations in each well and averaged for analysis. Scratch size was calculated at 0 h and 12 h using the wound healing tool macro for ImageJ. Finally, cells were washed with PBS and TRIzol was added for RNA isolation.

Statistical analyses

For the candidate gene study, logistic regression was used to associate the 14q32 SNPs with cardiovascular outcomes adjusted for sex, age, country, and pravastatin treatment. All statistical analyses were performed with PLINK statistical software (http://pngu.mgh.harvard.edu/~purcell/plink/download.shtml#download). P-values <0.05 were considered statistically significant.

SNPs were pruned based on linkage, using LDLink software (https://analysistools.nci.nih.gov/LDlink/)[31,32]. For pruning, we used the CEU population as reference which corresponds to the PROSPER population (r^2= 0.3, MAF= 0.01).We performed correction for multiple testing, using both Bonferroni and false discovery rate (FDR) corrections within each gene region of the 14q32 locus, as our a priori interest lays

with the snoRNA gene region and the other regions were included to allow for correction of potential confounding by linkage. An FDR of 10% was chosen. We also performed correction for multiple testing on the pruned SNPs in the locus as a whole with a global test, using the tail strength method, including all genes in the 14q32 locus, looking at associations with heart failure. The tail strength measures how much P-values in a set differ from the expected uniform distribution under the null hypothesis and sums up these differences into single-test statistics[33]. We used a cutoff of 10% and 20% for missingness in individuals and markers, respectively. The global P-value was calculated using a logistic regression model on each SNP and summarizing the P-values using the tail strength. To account for residual LD between SNPs, 10^4 permutations were used to derive an empirical P-value. R version 3.5.0 was used for all calculations.

Normalized relative expression levels of noncoding RNAs expressed as mean + SEM. Differences between groups were assessed using student's t-tests. Because of large inter-sample variation, a Grubbs' test was used to identify significant outliers ($\alpha < 0.05$) in human 14q32 ncRNA expression levels, resulting in exclusion of three individual measurements. In the STEMI samples, the variance over time was analyzed using repeated measures one-way analyses of variance (ANOVA). Tukey's range test was used as a *post hoc* test to find significant variation between two measurement time points.

For *in vitro* assays two-tailed Student's t-tests or two-way ANOVA were used to compare groups. A level of P-value <0.05 was considered significant. A Grubbs' test was used to identify significant outliers ($\alpha = 0.05$), resulting in exclusion of two individual scratch assays. However, the data still include a minimum of three independent experiments for each snoRNA.

Results

Association of 14q32 genetic variations with cardiovascular disease

The 14q32 locus is depicted in Figure 1. To establish a role of 14q32 snoRNAs in human cardiovascular disease, we focused on SNPs in the 14q32 locus that were genotyped in 5244 participants of the PROSPER study. Characteristics of PROSPER participants are given in Supplementary data, Table S1, all data on extracted 14q32 SNPs are given in the Supplementary data, Data S2 file. When zooming in on the different genes in the locus, six SNPs in the protein coding gene DLK1 were included, of which one associated with coronary events; 53 SNPs in the lncRNA MEG3 gene were included, of which eight associated with cardiovascular endpoints; seven SNPs in the lncRNA MEG8 gene were included, of which one associated with heart failure; and 11 SNPs in the lncRNA MEG9 gene were included of which three associated with vascular mortality and two with all-cause mortality. In the two regions that encode the vast majority of the snoRNAs and microRNAs within the locus, 51 and 42 SNPs were included in the array, respectively, of which 17 and 13 associated with cardiovascular endpoints and of these, 14 and 9 SNPs, respectively, associated with heart failure (Figure 2).

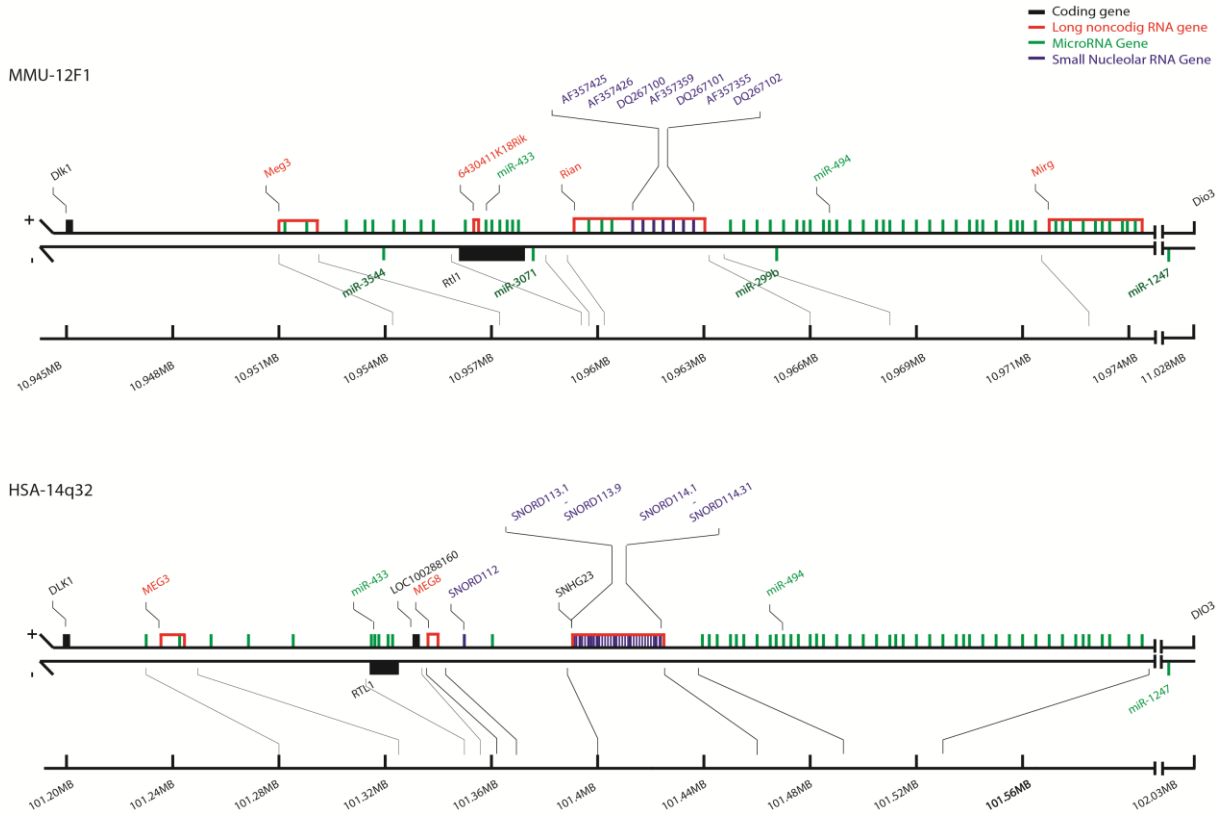

Figure 1 Schematic representation of the imprinted human 14q32 and murine 12F1 loci. Protein coding genes are depicted in black, lncRNA genes in red, microRNA genes in green, and snoRNA genes in blue.

We then pruned SNPs based on linkage, to correct for multiple testing. For DLK1, MEG3, RTL1, MEG8, the snoRNA region, the microRNA region, and MEG9, 6, 17, 3, 4, 8, 14, and 2 SNPs were kept, respectively. Data on kept and pruned SNPs per gene are given in the Supplementary data, Data S3 file. After Bonferroni correction per gene, one SNP in the snoRNA region (rs2145501) was significantly associated with heart failure. After FDR correction per gene, four SNPs in the snoRNA region were significantly associated with heart failure (rs2145501, rs2145504, rs2295657, and rs10133948). After both Bonferroni and FDR correction per gene, two SNPs in the MEG9 gene (rs2295655 and rs3742406) were significantly associated with vascular mortality and one SNP with all-cause mortality (rs2295655). The odds ratios, P-values, and corrected P-value thresholds are shown in Supplementary data, Table S2B. Multiple correction testing data on all pruned SNPs per gene are given in the Supplementary data, Data S4 file.

We also performed a global test on SNPs kept after pruning using the tail strength method to correct for multiple testing over the locus as a whole, looking at associations with heart failure. The global P-value was 0.018, meaning that the null-hypothesis of no associated SNPs in the locus is rejected and that the 14q32 locus associates significantly with heart failure.

SNPs in the locus were selected from a genome wide screening array dataset, in which SNPs are selected more or less evenly over the length of the genome and preferably in coding sequences. Since there are no coding sequences on the positive strand of the 14q32 locus, except for DLK1, none of the SNPs included in the analyses were located directly in a snoRNA gene. Therefore, we rely on the fact that SNPs that are located in proximity of each other are often inherited together, also referred to as linkage. Non-functional SNPs can be associated with cardiovascular endpoints because they are linked to a different, functional SNP. We determined r^2 values, a measure of linkage between SNPs. We found evidence of linkage within the MEG3 gene, within the microRNA-cluster, and within the snoRNA-cluster, which underlines their individual biological importance. However, we also found that there was virtually no linkage between the SNPs in the snoRNA-cluster and those in the microRNA-cluster. In fact, there is a recombination hotspot in between both clusters. There is another recombination hotspot between MEG3 and the snoRNA-cluster, as well as one between the microRNA-cluster and MEG9. This is in fact a crucial finding, because it demonstrates that the 14q32 snoRNAs associate with cardiovascular endpoints, independently of the microRNAs and MEG3 (Supplementary data, Figure S1A–C). A more detailed view of linkage within the snoRNA-cluster is given in Supplementary data, Figure S2.

As confirmation of our genetic association data, we performed a lookup of 14q32 SNPs in the publicly available meta-analysis dataset of cardiogram (www.cardiogramplusc4d.org). To our knowledge, public data on heart failure specifically are not available yet, but cardiogram focuses on coronary artery disease. All extracted cardiogram data are provided in the Supplementary data, Data S5 file, and significant associations directly in (the vicinity of) 14q32 noncoding RNA genes are given in Supplementary data, Table S6.

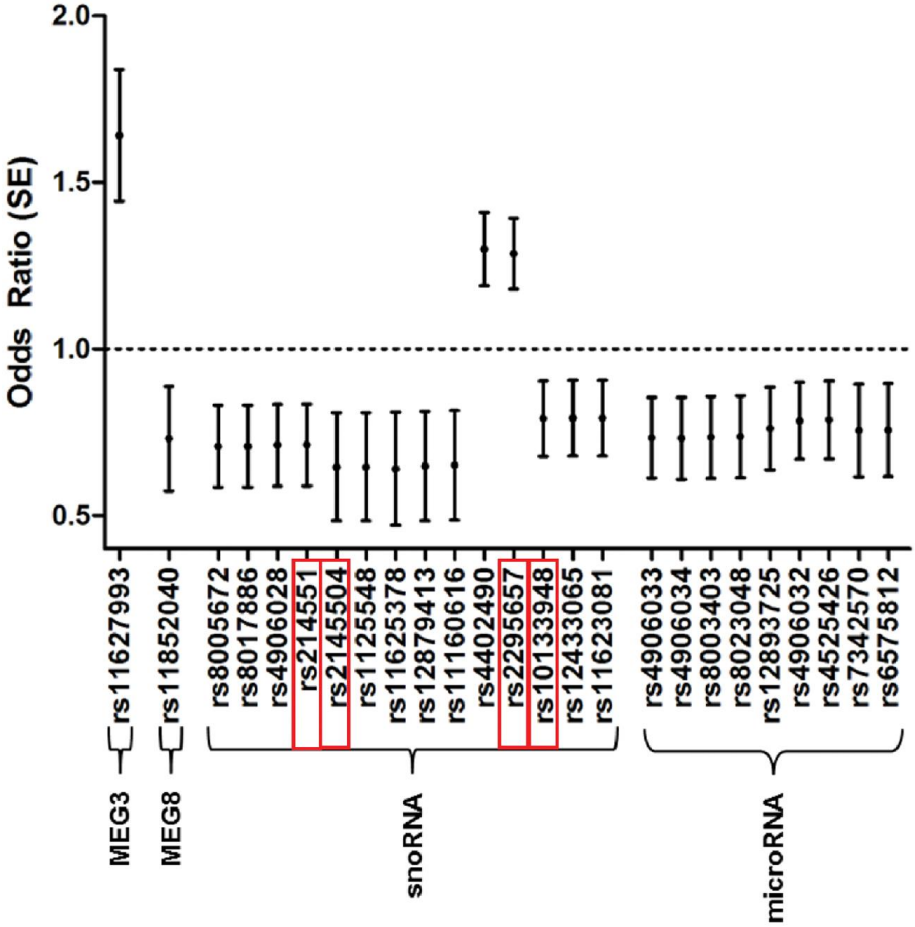

Figure 2 14q32 SNPs and heart failure. Odds ratios, ± standard errors, are given of SNPs that associate significantly with heart failure. SNPs are given in order of their chromosomal location and accolades indicate their respective regions in the 14q32 locus. Only the four SNPs outlined in red remain significant after correction for multiple testing.

Global expression of 14q32 snoRNAs

The cluster contains three highly related copy-sets of SNORD112 (one copy), SNORD113 (nine copies) and SNORD114 (31 copies). Since the snoRNAs are highly similar in sequences, rt/qPCR primers can only reliably discriminate 7 of the 41 snoRNAs, namely SNORD112, SNORD113.2, SNORD113.6, SNORD113.7, SNORD113.8, SNORD113.9, and SNORD114.1. We measured these seven snoRNAs in a biobank of 95 human vascular tissue samples, collected

during general surgery within the LUMC (Supplementary data, Table S3). With the exception of SNORD113.2, all measured 14q32 snoRNAs were abundantly expressed throughout the vasculature (Supplementary data, Figure S3A–G). Global snoRNA expression was highest however in the arteries and veins of the head and neck, again with the exception of SNORD113.2, which was expressed most abundantly in vessels of the lower limbs and in mammarian arteries (Figure 3).

Samples were collected during general surgery for any indication. However, most vessels were collected during vascular surgery for peripheral artery disease and coronary artery bypass grafting on the one hand or tumour resections on the other. However, none of the snoRNAs were differentially expressed between benign and perimalignant vessels. Nor did snoRNA expression associate with age or sex (data not shown).

We also assessed 14q32 snoRNA expression in four types of human primary vascular cells, isolated from the umbilical cord, namely HUVECs, HUAECs, HUASMCs, and HUAFs. Although we observed consistent snoRNA expression in all four cell types, expression was clearly enriched in HUASMCs (Supplementary data, Figure S4).

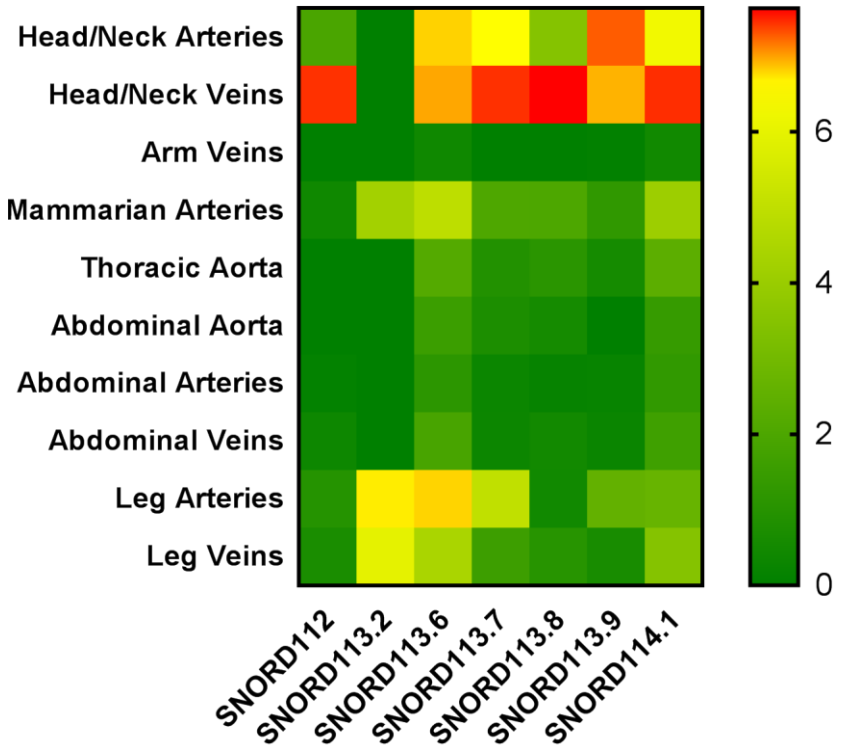

Figure 3 Heatmap of snoRNA expression in human vasculature. SnoRNAs are grouped in vessel origin and in order of their genetic localization. For every snoRNA, relative expression, calculated using the 2^{-dCt} method, in each vessel group was normalized against the average expression in all samples. Relative expression below average is green, around average is yellow, and above average is orange to red. The total number of vessels included was 95.

14q32 snoRNA expression in failed human coronary arterial-venous bypass grafts

We compared 14q32 snoRNA expression in naive VSMs and failed arterial-venous bypasses. Naïve VSMs were harvested during bypass surgery and served as 'baseline' controls for failed coronary arterial-venous bypass grafts. In failed bypasses, expression levels of 14q32 snoRNAs SNORD112 and SNORD113.6 remained more or less stable. Expression levels of SNORD113.2, SNORD113.7, SNORD113.8, SNORD113.9, and SNORD114.1 on the other hand appeared upregulated between two-fold and 20-fold (Figure 4A–G).

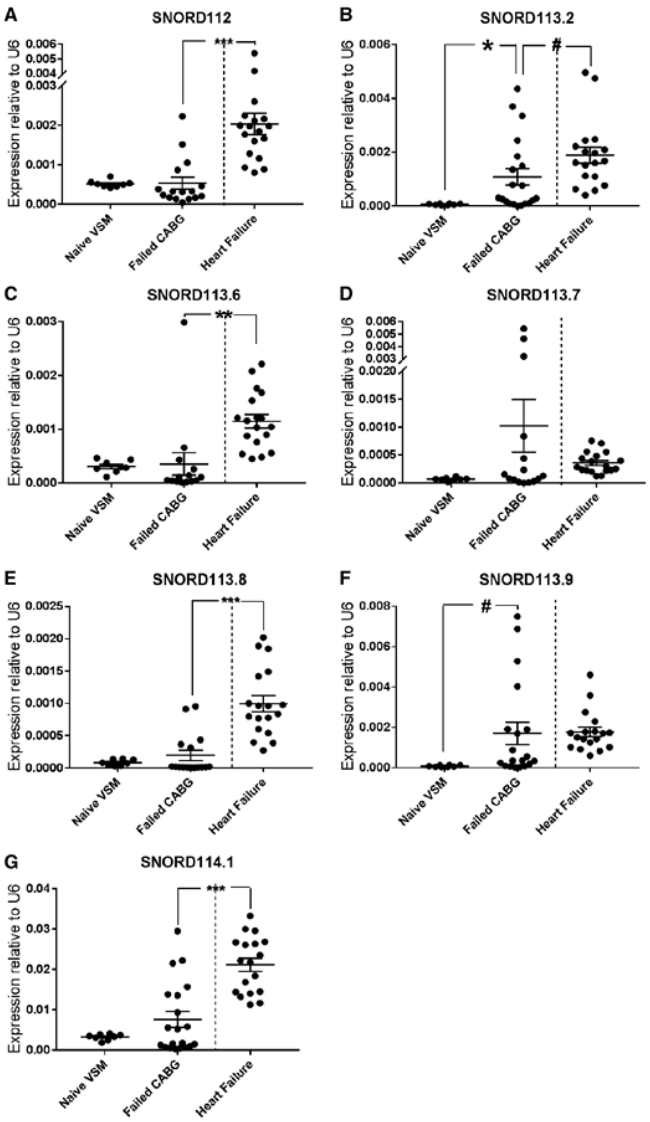

Figure 4 Regulation of the 14q32 small ncRNAs in human vein graft disease and expression in human failing hearts (A–G). Relative expression, calculated using the 2^{-dCt} method, of 14q32 microRNAs and snoRNAs in failed coronary bypasses (right bars; N= 20), compared with naive vena saphena magna harvested during bypass surgery (left bars; N= 8), as well as expression levels in human end-stage failing hearts (N= 18). Mean values are given and errors bars represent SEMs. #P<0.1; *P<0.05; **P<0.01; ***P<0.001 (t-test).

14q32 snoRNA expression in end-stage failing human hearts

As we observed the strongest association between SNPs in the snoRNA region and heart failure, we also looked at snoRNA expression in tissue samples from explanted end-stage failing human hearts. For obvious reasons, we had no healthy heart tissue samples for comparison. However, as shown in Figure 4A–G, all measured 14q32 snoRNAs were expressed in failing human hearts. When compared with expression in failing bypass grafts, expression was higher in heart failure samples for five out seven measured snoRNAs [SNORD112: 3.8-fold (P> 0.001); SNORD113.2: 1.7-fold (P = 0.07); SNORD113.6: 3.2-fold (P> 0.01); SNORD113.8: 5.1-fold (P> 0.001); and SNORD114.1: 2.8-fold (P < 0.001), and similar for the remaining SNORD113.7 (P = 0.13) and SNORD113.9 (P=0.91)].

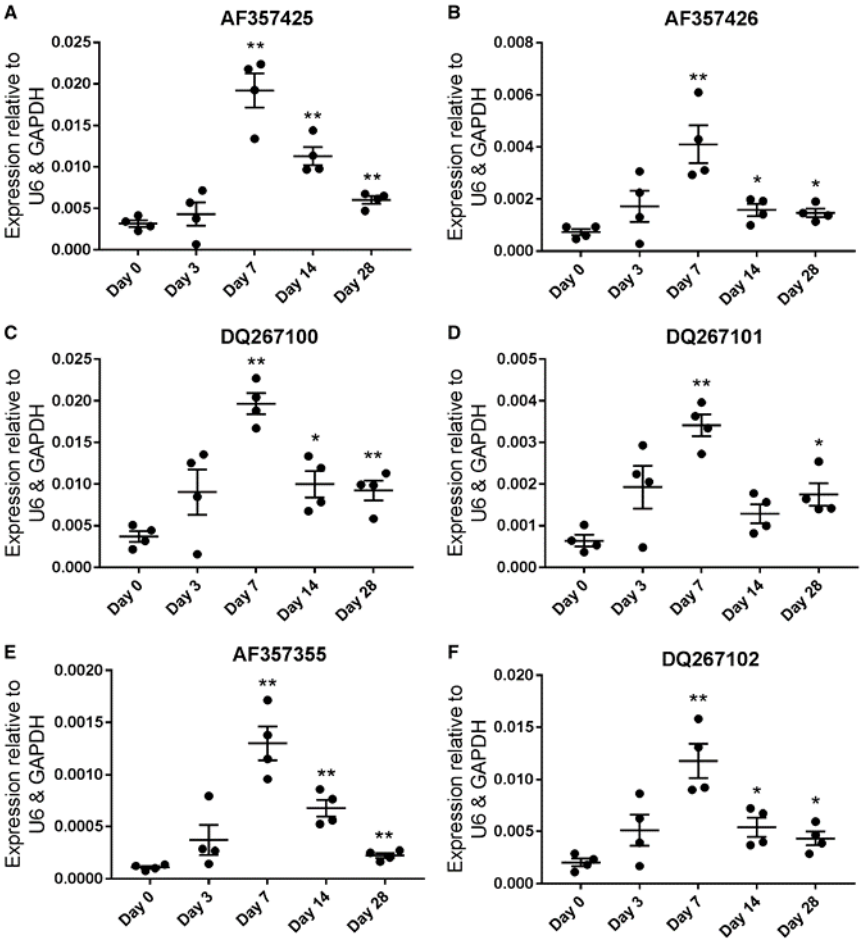

Figure 5 Regulation of the 12F1 snoRNAs in murine vein grafts (A–F). Relative expression, calculated using the 2^{-dCt} method, over time, relative to naive venae cavae, in vein grafts in ApoE*3L mice. Mean values are given and errors bars represent SEMs. *P<0.05; **P<0.01 (t-test). Each time point includes vein grafts from four mice, except for time point 0, which contains four pools of naive caval veins from three mice (12 mice in total).

Murine snoRNA expression in a model for arteriovenous bypass failure

The 14q32 noncoding RNA cluster is conserved in eutheria and is transcribed from the imprinted 12F1 locus in mice (Figure 1).We compared expression of six different 12F1 snoRNAs in murine vein grafts, a model for arterial-venous bypass failure. Expression of all 12F1 snoRNAs increases after vein graft surgery and peaks at 7 days after vein grafting. After 7 days, levels decrease, but they do not normalize and remain elevated until Day 28 (Figure 5).

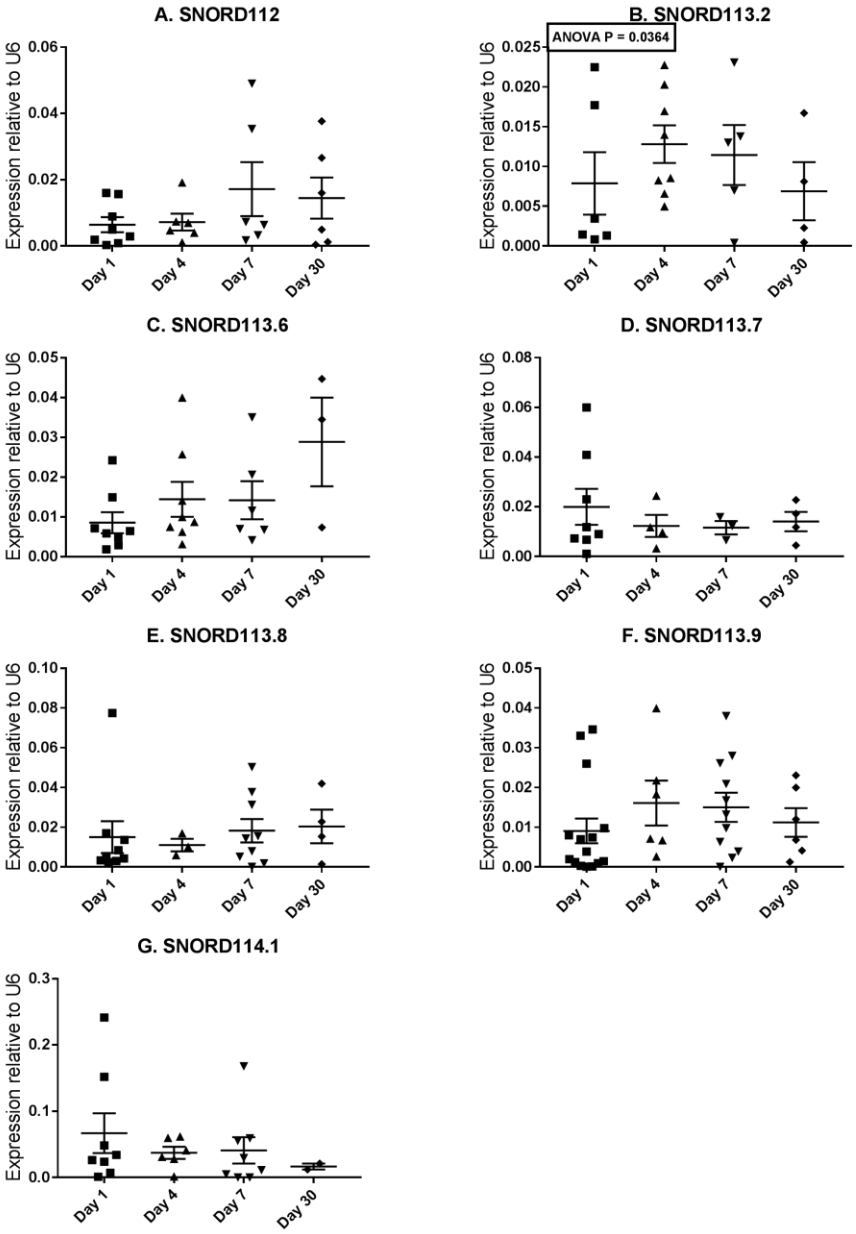

Figure 6 Regulation of circulating 14q32 snoRNA expression (A–G). Relative expression, calculated using the 2^{-dCt} method, of 14q32 snoRNAs, in plasma of patients with STEMI, collected over time. Mean values are given and errors bars represent SEMs. P-value for ANOVA is given for SNORD113.2. Although 23 patients were included in all measurements, some snoRNAs remained below detection levels in some patient samples.

14q32 circulating snoRNAs in ST-elevation myocardial infarction

In our STEMI-patient cohort, we measured the same seven 14q32 snoRNAs in plasma, drawn at hospitalization, and on Day 4, Day 7, and Day 30 after hospitalization. All seven snoRNAs could be detected in plasma, albeit in low levels (some snoRNAs remained below the detection limit in some individuals). SNORD113.2 levels were regulated over time in response to STEMI [P= 0.0364; F(3,22) = 3.381]. SNORD113.2 levels were increased two-fold between Day 4 and Day 30 (P = 0.0424), suggesting a sub-acute increased expression at Day 4 in comparison to the assumed normal expression levels at Day 30 (Figure 6B). Remaining snoRNAs appeared regulated over time as well but significant changes in expression were not observed (Figure 6A and C–G).

Potential mechanisms of action

To gain more insight into the potential role of 14q32 snoRNAs in cardiovascular pathology, we looked at different aspects of snoRNA biology. We performed RIP in both human and murine cells to determine which RBPs can bind the 14q32/12F1 snoRNAs. We found no evidence of snoRNA-binding to the spliceosome in either human or murine cells (SNRNP70; data not shown). In primary human umbilical arterial adventitial fibroblasts (HUAAFs), all 14q32 snoRNAs measured were bound to Fibrillarin and to a lesser extent also to AGO1. Binding to Fibrillarin was consistent and outspoken for all 14q32 snoRNAs measured, even though expression of SNORD113.2 was relatively low in all fractions, including the whole-cell lysate (10% input) (Figure 7A). 14q32 snoRNAs were clearly enriched in the Fibrillarin fraction compared to the Fibrillarin target U6 (U6 is a snRNA that methylated by Fibrillarin), even though U6 expression in human fibroblasts is approximately 1000-fold higher than 14q32 snoRNA expression (Supplementary data, Figure S4).

The murine 12F1 snoRNAs did not bind to Ago1, but all 12F1 snoRNAs, with the exception of DQ267101, were clearly enriched in the Fibrillarin fraction (Figure 7B). Fibrillarin is the methyltransferase that performs snoRNA-directed 2'O-ribose-methylation of target ncRNAs. Therefore, these data indicate that 14q32/12F1 snoRNAs direct 2'O-ribose-methylation via Fibrillarin of non-canonical RNA targets. Furthermore, 14q32 snoRNAs may interact with the microRNA processor protein AGO1.

3GAs [formerly known as Gene Silencing Oligonucleotides (GSOs)], which have proven very reliable in microRNA-inhibition[4], proved less efficient as snoRNA-inhibitors; 3GAs directed towards the 5'-end of the snoRNA knocked-down snoRNA expression by 40–80% (data not shown). SnoRNAs have proven notoriously difficult to inhibit, likely due to their predominantly nucleolar localization and more complex structures[34]. However, 3GAs directed to the 3'-end lead to up-regulation of all 12F1 snoRNAs, except for AF3574276,

which showed virtually no expression in murine fibroblasts (Figure 7C). SnoRNAs are processed by exonucleases[35,36] and 3GA-binding to the 3'-end may protect against exonuclease digestion.

We then used 3'-end-directed 3GAs to overexpress the 12F1 snoRNAs individually in mouse fibroblasts and performed scratch wound healing assays to assess changes in proliferation and migration. Upregulation of snoRNA AF357425 led to a significantly impaired scratch wound healing (32% reduction compared with 3GA-Control, P= 0.0065), whereas up-regulation of snoRNA DQ267102 showed a similar trend (19% reduction compared with 3GA-Control, P=0.083) (Figure 7D).

snoRNA conservation

So far, only seven 12F1 snoRNAs have been annotated in mice vs. 41 14q32 snoRNAs in humans (NCBI Gene). However, 19 more murine 12F1 snoRNAs have been predicted based on sequence, but have not been confirmed as existing snoRNAs yet (UCSC Genome Browser). We were able to design unique rt/qPCR primers for 16 of the 19 additional predicted murine snoRNAs and measured their potential expression in murine fibroblasts (Supplementary data, Figure S5). Not only were these 16 snoRNAs all expressed, but also at a higher level than the seven annotated snoRNAs. rt/qPCR is not a confirmative experiment to demonstrate that these sequences are mature snoRNAs, we could pick up remaining Rian pre-lncRNA, or not yet degraded Rian introns. However, it is feasible that the murine 12F1 locus is more closely related to the human 14q32 locus in snoRNA abundance than previously assumed. We then aligned the sequences of the human and murine snoRNAs and, although there are overlapping regions, there also was large variability. However, if we assume that these snoRNAs function via Fibrillarin, then we know the 'seed sequences' of the snoRNAs, namely the nine nucleotides upstream of the D-boxes. If we align these, we observed clearly conserved seed sequences of murine and human snoRNAs (Supplementary data, Figure S6). Specifically, murine snoRNAs (names starting with AF, DQ, or GM) cluster with human snoRNAs (names starting with SNORD) based on sequence, rather than with other murine snoRNAs and vice versa. Furthermore, the alternative seed sequences, the nine nucleotides upstream of potential D'-boxes, are also largely conserved.

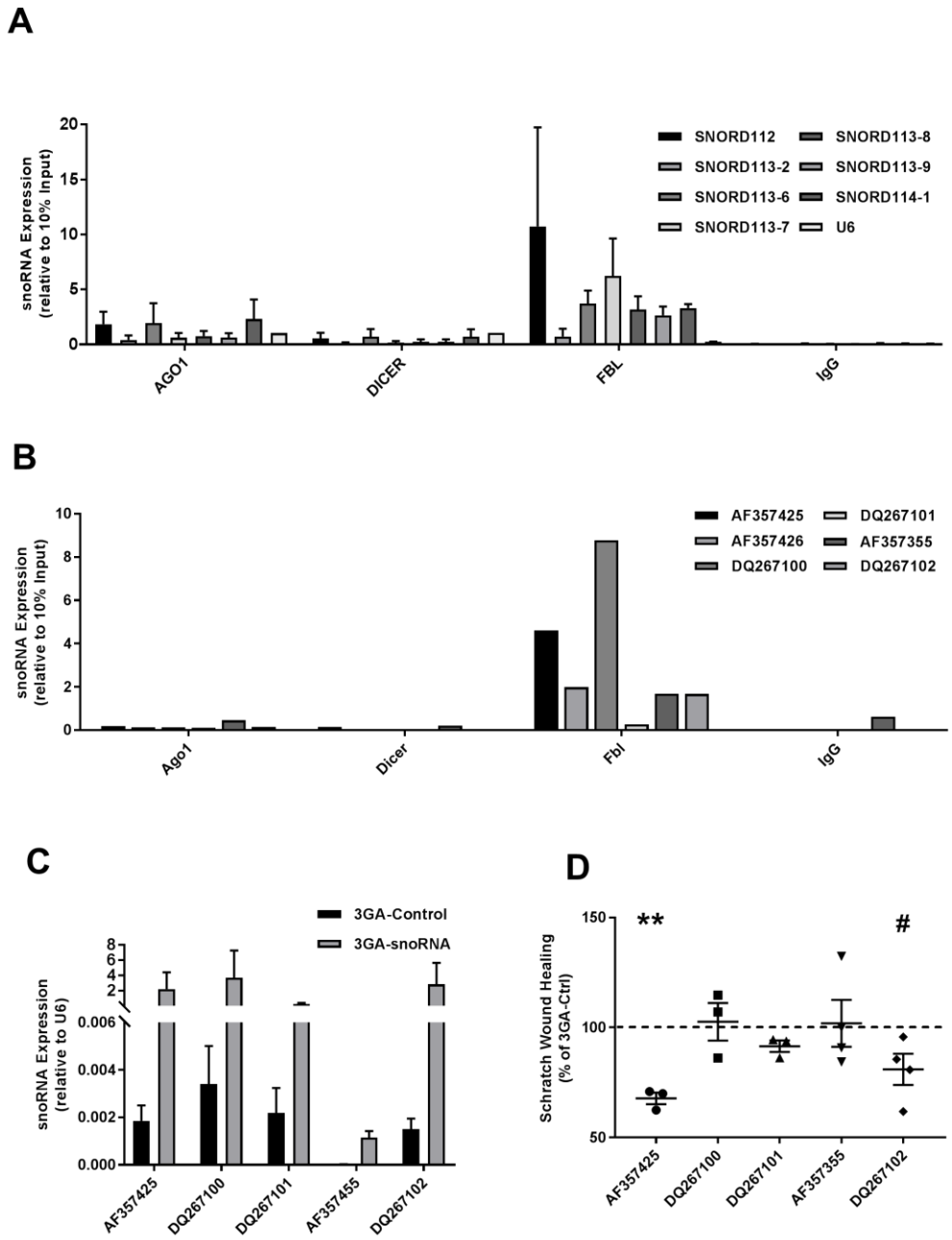

Figure 7 Functionality screenings on 14q32 and 12F1 snoRNAs. (A) RIP, followed by RNA isolation and rt/qPCR on primary HUAAFs. Expression levels of each snoRNA were normalized to snoRNA expression in untreated cell lysates (input) using the 2^{-dCt} method. IgG pull-down was used as negative control. The data represent three independent experiments performed in triplicate. (B) RIP, followed by RNA isolation and rt/qPCR on the murine fibroblast 3T3 cell line. Expression levels of each snoRNA were normalized to snoRNA expression in untreated cell lysates (input) using the 2^{-dCt} method. IgG pulldown was used as negative control. The data represent technical triplicates. (C) *In vitro* up-regulation of snoRNAs using 3'-end-directed 3GAs in murine primary fibroblasts. Expression levels were normalized to U6 using the 2^{-dCt} method. (D) Scratch-wound healing in primary murine fibroblasts at 12 h after scratch-wound placement. Data are presented as mean% of 3GA-Control ± SEM. #P< 0.1 and **P< 0.01 compared with 3GA-Control (t-test). Each data point represents an independent experiment performed in triplicate.

Discussion

In the present study, we have gathered evidence for an independent role of orphan snoRNAs in cardiovascular disease. First, we demonstrated significant associations of SNPs in the 14q32 snoRNA locus with cardiovascular events in a large population-based study. Second, we showed differential expression of 14q32 snoRNAs throughout the human vasculature. And third, we show regulation of 14q32 snoRNAs, in human tissue samples and in human plasma after cardiovascular disease. The 14q32 microRNAs and lncRNAs have previously been implied in cardiovascular pathology. However, here we uncover evidence that the 14q32 orphan snoRNAs play an independent role in cardiovascular disease for the first time.

Such an individual and independent role of 14q32 snoRNAs in cardiovascular disease was supported by our findings in our candidate gene study performed in the PROSPER study. Not only did we find the highest density of significantly associated SNPs of all 14q32 regions in the snoRNA-cluster, the fact that there are recombination hotspots that separate the snoRNA-region from the MEG3 and microRNA-cluster in the 14q32 locus also strongly implies an independent role of 14q32 snoRNAs in cardiovascular pathology. After correction for multiple testing per gene, only four SNPs in the snoRNA-region, as well two SNPs in the more remote MEG9 gene, remained significantly associated with cardiovascular endpoints. The snoRNA-SNPs associated specifically with heart failure. Even though we have no comparison to healthy human heart tissue, we do show that the 14q32 snoRNAs are abundantly expressed in the failing human heart.

However, we must keep in mind that on the used genome wide screening arrays, SNPs are selected preferably in coding sequences, and thus, none of the SNPs included in our analyses was located directly within a snoRNA gene itself. With the revolution of ncRNA research, it appears that we have stumbled upon an unexpected weakness in all the large genomic studies that have been performed in recent years, as most noncoding regions have been excluded or at least understudied.

We have previously described a regulatory role for several 14q32 microRNAs in vascular remodelling, in neovascularization, as well as in atherosclerosis and restenosis[4,5,37]. We also found that 14q32 microRNAs are regulated in distinct temporal expression patterns during vascular remodelling and that both the microRNA's temporal regulation, as well as its basal expression levels, is independent of its genomic location within the cluster. Looking at the 14q32 snoRNAs, we found a similar phenomenon. For example, even though all the snoRNAs are processed from adjacent introns of the SNHG23 host gene, SNORD113.2 showed very distinct expression patterns throughout the vasculature. Furthermore, the 14q32 snoRNAs showed differential regulation after both vein graft failure and after STEMI.

These findings indicate a leading role for posttranscriptional regulation processes in 14q32 snoRNA expression. However, they also indicate individual roles for all 14q32 snoRNAs in vascular remodelling and cardiovascular disease. Thus, whether or not a snoRNA is regulated during cardiovascular disease appears independent of its genomic location, but maybe dependent on its function instead.

Perhaps our best clues about these functions and about the mechanisms-of-action of orphan snoRNAs come from a highly similar ncRNA cluster, located on human locus 15q11. Like the 14q32 locus, the 15q11 cluster is imprinted. The locus also encodes multiple ncRNA genes, including two copy sets of orphan C/D box snoRNAs, SNORD115 (48 copies), and SNORD116 (29 copies). Deletions in the 15q11 locus cause Prader–Willi syndrome, which is characterized by cognitive disabilities, low muscle tone, short stature, incomplete sexual development, and a chronic feeling of hunger that can lead to morbid obesity. It is believed that the snoRNAs, particularly SNORD116, play a major role in Prader–Willi pathology. Studies have shown that 15q11 orphan snoRNAs can influence mRNA expression levels of over 200 genes, as well as each other's[38]. The 15q11 snoRNAs have been shown to direct alternative splicing of target mRNAs as well as influence mRNA editing[39,40]. In exploratory experiments, we did not find evidence of 14q32 snoRNA interactions with the spliceosome, even though this does not fully exclude a function for 14q32 snoRNAs in alternative splicing. However, we did find that both the human 14q32 snoRNAs and the murine 12F1 snoRNAs bind to predominantly to Fibrillarin, the canonical 2'O-ribose-methyltransferase associated with C/D box snoRNAs. Furthermore, the canonical snoRNA seed sequences, the nine nucleotide directly upstream of the C- and D'-boxes are highly conserved between the human 14q32 and murine 12F1 snoRNAs. This implies that 14q32 snoRNAs direct 2'O-ribose-methylation of their target RNAs and that their target-set, rather than their mechanism-of-action, is noncanonical. 2'O-ribose-methylation can protect RNAs from editing[40], which would fit with the findings for the 15q11 cluster.

Partial deletions and loss of imprinting also occur in the 14q32 locus and lead to a broad range of different pathologies. However, cluster-wide deletions are embryonically lethal. Interestingly, knockout of 12F1 lncRNA Meg3 in mice led to over-expression of several pro-angiogenic genes, including VEGF and DLL4, and to a drastically increased vascular capillary density in mouse embryos[41].

Besides alternative splicing and mRNA-editing, two other functions have been described for orphan snoRNAs. Some snoRNAs, like many lncRNAs, may function as competitive endogenous RNAs (ceRNAs), where they compete for binding of a microRNA with the microRNA's target mRNAs[42]. Other snoRNAs are processed into smaller RNAs and loaded into the RNA-induced silencing complex, where they function as snoRNA-derived microRNAs

and inhibit translation of their own set of target mRNAs[43]. We found that most human 14q32 snoRNAs indeed interact with the microRNA-processor as they also bind to AGO1. The binding to AGO1 could indicate a microRNA-like function; however, it is more likely that snoRNAs direct 2'O-ribose methylation of precursor microRNAs, via binding to the 2'O-ribose methyl-transferase Fibrillarin, as we recently showed that microRNAs are subject to Fibrillarin-dependent 2'O-ribose methylation[44]. This hypothesis is strengthened by the fact that the snoRNA seed sequences are conserved between mice and humans. Conservation in snoRNA seed sequences, implies conservation in the snoRNAs' target RNAs. MicroRNAs are one of the highest conserved RNA species. Therefore, it is plausible that the 14q32 snoRNAs target microRNAs, rather than rRNAs or snRNAs.

In summary, we have collected multiple lines of evidence for an independent role of 14q32 orphan snoRNAs in cardiovascular disease. Genetic variations in the 14q32 snoRNA-cluster are significantly associated with cardiovascular events, 14q32 snoRNAs are differentially expressed throughout the human vasculature and 14q32 snoRNA expression levels are regulated during cardiovascular disease. Therefore, we advocate that snoRNAs merit similar attention as other ncRNAs, such as microRNAs and lncRNAs, in future basic and clinical research, both within the field of cardiovascular disease and in other fields of research.

Acknowledgements

We thank Daphne van den Homberg for technical support. We kindly acknowledge Sudhir Agrawal and Idera Pharmaceuticals for the design and supply of the 3GAs.

References

1. Bartel DP. MicroRNAs: genomics, biogenesis, mechanism, and function. Cell 2004; 116:281–297.
2. Nossent AY, Eskildsen TV, Andersen LB, Bie P, Bronnum H, Schneider M, Andersen DC, Welten SM, Jeppesen PL, Hamming JF, Hansen JL, Quax PH, Sheikh SP. The 14q32 microRNA-487b targets the antiapoptotic insulin receptor substrate 1 in hypertension-induced remodeling of the aorta. Ann Surg 2013;258:743–751.
3. Welten SM, Goossens EA, Quax PH, Nossent AY. The multifactorial nature of microRNAs in vascular remodelling. Cardiovasc Res 2016;110:6–22.
4. Welten SM, Bastiaansen AJ, de JR, de Vries MR, Peters EH, Boonstra M, Sheikh SP, La MN, Kandimalla ER, Quax PH, Nossent AY. Inhibition of 14q32 MicroRNAs miR-329, miR-487b, miR-494 and miR-495 increases neovascularization and blood flow recovery after ischemia. Circ Res 2014;115:696–708.
5. Wezel A, Welten SM, Razawy W, Lagraauw HM, de Vries MR, Goossens EA, Boonstra MC, Hamming JF, Kandimalla ER, Kuiper J, Quax PH, Nossent AY, Bot I. Inhibition of MICRORNA-494 reduces carotid artery atherosclerotic lesion development and increases plaque stability. Ann Surg 2015;262:841–847; discussion 847–848.
6. Michalik KM, You X, Manavski Y, Doddaballapur A, Zornig M, Braun T, John D, Ponomareva Y, Chen W, Uchida S, Boon RA, Dimmeler S. Long noncoding RNA MALAT1 regulates endothelial cell function and vessel growth. Circ Res 2014;114:1389–1397.
7. Boon RA, Hofmann P, Michalik KM, Lozano-Vidal N, Berghäuser D, Fischer A, Knau A, Jae´ N, Schu¨rmann C, Dimmeler S. Long noncoding RNA Meg3 controls endothelial cell aging and function: implications for regenerative angiogenesis. J Am Coll Cardiol 2016;68:2589–2591.
8. Busch A, Eken SM, Maegdefessel L. Prospective and therapeutic screening value of non-coding RNA as biomarkers in cardiovascular disease. Ann Transl Med 2016;4:236.
9. Dechamethakun S, Muramatsu M. Long noncoding RNA variations in cardiometabolic diseases. J Hum Genet 2016;62:97–104.
10. Lorenzen JM, Thum T. Long noncoding RNAs in kidney and cardiovascular diseases. Nat Rev Nephrol 2016;12:360–373.
11. Ballantyne MD, McDonald RA, Baker AH. lncRNA/MicroRNA interactions in the vasculature. Clin Pharmacol Ther 2016;99:494–501.
12. Creemers EE, van Rooij E. Function and therapeutic potential of noncoding RNAs in cardiac fibrosis. Circ Res 2016;118:108–118.
13. Archer K, Broskova Z, Bayoumi AS, Teoh JP, Davila A, Tang Y, Su H, Kim IM. Long non-coding RNAs as master regulators in cardiovascular diseases. Int J Mol Sci 2015; 16:23651–23667.
14. Ounzain S, Burdet F, Ibberson M, Pedrazzini T. Discovery and functional characterization of cardiovascular long noncoding RNAs. J Mol Cell Cardiol 2015;89:17–26.
15. Devaux Y, Zangrando J, Schroen B, Creemers EE, Pedrazzini T, Chang CP, Dorn GW, Thum T, Heymans S. Long noncoding RNAs in cardiac development and ageing. Nat Rev Cardiol 2015;12:415–425.
16. Philippen LE, Dirkx E, da Costa-Martins PA, de Windt LJ. Non-coding RNA in control of gene regulatory programs in cardiac development and disease. J Mol Cell Cardiol 2015;89:51–58.
17. Thum T, Condorelli G. Long noncoding RNAs and microRNAs in cardiovascular pathophysiology. Circ Res 2015;116:751–762.
18. Uchida T, Wada H, Mizutani M, Iwashita M, Ishihara H, Shibano T, Suzuki M, Matsubara Y, Soejima K, Matsumoto M, Fujimura Y, Ikeda Y, Murata M. Identification of novel mutations in ADAMTS13 in an adult patient with congenital thrombotic thrombocytopenic purpura. Blood 2004;104:2081–2083.
19. Boon RA, Jae N, Holdt L, Dimmeler S. Long noncoding RNAs: from clinical genetics to therapeutic targets? J Am Coll Cardiol 2016;67:1214–1226.

20. Kiss T. Small nucleolar RNA-guided post-transcriptional modification of cellular RNAs. EMBO J 2001;20:3617–3622.
21. Brandis KA, Gale S, Jinn S, Langmade SJ, Dudley-Rucker N, Jiang H, Sidhu R, Ren A, Goldberg A, Schaffer JE, Ory DS. Box C/D small nucleolar RNA (snoRNA) U60 regulates intracellular cholesterol trafficking. J Biol Chem 2013;288:35703–35713.
22. Michel CI, Holley CL, Scruggs BS, Sidhu R, Brookheart RT, Listenberger LL, Behlke MA, Ory DS, Schaffer JE. Small nucleolar RNAs U32a, U33, and U35a are critical mediators of metabolic stress. Cell Metab 2011;14:33–44.
23. Cavaille J, Seitz H, Paulsen M, Ferguson-Smith AC, Bachellerie JP. Identification of tandemly-repeated C/D snoRNA genes at the imprinted human 14q32 domain reminiscent of those at the Prader-Willi/Angelman syndrome region. Hum Mol Genet 2002;11:1527–1538.
24. Shepherd J, Blauw GJ, Murphy MB, Bollen EL, Buckley BM, Cobbe SM, Ford I, Gaw A, Hyland M, Jukema JW, Kamper AM, Macfarlane PW, Meinders AE, Norrie J, Packard CJ, Perry IJ, Stott DJ, Sweeney BJ, Twomey C, Westendorp RG. Pravastatin in elderly individuals at risk of vascular disease (PROSPER): a randomised controlled trial. Lancet 2002;360:1623–1630.
25. Shepherd J, Blauw GJ, Murphy MB, Cobbe SM, Bollen EL, Buckley BM, Ford I, Jukema JW, Hyland M, Gaw A, Lagaay AM, Perry IJ, Macfarlane PW, Meinders AE, Sweeney BJ, Packard CJ, Westendorp RG, Twomey C, Stott DJ. The design of a prospective study of pravastatin in the elderly at risk (PROSPER). PROSPER Study Group. PROspective study of pravastatin in the elderly at risk. Am J Cardiol 1999;84:1192–1197.
26. Trompet S, de Craen AJ, Postmus I, Ford I, Sattar N, Caslake M, Stott DJ, Buckley BM, Sacks F, Devlin JJ, Slagboom PE, Westendorp RG, Jukema JW. Replication of LDL GWAs hits in PROSPER/PHASE as validation for future (pharmaco)genetic analyses. BMC Med Genet 2011;12:131.
27. Ripa RS, Jorgensen E, Wang Y, Thune JJ, Nilsson JC, Sondergaard L, Johnsen HE, Kober L, Grande P, Kastrup J. Stem cell mobilization induced by subcutaneous granulocyte-colony stimulating factor to improve cardiac regeneration after acute ST-elevation myocardial infarction: result of the double-blind, randomized, placebocontrolled stem cells in myocardial infarction (STEMMI) trial. Circulation 2006;113:1983–1992.
28. Simons KH, Peters HAB, Jukema JW, de Vries MR, Quax PHA. A protective role of IRF3 and IRF7 signalling downstream TLRs in the development of vein graft disease via type I interferons. J Intern Med 2017;282:522–536.
29. Valleron W, Laprevotte E, Gautier EF, Quelen C, Demur C, Delabesse E, Agirre X, Prosper F, Kiss T, Brousset P. Specific small nucleolar RNA expression profiles in acute leukemia. Leukemia 2012;26:2052–2060.
30. Mitchell PS, Parkin RK, Kroh EM, Fritz BR, Wyman SK, Pogosova-Agadjanyan EL, Peterson A, Noteboom J, O'Briant KC, Allen A, Lin DW, Urban N, Drescher CW, Knudsen BS, Stirewalt DL, Gentleman R, Vessella RL, Nelson PS, Martin DB, Tewari M. Circulating microRNAs as stable blood-based markers for cancer detection. Proc Natl Acad Sci USA 2008;105:10513–10518.
31. Machiela MJ, Chanock SJ. LDlink: a web-based application for exploring populationspecific haplotype structure and linking correlated alleles of possible functional variants. Bioinformatics 2015;31:3555–3557.
32. Machiela MJ, Chanock SJ. LDassoc: an online tool for interactively exploring genomewide association study results and prioritizing variants for functional investigation. Bioinformatics 2018;34:887–889.
33. Taylor J, Tibshirani R. A tail strength measure for assessing the overall univariate significance in a dataset. Biostatistics 2005;7:167–181.
34. Ploner A, Ploner C, Lukasser M, Niederegger H, Huttenhofer A. Methodological obstacles in knocking down small noncoding RNAs. RNA 2009;15: 1797–1804.

35. Cavaille J, Bachellerie JP. Processing of fibrillarin-associated snoRNAs from premRNA introns: an exonucleolytic process exclusively directed by the common stembox terminal structure. Biochimie 1996;78:443–456.
36. Kiss T, Filipowicz W. Exonucleolytic processing of small nucleolar RNAs from premRNA introns. Genes Dev 1995;9:1411–1424.
37. Welten SMJ, de Jong RCM, Wezel A, de Vries MR, Boonstra MC, Parma L, Jukema JW, van der Sluis TC, Arens R, Bot I, Agrawal S, Quax PHA, Nossent AY. Inhibition of 14q32 microRNA miR-495 reduces lesion formation, intimal hyperplasia and plasma cholesterol levels in experimental restenosis. Atherosclerosis 2017;261:26–36.
38. Falaleeva M, Surface J, Shen M, de la Grange P, Stamm S. SNORD116 and SNORD115 change expression of multiple genes and modify each other's activity. Gene 2015;572:266–273.
39. Kishore S, Khanna A, Zhang Z, Hui J, Balwierz PJ, Stefan M, Beach C, Nicholls RD, Zavolan M, Stamm S. The snoRNA MBII-52 (SNORD 115) is processed into smaller RNAs and regulates alternative splicing. Hum Mol Genet 2010;19:1153–1164.
40. Vitali P, Basyuk E, Le ME, Bertrand E, Muscatelli F, Cavaille J, Huttenhofer A. ADAR2-mediated editing of RNA substrates in the nucleolus is inhibited by C/D small nucleolar RNAs. J Cell Biol 2005;169:745–753.
41. Gordon FE, Nutt CL, Cheunsuchon P, Nakayama Y, Provencher KA, Rice KA, Zhou Y, Zhang X, Klibanski A. Increased expression of angiogenic genes in the brains of mouse meg3-null embryos. Endocrinology 2010;151:2443–2452.
42. Taulli R, Pandolfi PP. "Snorkeling" for missing players in cancer. J Clin Invest 2012;122: 2765–2768.
43. Ender C, Krek A, Friedlander MR, Beitzinger M, Weinmann L, Chen W, Pfeffer S, Rajewsky N, Meister G. A human snoRNA with microRNA-like functions. Mol Cell 2008;32:519–528.
44. van der Kwast R, van Ingen E, Parma L, Peters HAB, Quax PHA, Nossent AY. Adenosine-to-inosine editing of microRNA-487b alters target gene selection after ischemia and promotes neovascularization. Circ Res 2018;122:444–456.

Supplementary data

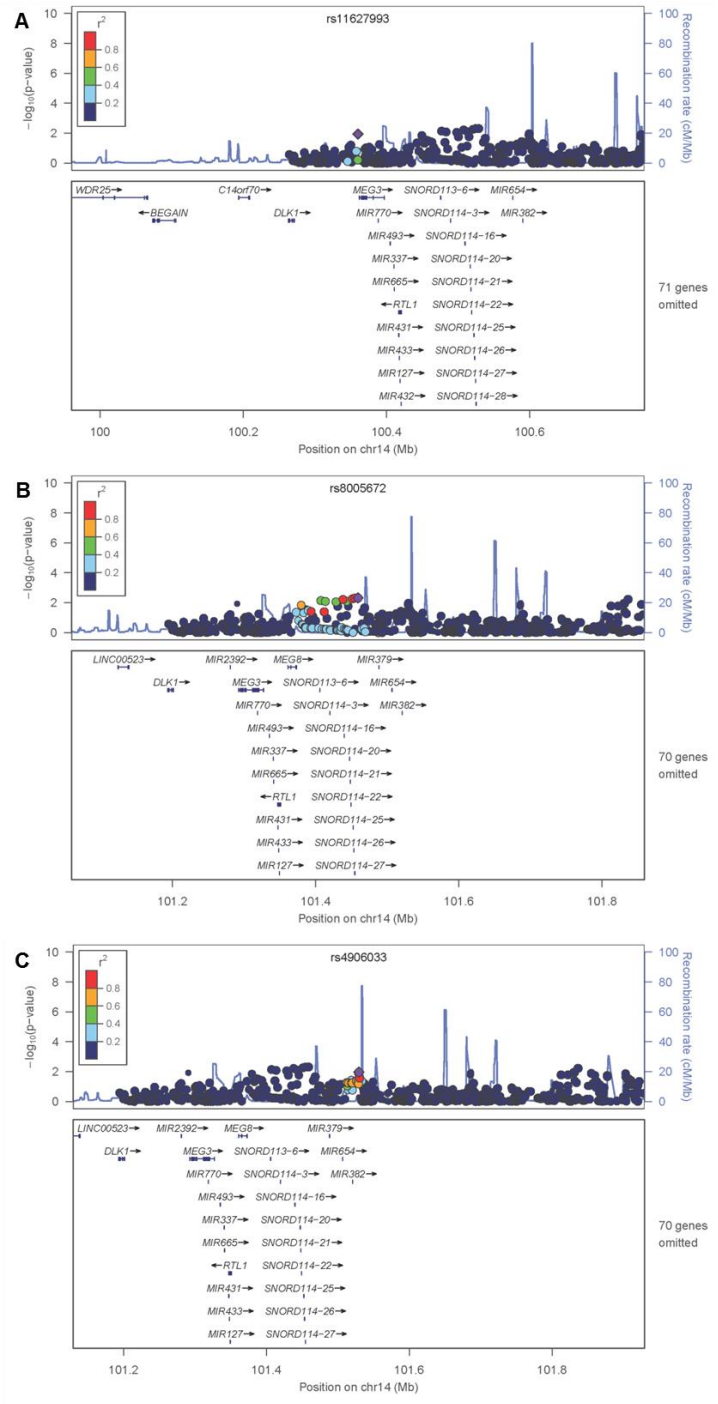

Supplemental Figure 1 Linkage of selected SNPs in *MEG3*, the snoRNA and microRNA clusters of the 14q32 locus. (A-C) Locuszoom images of r^2-values for SNPs in the *MEG3* (rs11627993), snoRNA (rs8005672) and microRNA (rs4906033) regions, respectively. The p-values correspond to the association between the SNPs and Heart Failure. Blue peaks represent recombination hotspots.

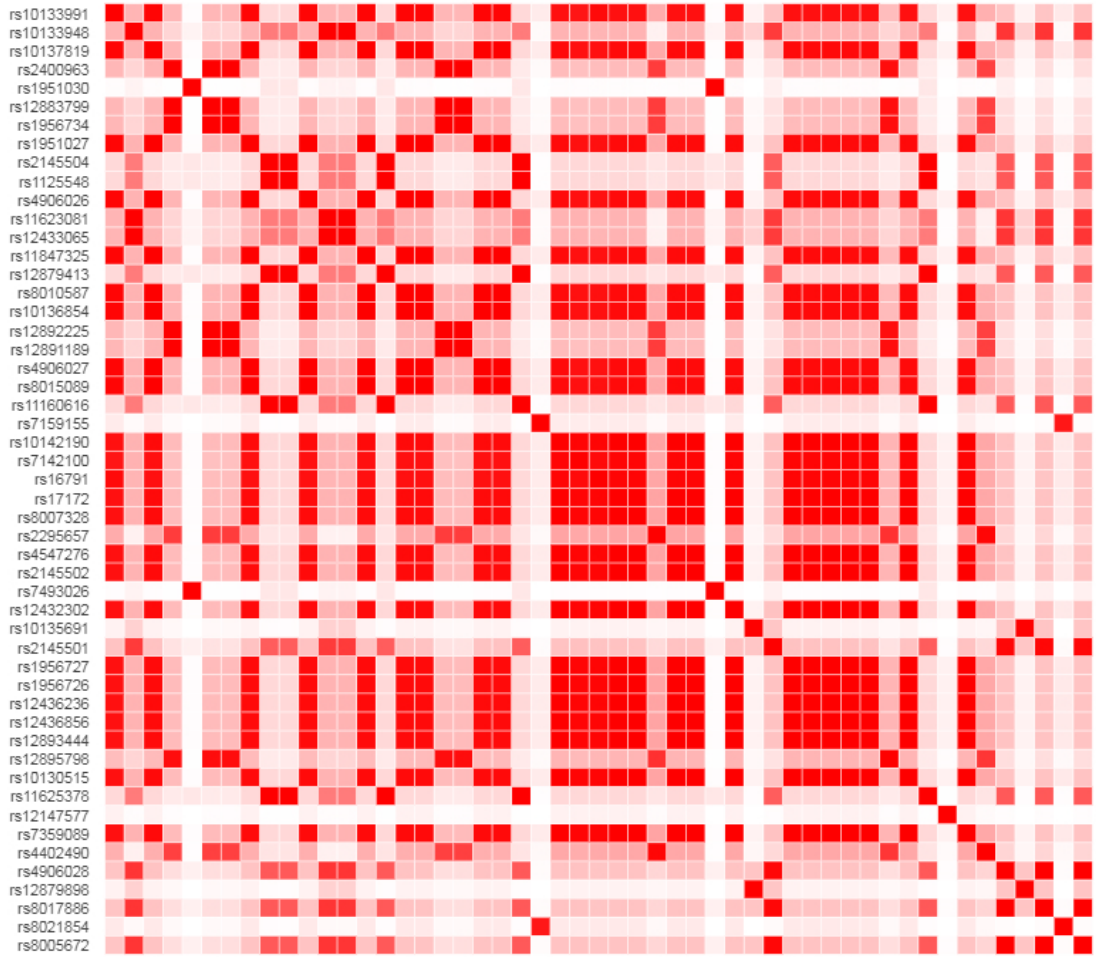

Supplemental Figure 2 Linkage between SNPs in the snoRNA cluster in the CEU-population. The same SNPs, in the same order, are placed on the X-axis as on the Y-axis. Linkage, expressed as r^2, is shown as a gradient from red to white, where red squares represent two SNPs that are in full linkage-disequilibrium and white squares represent two SNPs that are not linked at all.

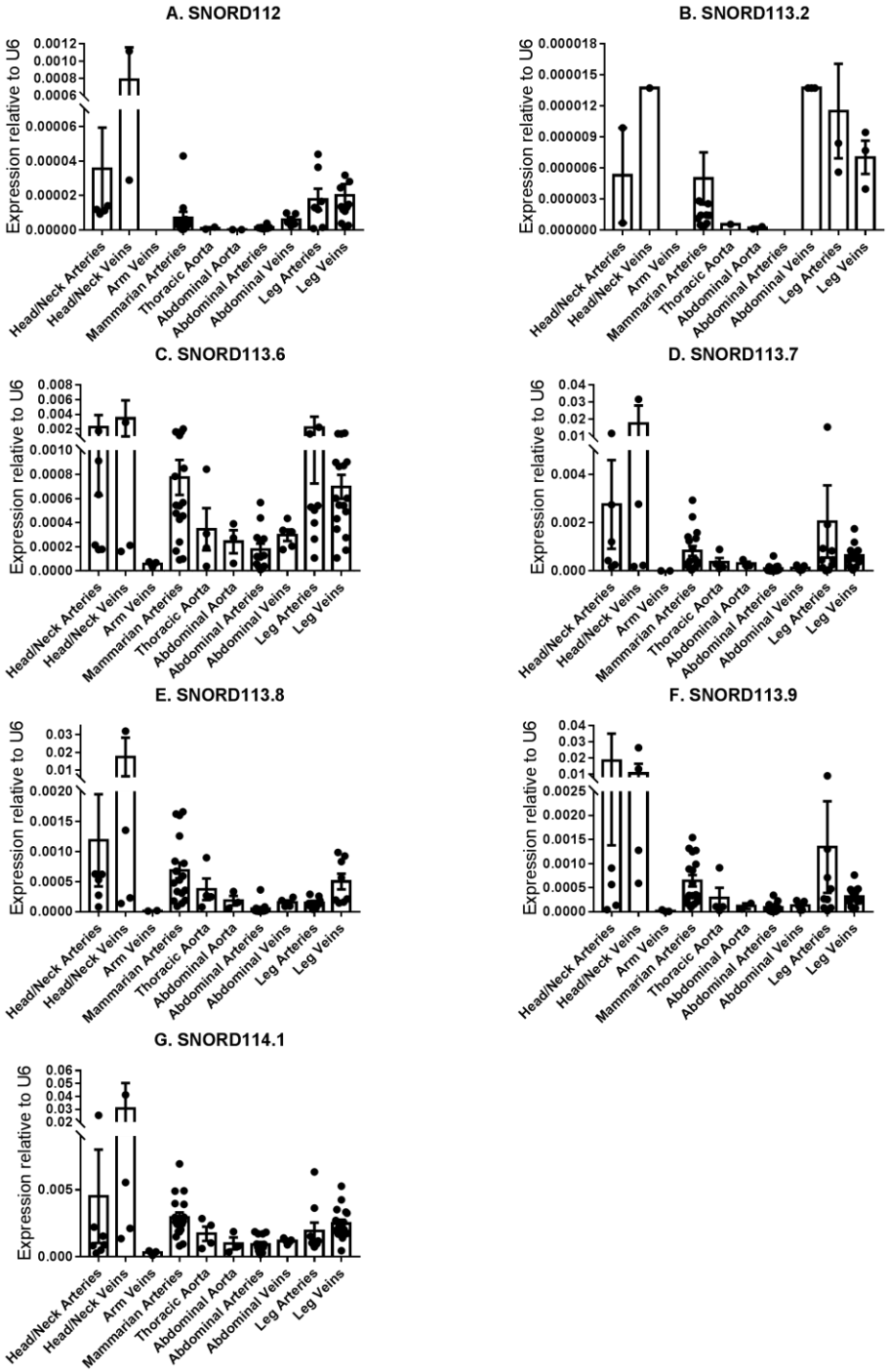

Supplemental Figure 3 Expression profiles of 14q32 snoRNAs throughout the human vasculature. Mean values are given and errors bars represent SEMs. U6 expression was used for normalization using the $2^{-\Delta Ct}$ method. N=95.

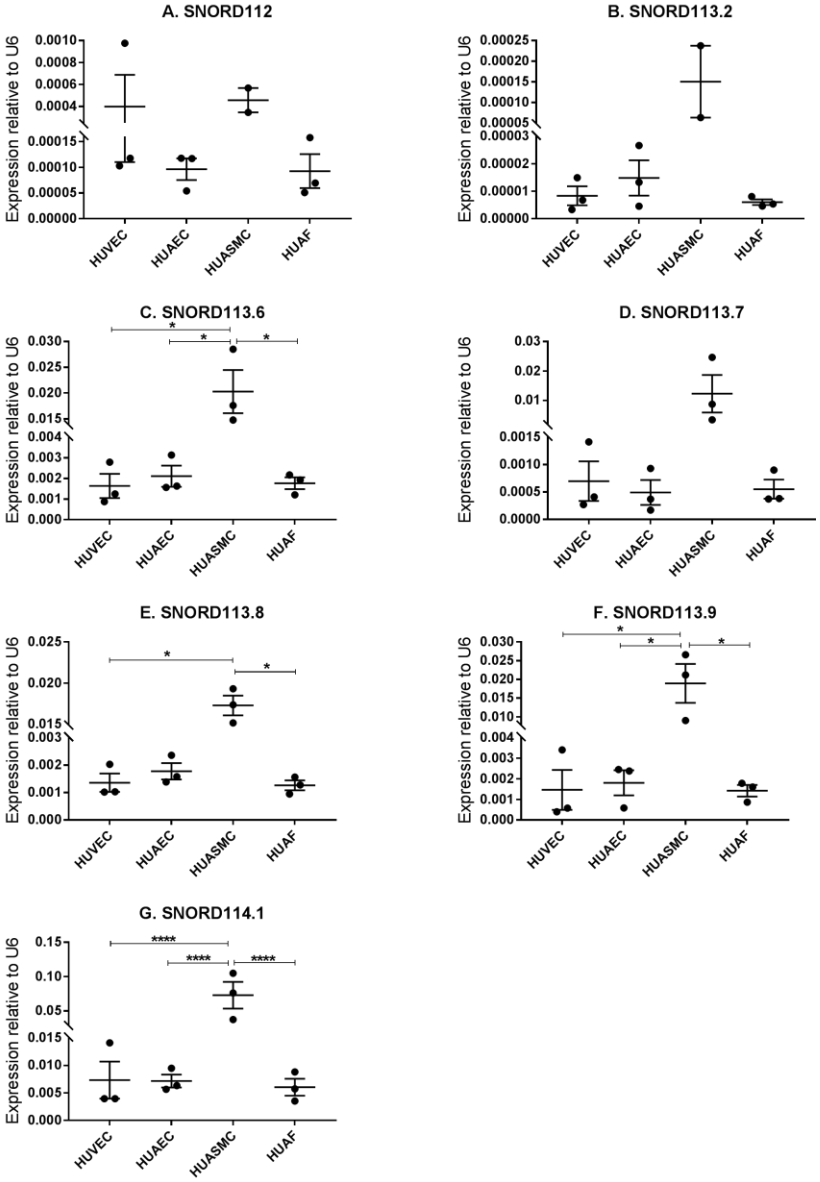

Supplemental Figure 4 Expression of 14q32 snoRNAs in primary human vascular cells. Mean values are given and errors bars represent SEMs. U6 expression was used for normalization using the $2^{-\Delta Ct}$ method. HUVEC: human umbilical venous endothelial cell; HUAEC: human umbilical arterial endothelial cell; HUASMC: human umbilical arterial smooth muscle cell; HUAF = human umbilical arterial fibroblast. * $p < 0.05$; ** $p < 0.01$ (t-test): N=3.

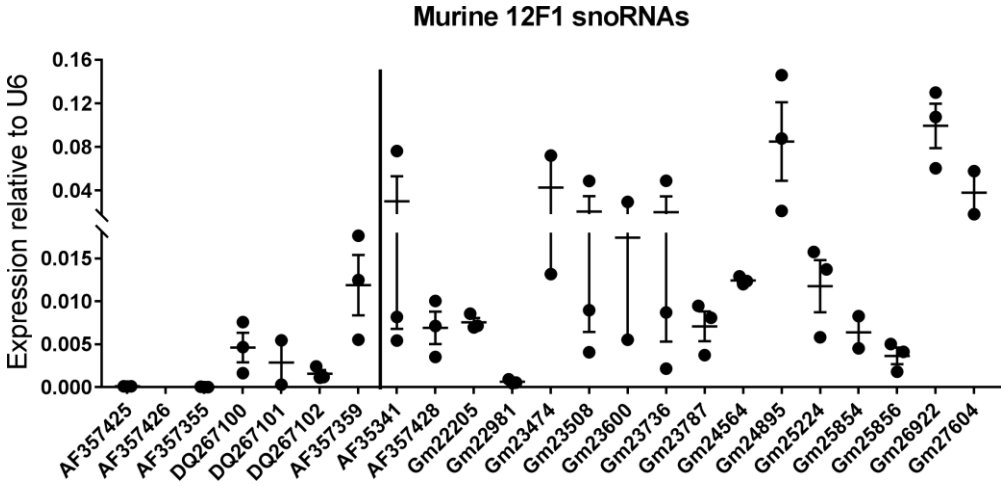

Supplemental Figure 5 Expression of annotated and predicted 12F1 snoRNAs in primary murine fibroblasts. Measurement were performed on three independent RNA isolations from independently cultured fibroblasts and errors bars represent SEMs. U6 expression was used for normalization using the $2^{-\Delta Ct}$ method. Annotated snoRNAs are depicted left of the vertical line, predicted snoRNAs are depicted right of the vertical line.

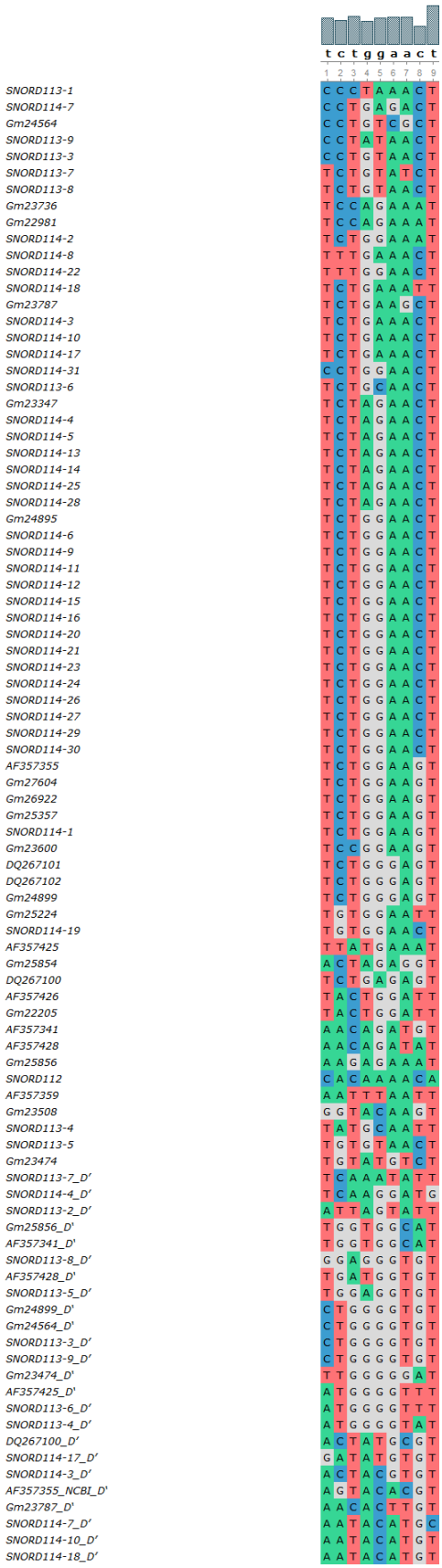

Supplemental Figure 6 Sequence-based alignment of canonical 'seed sequences'. The nine nucleotides directly upstream of C'- and D'-boxes, of human 14q32 snoRNAs (names starting with 'SNORD') and murine 12F1 snoRNAs (names starting with 'AF', 'DQ', or 'GM') are ordered based on sequence similarity.

Supplemental Table 1 Baseline characteristics of the PROSPER/PHASE study

	PROSPER/PHASE study (n=5244)
Continuous variables (mean, SD)	
Age (years)	75.3 (3.4)
Education (years)	15.1 (2.0)
Systolic blood pressure (mmHg)	154.6 (21.9)
Diastolic blood pressure (mmHg)	83.7 (11.4)
Height (cm)	165.2 (9.4)
Weight (kg)	73.3 (13.4)
Body mass index ($kg/m^{2)}$	26.8 (4.2)
Total cholesterol (mmol/L)	5.7 (0.9)
LDL cholesterol (mmol/L)	3.8 (0.8)
HDL cholesterol (mmol/L)	1.3 (0.4)
Triglycerides (mmol/L)	1.5 (0.7)
Categorical variables (n, %)	
Males	2524 (48.1)
Current smoker	1392 (26.5)
History of diabetes	544 (10.4)
History of hypertension	3257 (62.1)
History of angina	1424 (27.2)
History of claudication	354 (6.8)
History of myocardial infarction	708 (13.5)
History of stroke or TIA	586 (11.2)
History of vascular disease*	2336 (44.5)

*Any of stable angina, intermittent claudication, stroke, transient ischemic attack, myocardial infarction, peripheral artery disease surgery, or amputation for vascular disease more than 6 months before study entry.

Supplemental Table 2a All significant associations in the PROSPER/PHASE study.

Genomic Region	SNP	OR	P
Fatal or Non-Fatal Stroke and/or Coronary Events			
MEG3	rs12890215	1.136	0,04609
	rs4378559	1.135	0,0467
	rs11160607	1.133	0,04982
snoRNA	rs12879898	0.692	0,02596
Coronary Events			
DLK1	rs2273608	1,25	0,0246
MEG3	rs12431658	0,3566	0,04561
snoRNA	rs8021854	0,7249	0,02654
	rs12879898	0,6597	0,03137
	rs7159155	0,6605	0,0401
Cardiovascular Events			
MEG3	rs10144253	0,1229	0,03933
snoRNA	rs12879898	0,685	0,01651

Fatal or Non-Fatal Stroke and/or TIA			
microRNA	rs7342570	1.201	0,04927
Vascular Mortality			
snoRNA	rs2295657	1.231	0,02995
	rs12879898	0,5374	0,04767
MEG9	rs3742406	0,7996	0,01885
	rs2295655	0,7457	0,008417
	rs2295654	0,7422	0,007603
All-Cause Mortality			
MEG3	rs11160608	0,871	0,03604
	rs4906023	0,8731	0,03944
microRNA	rs11628379	0,7053	0,01991
	rs10132916	0,8514	0,03453
	rs12886869	0,8545	0,0389
	rs7161441	0,8458	0,03994
MEG9	rs2295655	0,8371	0,02158
	rs2295654	0,8337	0,01909
Hospitalization for Heart Failure			
MEG3	rs11627993	1.643	0.01165
MEG8	rs11852040	0,731	0,04402
snoRNA	rs8005672	0,7081	0,004873
	rs8017886	0,7083	0,004909
	rs4906028	0,7114	0,005507
	rs2145501	0,7128	0,006064
	rs2145504	0,6443	0,007216
	rs1125548	0,6443	0,007216
	rs11625378	0,639	0,008033
	rs12879413	0,6488	0,008168
	rs11160616	0,6512	0,00869
	rs4402490	1.299	0,01707
	rs2295657	1.286	0,01749
	rs10133948	0,7907	0,03894
	rs12433065	0,7921	0,04036
	rs11623081	0,7923	0,04062
microRNA	rs4906033	0,7314	0,01078
	rs4906034	0,7314	0,01078
	rs8003403	0,7347	0,01207
	rs8023048	0,7369	0,01298
	rs12893725	0,7612	0,02769
	rs4906032	0,784	0,03616
	rs4525426	0,7867	0,03984
	rs7342570	0,7551	0,04378
	rs6575812	0,7569	0,04711

Supplemental Table 2b Significant associations in the PROSPER/PHASE study after Correction for Multiple Testing, using False Discovery Rate (FDR; all SNPs in this table), or Bonferroni Correction (rs-numbers in bold print).

Genomic Region	SNP	OR	P	FDR-10% cut-off value for significance	Bonferroni cut-off value for significance
Hospitalization for Heart Failure					
snoRNA	**rs2145501**	0.7128	0.006064	0,0125	0,00625
	rs2145504	0.6443	0.007216	0,025	0,00625
	rs2295657	1.286	0.01749	0,0375	0,00625
	rs10133948	0.7907	0.03894	0,05	0,00625
Vascular Mortality					
MEG9	**rs2295655**	0,7457	0,00842	0,05	0,025
	rs3742406	0,7996	0,01885	0,1	0,025
All-Cause Mortality					
MEG9	**rs2295655**	0,8371	0,0216	0,05	0,025

Supplemental Table 3 Vascular tissue samples used for snoRNA analysis

	N	Mean age (SD)	Male (%)	Peri-malignancy (%)
Upper limb veins	3	51.3 (12.1)	100	0
Lower limb arteries	11	63.3 (14.0)	81.8	0
Lower limb veins	18	67.7 (13.4)	61.1	0
Abdominal arteries	14	67.6 (9.3)	64.3	64.3
Abdominal veins	5	63.0 (12.1)	80.0	60.0
Head and neck arteries	9	54.0 (28.0)	33.3	22.2
Head and neck veins	5	52.8 (18.8)	60.0	40.0
Abdominal aorta	4	65.8 (14.1)	25.0	0
Thoracic aorta	5	69.8 (16.7)	40.0	0
Mammarian arteries	18	62.0 (9.3)	72.2	0
Atrial appendage	1	50 (-)	100	0
Radial artery	1	42 (-)	100	0
Umbilical artery	1	0 (-)	unknown	0
Total	95	61.8 (16.5)	63.2	16.8

Supplemental Table 4 3GA Sequences.

Oligonucleotide	Sequence
3GA-Control	3’-TGTACGACTCCATAACGGT-X-TGGCAATACCTCAGCATGT-3’
3GA-AF357425	3’-GGGTTTAATCACTGTCCTC-X-CTCCTGTCACTAATTTGGG-3’
3GA-AF357426	3’-AGTATGTTGTCATCGTCTA-X-ATCTGCTACTGTTGTATGA-3’
3GA-DQ267100	3’-ACCTCAGACTCTCAGACGC-X-CGCAGACTCTCAGACTCCA-3’
3GA-DQ267101	3’-TGGAACTCAGACTCCCAGA-X-AGACCCTCAGACTCAAGGT-3’
3GA-AF357355	3’-TGAATCTCAGACTTCCAGA-X-AGACCTTCAGACTCTAAGT-3’
3GA-DQ267102	3’-ACCTCAGACTCCCAGACCT-X-TCCAGACCCTCAGACTCCA-3’

‘X’: Phosphorothioate linker

‘NNN’: 2’-O-methyl-modified DNA nucleotides

Supplemental Table 5 qPCR Primer Sequences

Oligonucleotide	Sequence
sno112.FW	TGGACCAATGATGAGACAGTG
sno112.Rev	GTGCAGAACTGGATTAATCATG
sno113.2-FW	TAGCCAATCATTAGTATTCTGAGC
sno113.2-Rev	AACCTCTGAGTTACAGAATCTA
sno113.6-FW	TGGACCAGTGATGAATATCATG
sno113.6-Rev	TGGACCTCAGAGTTGCAGATG
sno113.7-FW	TGGATCAATGATGAGTATGCGT
sno113.7-Rev	GACCTCAGAGATACAGACAGG
sno113.8-FW	TGGACCAATGATGAGATTGG
sno113.8-Rev	GGACCTCAGAGTTACAGATGGC
sno113.9-FW	GGATCAATGATGAGTACCCTG
sno113.9-Rev	TGGACCTCAGAGTTATAGGG
sno114.1-FW	GGACCTATGATGATGACTGG
sno114.1-Rev	TGGACCTCAGACTTCCAGACC
DQ267100-FW	CAATGATGACTGTGGGTGCT
DQ267100-RV	CCTCAGACTCTCAGACGCATA
DQ267102-FW	GATGACCTCTGGTGCCGTAT
DQ267102-RV	TGGACCTCAGACTCCCAGAC
DQ267101-FW	TCAATGATGACCAGCGGTAG
DQ267101-RV	TGGAACTCAGACTCCCAGAT
AF357426-FW	TGACCTTGTCTATATTATAAGTCAT
AF357426-FW	ACCTCAGAATCCAGTATGTTGTCA
AF357355-FW	GGGTGGGTTATGAGTTGTGG
AF357355-RV	TCTCAGACTTCCAGACATGTACTCA
AF357425-FW	AGGAGCATGGGGTTTCTGAC
AF357425-RV	TTTCATAAGGGTTTAATCACTGTCC
Gm26922_FW	ACAAAGGGTGGCGTATGAGT
Gm26922_RV	TCAGACTTCCAGACATGTACTCA

AF357428_FW	AGGACCGATGATGAGATCTGA
AF357428_RV	TGTTCATGTCATCGAGAAACACT
AF357341_FW	ATCTGGTGGCATCTGACTGT
AF357341_RV	GACATCTGTTCTCATGGCTGT
Gm23508_FW	CCTCTGGTAGCACACGATTTG
Gm23508_RV	CAGACTTCCAGACCTGTACCC
Gm25224_FW	TGATGACTCTGGTGGTGTGG
Gm25224_RV	GGACCTGAGAATTCCACATATGC
Gm23600_FW	AATGATGGCCAGTGATGATGT
Gm23600_RV	GACGACCAGACCTGTAGCTA
Gm23736_FW	TGATGAGATCTGGTGGCGTT
Gm23736_RV	GGATACTTGGCGTTCATGGAG
Gm23474_FW	TCAGTGAGGAGAACTTGGGG
Gm23474_RV	GACCTCAGAGACATACATGGGT
Gm27604_FW	TCTTGTTGGAGGTGAGCAGT
Gm27604_RV	CTCAGACTTCCGGACCTGTT
Gm24564_FW	CTGACCAATGATGAGAATTCTGG
Gm24564_RV	AGCGACAGGGTTAATCATAATCA
Gm24895_FW	GGCCAATGATGACGAGGTTT
Gm24895_RV	TGGACCTCAGACCTCTAGTGA
Gm25854_FW	ACCGGTGGCATTTGACTCAT
Gm25854_RV	GGATCTTGGTGTTTCAGACTCA
Gm22205_FW	TGACTGATCCTGAGCACTGT
Gm22205_RV	AGATCTCAAAGTTCCAGACATGT
Gm25856_FW	CAATGATGAGATCTGGTGGCA
Gm25856_RV	AGATTTCTCTTGACATGGATGCC
Gm22981_FW	GGACCGATGATGAGATCTGG
Gm22981_RV	TTCTGGATACTTGGCGTTCA
Gm23787_FW	CCAAGGTATGAGAGAGATGACG
Gm23787_RV	GGACCTCTGAGCTTCAGACAA
U6-FW	AGAAGATTAGCATGGCCCCT
U6-RV	ATTTGCGTGTCATCCTTGCG
GAPDH-FW	CACCACCATGGAGAAGGC
GAPDH-RV	AGCAGTTGGTGGTGCAGGA

Supplemental Table 6 Associations of SNPs, inside 14q32 gene regions, with CAD in the Cardiogram Meta-Analysis.

Genomic Region	SNP	Log Odds (OR)	P
DLK1	rs1555406	0,0510275 (1,124676187)	0,020927
IG-DMR	rs12437020*	-0,039967 (0,912080981)	0,037739
RTL1/ MIR493-MIR136	rs4906018	0,0389087 (1,093726412)	0,018723
	rs1077411*	0,0495353 (1,120818524)	0,037604
	rs1077412*	0,0612703 (1,151516857)	0,02932
snoRNA	rs1956734*	-0,041743 (0,908357487)	0,016671
	rs2295657*	-0,038137 (0,915931299)	0,019897
	rs10135691	0,0487901 (1,118896976)	0,031895
	rs4402490	0,034168 (1,081852368)	0,03986
	rs12879898	-0,050005 (0,891240267)	0,049692
MEG9	rs2007291	0,039289 (1,094684579)	0,022437

*Also associates with cardiovascular endpoints in PROSPER

Chapter 4

miRMap: profiling 14q32 microRNA expression and DNA methylation throughout the human vasculature

Frontiers in Cardiovascular Medicine 2019 Aug 8;6:113

EAC Goossens[1,2]
MR de Vries[1,2]
KH Simons[1,2]
H Putter[3]
PHA Quax[1,2]
AY Nossent[1,4,5]

[1]Department of Surgery and [2]Einthoven Laboratory for Experimental Vascular Medicine, Leiden University Medical Center, Leiden, The Netherlands; [3]Department of Biomedical Data Sciences, Leiden University Medical Center, Leiden, Netherlands, [4]Department of Laboratory Medicine, Medical University of Vienna, Vienna, Austria, [5]Department of Internal Medicine II, Medical University of Vienna, Vienna, Austria

Abstract

Aims: MicroRNAs are regulators of (patho)physiological functions with tissue-specific expression patterns. However, little is known about inter-vascular differences in microRNA expression between blood vessel types or vascular beds. Differences in microRNA expression could influence cardiovascular pathophysiology at specific sites in the vasculature. Therefore, we aimed to map expression profiles of vasoactive 14q32 microRNAs throughout the human vasculature, as well as expression of vasoactive target genes of the 14q32 microRNAs. Furthermore, we aimed to map the DNA methylation status of the 14q32 locus, which has been linked to cardiovascular disease.

Methods and Results: We collected 109 samples from different blood vessels, dissected during general surgery. Expression of a representative set of 17 14q32 microRNAs was measured in each sample. All 17 microRNAs showed a unique expression pattern throughout the vasculature. 14q32 microRNA expression was highest in lower limb vessels and lowest in head and neck vessels. All 17 microRNAs were expressed more abundantly in arteries than in veins. Throughout the human vasculature, we observed trends toward an inverse correlation between expression levels of the 14q32 microRNAs and their vasoactive target genes. DNA methylation of the 3 Differentially Methylated Regions (DMRs) along the 14q32 locus did not associate with primary or mature microRNA expression. However, hyper-methylation in venous coronary artery bypass grafts compared to arterial bypass grafts was observed in the Intergenic-DMR and MEG3-DMR. In patients with end-stage peripheral arterial disease we found differential DNA methylation throughout all DMRs in their lower limb veins. These findings were confirmed in a mouse model for vein-graft disease in which we found regulated 14q32 DNA methylation during the active phase of vascular remodelling. In ischemic tissues of a murine hind limb ischemia model we observed an increase in DNA methylation associated with increased ischemia over time.

Conclusions: We show that 14q32 microRNAs are abundantly expressed in the human vasculature and that expression differs significantly between different blood vessels. 14q32 DNA methylation also varies throughout the vasculature and is associated with vascular health, independently of microRNA levels. These findings could have important implications for future research and for future site-specific targeting of epigenetics-based therapeutics.

Introduction

Cardiovascular disease is the collective term for a variety of diseases that have the highest morbidity and mortality rates worldwide[1]. The pathophysiology of cardiovascular disease is multifactorial and different locations in the human vasculature are prone to different types of cardiovascular disease. For example, atherosclerosis occurs predominantly in large and medium sized arteries at locations with disturbed flow, such as bifurcations and curvatures[2], whereas arterial aneurysm formation occurs often in the aortic wall or in intracranial arterial walls[3,4]. This suggests that local differences in the vasculature are important in the pathophysiology of cardiovascular disease. In this study, we focus on microRNAs and differences in their intervascular expression levels.

MicroRNAs (miRs) are a class of small endogenous noncoding RNA molecules of approximately 22 nucleotides in length. Mature microRNAs are single-stranded RNA molecules that bind to the 3'-untranslated region (3'UTR) of their target mRNAs in order to inhibit mRNA translation into proteins.

Individual microRNAs have the ability to inhibit the expression of multiple, up to several hundred, target genes. Therefore, they can function as master switches in (patho)physiological processes[5], including cardiovascular disease. MicroRNAs have been shown to regulate different cardiovascular remodelling processes and pathologies[6-9]. Moreover, it was recently found that microRNA expression differs between atherosclerotic plaques and non-atherosclerotic arteries[10-12]. MicroRNAs are potentially important new therapeutic targets in the treatment of cardiovascular disease[13-15].

Our group was the first to describe that a large gene cluster of 54 individual microRNA genes on the long arm of human chromosome 14 (14q32) plays a major role in various forms of vascular remodelling and cardiovascular disease. The 14q32 locus is also known as DLK1-DIO3 locus. For example, inhibition of miR-329, miR-494, miR-487b, and miR-495 in mice stimulated neovascularization after hindlimb ischemia[16], but inhibition of miR-494 in mice also decreased atherosclerosis and increased plaque stability[17]. Moreover, inhibition of miR-495 reduced accelerated atherosclerosis and intimal hyperplasia in mice[18]. Furthermore, miR-487b plays a role in angiotensin II-induced aneurysm formation in rats[19]. Wang et al. also observed the antiangiogenic effect of miR-329[20]. Moreover, knockdown of miR-494 resulted in an increase in the heart's sensitivity to ischemia-reperfusion injury after myocardial infarction in mice[21]. Finally, the 14q32 microRNA cluster was also shown to be associated with bicuspid aortic valve disease[22].

We know that different vascular beds show different susceptibilities to various types of cardiovascular disease and that microRNAs play an important role in cardiovascular pathology[14]. Yet, we know little about expression profiles of vasoactive microRNAs

throughout the vasculature. MicroRNA expression in general is highly tissue-specific[23], which was already shown by Wienholds et al[24]. However, microRNA expression can also vary significantly between regions within tissues. For example, the vascular microRNA miR-126 has been shown to be vascular endothelial cell-specific[25], whereas another vascular microRNA, miR-145, is mainly expressed in vascular smooth muscle cells[12,26]. Both microRNAs have important roles in neovascularization, atherosclerosis, and aneurysm formation[14,27-30]. 14q32 microRNAs also show differential expression throughout the vasculature. For example miR-329, which is abundantly expressed in the femoral artery of mice, showed low to no expression in the carotid artery and miR-494, on the other hand, is expressed in the carotid artery and is upregulated in unstable human carotid artery lesions[17].

Besides expression of the 14q32 microRNAs, DNA methylation status of the 14q32 locus also plays a role in cardiovascular disease[31]. DNA methylation is subject to mutagenic loss, but is conserved in CpG-islands that are predominantly located in promotor regions of genes[32]. DNA methylation varies between individuals and, therefore, CpG-rich regions are called Differentially Methylated Regions (DMRs). The human 14q32 locus contains 3 DMRs, namely an Intergenic DMR (IG-DMR), located between the DLK1 and the MEG3 genes, a DMR partially overlapping the promotor region of MEG3 (MEG3-DMR), and a DMR located near the MEG8 gene (MEG8-DMR), all upstream of the microRNA gene cluster. Variations in the 14q32 DNA methylation status are associated with differences in microRNA expression in type 2 diabetes mellitus[33], murine lupus[34], and oncogenesis[35-39]. More importantly, similar to the 14q32 microRNA expression, methylation of the 14q32 locus has been shown to associate with atherosclerosis[31] and with peripheral arterial disease[40].

In this study, we aimed to map expression profiles of 14q32 microRNAs as well as DNA methylation throughout the human vasculature. We collected 109 different blood vessel samples in a biobank that were harvested during general surgery. We profiled the expression of a representative subset of the 14q32microRNAs and quantified the DNA methylation status within the three 14q32 DMRs. As microRNAs act through expression levels of their target genes, expression levels of confirmed vasoactive target genes for each of the profiled 14q32 microRNAs were measured. We investigated the impact of potential confounding factors on 14q32 microRNA expression and DNA methylation, including age, sex, and malignancies, which have been shown to associate with microRNA expression[41-43] and DNA methylation[35,36,38,39,44-46] profiles in general. Finally, we confirmed DNA methylation in relevant mouse models of cardiovascular disease i.e., vein graft disease and hind limb ischemia.

Materials and methods

Sample Collection

The miRMap biobank was compiled of 109 different human vascular tissue samples (Supplementary Table 1), which were collected during gastroenterological-, head- and neck-, vascular-, and thoracic surgery performed at the Leiden University Medical Center for various indications. Only surplus vessel tissue was used. Samples were collected in sterile Phosphate Buffered Saline (PBS) (30mL) with heparin (30µL of 1,000units/mL) immediately after dissection and were snap frozen at −80°C after draining of the liquid within 2 hours after collection.

All samples were anonymized and data that were collected from patients were only name of vessel, indication of surgery, sex, and age during surgery, so outcomes could not be traced back to individual persons. Collection, storage, and processing of the samples were performed in compliance with the Medical Treatment Contracts Act (Wet op de Geneeskundige Behandelingsovereenkomst (WGBO), art. 7:446-468 Burgerlijk Wetboek, 1995) and the Code of Conduct for Health Research using Body Material (Good Practice Code, Dutch Federation of Biomedical Scientific Societies, 2002) and the Dutch Personal Data Protection Act (Wet Bescherming Persoonsgegevens, 2001), according to Dutch law for using human tissue rest material in biobanks, following the principles outlined in the Declaration of Helsinki. As we only used surplus, anonymized material, Informed Consent was not required under Dutch law, and therefore not obtained.

Lower limb veins from six patients suffering from peripheral arterial disease in critical ischemic conditions were obtained during lower limb amputation surgery and collected in the Ampubase biobank in the Leiden University Medical Center (Supplementary Table 1). Inclusion criteria for the biobank were minimum age of 18 years and lower limb amputation, excluding ankle, foot, or toe amputations. The exclusion criteria were suspected or confirmed malignancy and inability to give informed consent. Directly after amputation, vessels were dissected from the amputated limb and snap-frozen at −80°C.

Sample collection was approved by the Medical Ethics Committee of the Leiden University Medical Center (Protocol No. P12.265) and written informed consent was obtained from all participants.

Hind Limb Ischemia Model

All animal experiments were approved by the committee on animal welfare of the Leiden University Medical Center (Leiden, The Netherlands) and all animal procedures were performed conform the guidelines from Directive 2010/63/EU of the European Parliament on the protection of animals used for scientific purposes. Wildtype C57Bl/6 mice (all male, aged

8–12 weeks, housed with water and chow ad libitum) anesthetized by intraperitoneal injection of midazolam (5mg/kg, Roche Diagnostics), medetomidine (0.5mg/kg, Orion), and fentanyl (0.05mg/kg, Janssen Pharmaceuticals). Left hind limb ischemia was induced by a single electrocoagulation of the left femoral arteria proximal to the superficial epigastric artery. Anesthesia was antagonized after surgery with flumazenil (0.5mg/kg, Fresenius Kabi) and atipamezole (2.5mg/kg, Orion). Buprenorphine (0.1mg/kg MSD Animal Health) was provided post-surgery as painkiller. Mice were anesthetized as described above. One group of mice (n = 4) was sacrificed without any intervention as baseline control group. Other groups were sacrificed 1 day and 3 days after hind limb surgery (4 mice per group). Hind limb muscles (adductor muscle, gastrocnemius muscle, and soleus muscle) from the ligated left hind limb and its internal control the right hind limb were removed and snap-frozen at −80°C.

Vein Graft Disease Model

ApoE3*Leiden mice, all male, aged 10–20 weeks, were housed with water and a western-type diet (ABdiets, ad libitum). This led to hypercholesterolemia above 12mmol/L, as determined before surgery (Roche Diagnostics). Vein graft surgery was performed by interposition of a donor caval vein in the carotid artery of recipient mice as previously described by De Vries et al[47]. Mice were anesthetized with midazolam (5mg/kg, Roche Diagnostics), medetomide (0.5mg/kg, Orion), and fentanyl (0.05mg/kg, Janssen Pharmaceuticals) and mice were monitored for adequacy of anesthesia by keeping track of breathing frequency and response to toe pinching. After surgery, anesthesia was antagonized with atipamezole (2.5mg/kg, Orion) and flumazenil (0.5mg/kg, Fresenius Kabi). As pain relieve buprenorphine (0.1mg/kg, MSD Animal Health) was provided post-surgery. Mice were sacrificed after 14 or 28 days (7 mice per group) by exsanguination under anesthesia. One mouse of the 14 days group was taken out because humane endpoint criteria were met. Vein grafts and native caval veins were harvested and snap-frozen at −80°C.

Isolation of Human Umbilical Venous Endothelial Cells (HUVECs), Human Umbilical Arterial Endothelial Cells (HUAECs), Human Umbilical Arterial Smooth Muscle Cells (HUASMCs), and Human Umbilical Arterial Myofibroblasts (HUAFIBs)

Umbilical cords were collected from full-term pregnancies and stored in sterile PBS at 4°C and cell isolation was performed within 7 days. Umbilical cord vascular cells were isolated as previously described by Welten et al[16]. In brief, for HUVEC/HUAEC isolation, a cannula was inserted in the umbilical vein or in one of the umbilical arteries and flushed with sterile PBS. The vessels were infused with 0.075% collagenase type II (Worthington) and incubated at

37°C for 20min. The collagenase solution was collected and the vessels were flushed with PBS in order to collect all detached endothelial cells. The cell suspensions were centrifuged at 300g for 5min and the pellet was resuspended in HUVEC/HUAEC culture medium [M199 (PAA) with 10% heat inactivated human serum (PAA), 10% heat inactivated newborn calf serum (PAA), 1% of penicillin (10,000U/mL) and 1% of streptomycin (10,000U/mL) (MP Biomedicals), 150µg/ml endothelial cell growth factor (kindly provided by Dr. Koolwijk, VU Medical Center, Amsterdam, the Netherlands) and 0.1% (1,000units/mL) heparin (LEOPharma)]. HUAECs and HUVECs were cultured in plates coated with 1% gelatin.

The second artery was removed and cleaned from remaining connective tissue. Endothelial cells were removed by gently rolling the artery over a blunted needle. The tunica adventitia and tunica media were separated using surgical forceps. After overnight incubation in HUASMC/HUAFIB culture medium (DMEM GlutaMAXTM (Invitrogen, GIBCO), 10% heat inactivated fetal bovine serum (PAA), 10% heat inactivated human serum, 1% penicillin (10,000U/mL)/streptomycin (10,000U/mL) and 1% non-essential amino acids (100X, ref 11140–035) (GIBCO, Life Technologies), both tunicae were incubated separately in a 2mg/ml collagenase type II solution (Worthington) at 37°C. Cell suspensions were filtered over a 70µm cell strainer and centrifuged at 300g for 10min. Cell pellets were resuspended and plated in culture medium. Cells isolated from the tunica adventitia were washed with culture medium after 90min to remove slow-adhering non-fibroblast cells.

Primary Cell Culture

Cells were cultured at 37°C in a humidified 5% CO_2 environment. Cell-type specific culture medium was refreshed every 2–3 days. Cells were passed at 90–100% (HUVECs, HUAECs, and HUASMCs) or 70–80% confluency (HUAFIBs). HUVECs, HUASMCs, and HUAFIBs were used up to passage six and HUAECs up to passage three. Stocks of isolated HUVECs, HUASMCs, and HUAFIBs up to passage four and HUAECs up to passage two were stored at −180°C in DMEM GlutaMAX™ containing 20% FBS and 10% DMSO (Sigma).

RNA Isolation

For RNA isolation, frozen human vascular tissues were crushed in liquid nitrogen and total RNA was isolated from tissue powder as well as from cultured cells by standard TRIzol-chloroform extraction, according to the manufacturer's instructions (Thermo Fisher Scientific). RNA concentrations were measured using Nanodrop™ 1000 Spectrophotometer (Thermo Fisher Scientific).

MicroRNA Quantification

For microRNA quantification, RNA was reversed transcribed using the Taqman™ MicroRNA Reverse Transcription Kit (Thermo Fisher Scientific) and subsequently quantified using microRNA-specific Taqman™ qPCR kits (Thermo Fisher Scientific) on the VIIa7 (Thermo Fisher Scientific). MicroRNA expression was normalized against U6 small nuclear RNA. MicroRNAs analyzed, in order of their genetic location along the 14q32 cluster, were hsa-miR-433-3p (miR-433-3p), hsa-miR-127-3p (miR-127-3p), hsa-miR-136-5p (miR-136-5p), hsa-miR-370-3p (miR-370-3p), hsa-miR-411-5p (miR-411-5p), hsa-miR-329-3p (miR-329-3p), hsa-miR-494-3p (miR-494-3p), hsa-miR-543-3p (miR-543-3p), hsa-miR-495-3p (miR-495-3p), hsa-miR-376c-3p (miR-376c-3p), hsa-miR-300-3p (miR-300-3p), hsa-miR-487b-3p (miR-487b-3p), hsa-miR-539-5p (miR-539-5p), hsa-miR-544a-3p (miR-544a-3p), hsa-miR-134-5p (miR-134-5p), hsa-miR-485-5p (miR-485-5p), hsa-miR-410-3p (miR-410-3p). Of the 54 microRNAs located on the 14q32 locus, we measured the expression of 17 microRNAs in our biobank of human vascular tissue samples. The genes encoding these microRNAs were distributed equally along the locus (Figure 1A) and in a previously published Reverse Target Prediction analysis, these microRNAs were demonstrated to be of potential interest in vascular remodelling[16]. Vessels were divided into groups based on location of origin, with each group consisting of samples from at least 3 different individuals. For comparisons between patients with coronary artery disease (CAD) and peripheral artery disease (PAD), we looked both at arteries and veins. For CAD, we included arteriae mammariae and venae saphenae magnae (VSM), both used and prepared for coronary artery bypass grafting, but discarded as surplus length of the bypass. For PAD, we included lower limb arteries and lower limb veins that were either prepared for femoral popliteal bypass grafting, but discarded as surplus length of the bypass, or removed along with amputated tissue after lower limb amputation. Expression levels of microRNAs were calculated relative to U6 expression and expressed as 2^{-dCt}.

Primary microRNA Quantification

RNA was reverse transcribed using “high-capacity RNA to cDNA kit” (Thermo Fisher Scientific) and quantified by qPCR using SybrGreen reagents (Qiagen) on the VIIa7. Primary microRNA expression was normalized against U6 and expressed as 2^{-dCt}. Primary microRNAs and primer sequences are provided in Supplementary Table 4.

DNA Methylation Assessment

DNA methylation was determined using methylation-sensitive endonucleases, as described previously by Moradi et al[37]. Genomic DNA was isolated using DNeasy Blood & Tissue Kit (Qiagen). Of 109 vessel tissue samples only 78 samples could be used for DNA methylation

quantification due to shortage of tissue or to a very low DNA yield (<2ng/µL). All Ampubase biobank samples had DNA yield > 2ng/µL. In the murine hind limb ischemia model and in the vein graft model all samples had sufficient DNA yield. After treating the DNA with methylation-sensitive restriction enzymes (Supplementary Table 2; 10units/reaction according to Manufacturer's Protocol (NEB) with 200ng DNA per reaction), uncut, and thus methylated, DNA was quantified by qPCR using SybrGreen reagents (Qiagen) on the VIIa7. The estimated methylated DNA fraction (EMF) was expressed relative to an restriction enzyme independent control sequence. Primer sequences and the corresponding CpGs that are potentially cut by methylation-sensitive restriction enzymes are provided in Supplementary Tables 2 and 3. Estimated methylation fractions (EMF) were calculated relative to a methylation-independent control, i.e., a stretch of DNA from the same genomic region that did not contain methylation-sensitive restriction sites.

MicroRNA Targets and DNA Methyltransferases (DNMTs)

For each microRNA, we selected at least one previously confirmed target gene that plays a confirmed role in vascular remodelling. Ninety five out of 109 samples had sufficient RNA yield for mRNA quantification (≥40ng/µL). mRNA was reverse transcribed using "high-capacity RNA to cDNA kit" (Thermo Fisher Scientific) and quantified by qPCR using SybrGreen reagents on the VIIa7. mRNA expression was normalized against GAPDH and expressed as 2^{-dCt}. Target mRNAs, DNMTs and primer sequences are provided in Supplementary Table 4.

Statistical Analyses

Mean values per group are presented ± SEM. Differences between groups were evaluated using Student's t-tests with a significance level of $\alpha < 0.05$. P-values were adjusted for multiple testing using Holm-Sidak's method.

A Grubbs' test was used to identify significant outliers ($\alpha < 0.05$) resulting in exclusion of maximum of one value per data group per microRNA, except for miR-494 in which dataset we excluded three relative expression values in lower leg arteries because of their extremely high value.

Fisher's exact test was performed to evaluate the overall trends toward increases or decreases for all microRNAs between veins and arteries and between non-malignant and perimalignant vessels.

To evaluate the possible impact of age on expression levels between (primary) microRNA levels and DNA methylation, between DNMT expression and (primary) microRNA expression and between DNMT expression and DNA methylation, linear regression analyses were performed in GraphPad Prism 8.

For the heat map, expression levels of each microRNA were normalized to its own average expression in all samples in the biobank.

One-way ANOVA statistical analysis was performed to detect differences in vascular wall cell types and to assess differences between vessel groups in coronary artery disease (CAD) and peripheral artery disease (PAD) and for DNA methylation in murine vein graft disease using $\alpha < 0.05$. To test significance between two groups of the one-way ANOVA analysis, multiple tests were performed and correction for multiple testing with Holm-Sidak's method was done.

To evaluate the possible change of DNA methylation over time, log-transformed, between treated and untreated hind limb muscles within the three DMRs, a mixed model was used in IBM SPSS Statistics 23 ($\alpha < 0.05$), with time (categorical), muscle, left/right, and DMR as fixed effects, and random intercepts per mouse.

Results

Global Expression Patterns of 14q32 microRNAs

Of the 54 microRNA genes located on the 14q32 locus, we measured expression of a selection of a representative subset of 17 microRNAs in our biobank of 109 human vascular tissue samples originating from various locations throughout the human vasculature. These microRNAs were distributed equally along the locus (Figure 1A) and in a previously published Reverse Target Prediction analysis, these microRNAs were demonstrated to be of potential interest in vascular remodelling[16]. Expression data were divided into groups based on location of origin of the collected blood vessels. In Figure 1B a heat map of the overall expression of 14q32 microRNAs is presented. Expression of the 14q32 microRNAs was highest in lower limb vessels and abdominal arteries. Some microRNAs, which genes are located next to each other, showed similar expression patterns, such as miR-134-5p and miR-485-5p. However, miR-543-3p and miR-495-3p, also direct genetic neighbors in the cluster, differ in expression pattern. MiR-494-3p and miR-487b-3p, although not located in close proximity from each other within the locus, do show resemblances in relative expression throughout various vessel types. All measured microRNAs, however, showed unique expression patterns, suggesting independent regulation of expression.

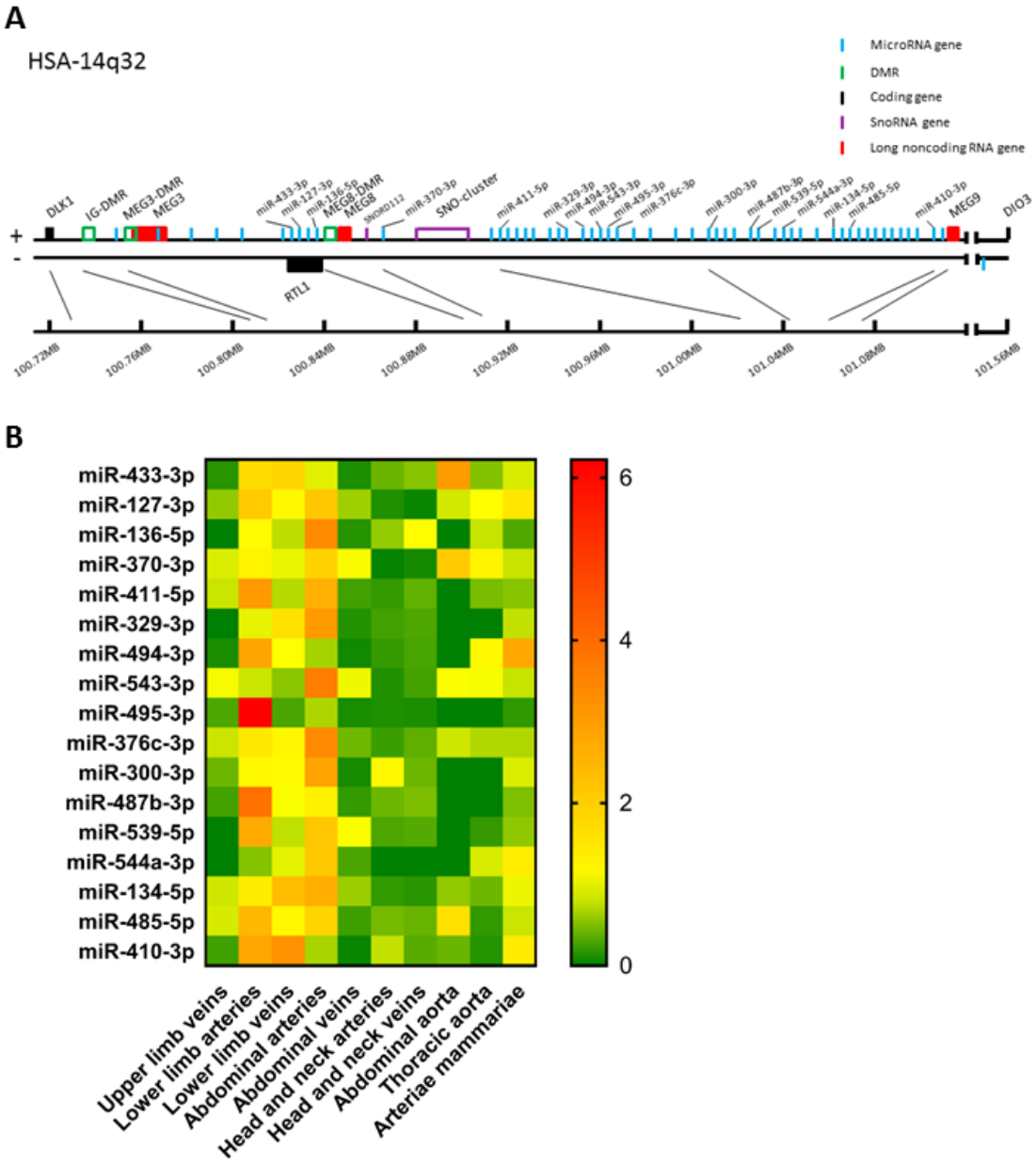

Figure 1 (A) Schematic presentation of the human 14q32 locus. Protein coding genes are depicted in black, long noncoding RNA genes in red, measured microRNA genes in blue, DMRs in green, and snoRNA genes in purple. (B) Heat map of all analyzed microRNAs. For every microRNA, expression in each vessel group was normalized against the average expression of the microRNA in all samples. Relative expression below average is green, around average is yellow and above average is orange to red. Vessels were divided into the following groups: upper limb veins (N = 3), lower limb arteries (N = 14), lower limb veins (N = 20), abdominal arteries (N = 17), abdominal veins (N = 6), head and neck arteries (N = 9), head and neck veins (N = 7), abdominal aorta (N = 4), thoracic aorta (N = 5), and arteriae mammariae (N = 21). MicroRNAs are arranged in the order of chromosomal location of the microRNA gene.

Individual 14q32 microRNA Expression Throughout the Vasculature

Next, we analyzed the relative expression levels of each microRNA in different types of vessels (Figure 2). As presented in Figure 1B, microRNA expression in general was highest in vessel tissues in the lower limbs and the abdomen, and lowest in the head- and neck area. On individual levels, we observed a significant difference in expression between the abdominal arteries and veins for miR-433-3p, miR-127-3p, miR-136-5p, miR-411-5p, miR-329-3p, miR-494-3p, miR-495-3p, miR-376c-3p, miR-300-3p, miR-487b-3p, miR-539-5p, miR-134-5p, miR-485-5p, and miR-410-3p. Similar observations were made for lower limb arteries and veins for miR-127-3p, miR-495-3p, miR-487b-3p, and miR-485-5p. As mentioned above, some microRNAs closely located to each other within the cluster show similar expression profiles, but others vary widely, suggesting a tight and active regulation of expression of each individual microRNA in each different blood vessel. Furthermore, relative expression ranged from <0.0001 in lower limb vessels and abdominal veins (miR-544a-3p, Figure 2N) to 0.4 in abdominal aortas (miR-433-3p, Figure 2A). Among four 14q32microRNAs, miR-329-3p, miR-487b-3p, miR-494-3p, and miR-495-3p, for which we previously reported a functional role in vascular remodelling[16-19], miR-329-3p showed very low expression, whereas its neighbor in the cluster, miR-494-3p, showed a 100-fold higher expression (Figures 2F,G). Expression levels of these four microRNAs were all below the detection level in abdominal aortic tissue, however they were all harvested during aneurysm repair surgery (Figures 2F,G,I,L). This again implies that microRNA expression is independently regulated.

Arterial vs. Venous microRNA Expression

As we observed differences in expression of 14q32 microRNAs between arteries and veins of the same tissue (e.g., lower limb, abdomen, head, and neck), we divided samples into two groups, namely arteries (N = 73) and veins (N = 36). Arterial and venous expression of each individual microRNA is depicted in Figure 3. None of the 14q32 microRNAs, individually, showed significant expression differences between arteries and veins after adjusting for multiple testing. However, the overall observation that microRNA expression in arterial samples is higher than in venous samples for each microRNA, was significant ($p = 0.0027$).

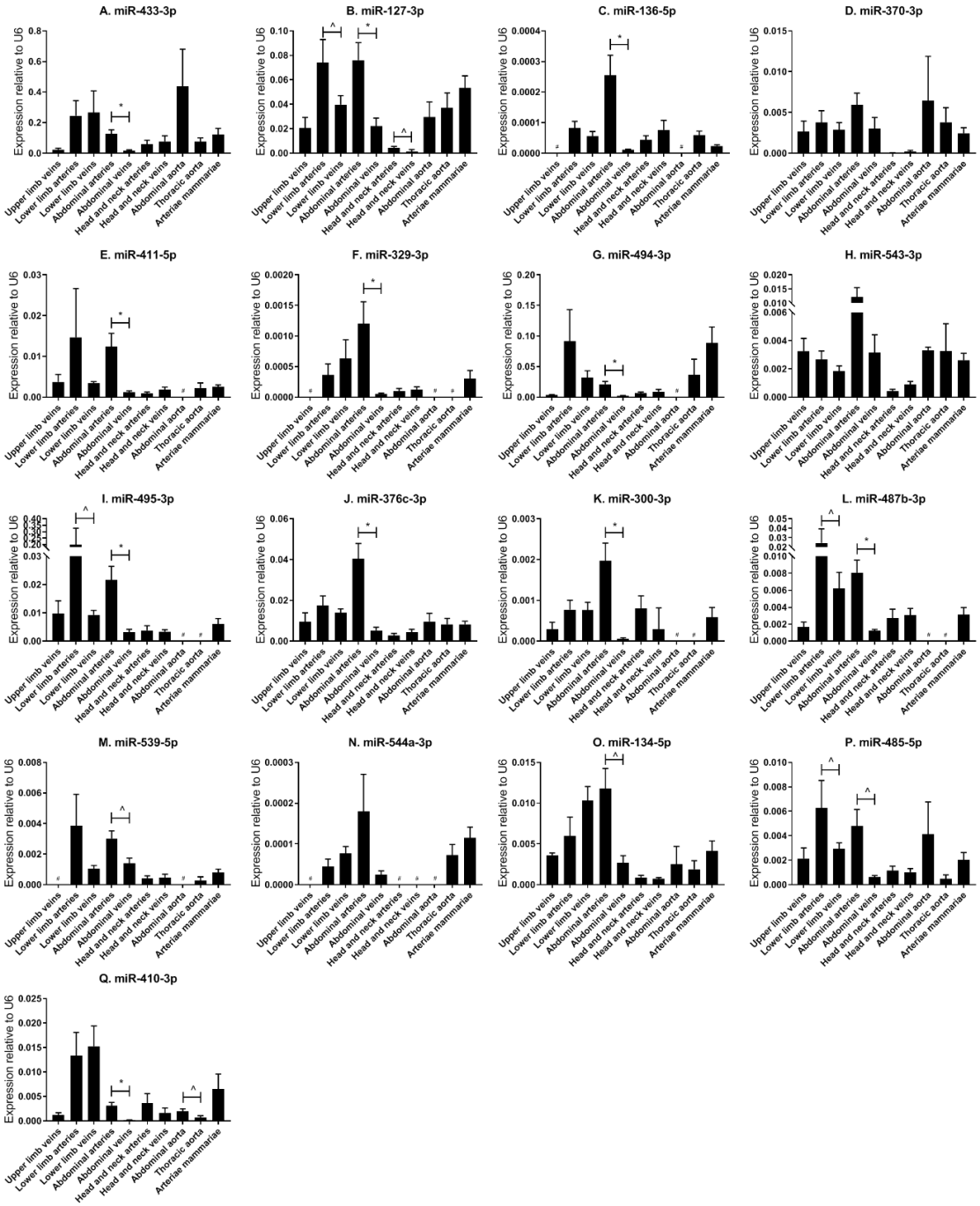

Figure 2 (A–Q) MicroRNA expression profiles in human vessel groups. Vessels were divided into the following groups: upper limb veins (N = 3), lower limb arteries (N = 14), lower limb veins (N = 20), abdominal arteries (N = 17), abdominal veins (N = 6), head and neck arteries (N = 9), head and neck veins (N = 7), abdominal aorta (N = 4), thoracic aorta (N = 5), and arteriae mammariae (N = 21). Each microRNA shows vessel group specific expression patterns. Mean expression per group is shown. The error bars represent the SEMs. ^$p < 0.1$, *$p < 0.05$, # <3 samples showed expression and samples were therefore not included in the analyses. Student's t-test was used with a significance level of $\alpha < 0.05$. MicroRNAs are arranged in the order of chromosomal location of the microRNA gene.

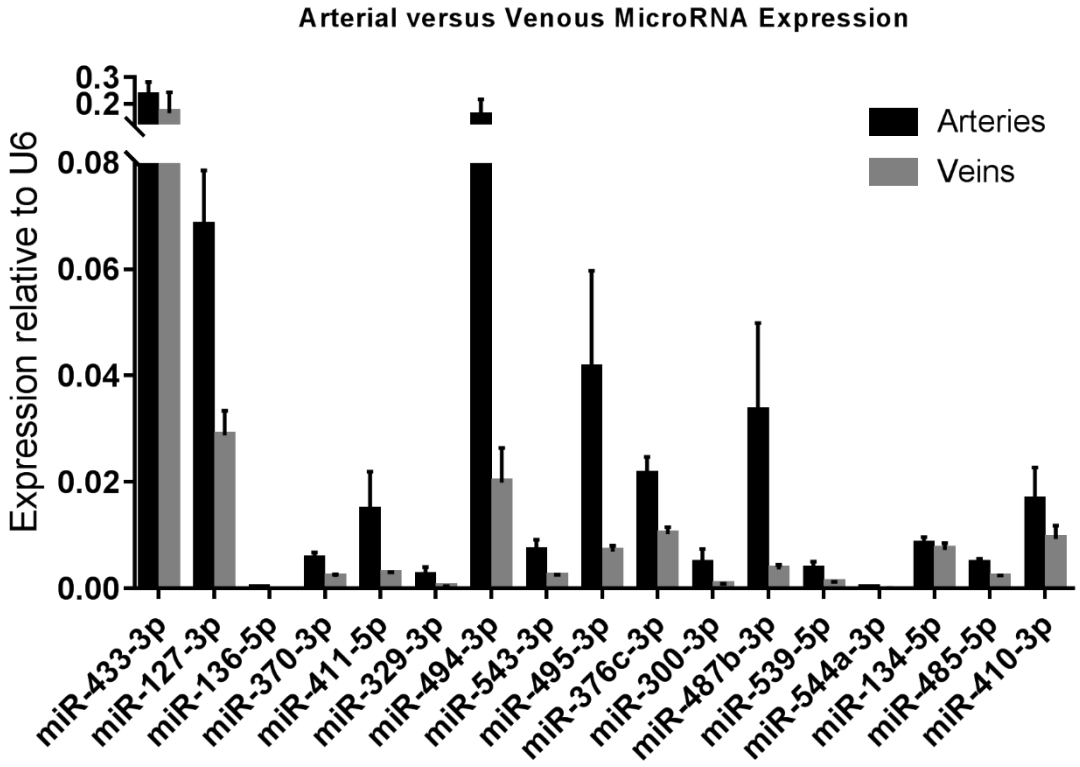

Figure 3 Arterial vs. Venous MicroRNA Expression. Arteries (N = 73) vs. Veins (N = 36) in miRMap. Mean expression per group is shown. The error bars represent the SEMs. MicroRNAs are arranged in the order of chromosomal location of the microRNA gene.

14q32 microRNA Expression in Vascular Cell Layers of Human Umbilical Cords

In order to determine in which segment of the vascular wall the 14q32 microRNAs are most abundantly expressed, we measured microRNA expression in cultured primary human umbilical cord cells, realizing of course that the umbilical cord arteries and veins are just two types of blood vessels and that the next findings may differ in other vessel types. We included human umbilical venous endothelial cells (HUVECs), human umbilical arterial endothelial cells (HUAECs), human umbilical arterial smooth muscle cells (HUASMCs), and human umbilical arterial fibroblasts (HUAFIBs). The expression of 14q32 microRNAs in umbilical cord endothelial cells (both venous and arterial) was relatively low compared to arterial smooth muscle cells and arterial fibroblasts. Arterial endothelial cell microRNA expression was also lower than both arterial smooth muscle cell and arterial fibroblast microRNA expression (Figures 4A–Q). We found that HUASMC expression for miR-127-3p was high compared to all other primary vascular cell types (Figure 4B). A similar pattern was found for miR-370-3p and miR-495-3p (Figures 4D,I).

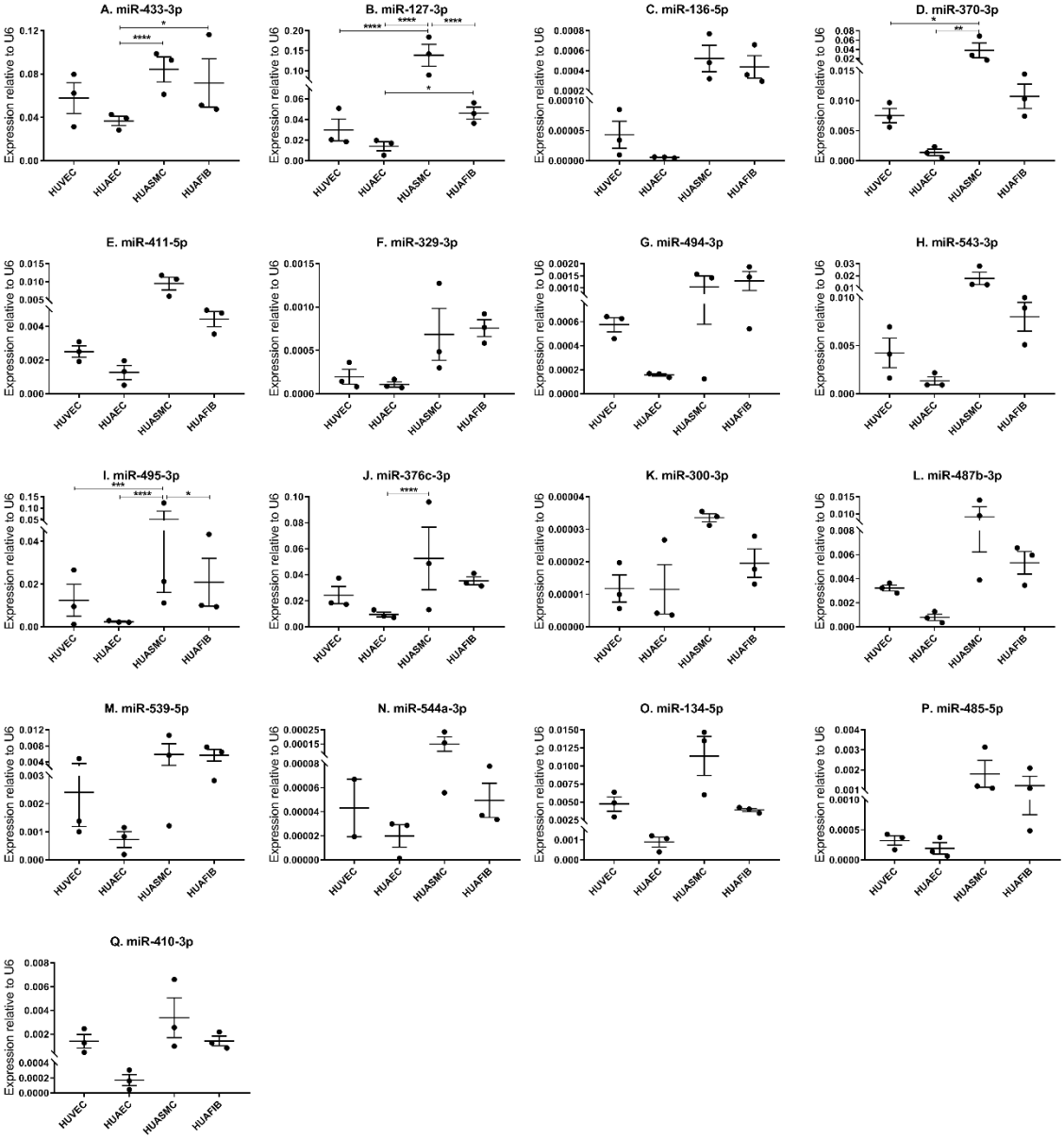

Figure 4 (A–Q) MicroRNA expression in human umbilical cord vascular cell layers. Human umbilical venous endothelial cells (HUVEC, N = 3), human umbilical arterial endothelial cells (HUAEC, N = 3), human umbilical arterial smooth muscle cells (HUASMC, N = 3), and human umbilical arterial fibroblasts (HUAFIB, N = 3). Mean expression per group is shown. The error bars represent the SEMs. *$p < 0.05$, **$p < 0.01$, ***$p < 0.005$, ****$p < 0.001$. One-way ANOVA statistical analysis was performed with a significance level of $\alpha < 0.05$. MicroRNAs are arranged in the order of chromosomal location of the microRNA gene.

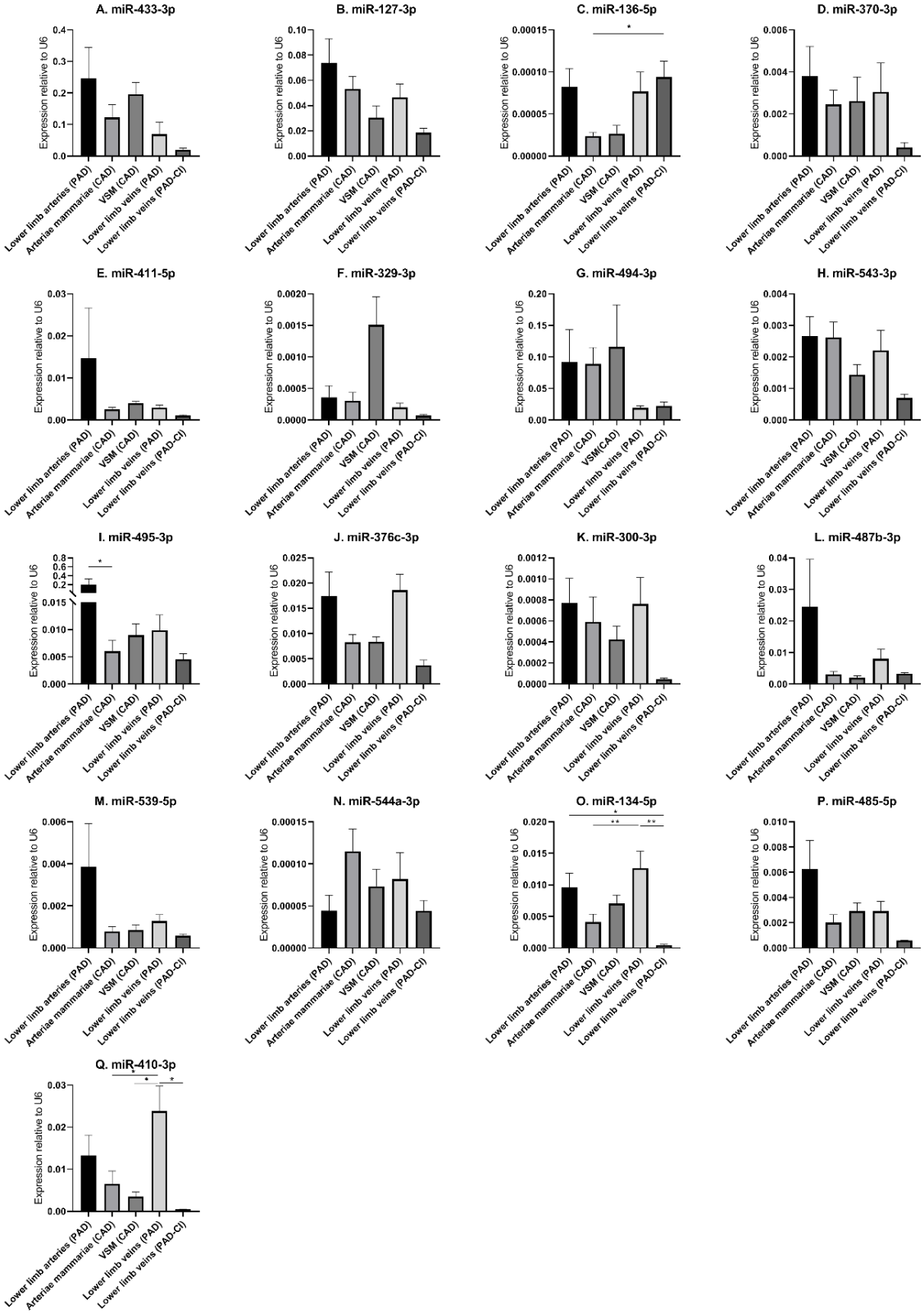

Figure 5 (A–Q) MicroRNA expression in human vessel groups of peripheral and coronary artery disease patients. Vessels were divided into the following groups: lower limb arteries from patients with PAD (N = 14), arteriae mammariae from patients with CAD (used as arterial graft; N = 21), lower limb veins from patients with CAD (used as vein graft; N = 8), lower limb veins from patients with PAD (N = 12), lower limb veins from patients with critical ischemia (PAD-CI; N = 6). Mean expression per group is

shown. The error bars represent the SEMs. *$p < 0.05$, **$p < 0.01$. One-way ANOVA statistical analysis was performed with multiple testing for differences between all bars individually with a significance level of $\alpha < 0.05$, corrected for multiple testing. MicroRNAs are arranged in the order of chromosomal location of the microRNA gene.

14q32 microRNA Expression in Patients With Cardiovascular Disease

In order to determine whether the 14q32 microRNAs are also regulated in samples from patients with cardiovascular disease, we selected four groups of blood vessels from the miRMap biobank, harvested during bypass surgery in Coronary Artery Disease (CAD) patients or intermittent Peripheral Artery Disease (PAD) patients. From both CAD and PAD patients, we selected arterial and venous. Furthermore, we selected a group of lower limb veins from patients with PAD in Critical Ischemic conditions (PAD-CI). As shown in Figure 5, except for miR-136-5p and miR-494-3p, microRNA expression is higher in the less ischemic lower limb veins in intermittent PAD compared to the PAD-CI samples.

14q32 microRNA Target Gene Expression

For each of the 17 measured 14q32 microRNAs, we selected at least one confirmed target gene with a confirmed vascular function. Vessel groups that show high expression for a specific microRNA, show lower expression of the selected target mRNA and vice versa. This is shown in Figure 6 for the abdominal and thoracic aorta groups, for the arteria mammaria group and for the lower limb vessels. Both high and low microRNA expression show inversed expression of the measured target mRNAs, for example for miR-433-3p, miR-370-3p, and miR-544a-3p (Figures 6A,D,P).

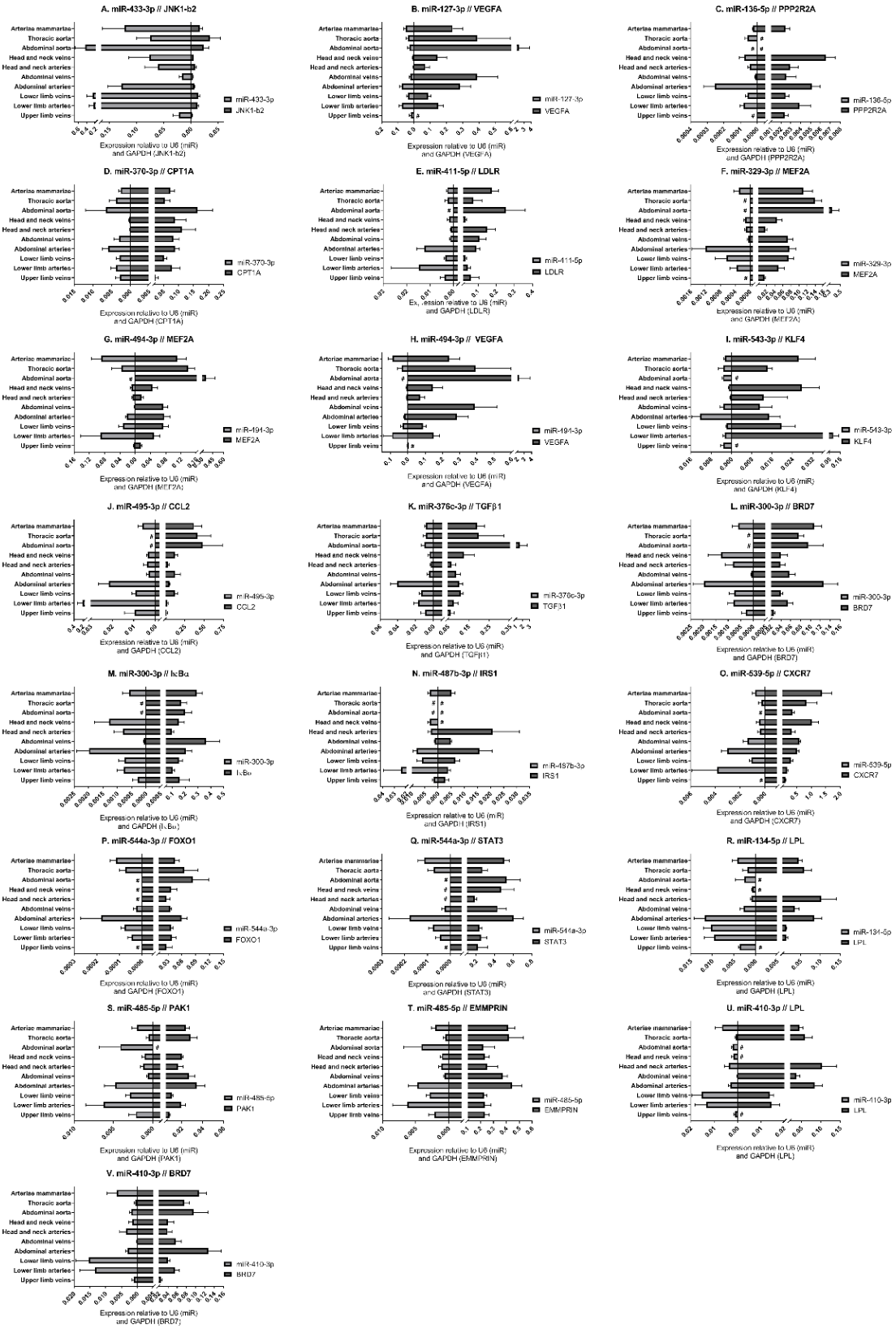

Figure 6 (A–V) MicroRNA target genes. Vessels were divided into the following groups: upper limb veins (N = 3), lower limb arteries (N = 11), lower limb veins (N = 18), abdominal arteries (N = 14), abdominal veins (N = 5), head and neck arteries (N = 9), head and neck veins (N = 5), abdominal aorta (N = 4), thoracic aorta (N = 5), and arteriae mammariae (N = 18). MicroRNA expression and target gene expression tend to show inversed expression in different vessel groups. Mean expression per group is

shown. The error bars represent the SEMs. # <3 samples showed expression and samples were therefore not included in the analyses. MicroRNAs arranged in the order of chromosomal location of the microRNA gene.

Methylation of 14q32 DNA Throughout Vasculature

We measured the estimated methylation fraction (EMF) of multiple CpGs in the 3 DMRs located along the 14q32 locus (Figure 1A) in 78 miRMap samples. Although we observed distinct patterns of differential methylation throughout the human vasculature for the three different DMRs (Figure 7), we did not observe differences between arteries and veins of the human vasculature. Moreover, we did not find direct correlations between 14q32 EMF and 14q32 microRNA expression individually (data not shown). Since DNA methylation is suggested to mainly affect transcription and the primary form of microRNA is directly affected by transcriptional changes, we also assessed whether there was a correlation between pri-microRNA expression of 4 14q32 microRNAs that are highly regulated in cardiovascular remodelling (miR-329, miR-487b, miR-494, and miR-495) and 14q32 DNA methylation. As shown in Figure 8, none of the pri-microRNAs correlated significantly with EMF of any DMR along the 14q32 locus.

Changes in DNA methylation of the 14q32 cluster in atherosclerotic lesions were previously reported[31]. To further investigate this, we used the previously described four groups of blood vessels from the miRMap biobank, harvested during bypass surgery in CAD or PAD patients, as well as the group of lower limb veins from patients with PAD-CI. We found that in the IG-DMR (IG-DMR-CG6) and in the MEG3-DMR, but not in the MEG8-DMR, venous coronary artery bypass grafts [venae saphenae magnae (VSM)] had a higher EMF than arterial coronary artery bypass grafts (arteriae mammariae; Figures 9B–E). The EMFs did not differ between arterial and venous samples from PAD patients. Furthermore, EMF in venous samples of patients with PAD-CI, collected during amputation, showed a different EMF for each CpG site. EMFs of PAD-CI veins were high compared to PAD veins for IG-DMR-CG4-2, MEG3-DMR-1B, and MEG8-DMR-1H (Figures 9A,E,G), but low in IG-DMR-CG6-1 (Figure 9B). MEG8-DMR-1A did not show any differences between groups (Figure 9F). Together, these data suggest that site specific DNA methylation is linked to cardiovascular disease status directly, rather than indirectly via changes in microRNA expression.

To identify whether there is significant correlation between primary microRNA (pri-miR) transcripts and DNA Methyltransferase (DNMT) genes, we measured DNMT gene expression. As we already found that DNA methylation is changed in vascular remodelling processes, we focused on peripheral artery disease (PAD) vascular samples and coronary artery disease (CAD) vascular samples. Figure 10D shows that none of the DNMT genes correlated significantly with pri-microRNAs in miRMap CAD and PAD samples. Mature microRNAs did not

associate as well (data not shown). However, it is interesting that DNMT genes expression varies in samples with different cardiovascular diseases, especially between vessels in different stages of PAD. Both DNMT1, which functions in DNA methylation maintenance and DNMT3A, a *de novo* DNA methylation enzyme, are highly expressed in lower limb arteries of PAD patients, show lower expression in lower limb veins of PAD patients and lowest expression is present in lower limb veins of PAD patients with critical ischemia (Figures 10A–C). This implies that DNMT gene expression, like 14q32 DNA methylation, could be linked to cardiovascular disease directly. Furthermore, we assessed whether there is a correlation between DNA methylation and DNMT gene expression (Supplementary Figure 1). A significant correlation could only be found between DNMT3A and MEG3-DMR-1A (p = 0.03).

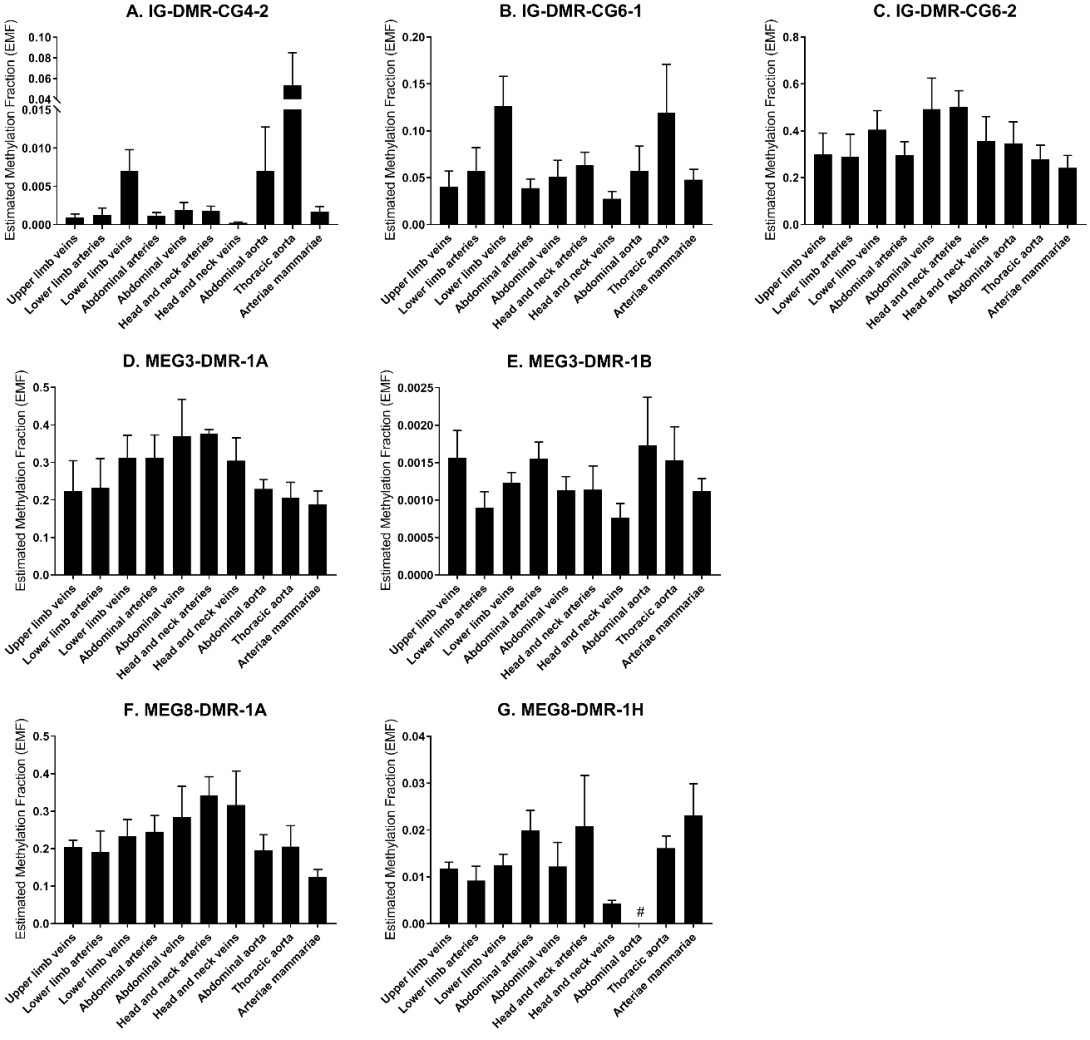

Figure 7 (A–G) DNA-methylation at the 3 DMRs along the 14q32 locus in vessel groups. Vessels were divided into the following groups: upper limb veins (N = 3), lower limb arteries (N = 6), lower limb veins (N = 17), abdominal arteries (N = 12), abdominal veins (N = 4), head and neck arteries (N = 5), head and neck veins (N = 5), abdominal aorta (N = 3), thoracic aorta (N = 5), and arteriae mammariae (N = 16). Estimated Methylation Fraction (EMF) relative to restriction enzyme-independent control. Mean expression per group is shown. The error bars represent the SEMs. #<3 samples showed EMF and samples were therefore not included in the analyses.

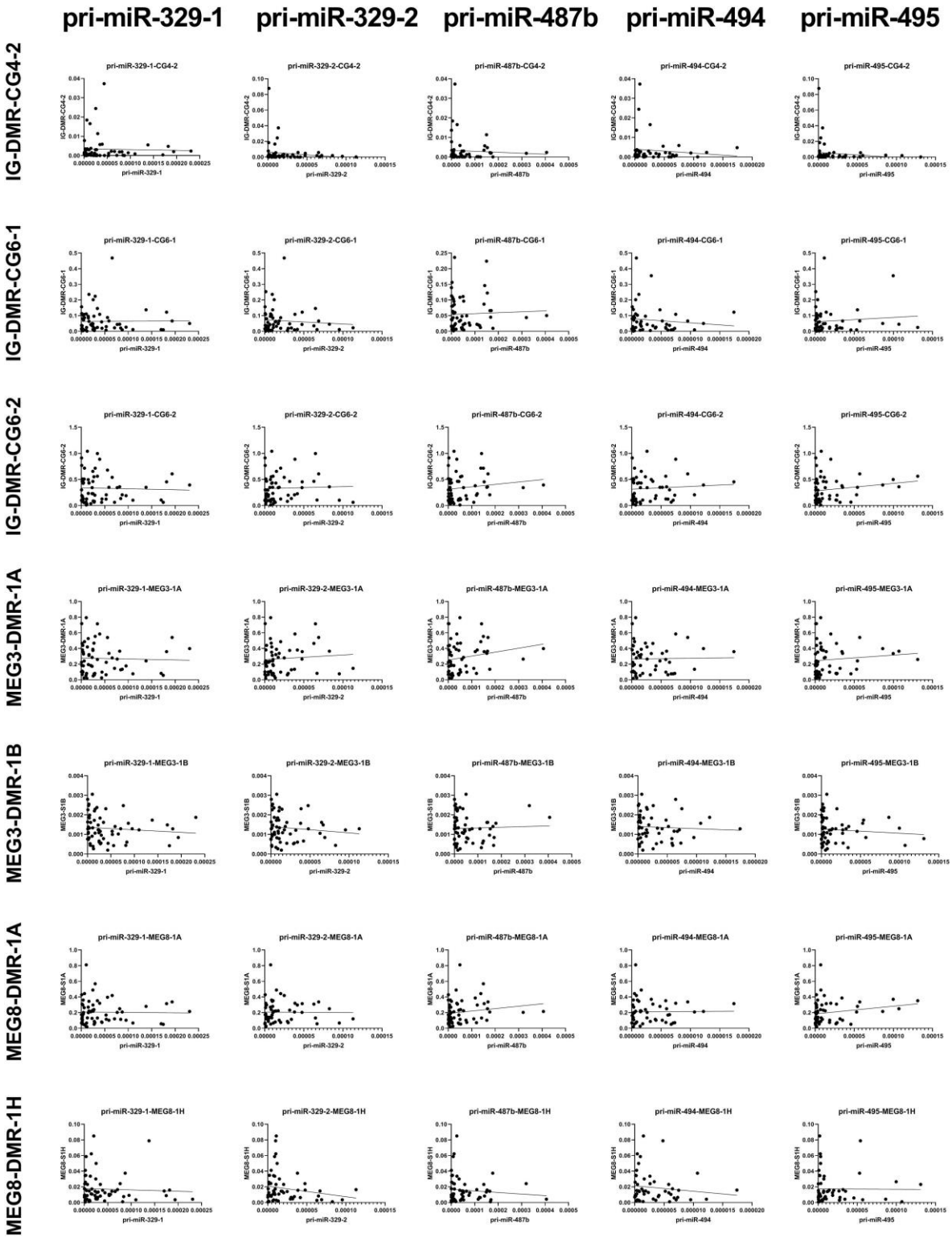

Figure 8 Correlations between primary 14q32 microRNAs and 14q32 DNA methylation. Primary microRNA (pri-miR) expression levels (relative to U6) compared to estimated DNA methylation fraction [EMF (relative to restriction enzyme-independent control)]. Linear regression analyses did not show statistically significant correlations.

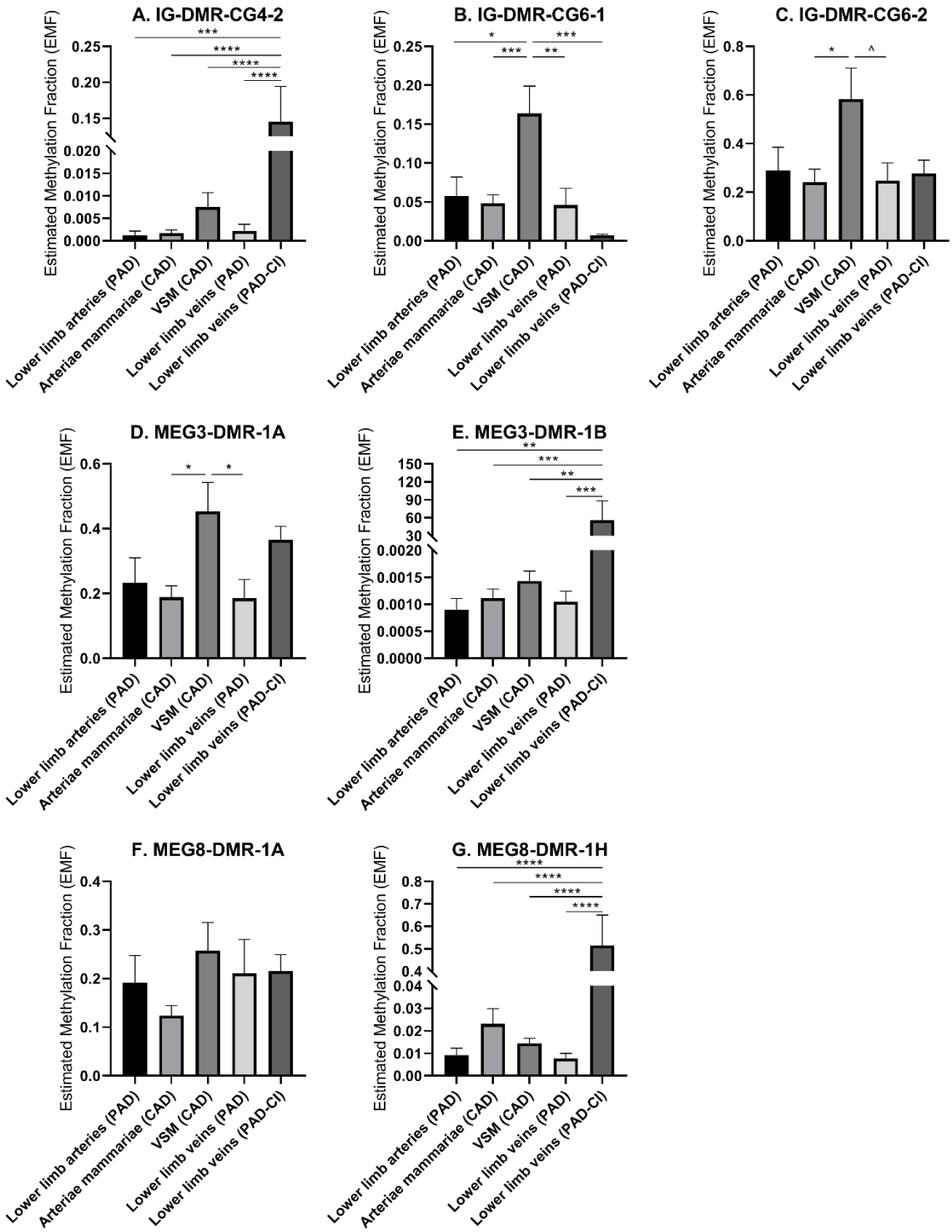

Figure 9 (A–G) Methylation of DNA in 14q32 DMRs in human vessel groups of peripheral and coronary artery disease patients. Vessels were divided into the following groups: lower limb arteries from patients with PAD (N = 6), arteriae mammariae from patients with CAD (used as arterial graft; N = 16), VSMs from patients with CAD (used as vein graft; N = 8), lower limb veins from patients with PAD (N = 9), lower limb veins from patients with critical ischemia (PAD-CI; N = 6). Estimated Methylation Fraction (EMF) relative to restriction enzyme-independent control. Mean expression per group is shown. The error bars represent the SEMs. ^p < 0.1, *p < 0.05, **p < 0.01, ***p < 0.005, ****p < 0.001. One-way ANOVA statistical analysis was performed with multiple testing for differences between all bars individually with a significance level of $\alpha < 0.05$, corrected for multiple testing.

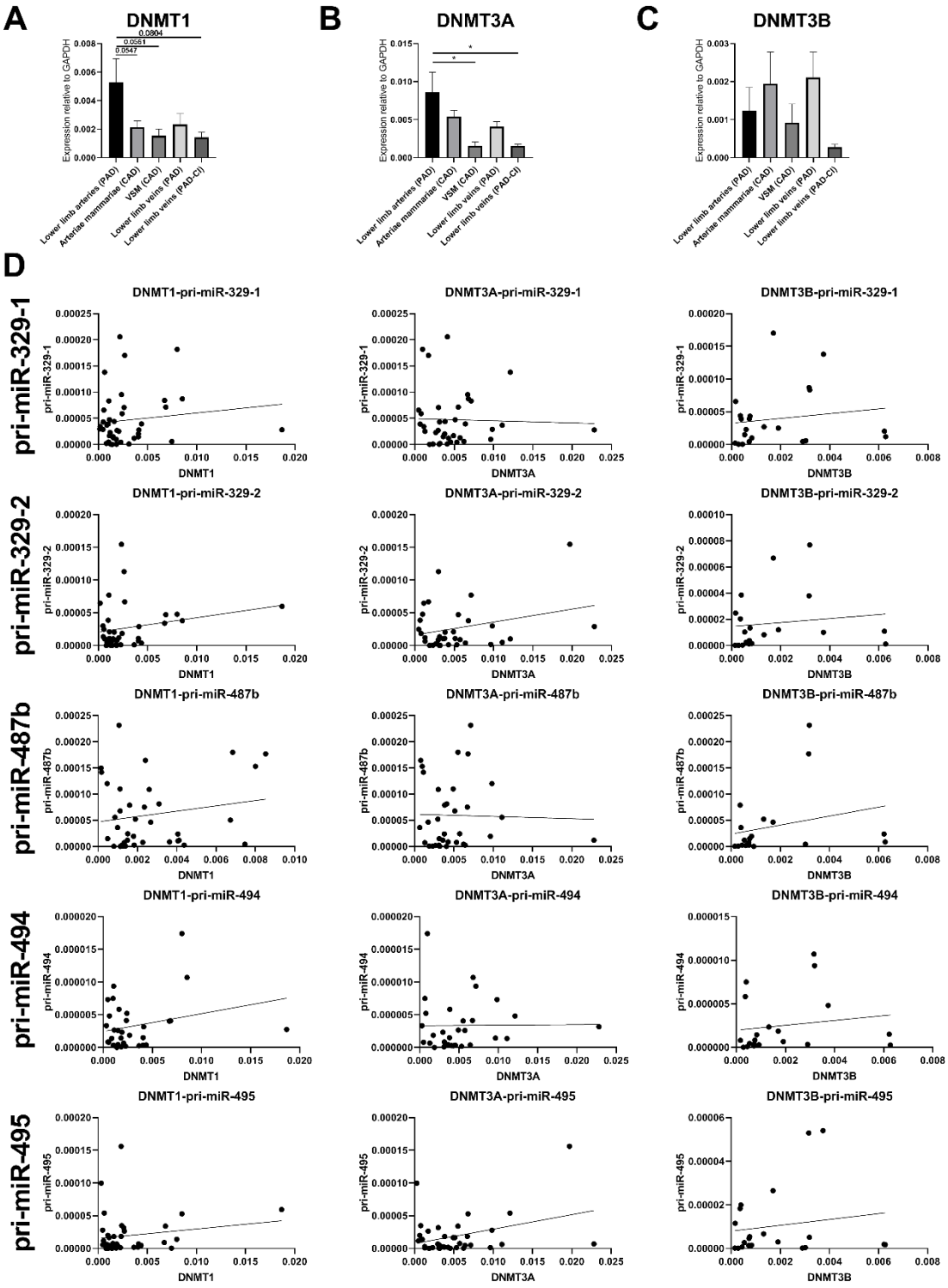

Figure 10 Gene expression of DNMT1, DNMT3A, and DNMT3B and correlations with pri-microRNA expression. Vessels were divided into the following groups: lower limb arteries from patients with PAD (N = 11), arteriae mammariae from patients with CAD (used as arterial graft; N = 18), VSMs from patients with CAD (used as vein graft; N = 8), lower limb veins from patients with PAD (N = 10), lower limb veins from patients with critical ischemia (PAD-CI; N = 6). The error bars represent the SEMs. *$p < 0.05$. One-way ANOVA statistical analysis was performed with multiple testing for differences between all bars individually with a significance level of $\alpha < 0.05$, corrected for multiple testing. Linear regression analyses do not show statistically significant correlations.

14q32 DNA Methylation in Murine Models for Cardiovascular Disease

To confirm the associations of 14q32 DNA methylation with both vein graft disease and peripheral artery disease, we used two different mouse models. In a murine model for vein graft disease, we found that 14q32 DNA methylation was changed during the active phase of vascular remodelling, i.e., at 2 weeks after vein graft surgery (Figure 11). After 28 days a more stable phase of vein graft disease[48,49], EMF seems to go back toward the EMF of the native vena cava (Figure 11). DNA methylation, however, was not shown to increase or decrease DMR-specifically, as we found both EMF increases and EMF decreases at 2 weeks after vein graft surgery within one DMR, namely IG-DMR (Figures 11E,F).

Hind limb ischemia was induced via femoral artery ligation, to mimic PAD in mice. We have previously shown a large scale upregulation for 14q32 microRNAs in response to hind limb ischemia in mice[16]. Here, we measured 14q32 DNA methylation of the three DMRs (Dlk1-DMR, IG-DMR, and Glt2-DMR) in three different muscles (adductor muscle, gastrocnemius muscle, and soleus muscle) at three different time points (Figure 12). Using a Mixed Model in SPSS, on all data together, we found a significant change in DNA methylation over time in ischemic muscle tissues in the three DMRs ($p = 0.009$).

Together, these findings indicate that associations between 14q32 microRNA expression and cardiovascular disease as well as between DNA methylation and cardiovascular disease are conserved over species.

Potential Confounding Factors

As microRNA expression and DNA methylation can be influenced by different factors, we assessed the influence of the most common confounding factors: sex, age, and malignancy. In the miRMap biobank, neither 14q32 microRNA expression nor DNA methylation differed between men and women. Furthermore, no correlation with age was observed (data not shown). Finally, we selected vessels resected from locations near resected tumors (abdominal and head and neck tumors) and compared expression with vessels originating from these same locations from patients without malignancies (Supplementary Figure 2A). Although we did not observe significant differences for individual microRNAs, of the 17 measured microRNAs, 16 microRNAs showed higher expression in the peri-malignancy samples ($p = 0.0167$). For DNA methylation, no differences in EMF nor a trend toward hypo- or hyper-methylation in any of the groups was observed (Supplementary Figure 2B).

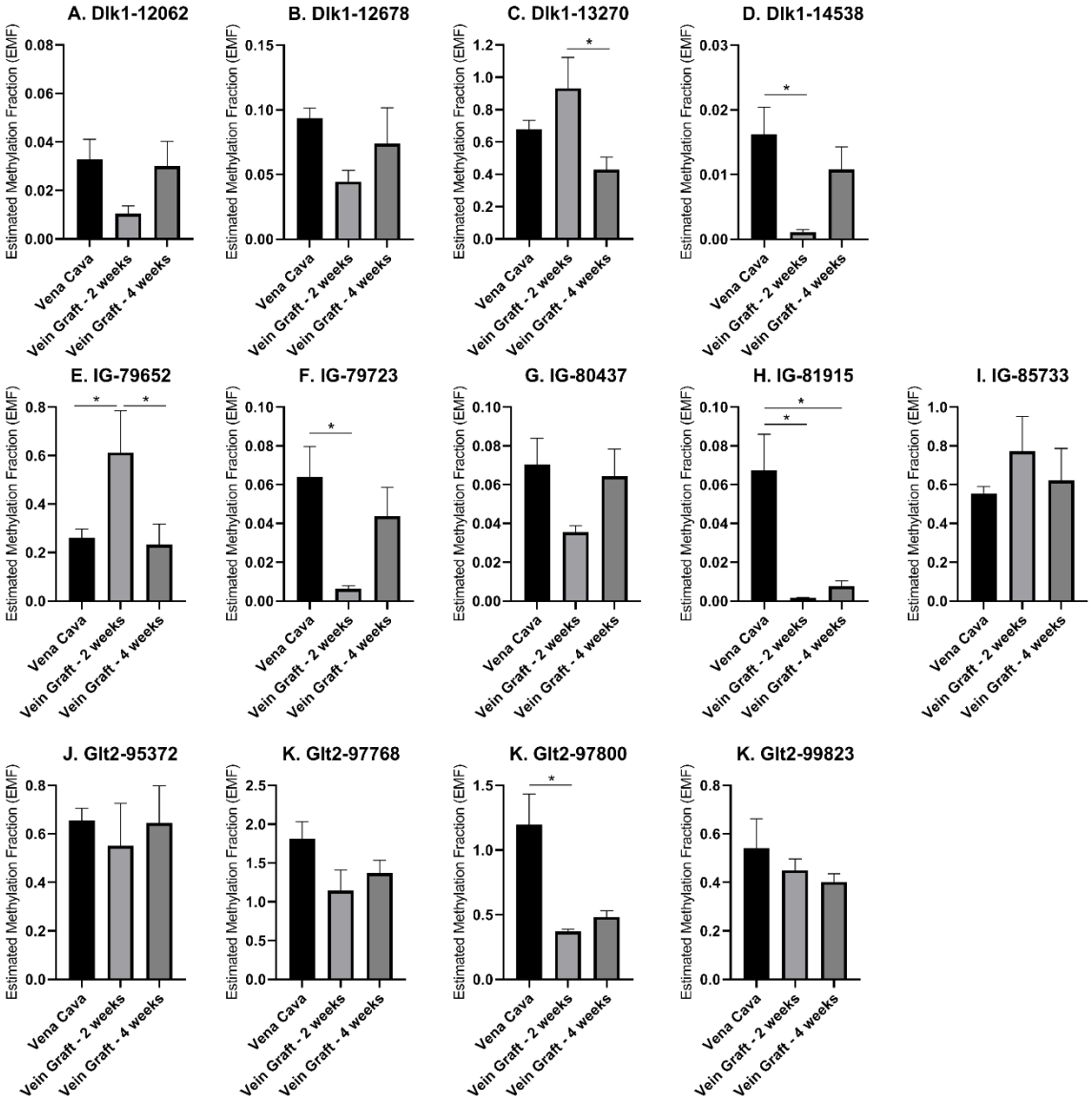

Figure 11 (A–M) 14q32 DNA methylation in murine vein graft disease. Native venae cavae (N = 13) were compared to venae cavae used as vein grafts, harvested either after 2 weeks (N = 6) and after 4 weeks (N = 7) in the different CpG-positions along the genome. At 2 weeks after surgery, Estimated Methylation Fraction (EMF) was up- or downregulated and at 4 weeks after surgery this change seemed to go back to the EMF of the native venae cavae. EMF is expressed relative to restriction enzyme-independent control. Mean expression per group is shown. The error bars represent the SEMs. *p < 0.05. One-way ANOVA statistical analysis was performed with multiple testing for differences between all bars individually with a significance level of $\alpha < 0.05$, corrected for multiple testing.

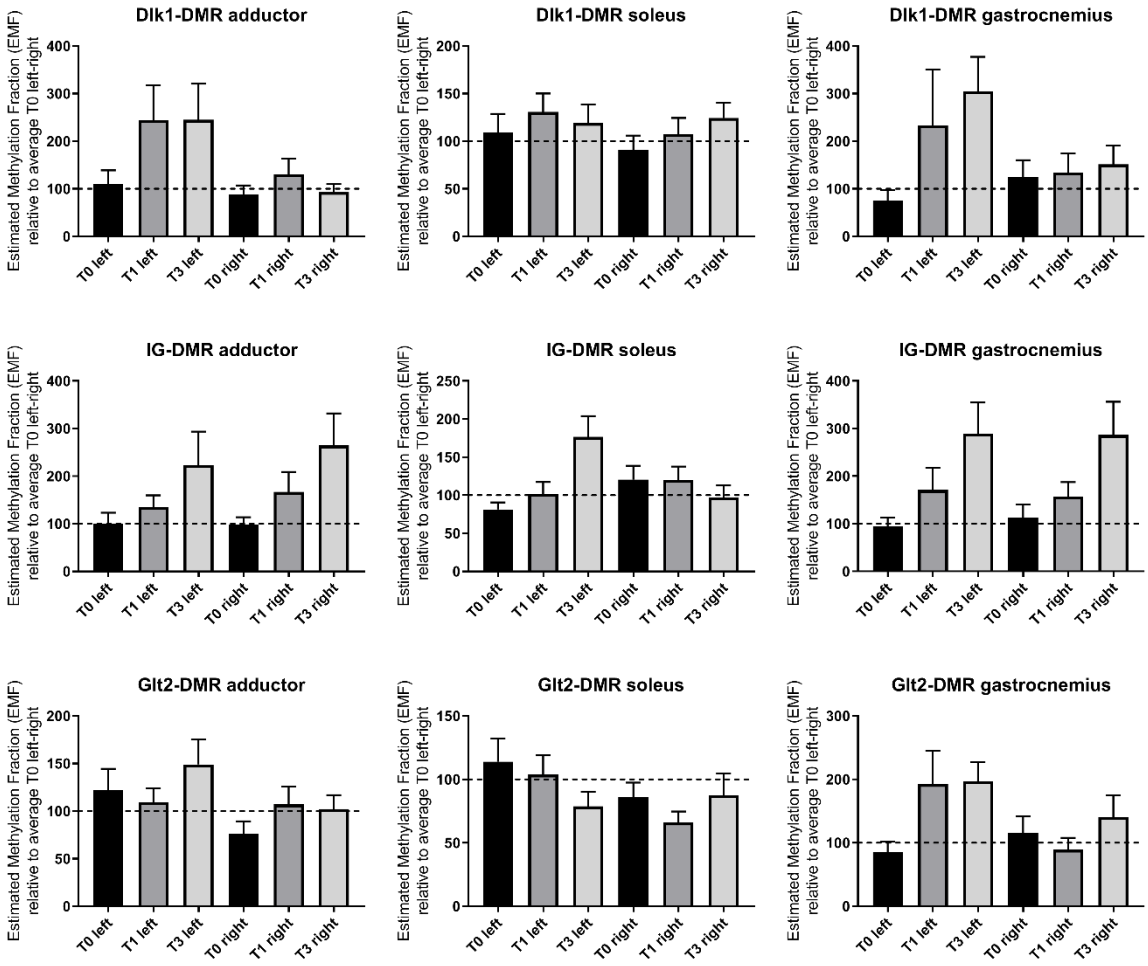

Figure 12 14q32 DNA methylation in murine hind limb ischemia model. Hind limb muscles (adductor, soleus and gastrocnemius) harvested before (N = 4), 1 day after (N = 4), and 3 days after left femoral artery ligation (N = 4). Muscles from the right paw were used as internal control. Estimated Methylation Fraction (EMF) relative to restriction enzyme-independent control is expressed relative to the average EMF of T0 in left and right (set to 100% and indicated as the dotted line). Mean expression per group is shown. The error bars represent the SEMs. On all data together, a Mixed Model is performed and showed a significant change in DNA methylation over time in ischemic muscle tissues in the three DMRs (p = 0.009).

Discussion

All 14q32 microRNAs measured in this study are expressed in the human vasculature, but not all microRNAs are expressed in all vessel types. In fact, each 14q32microRNA had its own unique expression “fingerprint” throughout the vasculature. Expression levels of the 14q32 microRNAs varied widely in each type of vessel. These findings confirm the existence of tight individual regulation of 14q32microRNA expression which should be taken into account in future studies. Moreover, our study demonstrates the complexity of human microRNA expression patterns, which has been studied extensively in different blood components[50,51], but not in the vessel wall itself. This may have implications for future microRNA-based

therapies, either as a limitation, if the target microRNA is not expressed at a vascular target site, or as a potential advantage when highly specific vessel type microRNA expression allows us to modulate microRNA function locally, avoiding systemic vascular side effects[14]. DNA methylation of the 14q32 locus also varied over different blood vessels, but was not directly associated with microRNA expression, as was claimed by previous reports[31,35]. Our results underline the complex transcriptional landscape of noncoding RNAs in general.

Interestingly, we observed the highest expression in lower limb vascular tissues and lowest expression in head- and neck vascular tissues was clearly observed. Both vessel groups originate from locations prone to atherosclerosis. However, even though the pathophysiologies of both carotid artery disease and peripheral artery disease are consistent[2] and affected by the same risk factors[52], we found differential expression of 14q32 microRNAs, which have previously been shown to associate with atherosclerotic disease[17].

The observation that all measured 14q32 microRNAs had higher expression in arteries than in veins can be explained by a previous finding that 14q32 microRNAs are expressed abundantly in fibroblasts, which are highly present in the adventitial layer of arteries[16,19]. This was confirmed by the high arterial fibroblast 14q32 microRNA expression. Furthermore, it was observed that arterial smooth muscle cells also showed high expression. This was reported previously for a non-14q32 microRNA, miR-195[53]. This microRNA showed more prominent expression in human aortic smooth muscle cells than in HUVECs[53], however, this could also be an effect of the vascular bed, rather than the cell type. Although vascular SMCs and adventitial fibroblasts are mainly associated with arteries, they are also present in veins, albeit less prominent. Our finding that 14q32 microRNA expression is higher in both HUASMCs and HUAFIBs and low in both HUVECs and HUAECs, suggests that these vascular wall cell layers are the major contributors to 14q32 microRNA expression in the vascular wall, at least in umbilical cord vessels.

The fact that we observed microRNA-specific expression fingerprints implies individual regulation of 14q32 microRNA expression. MicroRNA expression can be regulated by many different factors, both acting during transcription and during post-transcriptional processing. RNA Binding Proteins (RBPs) for example, are post-transcriptional regulators of microRNA expression. RBPs are able to bind precursor microRNAs and promote or inhibit microRNA maturation. Thereby, RBPs directly influence microRNA expression. Myocyte Enhancer Factor 2A (MEF2A) is such an RBP, which regulates posttranscriptional regulation of both miR-329 and miR-494[54], but Cold-Inducible RNA-Binding Protein (CIRBP) and Hydroxyacyl-CoA DeHydrogenase trifunctional multienzyme complex subunit Beta (HADHB) are also RBPs that regulate 14q32 microRNAs miR-329 and miR-495[55]. However, even between these microRNAs, differences in expression levels and patterns were found. This suggests that

MEF2A, CIRBP, and HADHB are only a small part of the complex regulation of microRNA expression. As already suggested by Treiber et al, the interaction between RBPs and microRNAs is a complex mechanism[56] and further studies are needed to elucidate the full mechanism of and interplay between transcriptional and post-transcriptional factors that affect localized microRNA expression.

Expression of target genes of 14q32 microRNAs was also assessed. In a previous study MEF2A was identified as direct target of miR-329[16]. Here, we found that lower expression of miR-329-3p, as well as miR-494-3p, corresponds with higher expression of MEF2A and vice versa. VEGFA is a confirmed target of miR-494[16], as well as of miR-127[57], and we found that expression of these microRNAs is indeed inversely correlated with expression of VEGFA throughout the vasculature. MiR-495 targets CCL2 and thereby affects proliferation and apoptosis of HUVECs[58]. In the vessel where CCL2 is highest expressed, the aorta, miR-495-3p was not expressed. We show here that miR-433-3p is highly expressed in the human vasculature. It has been shown previously that miR-433 is also abundantly expressed in cardiac fibrosis[59] and that the miR-433 target gene JNK1-b2, shows decreased expression in cardiac fibrosis. We confirmed the inversed relation between miR-433 and JNK1-b2 in miRMap. MiR-370 has been described to directly inhibit CPT1A expression and thereby reduce fatty acid β-oxidation in lipid metabolism[60]. We also found an inversed correlation between miR-370 expression and CPT1A expression. FOXO1 has been described to be a direct target of miR-544 in colorectal cancer development[61]. FOXO1 itself has been found to inhibit endothelial growth and proliferation[62] and wound closure and vascular density was reduced upon deletion of FOXO1[63]. Again, we observed an inverse relationship between miR-544 and FOXO1 expression profiles. Therefore, we could conclude that the measured 14q32 microRNAs act as regulators of their target mRNAs in vascular remodelling.

DNA methylation in the 14q32 locus is associated with tissue specificity in oncogenesis[64], but it is also associated to several (patho)physiological conditions in cardiovascular diseases like atherosclerosis[31] and cardiac fibrosis[65]. Therefore, we quantified DNA methylation of multiple CpGs in the three different DMRs along the 14q32 locus in order to assess a possible relation between 14q32 DNA methylation and the different vascular origins. Differential DNA methylation was measured, but we did not find clear patterns overall throughout the human vasculature. Although it had previously been shown that hypo-methylation of the 14q32 DMRs is associated with increased 14q32 microRNA expression and vice versa[31,35], we did not find a direct correlation between 14q32 DNA methylation and 14q32 microRNA expression in miRMap. Moreover, DNA methylation did not correlate with pri-microRNA expression. The lack of direct associations between DNA methylation and microRNA expression indicates that DNA methylation can have other functions than merely regulation of transcription. An

example of such “novel” functions was published by Shayevitch et al, demonstrating that DNA methylation can function as regulator of alternative splicing of mRNA[66]. This suggests that transcription and interaction between epigenetic features is a much more complex mechanism than has been thought and such alternative functions of the epigenome require further in-depth investigations in the future.

In patients with CAD who underwent coronary artery bypass grafting, significantly higher 14q32 DNA methylation of two DMRs was found in pre-implantation venous bypass grafts than in pre-implantation arterial bypass grafts. We know that coronary artery bypass graft patency is still significantly higher in arterial than in venous bypass grafts[67-69]. Future research into the effect of 14q32 DNA methylation on graft patency is needed to assess a direct relationship. Furthermore, we found a highly genomic location-dependent DNA methylation status of critical ischemic lower limb veins compared to intermittent ischemic lower limb veins. 14q32 DNA methylation status is associated with atherosclerosis[31] and ischemic arterial disease[40]. The observed differential DNA methylation statuses imply that DNA methylation itself is a disease dependent mechanism of gene expression regulation, independent of microRNA expression. Furthermore, it is interesting that DNMT gene expression varies in samples with different cardiovascular diseases, especially between vessels in different stages of PAD. Both DNMT1, which functions in DNA methylation maintenance, and DNMT3A, a *de novo* DNA methylation enzyme, are highly expressed in lower limb arteries of PAD patients and lowest expression is present in lower limb veins of PAD patients with critical ischemia. This implies that DNMT gene expression, like 14q32 DNA methylation could be linked to cardiovascular disease directly. A significant correlation between DNMT gene expression and 14q32 DNA methylation could only be found between DNMT3A and MEG3-DMR-1A. The absence of other significant correlations within this analyses could be explained by the fact that we have measured the status of DNA methylation and RNA expression at one timepoint, whereas DNA methylation is a dynamic process and we only measured in a static situation. Future research is needed to fully elucidate this independent mechanism and the interplay between DNA methylation and cardiovascular disease.

Conservation between the human 14q32 locus and the murine 12F1 locus has been described previously[23]. In murine models for PAD and vein graft disease, we found increasing DNA methylation over time after hind limb ischemia. Furthermore, we observed changes in DNA methylation at 2 weeks after vein grafting, when vascular remodelling is most active vs. a normalization of the DNA methylation status at 4 weeks after vein grafting. At 4 weeks, the remodelling process of the vein graft model slows down toward a new stable state[48,49]. This suggests that 14q32 DNA methylation status is actively regulated during vascular remodelling. Unfortunately, we have no way to determine the exact stage of remodelling in the human

atherosclerotic vascular samples that we obtained. However, the findings that DNA methylation directly associates with cardiovascular disease in the human vasculature, was fully supported by our murine models.

Confounding factors that the miRMap study design allowed us to include, namely sex, age, and malignancy, and that are known to affect development and progression of cardiovascular diseases[41-43], were assessed. We did not find a correlation of age and sex with 14q32 microRNA expression as well as with 14q32 DNA methylation. However, in 16 out of 17 14q32 microRNAs, expression in peri-malignancy vessels was higher than in non-malignant control vessels, indicating that malignancies do influence 14q32 microRNA expression in blood vessels in their vicinity. On the other hand, 14q32 DNA methylation did not differ between vessels closely located to malignancies and their control vascular tissues, unlike what has been described in literature for several types of cancer[35,36,39]. However, this was in the malignancy itself and not in vascular tissue nearby.

In conclusion, 14q32 microRNAs showed to be highly diverse in expression pattern throughout the human vasculature. In this study, we focused on the 14q32 microRNA cluster, but it is likely that other vasoactive microRNAs outside the 14q32 cluster, like the endothelial-specific microRNA miR-126 and the smooth muscle cell-specific microRNA miR-145, show specific vascular fingerprints as well. Furthermore, although DNA methylation could not be linked to microRNA expression, it is directly linked to both cardiovascular disease status and vessel location. Vessel-specific microRNA expression and DNA methylation profiles could impact both the development and treatment of cardiovascular disease, merit more attention in future studies into the mechanistic role of microRNAs and DNA methylation in cardiovascular pathology and should be taken into account in treatment of cardiovascular diseases via microRNAs.

Acknowledgements

We thank the surgeons of the LUMC for their help in tissue sample collection and M.W. Pollemans for the technical support.

Funding

This work was supported by an MD/PhD Fellowship from the LUMC to Eveline Goossens.

References

1. WHO. Available online at: http://www.who.int/mediacentre/factsheets/fs317/en/ (2017).
2. Cunningham KS, Gotlieb AI. The role of shear stress in the pathogenesis of atherosclerosis. Lab Invest. (2005) 85:9–23. doi: 10.1038/labinvest.3700215
3. Fan XJ, Zhao HD, Yu G, Zhong XL, Yao H, Yang QD. Role of inflammatory responses in the pathogenesis of human cerebral aneurysm. Genet Mol Res. (2015) 14:9062–70. doi: 10.4238/2015.August.7.15
4. Golledge J, Muller J, Daugherty A, Norman P. Abdominal aortic aneurysm: pathogenesis and implications for management. Arterioscler Thromb Vasc Biol. (2006) 26:2605–13. doi: 10.1161/01.ATV.0000245819.32762.cb
5. Rajewsky N. microRNA target predictions in animals. Nat Genet. (2006) 38(Suppl.)S8–13. doi: 10.1038/ng1798
6. Bonauer A, Boon RA, Dimmeler S. Vascular microRNAs. Curr Drug Targets. (2010) 11:943–9. doi: 10.2174/138945010791591313
7. Thum T, Galuppo P, Wolf C, Fiedler J, Kneitz S, van Laake LW, et al. MicroRNAs in the human heart: a clue to fetal gene reprogramming in heart failure. Circulation. (2007) 116:258–67. doi: 10.1161/CIRCULATIONAHA.107.687947
8. van Rooij E, Sutherland LB, Liu N, Williams AH, McAnally J, Gerard RD, et al. A signature pattern of stress-responsive microRNAs that can evoke cardiac hypertrophy and heart failure. Proc Natl Acad Sci USA. (2006) 103:18255–60. doi: 10.1073/pnas.0608791103
9. Wang S, Aurora AB, Johnson BA, Qi X, McAnally J, Hill JA, et al. The endothelial-specific microRNA miR-126 governs vascular integrity and angiogenesis. Dev Cell. (2008) 15:261–71. doi: 10.1016/j.devcel.2008.07.002
10. Parahuleva MS, Lipps C, Parviz B, Holschermann H, Schieffer B, Schulz R, et al. MicroRNA expression profile of human advanced coronary atherosclerotic plaques. Sci Rep. (2018) 8:7823. doi: 10.1038/s41598-018-25690-4
11. Markus B, Grote K, Worsch M, Parviz B, Boening A, Schieffer B, et al. Differential expression of MicroRNAs in endarterectomy specimens taken from patients with asymptomatic and symptomatic carotid plaques. PLoS ONE. (2016) 11:e0161632. doi: 10.1371/journal.pone.0161632
12. Wei Y, Nazari-Jahantigh M, Neth P, Weber C, Schober A. MicroRNA-126,−145, and−155: a therapeutic triad in atherosclerosis? Arterioscler Thromb Vasc Biol. (2013) 33:449–54. doi: 10.1161/ATVBAHA.112.300279
13. van Rooij E, Olson EN. MicroRNA therapeutics for cardiovascular disease: opportunities and obstacles. Nat Rev Drug Discov. (2012) 11:860–72. doi: 10.1038/nrd3864
14. Welten SM, Goossens EA, Quax PH, Nossent AY. The multifactorial nature of microRNAs in vascular remodelling. Cardiovasc Res. (2016) 110:6–22. doi: 10.1093/cvr/cvw039
15. Thum T. MicroRNA therapeutics in cardiovascular medicine. EMBO Mol Med. (2012) 4:3–14. doi: 10.1002/emmm.201100191
16. Welten SM, Bastiaansen AJ, de Jong RC, de Vries MR, Peters EA, Boonstra MC, et al. Inhibition of 14q32 MicroRNAs miR-329, miR-487b, miR-494, and miR-495 increases neovascularization and blood flow recovery after ischemia. Circ Res. (2014) 115:696–708. doi: 10.1161/CIRCRESAHA.114.304747
17. Wezel A,Welten SM, RazawyW, Lagraauw HM, de Vries MR, Goossens EA, et al. Inhibition of microRNA-494 reduces carotid artery atherosclerotic lesion development and increases plaque stability. Ann Surg. (2015) 262:841–7; discussion 847-848. doi: 10.1097/SLA.0000000000001466
18. Welten SMJ, de Jong RCM, Wezel A, de Vries MR, Boonstra MC, Parma L, et al. Inhibition of 14q32 microRNA miR-495 reduces lesion formation, intimal hyperplasia and plasma cholesterol levels in experimental restenosis. Atherosclerosis. (2017) 261:26–36. doi: 10.1016/j.atherosclerosis.2017.04.011

19. Nossent AY, Eskildsen TV, Andersen LB, Bie P, Bronnum H, Schneider M, et al. The 14q32 microRNA-487b targets the antiapoptotic insulin receptor substrate 1 in hypertension-induced remodeling of the aorta. Ann Surg. (2013) 258:743–53. doi: 10.1097/SLA.0b013e3182a6aac0
20. Wang P, Luo Y, Duan H, Xing S, Zhang J, Lu D, et al. MicroRNA 329 suppresses angiogenesis by targeting CD146. Mol Cell Biol. (2013) 33:3689– 99. doi: 10.1128/MCB.00343-13
21. Wang X, Zhang X, Ren XP, Chen J, Liu H, Yang J, et al. MicroRNA-494 targeting both proapoptotic and antiapoptotic proteins protects against ischemia/reperfusion-induced cardiac injury. Circulation. (2010) 122:1308–18. doi: 10.1161/CIRCULATIONAHA.110.964684
22. Martinez-Micaelo N, Beltran-Debon R, Aragones G, Faiges M, Alegret JM. MicroRNAs clustered within the 14q32 locus are associated with endothelial damage and microparticle secretion in bicuspid aortic valve disease. Front Physiol. (2017) 8:648. doi: 10.3389/fphys.2017.00648
23. Seitz H, Royo H, Bortolin ML, Lin SP, Ferguson-Smith AC, Cavaille J. A large imprinted microRNA gene cluster at the mouse Dlk1-Gtl2 domain. Genome Res. (2004) 14:1741–8. doi: 10.1101/gr.2743304
24. Wienholds E, Kloosterman WP, Miska E, Alvarez-Saavedra E, Berezikov E, de Bruijn E, et al. MicroRNA expression in zebrafish embryonic development. Science. (2005) 309:310–1. doi: 10.1126/science.1114519
25. van Solingen C, Seghers L, Bijkerk R, Duijs JM, Roeten MK, van Oeveren-Rietdijk AM, et al. Antagomir-mediated silencing of endothelial cell specific microRNA-126 impairs ischemia-induced angiogenesis. J Cell Mol Med. (2009) 13:1577–85. doi: 10.1111/j.1582-4934.2008.00613.x
26. Cheng Y, Liu X, Yang J, Lin Y, Xu DZ, Lu Q, et al. MicroRNA-145, a novel smooth muscle cell phenotypic marker and modulator, controls vascular neointimal lesion formation. Circ Res. (2009) 105:158–66. doi: 10.1161/CIRCRESAHA.109.197517
27. Harris TA, Yamakuchi M, Ferlito M, Mendell JT, Lowenstein CJ. MicroRNA-126 regulates endothelial expression of vascular cell adhesion molecule 1. Proc Natl Acad Sci USA. (2008) 105:1516–21. doi: 10.1073/pnas.0707493105
28. Schober A, Nazari-Jahantigh M, Wei Y, Bidzhekov K, Gremse F, Grommes J, et al. MicroRNA-126-5p promotes endothelial proliferation and limits atherosclerosis by suppressing Dlk1. Nat Med. (2014) 20:368–76. doi: 10.1038/nm.3487
29. Kin K, Miyagawa S, Fukushima S, Shirakawa Y, Torikai K, Shimamura K, et al. Tissue- and plasma-specific MicroRNA signatures for atherosclerotic abdominal aortic aneurysm. J Am Heart Assoc. (2012)1:e000745. doi: 10.1161/JAHA.112.000745
30. Anand S, Cheresh DA. Emerging role of micro-RNAs in the regulation of angiogenesis. Genes Cancer. (2011) 2:1134–8. doi: 10.1177/1947601911423032
31. Aavik E, Lumivuori H, Leppanen O, Wirth T, Hakkinen SK, Brasen JH, et al. Global DNA methylation analysis of human atherosclerotic plaques reveals extensive genomic hypomethylation and reactivation at imprinted locus 14q32 involving induction of a miRNA cluster. Eur Heart J. (2015) 36:993–1000. doi: 10.1093/eurheartj/ehu437
32. Jeltsch A, Jurkowska RZ. New concepts in DNA methylation. Trends Biochem Sci. (2014) 39:310–8. doi: 10.1016/j.tibs.2014.05.002
33. Kameswaran V, Bramswig NC,McKenna LB, PennM, Schug J, Hand NJ, et al. Epigenetic regulation of the DLK1-MEG3 microRNA cluster in human type 2 diabetic islets. CellMetabol. (2014) 19:135–45. doi: 10.1016/j.cmet.2013.11.016
34. Dai R, Lu R, Ahmed SA. The upregulation of genomic imprinted DLK1-Dio3 miRNAs in murine lupus is associated with global DNA hypomethylation. PLoS ONE. (2016) 11:e0153509. doi: 10.1371/journal.pone.0153509
35. Guo W, Dong Z, Liu S, Qiao Y, Kuang G, Guo Y, Shen S, Liang J. Promoter hypermethylation-mediated downregulation of miR-770 and its host gene MEG3, a long non-coding RNA, in the

development of gastric cardia adenocarcinoma. Mol Carcinogen. (2017) 56:1924–34. doi: 10.1002/mc.22650
36. Gonzalez-Vallinas M, Rodriguez-Paredes M, Albrecht M, Sticht C, Stichel D, Gutekunst J, et al. Epigenetically regulated chromosome 14q32 miRNA cluster induces metastasis and predicts poor prognosis in lung adenocarcinoma patients. Mol Cancer Res. (2018) 16:390–402. doi: 10.1158/1541-7786.MCR-17-0334
37. Moradi S, Sharifi-Zarchi A, Ahmadi A, Mollamohammadi S, Stubenvoll A, Gunther S, et al. Small RNA sequencing reveals Dlk1-Dio3 locus-embedded MicroRNAs as major drivers of ground-state pluripotency. Stem Cell Rep. (2017) 9:2081–96. doi: 10.1016/j.stemcr.2017.10.009
38. Xi S, Xu H, Shan J, Tao Y, Hong JA, Inchauste S, et al. Cigarette smoke mediates epigenetic repression of miR-487b during pulmonary carcinogenesis. J Clin Invest. (2013) 123:1241–61. doi: 10.1172/JCI61271
39. Oshima G, Poli EC, Bolt MJ, Chlenski A, Forde M, Jutzy JMS, et al. DNA methylation controls metastasis-suppressive 14q32-encoded miRNAs. Cancer Res. (2019) 79:650–62. doi: 10.1158/0008-5472.CAN-18-0692
40. Heuslein JL, Gorick CM, Price RJ. Epigenetic regulators of the revascularization response to chronic arterial occlusion. Cardiovasc Res. (2019) 115:701–12. doi: 10.1093/cvr/cvz001
41. Burgess KS, Philips S, Benson EA, Desta Z, Gaedigk A, Gaedigk R, et al. Age related changes in MicroRNA expression and pharmacogenes in human liver. Clin Pharmacol Ther. (2015) 98:205–15. doi: 10.1002/cpt.145
42. Kwekel JC, Vijay V, Han T, Moland CL, Desai VG, Fuscoe JC. Sex and age differences in the expression of liver microRNAs during the life span of F344 rats. Biol Sex Differ. (2017) 8:6. doi: 10.1186/s13293-017-0127-9
43. Enterina JR, Enfield KSS, Anderson C, Marshall EA, Ng KW, Lam WL. DLK1-DIO3 imprinted locus deregulation in development, respiratory disease, and cancer. Expert Rev Respir Med. (2017) 11:749–61. doi: 10.1080/17476348.2017.1355241
44. Xiao FH, Wang HT, Kong QP. Dynamic DNA methylation during aging: a “prophet” of age-related outcomes. Front Genet. (2019) 10:107. doi: 10.3389/fgene.2019.00107
45. El-Maarri O, Becker T, Junen J, Manzoor SS, Diaz-Lacava A, Schwaab R, et al. Gender specific differences in levels of DNA methylation at selected loci from human total blood: a tendency toward higher methylation levels in males. Hum Genet. (2007) 122:505–14. doi: 10.1007/s00439-007-0430-3
46. Liu J, Morgan M, Hutchison K, Calhoun VD. A study of the influence of sex on genome wide methylation. PLoS ONE. (2010) 5:e10028. doi: 10.1371/journal.pone.0010028
47. de Vries MR, Niessen HW, Lowik CW, Hamming JF, Jukema JW, Quax PH. Plaque rupture complications in murine atherosclerotic vein grafts can be prevented by TIMP-1 overexpression. PLoS ONE. (2012) 7:e47134. doi: 10.1371/journal.pone.0047134
48. de Vries MR, Parma L, Peters HAB, Schepers A, Hamming JF, Jukema JW, et al. Blockade of vascular endothelial growth factor receptor 2 inhibits intraplaque haemorrhage by normalization of plaque neovessels. J InternMed. (2019) 285:59–74. doi: 10.1111/joim.12821
49. Lardenoye JH, de Vries MR, Lowik CW, Xu Q, Dhore CR, Cleutjens JP, et al. Accelerated atherosclerosis and calcification in vein grafts: a study in APOE∗3 Leiden transgenic mice. Circ Res. (2002) 91:577–84. doi: 10.1161/01.RES.0000036901.58329.D7
50. Juzenas S, Venkatesh G, Hubenthal M, Hoeppner MP, Du ZG, Paulsen M, et al. A comprehensive, cell specific microRNA catalogue of human peripheral blood. Nucleic Acids Res. (2017) 45:9290–301. doi: 10.1093/nar/gkx706
51. Teruel-Montoya R, Kong X, Abraham S, Ma L, Kunapuli SP, Holinstat M, et al. MicroRNA expression differences in human hematopoietic cell lineages enable regulated transgene expression. PLoS ONE. (2014) 9:e102259. doi: 10.1371/journal.pone.0102259

52. Parsons C, Agasthi P, Mookadam F, Arsanjani R. Reversal of coronary atherosclerosis: role of life style and medical management. Trends Cardiovasc Med. (2018) 28:524–31. doi: 10.1016/j.tcm.2018.05.002
53. Wang YS, Wang HY, Liao YC, Tsai PC, Chen KC, Cheng HY, et al. MicroRNA-195 regulates vascular smooth muscle cell phenotype and prevents neointimal formation. Cardiovasc Res. (2012) 95:517–26. doi: 10.1093/cvr/cvs223
54. Welten SMJ, de Vries MR, Peters EAB, Agrawal S, Quax PHA, Nossent AY. Inhibition of Mef2a enhances neovascularization via post-transcriptional regulation of 14q32 MicroRNAs miR-329 and miR-494. Mol Ther Nucleic Acids. (2017) 7:61–70. doi: 10.1016/j.omtn.2017.03.003
55. Downie Ruiz Velasco A, Welten SMJ, Goossens EAC, Quax PHA, Rappsilber J, Michlewski G, et al. Posttranscriptional regulation of 14q32 MicroRNAs by the CIRBP andHADHB during vascular regeneration after ischemia.Mol Ther Nucleic Acids. (2019) 14:329–38. doi: 10.1016/j.omtn.2018.11.017
56. Treiber T, Treiber N, Plessmann U, Harlander S, Daiss JL, Eichner N, et al. A compendium of RNA-binding proteins that regulateMicroRNA biogenesis. Mol Cell. (2017) 66:270–84.e213. doi: 10.1016/j.molcel.2017.03.014
57. Pathak S, Meng WJ, Nandy SK, Ping J, Bisgin A, Helmfors L, et al. Radiation and SN38 treatments modulate the expression of microRNAs, cytokines and chemokines in colon cancer cells in a p53-directed manner. Oncotarget. (2015) 6:44758–80. doi: 10.18632/oncotarget.5815
58. Liu D, Zhang XL, Yan CH, Li Y, Tian XX, Zhu N, et al. MicroRNA-495 regulates the proliferation and apoptosis of human umbilical vein endothelial cells by targeting chemokine CCL2. Thromb Res. (2015) 135:146–54. doi: 10.1016/j.thromres.2014.10.027
59. Tao L, Bei Y, Chen P, Lei Z, Fu S, Zhang H, et al. Crucial role of miR-433 in regulating cardiac fibrosis. Theranostics. (2016) 6:2068– 83. doi: 10.7150/thno.15007
60. Iliopoulos D, Drosatos K, Hiyama Y, Goldberg IJ, Zannis VI. MicroRNA-370 controls the expression of microRNA-122 and Cpt1alpha and affects lipid metabolism. J Lipid Res. (2010) 51:1513–23. doi: 10.1194/jlr.M004812
61. Yao GD, Zhang YF, Chen P, Ren XB. MicroRNA-544 promotes colorectal cancer progression by targeting forkhead box O1. Oncol Lett. (2018) 15:991–7. doi: 10.3892/ol.2017.7381
62. Wilhelm K, Happel K, Eelen G, Schoors S, Oellerich MF, Lim R, et al. FOXO1 couples metabolic activity and growth state in the vascular endothelium. Nature. (2016) 529:216–20. doi: 10.1038/nature16498
63. Jeon HH, Yu Q, Lu Y, Spencer E, Lu C, Milovanova T, et al. FOXO1 regulates VEGFA expression and promotes angiogenesis in healing wounds. J Pathol. (2018) 245:258–64. doi: 10.1002/path.5075
64. Dmitrijeva M, Ossowski S, Serrano L, Schaefer MH. Tissue-specific DNA methylation loss during ageing and carcinogenesis is linked to chromosome structure, replication timing and cell division rates. Nucleic Acids Res. (2018) 46:7022–39. doi: 10.1093/nar/gky498
65. Watson CJ, Collier P, Tea I, Neary R, Watson JA, Robinson C, et al. Hypoxia induced epigenetic modifications are associated with cardiac tissue fibrosis and the development of a myofibroblast-like phenotype. Hum Mol Genet. (2014) 23:2176–88. doi: 10.1093/hmg/ddt614
66. Shayevitch R, Askayo D, Keydar I, Ast G. The importance of DNA methylation of exons on alternative splicing. RNA. (2018) 24:1351–62. doi: 10.1261/rna.064865.117
67. Goldman S, Zadina K, Moritz T, Ovitt T, Sethi G, Copeland JG, et al. Long-term patency of saphenous vein and left internal mammary artery grafts after coronary artery bypass surgery: results from a Department of Veterans Affairs Cooperative Study. J Am Coll Cardiol. (2004) 44:2149–56. doi: 10.1016/j.jacc.2004.08.064
68. Lytle BW, Loop FD, Cosgrove DM, Ratliff NB, Easley K, Taylor PC. Long-term (5 to 12 years) serial studies of internal mammary artery and saphenous vein coronary bypass grafts. J Thoracic Cardiovasc Surg. (1985) 89:248–58.

69. Gaudino M, Benedetto U, Fremes S, Biondi-Zoccai G, Sedrakyan A, Puskas JD, et al. Radial-artery or saphenous-vein grafts in coronary-artery bypass surgery. N Engl J Med. (2018) 378:2069–77. doi: 10.1056/NEJMoa1716026

Supplementary Data

Supplementary Table 1 Vascular tissue samples used for microRNA analysis

miRMap biobank	N	Mean age (SD)	Male (%)	Peri-malignancy (%)
Upper limb veins	3	51.3 (12.1)	100	0
Lower limb arteries	14	60.6 (15.1)	71.4	0
Lower limb veins	20	69.1 (13.1)	65.0	0
Abdominal arteries	17	65.4 (11.6)	70.6	64.7
Abdominal veins	6	58.3 (15.7)	83.3	66.7
Head and neck arteries	9	54.0 (28.0)	33.3	22.2
Head and neck veins	7	50.7 (21.5)	57.1	28.6
Abdominal aorta	4	65.8 (14.1)	25.0	0
Thoracic aorta	5	69.8 (16.7)	40.0	0
Arteriae mammariae	21	64.2 (10.0)	66.7	0
Atrial appendage	1	50 (-)	100	0
Radial artery	1	42 (-)	100	0
Umbilical artery	1	0 (-)	unknown	0
Total	109	61.4 (17.1)	63.3	17.4
Ampubase biobank	**N**	**Mean age (SD)**	**Male (%)**	**Peri-malignancy (%)**
Lower limb veins	6	61.6 (17.4)	100	0

Supplementary Table 2 Methylation-sensitive restriction enzymes used for DNA-methylation quantification.

Restriction Enzyme	Cut site
AciI	C|CGC
HhaI	GCG|C
BstUI	CG|CG
HpaII	C|CGG

Supplementary Table 3 Methylation sites and corresponding qPCR primer sequences and methylation-sensitive restriction enzymes.

Name of methylation site	CpG positions in genome (GRCh38/hg38)	Sequence Forward Primer	Sequence Reverse Primer	Enzyme
IG-DMR-CG4-2	100809537-8	CTTCCTGGCCCTTCCCTG	TGATAACCTGCGGATCTGAGA	AciI
IG-DMR-CG6-1	100810930-1 100810932-3 100810948-9	GGATCTGTGAGAAATGACTTCG	CAGGCACCTGGTGAGTCG	AciI
IG-DMR-CG6-2	100811108-9 100811115-6	CTAATTGCCAGCGATTTGC	TCCATTGTGGCCAGTTACAG	AciI
DMR-MEG3-A	100825889-90 100825914-5 100825929-30	CACGCAGGGAAAAAGCAC	ACCCAGATTGCAGCAAAGAA	AciI
DMR-MEG3-B	100825889-90 100825891-2			BstUI
DMR-MEG8-1A	100904620-1	CCTGGGCCACATTTCTGAG	CGCATCTGTCGCAGTTAAAA	AciI
DMR-MEG8-1H	100904603-4 100904623-4			HhaI
DMR-Control		TTGCTACAAAGGATCTGAGCTG	GTTGCAAACCAGGGTGAAGT	-
Name of methylation site	**CpG positions in genome (AJ320506.1)**	**Sequence Forward Primer**	**Sequence Reverse Primer**	**Enzyme**
Dlk1-DMR	12062	AGCTGCAATGCTCATTCCTAGTG	TAGTGGTCTATTCACCCAAGTGC	HpaII
	12678	GGAAAGGGCATGGGAGAGGAC	CCATCGTTCTCGCATGGGTTAGG	HhaI
	13270	AGGCCATCTGCTTCACCATCC	CGCTGTTATACTGCAACAGGAG	HhaI
	14538	GCCCAAGACTCCACCTCATGC	CACCCCACAAGCCATAGTGTC	HpaII
IG-DMR	79652	GGATCCTGACCTATGTGTACCTCTG	ACGGACCGTGTGTATGTGCTGTAG	HhaI
	79723			HpaII
	80437	TCTTGTGGCAAAGGTACGTGACTG	GTATGCTATGCATTTGTGCTGAAGG	HpaII
	81915	AGCTGACTTCCTTCAGCCACAGT	TTGACCCTGTGAGAGATGCTCAG	HpaII
	85733	AGTTTCTGGGAAACGTACAGAAGG	CACTTCTCTGCAAGGCCAAGTC	HhaI
Glt2-DMR	95372	GGTCGGGAGCGAGATGGGTTG	GCGTCCATGACACCCTAAATCAC	HhaI
	97768 97800	TCCCGTTCATGGCTCATGTGTCTC	GCCCTGGAAATGACCGCACACTC	HhaI HpaII
	99823	CCCTCTCAGTTTCCCAAACCTG	CCAAGGTATCCTGGAAGAGCTGAC	HpaII
DMR-Control		GGTGCCAGCAGAGACTTACACAG	CATGCCCTTTGACACTTAGTATGC	-

Supplementary Table 4 qPCR primer sequences for target mRNAs, pri-miRs and DNMTs

Primer	Sequence Forward Primer	Sequence Reverse Primer	Targeted by microRNA
HSA-CXCR7	ACAGCACAGCCAGGAAGG	TCCCTGGCTCTGAGTAGTCG	539
HSA-TGFβ1	GGCTACCATGCCAACTTCTG	CCGGGTTATGCTGGTTGTA	376c
HSA-KLF4	AGGGAGAAGACACTGCGTCA	ACGATCGTCTTCCCCTCTTT	543
HSA-JNK1-B2	AGAATCAGACTCATGCCAAGC	GGGATTTCTGTGGTGTGAAAA	433
HSA-CPT1a	ATCAAGAAATGTCGCACGAG	CATGGAGGCCTCGTATGTG	370
HSA-LPL	TAGCAGAGTCCGTGGCTACC	TGGCACCCAACTCTCATACA	410
HSA-LDLR	GAGGTGGCCAGCAATAGAAT	TCTCTGCTGATGACGGTGTC	411
HSA-MEF2A	GTGTCTGTGACAACCCCAAG	GAAGCCTTGAAGGGCTGAC	329, 494
HSA-VEGFA	GTGTGTGCCCACTGAGGAGT	TGTTGTGCTGTAGGAAGCTCA	127, 494
HSA-PPP2R2A	TGGTTACCCCAGAAAAATGC	ACCCTTCTGGTCTTTTGTCC	136
HSA-IRS1	ATACTCGAGTGACCTCAGCAAATCC TCTTC	ATAGCGGCCGCATACCTCCATCCC ACATCCA	487b
HSA-CCL2	TCTGTGCCTGCTGCTCATAG	CGAGCCTCTGCACTGAGAT	495
HSA-IκBα	TTTTGGTGTCCTTGGGTGCT	CAACAGGAGTGACACCAGGT	300
HSA-BRD7	CTGTTGCACTCAGGAATGAAAA	TCTGCTTTCGAGTTTTCTGCA	300, 410
HSA-FOXO1	AGTGGATGGTCAAGAGCGTG	GCACACGAATGAACTTGCTGT	544
HSA-STAT3	GTCAGTGACCAGGCAGAAGA	CACGTACTCCATCGCTGACA	544
HSA-PAK1	TCGAACCAGGTCATTCACAGA	GCTCTGGGGTTATCTGTGCA	485-5p
HSA-EMMPRIN	GTACTCCTGCGTCTTCCTCC	CCCCTCGTTGATGTGTTCTGA	485-5p
HSA-DNMT1	ATCTTCCTGACACCCTGCAT	CTCCCTGGTAGAATGCCTGA	
HSA-DNMT3A	AAGGAGGAGCGCCAAGAG	ATCACCGCAGGGTCCTTT	
HSA-DNDMT3B	ATGAAGGTTGGCGACAAGAG	CCCTGTGAGCAGCAGAAACT	
Pri-miR-329-1	TGGGGAAGAATCAGTGGTGT	GACCAGAAGGCCTCCAAGAT	
Pri-miR-329-2	TGTCAAGTTTGGGGAAGGAA	GACCAGAAGGCCTCCAAGAT	
Pri-miR-487b	AGGCAGTGGCTTTCTTTTCC	GAGGTGGGATCCAAACACAG	
Pri-miR-494	GATTCGGCAGTTCTGTTTTGA	CTGAAGGCTGCATCAGGAAC	
Pri-miR-495	CTGACCCTCAGTGTCCCTTC	ATGGAGGCACTTCAAGGAGA	

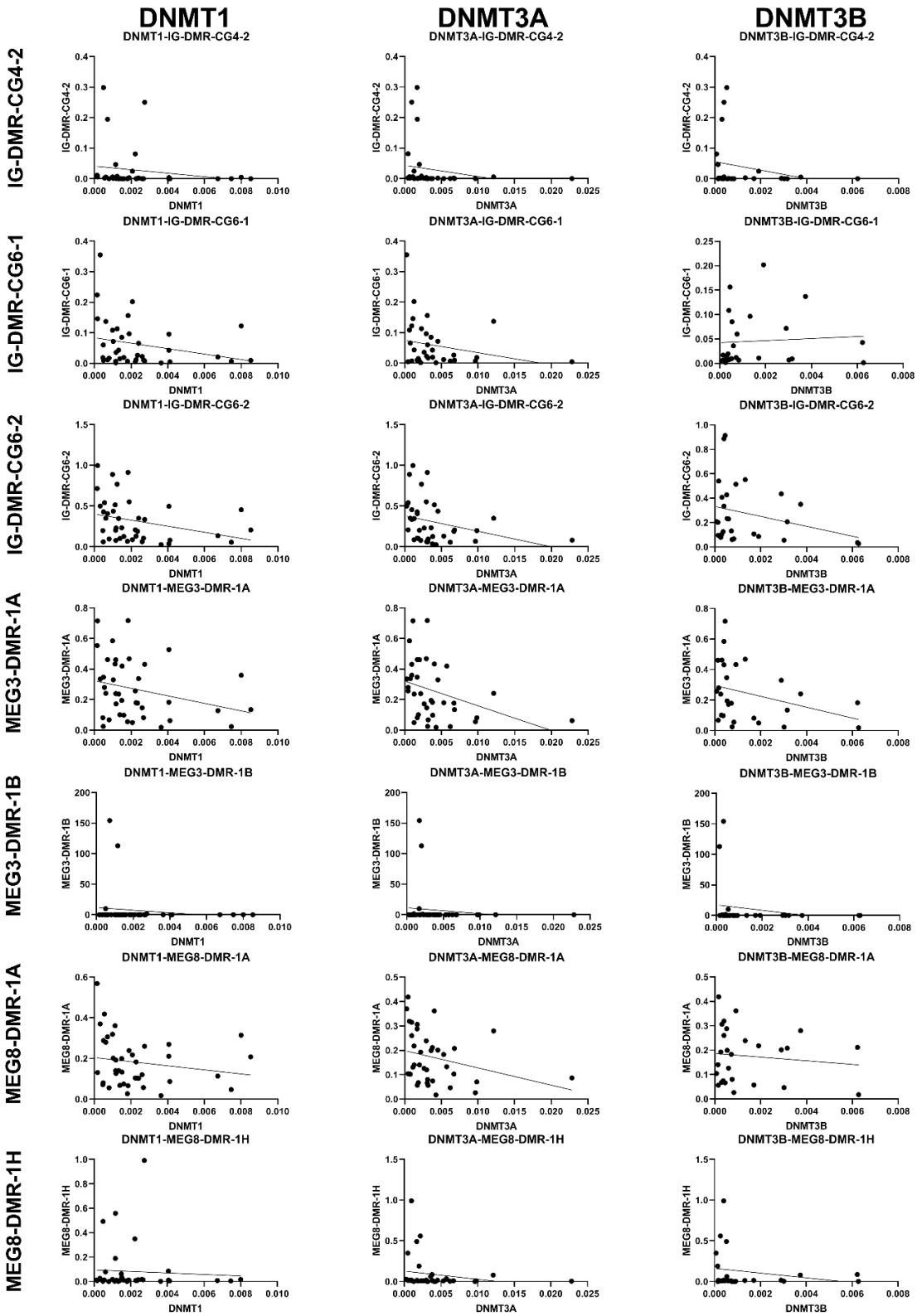

Supplementary Figure 1 Correlations between DNA methylation and DNMT gene expression. Vessels were divided into the following groups: lower limb arteries from patients with PAD (N=11), arteriae mammariae from patients with CAD (used as arterial graft) (N=18), VSMs from patients with CAD (used as vein graft) (N=8), lower limb veins from patients with PAD (N=10), lower limb veins from patients with critical ischemia (PAD-CI) (N=6). Linear regression analyses only showed statistically significant correlation between DNMT3A and MEG3-DMR-1A (p=0.03).

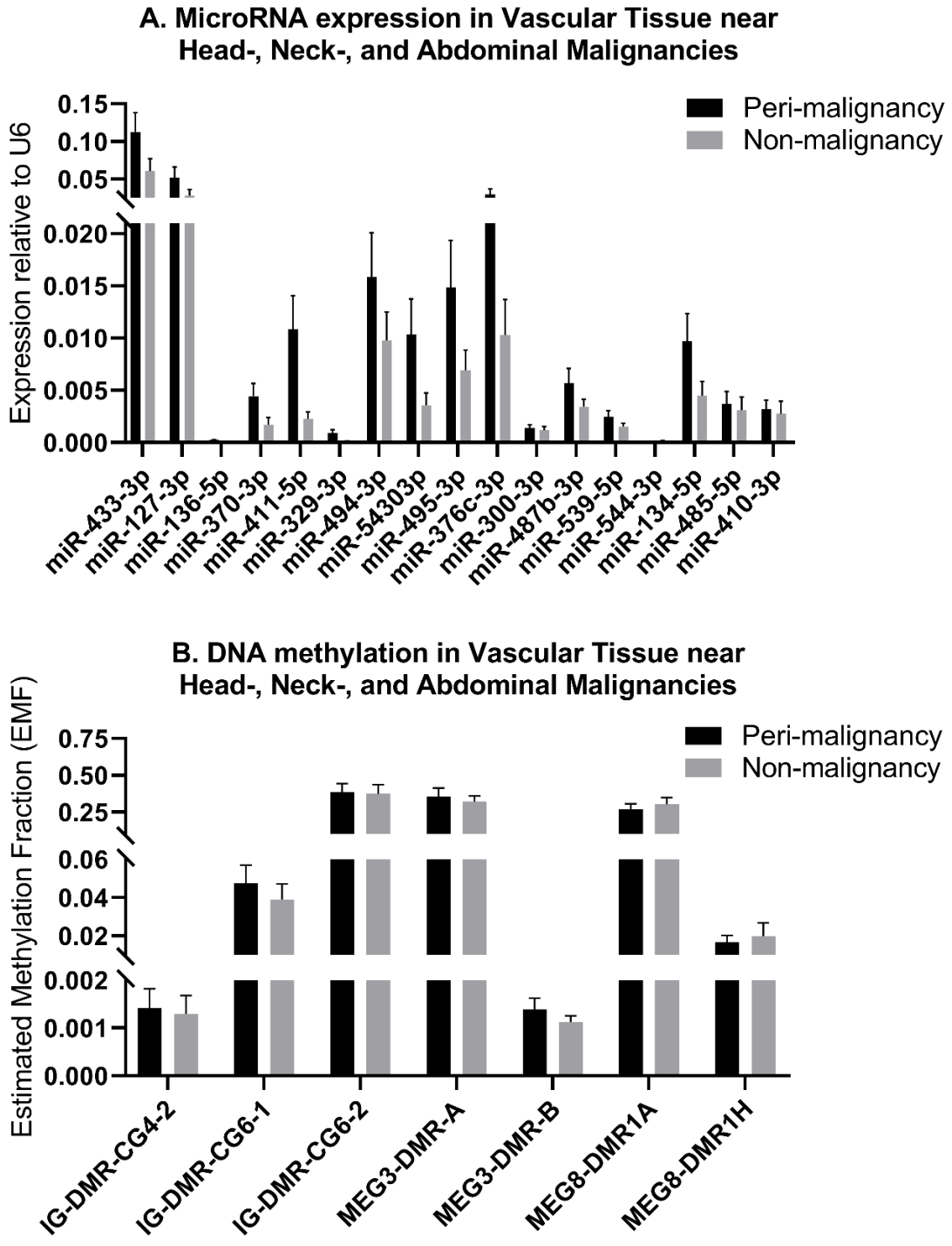

Supplementary Figure 2 A - Peri-malignancy vessel versus non-malignancy vessel microRNA expression. Peri-malignant vessels (N=19) versus non-malignant vessels (N=20) did not show significant differences for any of the analysed microRNAs. Mean expression per group is shown. The error bars represent the SEMs. MicroRNAs are arranged in the order of chromosomal location of the microRNA gene. B - Peri-malignancy vessel versus non-malignancy vessel DNA methylation. Peri-malignant vessels (N=13) versus non-malignant vessels (N=23) did not show significant differences for any of the analysed CpG sites. Mean expression per group is shown. The error bars represent the SEMs. CpG sites are arranged in the order of chromosomal location.

Part II

Chapter 5

Myostatin inhibits vascular smooth muscle cell proliferation and local 14q32 microRNA expression, but not systemic inflammation or restenosis

Submitted to International Journal of Molecular Sciences

EAC Goossens[1,2]
MR de Vries[1,2]
JW Jukema[3]
PHA Quax[1,2]
AY Nossent[1,2,4,5]

[1]Department of Surgery and [2]Einthoven Laboratory for Experimental Vascular Medicine, Leiden University Medical Center, Leiden, The Netherlands; [3]Department of Cardiology, Leiden University Medical Center, Leiden, Netherlands, [4]Department of Laboratory Medicine, Medical University of Vienna, Vienna, Austria, [5]Department of Internal Medicine II, Medical University of Vienna, Vienna, Austria

Abstract

Myostatin is a negative regulator of muscle cell growth and proliferation. Furthermore, myostatin directly affects expression of 14q32 microRNAs by binding the 14q32 locus. Direct inhibition of 14q32 microRNA miR-495-3p decreased postinterventional restenosis via inhibition of both vascular smooth muscle cell (VSMC) proliferation and local inflammation. Here we aimed to investigate the effects of myostatin in a mouse model for postinterventional restenosis.

In VSMCs *in vitro*, myostatin led to dose-specific downregulation of 14q32 microRNAs miR-433-3p, miR-494-3p and miR-495-3p. VSMC proliferation was inhibited, where cell migration and viability remained unaffected. In a murine postinterventional restenosis model, myostatin infusion did not decrease restenosis, neointimal area or lumen stenosis. Myostatin inhibited expression of both proliferation marker PCNA and of 14q32 microRNAs miR-433-3p, miR-494-3p and miR-495-3p dose-specifically in cuffed femoral arteries. However, 14q32 microRNA expression remained unaffected in macrophages and macrophage activation as well as macrophage influx into lesions were not decreased.

In conclusion, myostatin did not affect postinterventional restenosis. Although myostatin inhibits 14q32 microRNA expression and proliferation in VSMCs, myostatin had no effect on macrophage activation and infiltration. Our findings underline that restenosis is driven by both VSMC proliferation and local inflammation. Targeting only one of these components is insufficient to prevent restenosis.

Introduction

Atherosclerotic occlusions of the coronary artery and the femoral artery, causing coronary artery disease (CAD) and peripheral artery disease (PAD) respectively, can be treated by balloon angioplasty with or without stenting. However, in both CAD and PAD, restenosis often occurs due to a variety of factors[1]. Even when pro-atherogenic risk factors, such as hypercholesterolemia, are strictly controlled, restenosis can still develop. Upon physical manipulation of the occluded vessel during the angioplasty, the vascular wall becomes activated. On a cellular level, two vascular responses are crucial[1, 2]. On the one hand, vascular smooth muscle cells (VSMCs) that reside in the tunica media of the arterial wall, change their phenotype from contractile to synthetic, meaning that they start to proliferate and migrate into the tunica intima, forming a neointimal layer. On the other hand, inflammatory cells adhere to and infiltrate the affected vessel wall. Of these inflammatory cells, monocytes/macrophages are among the first to arrive and drive the inflammatory response. Inflammation allows for extracellular matrix remodelling, further facilitating the intimal hyperplasia. Although initiated locally, restenosis is driven by both local and systemic inflammation.

Patients with an atherosclerotic occlusion that are treated with balloon angioplasty, often receive drug-eluting stents (DES) that secrete drugs locally to inhibit restenosis[3, 4]. Many studies have been performed to find the most effective compound to reduce restenosis, focusing on anti-proliferative drugs. However, some compounds also target the inflammatory side of restenosis[5]. Sirolimus and paclitaxel are among the most frequently used compounds in DES. Sirolimus (rapamycin) has antiproliferative properties and is an immunosuppressing agent, inhibiting the local inflammatory reaction in restenosis[6]. Paclitaxel is antimitotic and therefore strongly antiproliferative in VSMCs[7], but does not act on inflammation and the therapeutic window is narrow[8]. Nowadays, DES that are mostly used, are sirolimus-like stents. Short term clinical outcomes between the two stents are similar, but long-term efficacy and safety favor sirolimus stents[8, 9]. Despite the existing stents however, restenosis remains a common issue in the fields of cardiology and vascular surgery and more efficient therapeutic strategies are still needed.

Myostatin, also known as Growth Differentiation Factor-8 (GDF-8), is a member of the TGF-β superfamily that negatively regulates skeletal muscle mass by inhibiting muscle hypertrophy and hyperplasia. Myostatin null mice show a dramatically increased skeletal muscle mass[10]. Accordingly, administration of myostatin causes muscle atrophy[11]. Myostatin is not only expressed in skeletal muscle cells, but also in cardiomyocytes and VSMCs[12, 13]. Although myostatin was shown to affect muscle cell function via extracellular binding to the activin type 2 receptor[14], intracellular effects, in which myostatin directly affects gene transcription, were

also observed[15]. One of the genomic regions that is affected by myostatin, is called the callipyge locus, also known as the 14q32 locus in humans. Callipyge originates from ancient Greek and means beautiful buttocks. Both absence of myostatin[15] and mutations in the 14q32 locus[16] can lead to a 'callipyge phenotype', which is defined by excessive muscle growth in cattle, sheep and mice. The callipyge locus contains three protein coding genes, but also a large conserved microRNA cluster, the 14q32 microRNA cluster (DIO3-DLK1 cluster, 12F1 in mice) that is known to play a role in many different vascular remodelling processes[17-21]. Upon knockout of myostatin in mice, microRNAs of the 12F1 locus were upregulated[15].

MicroRNAs are short noncoding RNA molecules that regulate gene expression by binding to the 3'-UTR of their target messenger RNA (mRNA), thereby inhibiting translation. As one microRNA has the ability to bind to multiple target genes, a single microRNA can affect entire (patho)physiological processes. This makes them promising targets in vascular remodelling, which is always a multifactorial process. In 2017, our group found that direct inhibition of 14q32 microRNA miR-495-3p reduces intimal hyperplasia, macrophage influx and overall lesion formation in experimental restenosis[17]. Myostatin has the potential to inhibit both VSMC proliferation and expression of miR-495-3p, as well as other 14q32 microRNAs, simultaneously. Therefore, we hypothesized that administration of myostatin will reduce postinterventional restenosis.

In this study, we made use of an established murine restenosis model[8, 17, 22-25]. In this model, a non-constrictive cuff is placed around both femoral arteries. Manipulation of the artery, as well as a foreign body response to the cuff, triggers both intimal hyperplasia and an inflammatory response[26]. We focused on the effects of myostatin infusion on VSMC proliferation, neointima formation, on macrophage infiltration into the lesions and of course on 14q32 microRNA expression. We looked specifically at miR-433-3p, miR-494-3p and miR-495-3p, as the genes encoding these microRNAs are located separately along the length of 14q32 locus, as it was previously shown that myostatin affects expression of the complete locus, rather than single microRNAs[15].

Materials and Methods

Animals and femoral artery cuff mouse model

This study was performed in compliance with Dutch government guidelines and the Directive 2010/63/EU of the European Parliament. All animal experiments were approved by the animal welfare committee of the Leiden University Medical Center. Male C57BL/6 mice (8-10 weeks old) with unrestricted access to food and water were used. Mice were randomized into groups based on age and weight. As described previously[17], mice underwent bilateral cuff surgery under adequate anesthesia and peri-operative analgesia, i.e. 5mg/kg midazolam

(Roche Diagnostics), 0.05mg/kg fentanyl (Janssen Pharmaceuticals) and 0.5mg/kg dexmedetomidine (Orion). After the incision, the iliac fat pad was located and the femoral artery was separated from the femoral vein and the femoral nerve and the non-constrictive polyethylene cuff was put into place and fixed with 2 6/0 sutures. The skin was closed with a continuous suture. Three groups of mice received Alzet Osmotic Pumps with myostatin (R&D systems, cat#788-G8/CF) in administration concentrations of 0.4µg/day, 0.2µg/day and 0.1µg/day and the control group received mini pumps with vehicle. Dosage of 0.4µg/day was described in literature to not have unwanted side effects as affecting body weight[27]. With the dose specific effect *in vitro*, we also choose to use 0.1µg/day and 0.2µg/day treatments. The pumps were placed subcutaneously in the neck and the skin was closed with two wound clips. Depending on the wound closure rate, at day 7-10 mice underwent Isoflurane anesthesia to remove the wound clips. In 0.2µg/day group, two mice died postoperatively. In 0.1µg/day group one mouse was taken out of the study as we observed during histological analysis that the femoral artery was not completely located in the cuff. At day 18, 19, 20 after surgery 200µL BrdU (5mg/ml) was injected i.p. for labeling of proliferating cells. On the day of sacrifice (21 days after surgery), the animals underwent terminal anesthesia, blood was drawn via heart puncture, after which a perfusion with PBS and formaldehyde was applied. Next, the cuffed arteries and hindlimb bones were collected for further processing.

Cell culture

Immortalized VSMCs[31] were cultured at 37°C in a humidified 5% CO2 environment. Culture medium (DMEM GlutaMAX™ (Invitrogen, GIBCO)), 10% heat inactivated fetal calf serum (PAA), 1% penicillin (10000U/mL) / streptomycin (10000U/mL)) was refreshed every 2-3 days. Cells were passed at 90% confluency using trypsin (Sigma). Stock solutions of isolated VSMCs up to passage four were stored at -180°C in 50% DMEM GlutaMAX™ containing 10% FCSi and 1% Penicillin/Streptomycin, 40% FCSi (PAA) and 10% DMSO (Sigma).

In vitro addition of myostatin to VSMCs

VSMCs were seeded in 12-well plates at 60.000 cells per well in culture medium. After 24 hours, cells were washed with PBS and each well was incubated with starve medium (DMEM GlutaMAX™ (Invitrogen, GIBCO) with 2% fetal bovine serum and 1% penicillin (10.000U/mL) / streptomycin (10.000U/mL) with or without recombinant myostatin (R&D systems, cat#788-G8) for 48 hours in different concentrations, 10nM and 20nM. For further microRNA analyses medium was aspired and cells were washed with PBS before adding 0.5mL TRIzol/well for RNA isolation. Each condition was performed in triplicate and each experiment was performed at least three times.

Scratch-wound healing assay

After 48 hours of incubation with 10nM recombinant myostatin or without recombinant myostatin medium was aspired and a scratch-wound was made across the diameter of each well using a p200 pipet tip. Next, cells were washed with PBS and fresh medium (DMEM GlutaMAX™ (Invitrogen, GIBCO)), 2% FBS, 1% penicillin (10.000U/mL) / streptomycin (10000U/mL)) was added. In order to monitor scratch-wound closure, live phasecontrast microscropy (Axiovert 40C, Carl Zeiss) was used for taking pictures immediately after (0h) and 21 hours after introducing the scratch-wound. Pictures were taken at two different locations in each well and averaged for analysis. Scratch size was calculated at 0h and 21h using the wound healing tool macro for ImageJ. Each single scratch assay condition was performed in triplicate and the scratch-wound healing assay was performed three times.

MTT viability assay

VSMCs were seeded in 96-wells plate with 4000 cells/well. After 24 hours, medium was aspired and cells were washed with PBS. Starve medium with 10nM and 20nM recombinant myostatin or without myostatin was added and cells were incubated for 48 hours. Negative control was culture medium with 10% DMSO as toxic agent and positive control was culture medium. 10µL of MTT (5mg/mL) was added and after 4 hours of incubation medium was removed carefully and replaced by isopropanol 0.1N HCl. Plate was incubated on shaker platform for 90 minutes at 250 rpm and absorbance was read at 540nm using Cytation5 (BioTek). Each single scratch assay condition was performed in quadruplicate and the viability assay was performed four times.

RNA isolation

Murine tissues were homogenized in TRIzol with electric pestle before starting RNA isolation. RNA isolation of both cultured cells and murine tissue was performed by standard TRIzol-chloroform extraction, according to the manufacturer's instructions (Thermo Fisher Scientific). RNA concentrations were measured using NanodropTM 1000 Spectrophotometer (Thermo Fisher Scientific).

MicroRNA Quantification

For microRNA quantification of miR-433-3p, miR-494-3p and miR-495-3p, in all samples RNA was reversed transcribed using the Taqman^{TM} MicroRNA Reverse Transcription Kit (Thermo Fisher Scientific) and subsequently quantified using microRNA-specific Taqman^{TM} qPCR kits

(Thermo Fisher Scientific) on the VIIa7 (Thermo Fisher Scientific). MicroRNA expression was normalized against U6 small nuclear RNA.

mRNA quantification

For quantification of mRNA, RNA was reverse transcribed using 'high-capacity RNA to cDNA kit' (Thermo Fisher Scientific) and quantified by qPCR using SybrGreen reagents (Qiagen) on the VIIa7. Primer sequences are provided in Supplementary Table 1.

Immunocytochemistry

VSMCs were plated on 0.2% gelatin coated cover slips in a 12-wells plate with 60.000 cells/well and incubated for 48 hours with 10nM recombinant myostatin and control was without myostatin. Cells were washed with PBS and fixated with 4% performaldehyde before permeabilization with 0.1% Triton (T8532, Sigma Aldrich). Primary anti-mouse-GDF8 antibody (ab71808, Abcam) was applied 1:50 and incubated overnight. Donkey anti-rabbit Alexa 647 (A31573) was applied 1:800 and after 60 minutes incubation Hoechst 34580 (Sigma-Aldrich, ref 63493) 1:1000 was applied. Cover slips were washed with PBS three times and pasted on glass slides mounted with Prolong™ Gold (P36930, Invitrogen). Pictures were taken with Confocal Microscopy.

Histological and immunohistochemical assessment of cuffed femoral arteries

Formaldehyde fixed cuffed femoral arteries were paraffin-embedded and 5µm thick cross sections of arteries were stained to visualize vessel morphology. For quantification of intimal thickening, elastic laminae were visualized with Weigert's elastin staining. For immunohistochemical analysis, the following antibodies were used: Myostatin (ab71808; Abcam), BrdU (ab221240; Abcam), Ki-67 (ab16667; Abcam), αSMA (1A4 clone, Dako), Mac-3 (550292; BD Pharmingen). Images of stained slides were obtained using Panoramic 250 Flash III (3DHISTECH). All quantifications were performed on six sequential representative sections per vessel segment using image analysis software (Qwin, Leica) for Weigert's elastin staining. All other quantifications were done using Panoramic Viewer software (3DHISTECH).

Bone marrow-derived macrophage isolation and stimulation

After sacrifice, femur and tibia bones from 0.0µg myostatin/day group (control group) and from 0.4µg myostatin/day group were collected and proximal and distal ends were removed. Bones were flushed with PBS with 25G needle (ref 300600, BD Microlance) and bone marrow was collected in 70µm cell strainer (BD Biosciences). After collection of bone marrow, cell

strainers were flushed with PBS and isolate was centrifuged. After removal of supernatant, washing steps were repeated two times. Washed pellet was resuspended in ACK lysing buffer (A10492, GIBCO) and kept on ice for 3 minutes. Lysis was stopped with culture medium (RPMI Medium 1640 (ref 52400-025, GIBCO) with 25% Fetal Bovine Serum (F7524, Sigma) and 1% penicillin/streptomycin). After two more washing steps with PBS, bone marrow monocytes were counted and seeded at 8.000.000 cells per dish (10cm diameter, Falcon, ref 351029) in 10mL culture medium with 2µL GM-CSF (ref 14-8331-80, eBiosciences). Monocytes of both groups were cultured either with and without *in vitro* treatment of 10nM myostatin. All conditions were performed in duplicate.

After 5 days, medium was refreshed and at day 8 after isolation, monocytes were maturated into macrophages and 10ng/mL LPS (K-235, Sigma) was added to trigger a cytokine release. 48 hours after stimulation, supernatant was collected, snap-frozen in liquid nitrogen and stored at -80°C. TRIzol was added and cell lysates were stored in -20°C before RNA isolation.

Enzyme-Linked Immuno Sorbent Assay (ELISA) of supernatant bone marrow-derived macrophages

ELISA analysis was performed following standard manufacturer's protocol for murine TNFα (ref 558534, BD OptEIA). Duplo samples of cultured macrophages were taken and each condition was tested in duplicate and using Cytation5 (BIOTEK) absorbance was read at 450nm and at 570nm. TNFα concentrations were calculated from standard curve.

Statistical analyses

Data are presented as mean + SEM. Indicated differences have the following levels of significance: *p<0.05, **p<0.01, ***p<0.001, ****p<0.0001. All tests were performed with a significance level of $\alpha<0.05$.

One sample t-test was performed to test differences of treated groups that are expressed relative to the control treatment, which is set to 100%. This test was used in myostatin addition and *in vivo* experiments and functional assays.

Between specific groups, the presence of differences was assessed with Student's t-test. These tests were used in comparison of PCNA expression in different treatment groups.

Kruskal-Wallis test was used to identify possible differences between treatment groups for MAC3 staining.

Results

In vitro uptake of myostatin in VSMC

Since myostatin can bind either to the cell surface receptor activin type II or can enter the nucleus, we first identified *in vitro* whether myostatin is taken up by VSMCs and, more specifically, is present in the nucleus. As shown in Figure 1A-C, myostatin was taken up into the VSMCs, concentrating mostly inside the nucleus. Endogenous expression of myostatin in the resting VSMC was negligible as in the negative control, where no myostatin was added, myostatin staining was absent (Figure 1D-F).

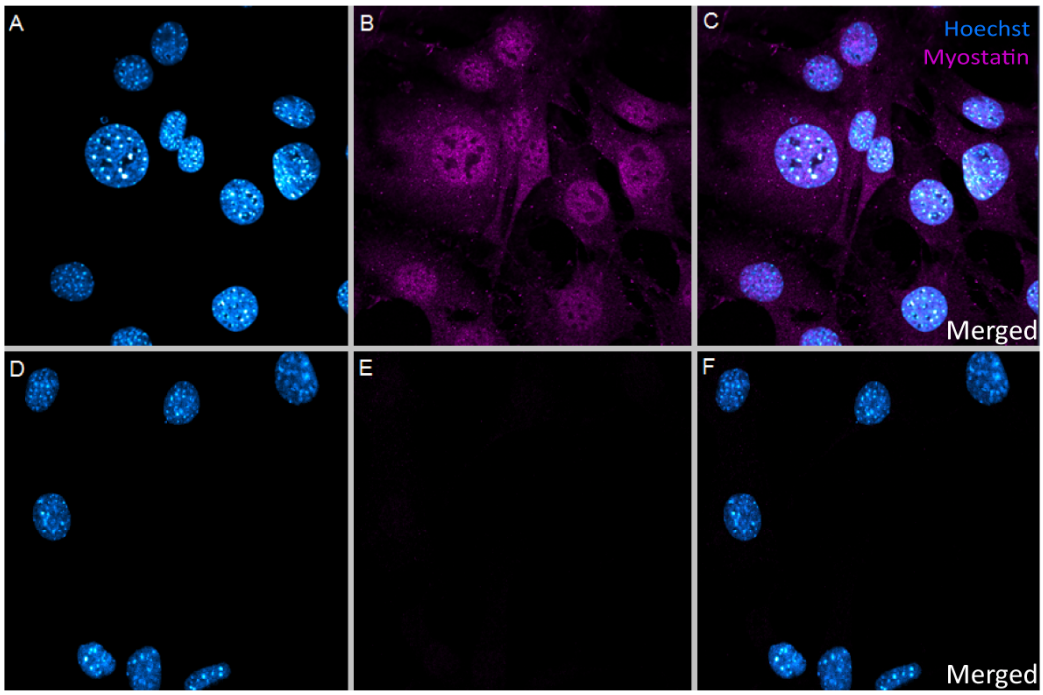

Figure 1A-F Immunocytochemical staining of VSMCs. A-C – VSMCs treated with 10nM myostatin showed uptake of myostatin in the cell, concentrating mostly in the nucleus. A – Hoechst only, B – Myostatin only, C – Merged image. D-F – VSMCs not treated with myostatin showed no endogenous myostatin presence in the cells at all. D – Hoechst only, E – Myostatin only, F – Merged image. Picture taken with 63x magnification.

Effect of myostatin on 14q32 microRNAs in VSMCs

We analyzed the effects of myostatin on expression levels of the specific 14q32 microRNAs miR-433-3p, miR-494-3p and miR-495-3p. Addition of 10nM or 20nM recombinant myostatin to VSMCs affected microRNA expression levels. For miR-433-3p, 10nM of myostatin downregulated microRNA expression ($p=0.04$), but 20nM did not affect miR-433-3p expression (Figure 2A). MiR-494-3p showed a downregulation after treatment with both 10nM and at 20nM myostatin (Figure 2B). MiR-495-3p was also downregulated by more than

80% after both 10nM and 20nM myostatin treatment (p=0.01 and p=0.01, respectively) (Figure 2C).

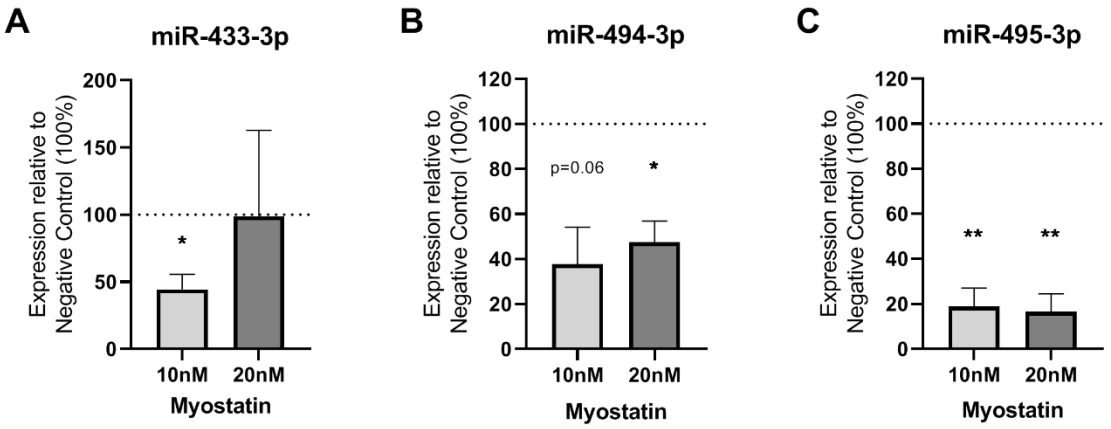

Figure 2A-C microRNAs in myostatin treated VSMCs relative to untreated control (100%). A – miR-433-3p expression in VSMCs treated with 10nM and 20nM myostatin only showed a downregulation at 10nM treatment (p=0.04). B – miR-494-3p expression in VSMCs treated with 10nM and 20nM myostatin was downregulated at 20nM treatment (p=0.03) and showed a trend towards downregulation at 10nM myostatin (p=0.06). C – miR-495-3p expression in VSMCs treated with 10nM and 20nM myostatin was decreased with more than 80% by both treatment concentrations (p=0.0098 and p=0.0088, respectively). Mean expression is shown and error bar represents SEM (N=3). One-sample t-test performed with 100% of control expression as hypothetical value. * p<0.05, ** p<0.01.

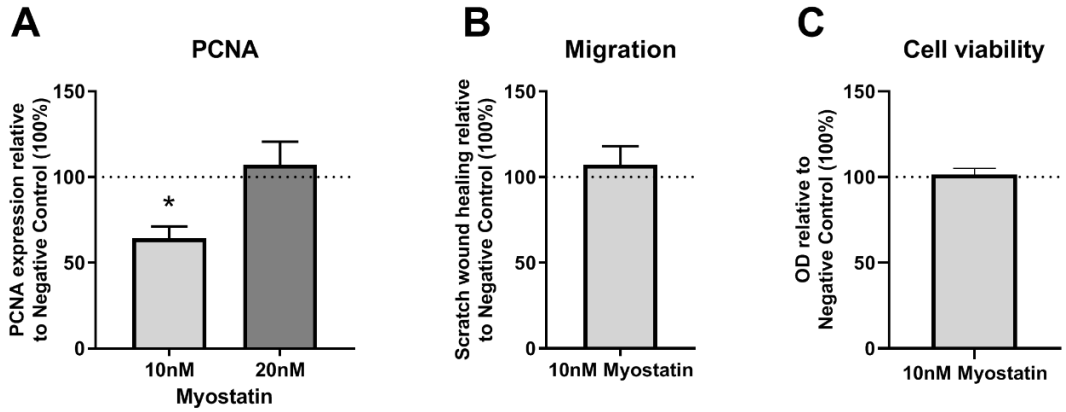

Figure 3A-C PCNA expression, cell migration and cell viability in myostatin treated VSMCs relative to non-myostatin treated control (100%). A – PCNA mRNA expression in myostatin treated VSMCs was downregulated at 10nM myostatin, but not at 20nM myostatin, N=3. B – Scratch wound healing in myostatin treated VSMCs was not changed, N=3. C – Cell viability in myostatin treated VSMCs remained unchanged, N=4. Mean expression is shown and error bars represent SEMs. One-sample t-test performed with 100% of Negative Control expression as control group.

Functional effects of MSTN on VSMCs

Proliferating Cell Nuclear Antigen (PCNA) mRNA expression, a measure of cell proliferation, was downregulated by approximately 40% when VSMCs were treated with 10nM myostatin compared to untreated cells (p=0.04) (Figure 3A). However, addition of 20nM myostatin did not result in downregulation of PCNA expression in cultured VSMCs. Migration and cell viability remained unaffected by 10nM myostatin, compared to the negative control (Figure 3B+C).

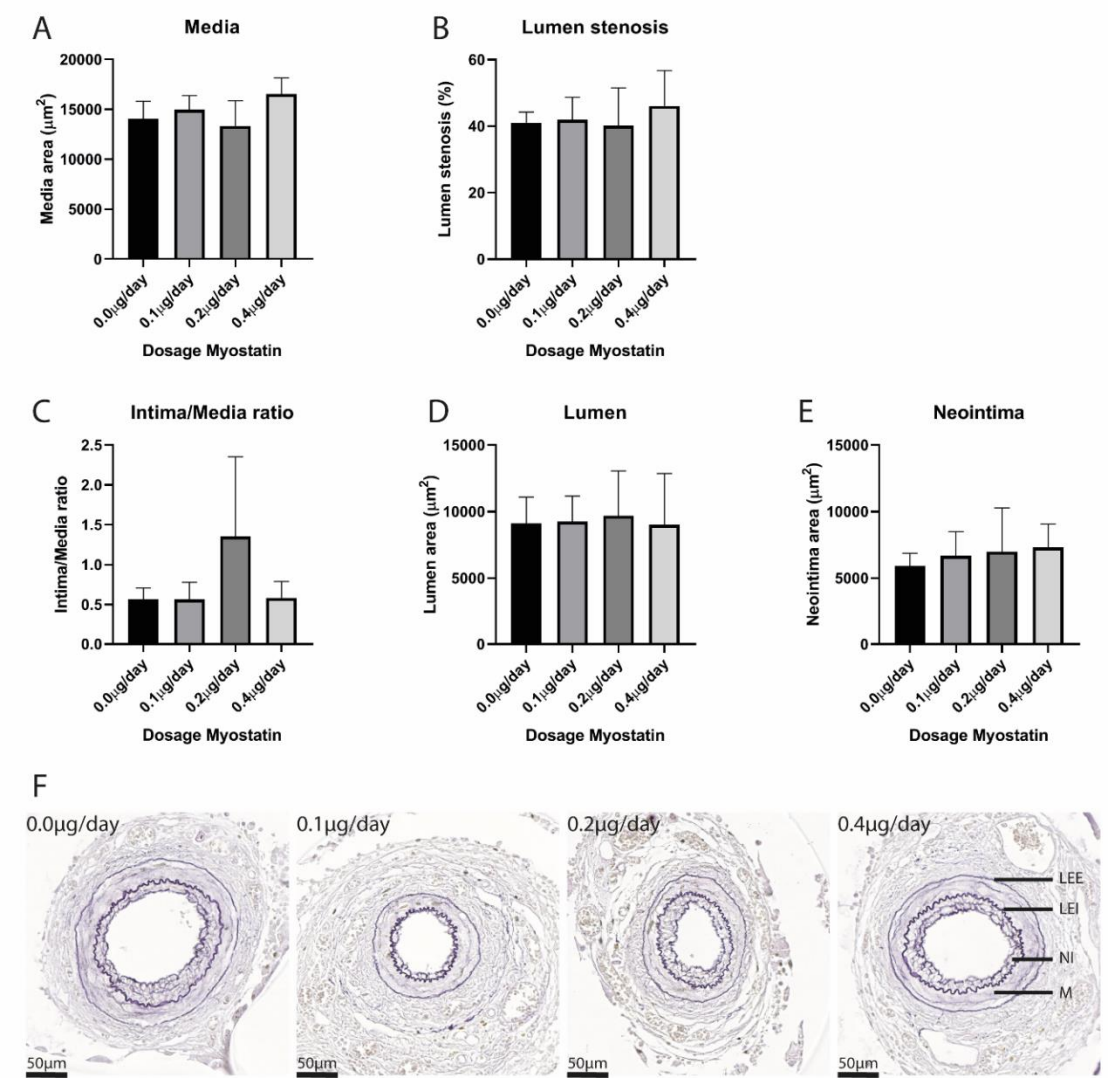

Figure 4A-F Quantification of restenosis in cuffed femoral arteries in different treatment groups. A – Media area was similar in different treatment groups. B – Lumen stenosis did not differ between treatment groups. C – Intima/Media ratio was similar in different treatment groups. D – Lumen area in different treatment groups was equal. E – Neointima area in different treatment groups did not differ. B-G Quantification of not occluded arteries. Mean expression is shown and error bar represents SEM. N=7 in control group, N=4 in 0.1µg/day, N=4 in 0.2µg/day, N=4 in 0.4µg/day. Student's t-test, performed between myostatin treated groups and control group with α=0.05, did not show any significant differences. F – representative examples of cuffed femoral arteries in different treatment groups. LEE = Lamina Elastica Externa, LEI = Lamina Elastica Interna, NI = Neointima, M = Media.

Restenosis in myostatin-treated mice

As there appeared to be a rest restricted therapeutic window in myostatin efficacy *in vitro*, we used multiple myostatin dosages *in vivo*. The highest dose of 0.4µg/day was based on previously published work by others[27]. With the dose-specific effect *in vitro*, we choose to also include two groups of mice treated with either 0.1µg/day or 0.2µg/day. Mice subjected to femoral artery cuff placement thus received 0.0µg/day (control group), 0.1µg/day, 0.2µg/day or 0.4µg/day of myostatin via continuous infusion from an osmotic pump. We analyzed intimal hyperplasia and restenosis in C57BL/6 mice that were sacrificed three weeks after femoral artery cuff placement. Arteries that showed 100% stenosis were excluded from the analyses (Supplementary Figure 1). In the remaining arteries, the medial layer area was similar in all groups (Figure 4A). Lumen stenosis and intima-media ratio did not differ either (Figures 4B+C). Finally, lumen area and neointima area were also similar in all groups (Figures 4D+E). Figure 4F shows representative femoral arteries with restenosis formation for each group.

Myostatin in cuffed femoral arteries

No endogenous myostatin expression was measured in the femoral arteries in any of the groups (data not shown). However, as shown in Figure 5A, the infused myostatin was effectively taken up by the cuffed arteries at all three dosages, where no myostatin was present in the control group.

Effect of myostatin treatment on proliferation

We then stained the cuffed femoral arteries for Ki-67, however hardly any positive cells were observed within the medial and intimal regions in any of the arteries (average of one cell/section) (Figure 5B). These Ki-67 positive cells stained negative for αSMA, indicating that VSMCs are not the cells that are still proliferating at this late time point (three weeks after cuff placement). Moreover, we performed a BrdU staining and again we observed no proliferating cells in the neointimal layer or medial layer of the femoral arteries (Figure 5C). PCNA mRNA expression, however, was decreased in myostatin-treated mice compared to controls (Figure 6).

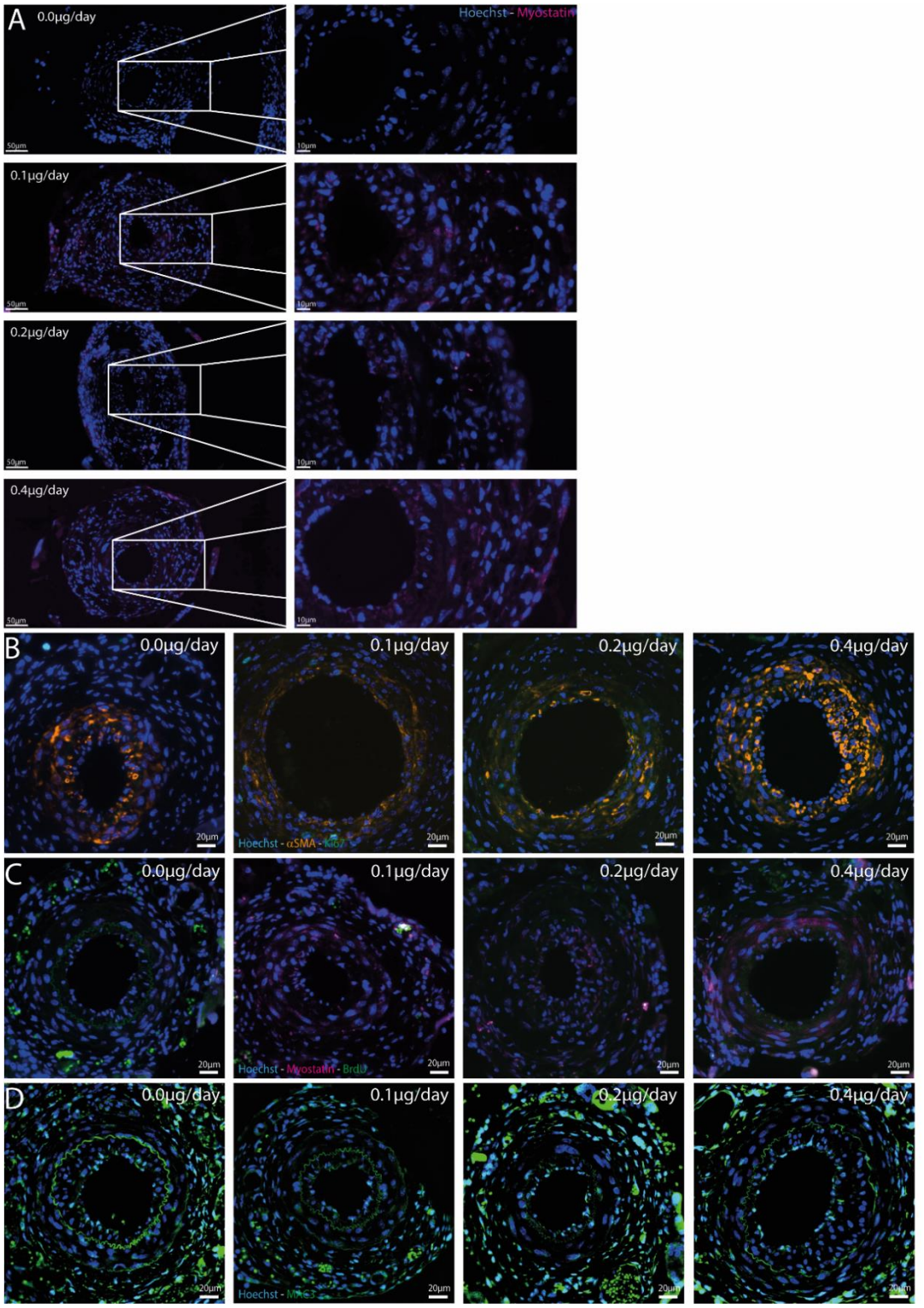

Figure 5A-D Immunofluorescent stainings in different treatment groups. A – Myostatin-Hoechst immunofluorescent double staining. Representative mouse of every treatment group is shown and zoom-in of femoral artery shows presence of myostatin in all treated groups, but not in the control group. B – Ki-67-αSMA-Hoechst immunofluorescent triple staining in cuffed femoral arteries of different treatment groups shows few proliferating cells, especially not in the αSMA area. C – BrdU-Myostatin-Hoechst immunofluorescent triple staining in cuffed femoral arteries of different treatment groups shows again little proliferating cells and those cells are not double stained with myostatin. D – Hoechst-MAC3 immunofluorescent double staining of cuffed femoral arteries showed macrophages in all groups in both the intimal and medial layers, but no differences were found.

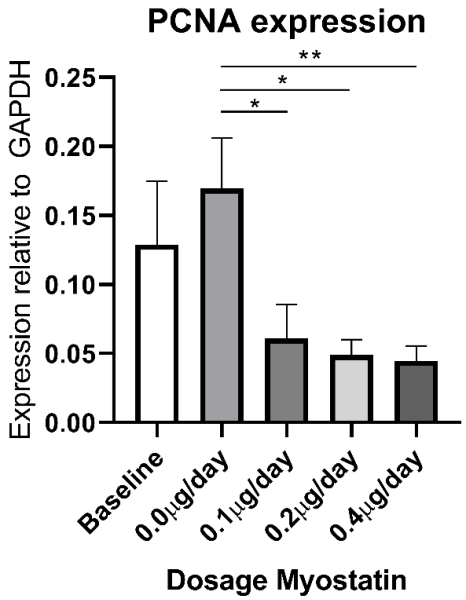

Figure 6 PCNA mRNA expression in femoral arteries of myostatin treated mice. PCNA mRNA expression in different treatment groups and control group is significantly lower in myostatin treated groups compared to control group showed significant differences between treated groups and control group. Mean expression is shown and error bar represents SEM (N=8 for 0.0, 0.1 and 0.4μg/day myostatin group, N=6 for baseline and 0.2μg/day group). Student's t-test performed between treated groups and control group with α=0.05. * $p<0.05$, ** $p<0.01$.

Effect of myostatin on macrophages

We then stained for MAC3 and observed that macrophages were present in both the neointimal and the medial layers of the cuffed femoral arteries in all mice (Figure 5D). However, the percentages of macrophages in the intimal layer, the medial layer and in both layers together, did not differ between groups (Supplemental Figures 2A-C). To further analyze the effect of myostatin on macrophage activation, isolated bone marrow monocytes of four control mice and four 0.4μg myostatin/day-treated mice were pooled per group and subjected to either 10nM additional myostatin in culture medium or culture medium only during maturation into macrophages *in vitro*. After maturation, macrophages were stimulated with 10ng/mL LPS for 48 hours and TNFα level was measured in the medium. TNFα secretion appeared lower in macrophages from myostatin-treated mice than from untreated mice, independent of the additional *in vitro* treatment with myostatin during the culturing period (Figure 7A and 7B). However, when we looked within the myostatin-treated or untreated mice, TNFα secretion appeared higher when myostatin was added during *in vitro* maturation of monocytes into macrophages (Figure 7C and 7D). It should be noted that neither effect was strong enough to detect any statistically significant differences.

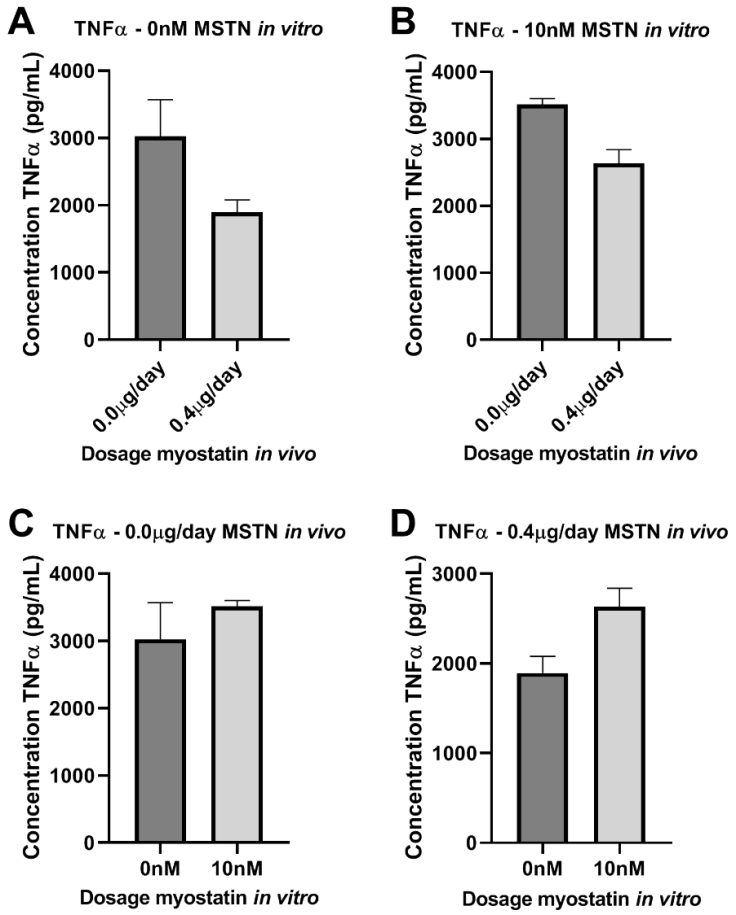

Figure 7A-E Effect of myostatin on macrophages. A-D – TNFα in supernatant of bone marrow macrophages stimulated with myostatin. A-B – *in vivo* treated mice with 0.0 vs. 0.4μg myostatin/day and not treated *in vitro* with myostatin (A) or *in vitro* treated with 10nM myostatin (B) did not show significant differences. C-D – *in vivo* not treated (C) or treated (D) and *in vitro* not treated or treated with myostatin did not show significant differences. Mean expression is shown as average of duplicate measurements of pooled cells and error bar represents SEM. Student's t-test did not show significant differences.

Effect of myostatin treatment on 14q32 microRNA expression in vivo

We assessed the effects of myostatin treatment on microRNA expression *in vivo* compared to the control group. As shown in Figure 8A-C, in the cuffed femoral arteries levels of the 14q32 microRNAs miR-433-3p, miR-494-3p and miR-495-3p were downregulated in response to myostatin, but again, only at specific dosages. For miR-433-3p, 0.4μg myostatin/day resulted in downregulation ($p=0.003$, Figure 8A), but at other dosages, no effect was observed. MiR-494-3p, however, showed decreased expression in both 0.1μg myostatin/day ($p=0.001$) and 0.4μg myostatin/day groups ($p<0.0001$, Figure 8B). MiR-495-3p expression level was downregulated by 50% in the 0.2μg myostatin/day treatment group ($p=0.0003$, Figure 8C). No miR-495 downregulation was observed in the 0.1μg/day and for 0.4μg/day myostatin groups (Figure 8C).

MicroRNA expression levels in bone marrow-derived macrophages were not downregulated in any of the treatment groups, i.e. long-term *in vivo* treatment with myostatin and control or *in vitro* treatment and control for any of the measured 14q32 microRNAs (Figure 8D-F).

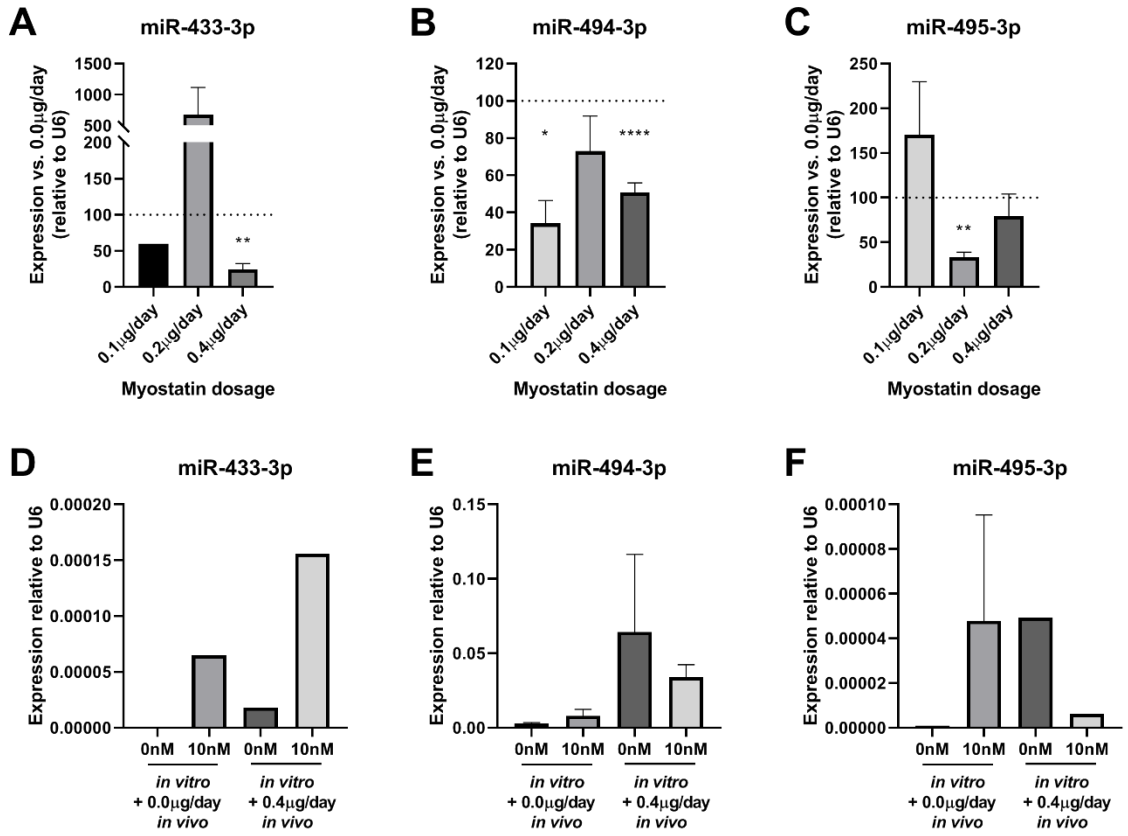

Figure 8A-F MicroRNA expression in femoral arteries and macrophages. A – miR-433-3p expression in femoral arteries of 0.1, 0.2, 0.4µg/day of myostatin relative to control mice (100%) showed significant downregulation of miR-433-3p at 0.4µg/day (p=0.003). B – miR-494-3p expression in femoral arteries of 0.1, 0.2, 0.4µg/day of myostatin relative to control mice (100%) showed significant downregulation of miR-494-3p at 0.1 (p=0.001) and 0.4µg/day (p<0.0001). C – miR-495-3p expression in femoral arteries of 0.1, 0.2, 0.4µg/day of myostatin relative to control mice (100%) showed significant downregulation of miR-495-3p at 0.2µg/day (p=0.0003). For A-C Mean expression is shown and error bars represent SEM (N=8 for 0.0, 0.1 and 0.4 treatment groups, N=6 for 0.2 treatment group). One-sample t-test performed with 100% expression of control group. * p<0.05, ** p<0.01, **** p<0.0001. D – miR-433-3p expression did not show any differences between groups. E – miR-494-3p expression did not show any differences between groups. F – miR-495-3p expression did not show any differences. For D-E bone marrow monocytes matured into macrophages from *in vivo* treated mice with 0.0 vs. 0.4µg myostatin/day and *in vitro* treated without myostatin or with 10nM myostatin. Maturated cells were stimulated with LPS to trigger an inflammatory reaction. Mean expression is shown as average of duplicate measurements of pooled macrophages and error bar represents SEM. Wilcoxon rank sum test did not show any differences.

Discussion

In this study, myostatin was investigated as regulator of VSMC proliferation and 14q32 microRNA expression with the ultimate goal to inhibit postinterventional restenosis. As anticipated, VSMC proliferation was inhibited and 14q32 microRNAs were downregulated in response to myostatin treatment, however, there were no effects on restenosis.

Myostatin is known to act mainly on skeletal muscle cells to inhibit their proliferation and growth[10, 11]. However, the facts that myostatin also functions in VSMCs[13] and that, in restenosis, exactly these VSMCs proliferate and migrate to form a neointimal layer[28], suggest that myostatin treatment could be a promising therapeutic compound for this important clinical problem. PCNA expression was downregulated by myostatin treatment both *in vitro* and *in vivo*, indicating that cell proliferation was indeed reduced by myostatin, where cell viability and migration remained unaffected. In contrast to the reduction in *in vivo* PCNA levels however, BrdU and Ki-67 were hardly detectable anymore in either the neointimal layer or the medial layer in any of the groups, indicating that, at the time of sacrifice, no active cell proliferation was ongoing in the lesions anymore. We can only speculate on the reasons for this discrepancy, however, most likely, the process of neointima formation is already complete after three weeks in this particular model.

It was previously shown that myostatin administration via injection of a Chinese Hamster Ovarian (CHO) cell line that overexpresses murine myostatin in athymic nude mice, compared to CHO-control cell injection, leads to muscle atrophy[11], which would be detrimental of course for any potential therapeutic compound. However, at the dosages used in this study, we did not observe any adverse effects of myostatin infusion. The arterial medial layers appeared normal in all groups, suggesting that VSMC-specific cytotoxic effects did not occur, which corresponds with our *in vitro* observation that myostatin did not affect cell viability. Furthermore, the elastic laminas, that in case of toxic side effects may show typical breaks[8], were intact in all patent vessels, confirming the absence of toxic effects.

As anticipated, myostatin treatment resulted in downregulation of 14q32 microRNA miR-433-3p, miR-494-3p and miR-495-3p expression, both *in vitro* in VSMCs and *in vivo* in the arterial wall of which VSMCs are the major cellular component. This fits with previous findings of myostatin's actions on the callipyge locus[15]. Both *in vitro* and *in vivo* we found that there is a defined therapeutic window however, with a dose-specific effect of myostatin on 14q32 microRNA downregulation in VSMCs. In macrophages, microRNA expression levels remained unaffected by myostatin treatment. As described previously, microRNAs show highly cell-type specific expression patterns[29] and have cell-type specific effects[30], which we confirmed in the present study.

The effect of myostatin on macrophages was further assessed in the cuffed femoral arteries. We did not observe differences in influx of macrophages in any of the treatment groups. This implies that myostatin does not affect migration and activation of macrophages in our restenosis model. Moreover, assessment of bone marrow-derived macrophages from myostatin-treated and control mice did not show any clear trend towards increased or decreased macrophage activation. Together with the lack of effect of myostatin on microRNA expression in these macrophages, we conclude that myostatin does not lead to sufficient changes in macrophage activation to contribute to a reduction in local inflammation in the artery and thus to a reduction in restenosis.

14q32 microRNAs act in multiple forms of vascular remodelling. Previous experimental studies showed that inhibition of 14q32 microRNAs decreases atherosclerosis and stimulates angiogenesis, but also decreases restenosis[17, 19, 21]. Thus, lower expression of 14q32 microRNAs stimulates beneficial remodelling and reduces maladaptive processes. In cardiovascular disease, this implies that downregulation of 14q32 microRNAs results in advantageous vascular remodelling. We anticipated that decreased levels of 14q32 microRNAs, as a result of myostatin infusion, would therefore lead to a reduction in intimal hyperplasia and restenosis in our model. This was not the case, however. We have previously shown that systemic inhibition of a single 14q32 microRNA, miR-495-3p, which was also downregulated in the femoral artery wall in the current study, resulted in a significant reduction in restenosis[17]. However, after systemic miR-495-3p inhibition, we also observed a reduction in the number of macrophages that infiltrated the lesions. Myostatin reduces miR-495-3p, as well as other 14q32 microRNAs, but in VSMCs only. Clearly, 14q32 microRNAs act on multiple cell types and tissues and inhibition in VSMCs alone is not enough to reduce maladaptive changes in the arterial wall.

Taken together, our findings demonstrate that systemically infused myostatin acts locally in the arterial wall to downregulate intracellular 14q32 microRNA expression and decreases VSMC proliferation, but myostatin does not decrease 14q32 microRNA expression levels in macrophages, nor does it affect their activation or infiltration in the arterial wall. As we could not decrease postinterventional restenosis, our myostatin study emphasizes the need to target both VSMC proliferation and inflammation in restenosis. Of the drugs available in the clinic nowadays, sirolimus is the only one that affects both VSMC proliferation and the inflammatory side of restenosis[6]. Other drug-eluting stents, like paclitaxel-eluting stents, only inhibit proliferation and are therefore less favorable[9].

In conclusion, myostatin inhibits expression of 14q32 microRNAs, as well as cell proliferation in VSMCs. *In vivo*, myostatin treatment also reduced 14q32 microRNA expression and VSMC proliferation in the femoral artery. However, 14q32 microRNA expression in bone marrow-

derived macrophages remained unaffected after myostatin treatment, nor did we observe changes in macrophage infiltration into the lesion. Moreover, myostatin treatment did not affect postinterventional restenosis. Our findings underline the fact that restenosis is driven by two major components, both VSMC proliferation and local inflammation. Therefore, therapeutic strategies to reduce postinterventional restenosis should aim to target both processes simultaneously.

Acknowledgements

We thank M.W. Pollemans for her technical support.

Funding

This work was supported by an MD/PhD Fellowship from the LUMC to Eveline Goossens.

References

1. Jukema, JW, Verschuren, JJ, Ahmed, TA, and Quax, PH (2011). Restenosis after PCI. Part 1: pathophysiology and risk factors. Nature reviews Cardiology 9: 53-62.
2. Lee, MS, David, EM, Makkar, RR, and Wilentz, JR (2004). Molecular and cellular basis of restenosis after percutaneous coronary intervention: the intertwining roles of platelets, leukocytes, and the coagulation-fibrinolysis system. The Journal of pathology 203: 861-870.
3. Moses, JW, Leon, MB, Popma, JJ, Fitzgerald, PJ, Holmes, DR, O'Shaughnessy, C, et al. (2003). Sirolimus-eluting stents versus standard stents in patients with stenosis in a native coronary artery. The New England journal of medicine 349: 1315-1323.
4. Stone, GW, Ellis, SG, Cox, DA, Hermiller, J, O'Shaughnessy, C, Mann, JT, et al. (2004). A polymer-based, paclitaxel-eluting stent in patients with coronary artery disease. The New England journal of medicine 350: 221-231.
5. Im, E, and Hong, MK (2016). Drug-eluting stents to prevent stent thrombosis and restenosis. Expert review of cardiovascular therapy 14: 87-104.
6. Suzuki, T, Kopia, G, Hayashi, S, Bailey, LR, Llanos, G, Wilensky, R, et al. (2001). Stent-based delivery of sirolimus reduces neointimal formation in a porcine coronary model. Circulation 104: 1188-1193.
7. Signore, PE, Machan, LS, Jackson, JK, Burt, H, Bromley, P, Wilson, JE, et al. (2001). Complete inhibition of intimal hyperplasia by perivascular delivery of paclitaxel in balloon-injured rat carotid arteries. Journal of vascular and interventional radiology : JVIR 12: 79-88.
8. Pires, NM, Eefting, D, de Vries, MR, Quax, PH, and Jukema, JW (2007). Sirolimus and paclitaxel provoke different vascular pathological responses after local delivery in a murine model for restenosis on underlying atherosclerotic arteries. Heart (British Cardiac Society) 93: 922-927.
9. King, L, Byrne, RA, Mehilli, J, Schomig, A, Kastrati, A, and Pache, J (2013). Five-year clinical outcomes of a polymer-free sirolimus-eluting stent versus a permanent polymer paclitaxel-eluting stent: final results of the intracoronary stenting and angiographic restenosis - test equivalence between two drug-eluting stents (ISAR-TEST) trial. Catheterization and cardiovascular interventions : official journal of the Society for Cardiac Angiography & Interventions 81: E23-28.
10. McPherron, AC, Lawler, AM, and Lee, SJ (1997). Regulation of skeletal muscle mass in mice by a new TGF-beta superfamily member. Nature 387: 83-90.
11. Zimmers, TA, Davies, MV, Koniaris, LG, Haynes, P, Esquela, AF, Tomkinson, KN, et al. (2002). Induction of cachexia in mice by systemically administered myostatin. Science 296: 1486-1488.
12. Sharma, M, Kambadur, R, Matthews, KG, Somers, WG, Devlin, GP, Conaglen, JV, et al. (1999). Myostatin, a transforming growth factor-beta superfamily member, is expressed in heart muscle and is upregulated in cardiomyocytes after infarct. Journal of cellular physiology 180: 1-9.
13. Verzola, D, Milanesi, S, Bertolotto, M, Garibaldi, S, Villaggio, B, Brunelli, C, et al. (2017). Myostatin mediates abdominal aortic atherosclerosis progression by inducing vascular smooth muscle cell dysfunction and monocyte recruitment. Scientific reports 7: 46362.
14. Tsuchida, K, Nakatani, M, Uezumi, A, Murakami, T, and Cui, X (2008). Signal transduction pathway through activin receptors as a therapeutic target of musculoskeletal diseases and cancer. Endocrine journal 55: 11-21.
15. Hitachi, K, and Tsuchida, K (2017). Myostatin-deficiency in mice increases global gene expression at the Dlk1-Dio3 locus in the skeletal muscle. Oncotarget 8: 5943-5953.
16. Magee, DA, Berry, DP, Berkowicz, EW, Sikora, KM, Howard, DJ, Mullen, MP, et al. (2011). Single nucleotide polymorphisms within the bovine DLK1-DIO3 imprinted domain are associated with economically important production traits in cattle. The Journal of heredity 102: 94-101.

17. Welten, SMJ, de Jong, RCM, Wezel, A, de Vries, MR, Boonstra, MC, Parma, L, et al. (2017). Inhibition of 14q32 microRNA miR-495 reduces lesion formation, intimal hyperplasia and plasma cholesterol levels in experimental restenosis. Atherosclerosis 261: 26-36.
18. Nossent, AY, Eskildsen, TV, Andersen, LB, Bie, P, Bronnum, H, Schneider, M, et al. (2013). The 14q32 MicroRNA-487b Targets the Antiapoptotic Insulin Receptor Substrate 1 in Hypertension-Induced Remodeling of the Aorta. Ann Surg 258: 743-753.
19. Welten, SM, Bastiaansen, AJ, de Jong, RC, de Vries, MR, Peters, EA, Boonstra, MC, et al. (2014). Inhibition of 14q32 MicroRNAs miR-329, miR-487b, miR-494, and miR-495 increases neovascularization and blood flow recovery after ischemia. Circ Res 115: 696-708.
20. Welten, SM, Goossens, EA, Quax, PH, and Nossent, AY (2016). The multifactorial nature of microRNAs in vascular remodelling. Cardiovascular research 110: 6-22.
21. Wezel, A, Welten, SM, Razawy, W, Lagraauw, HM, de Vries, MR, Goossens, EA, et al. (2015). Inhibition of MicroRNA-494 Reduces Carotid Artery Atherosclerotic Lesion Development and Increases Plaque Stability. Annals of surgery 262: 841-847; discussion 847-848.
22. Pires, NM, van der Hoeven, BL, de Vries, MR, Havekes, LM, van Vlijmen, BJ, Hennink, WE, et al. (2005). Local perivascular delivery of anti-restenotic agents from a drug-eluting poly(epsilon-caprolactone) stent cuff. Biomaterials 26: 5386-5394.
23. Pires, NM, Schepers, A, van der Hoeven, BL, de Vries, MR, Boesten, LS, Jukema, JW, et al. (2005). Histopathologic alterations following local delivery of dexamethasone to inhibit restenosis in murine arteries. Cardiovascular research 68: 415-424.
24. Eefting, D, Schepers, A, De Vries, MR, Pires, NM, Grimbergen, JM, Lagerweij, T, et al. (2007). The effect of interleukin-10 knock-out and overexpression on neointima formation in hypercholesterolemic APOE*3-Leiden mice. Atherosclerosis 193: 335-342.
25. de Jong, RCM, Ewing, MM, de Vries, MR, Karper, JC, Bastiaansen, A, Peters, HAB, et al. (2017). The epigenetic factor PCAF regulates vascular inflammation and is essential for intimal hyperplasia development. PloS one 12: e0185820.
26. Moroi, M, Zhang, L, Yasuda, T, Virmani, R, Gold, HK, Fishman, MC, et al. (1998). Interaction of genetic deficiency of endothelial nitric oxide, gender, and pregnancy in vascular response to injury in mice. The Journal of clinical investigation 101: 1225-1232.
27. Wilkes, JJ, Lloyd, DJ, and Gekakis, N (2009). Loss-of-function mutation in myostatin reduces tumor necrosis factor alpha production and protects liver against obesity-induced insulin resistance. Diabetes 58: 1133-1143.
28. Lardenoye, JH, Delsing, DJ, de Vries, MR, Deckers, MM, Princen, HM, Havekes, LM, et al. (2000). Accelerated atherosclerosis by placement of a perivascular cuff and a cholesterol-rich diet in ApoE*3Leiden transgenic mice. Circulation research 87: 248-253.
29. Goossens, EAC, de Vries, MR, Simons, KH, Putter, H, Quax, PHA, and Nossent, AY (2019). miRMap: Profiling 14q32 microRNA Expression and DNA Methylation Throughout the Human Vasculature. Frontiers in cardiovascular medicine 6: 113.
30. Rogg, EM, Abplanalp, WT, Bischof, C, John, D, Schulz, MH, Krishnan, J, et al. (2018). Analysis of Cell Type-Specific Effects of MicroRNA-92a Provides Novel Insights Into Target Regulation and Mechanism of Action. Circulation 138: 2545-2558.
31. den Dekker, WK, Tempel, D, Bot, I, Biessen, EA, Joosten, LA, Netea, MG, et al. (2012). Mast cells induce vascular smooth muscle cell apoptosis via a toll-like receptor 4 activation pathway. Arteriosclerosis, thrombosis, and vascular biology 32: 1960-1969.

Supplementary Data

Supplementary Table 1 Primer sequences used for rt/qPCR

	Forward sequence	Reverse sequence
MMU-PCNA	TCACAAAAGCCACTCCACTGT	CTTTAAGTGTCCCATGTCAGCA
MMU-MSTN	TGATCTTGCTGTAACCTTCCCA	TCATCGCAGTCAAGCCCAAAG
GAPDH	CACCACCATGGAGAAGGC	AGCAGTTGGTGGTGCAGGA

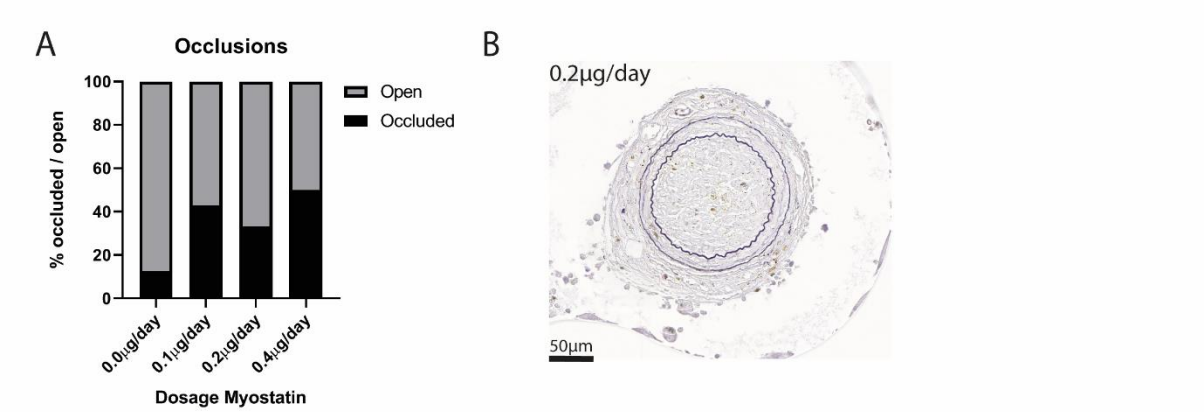

Supplementary Figure 1A-B Occluded cuffed femoral arteries in different treatment groups. A – Occlusion percentages in different treatment groups. Control group N=8, 0.1µg/day N=7, 0.2µg/day N=6, 0.4µg/day N=8. B – Representative example of occluded cuffed femoral artery. Chi Square test did not show significant differences between groups.

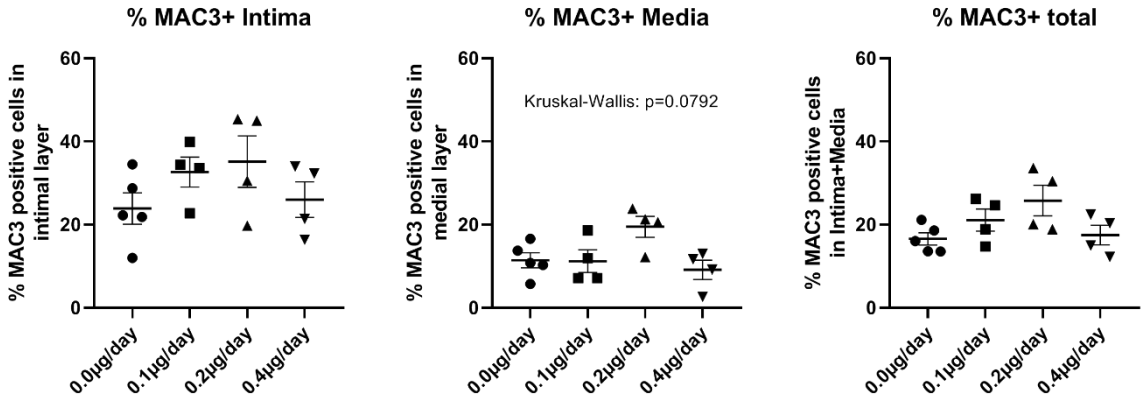

Supplementary Figure 2A-C Quantification of MAC3+ cells in different layers as percentage of total amount of cells in different treatment groups. A – Percentage of MAC3+ cells in the intimal layer did not differ between treatment groups. B – Percentage of MAC3+ cells in the medial layer did not differ between treatment groups. C - Percentage of MAC3+ cells in the intimal and medial layer together did not differ between treatment groups. Kruskal-Wallis test did not show any significant differences between groups.

Chapter 6

Inhibition of Cold-Inducible RNA-Binding Protein decreases 14q32 microRNA miR-495 expression and enhances *in vitro* angiogenesis

Manuscript in preparation

EAC Goossens[1,2]
L Zhang[1,2]
PHA Quax[1,2]
AY Nossent[1,3,4]

[1]Department of Surgery and [2]Einthoven Laboratory for Experimental Vascular Medicine, Leiden University Medical Center, Leiden, The Netherlands; [3]Department of Internal Medicine II and [4]Department of Laboratory Medicine, Medical University of Vienna, Vienna, Austria

Abstract

Aims: In peripheral artery disease (PAD) an occluded artery leads to downstream tissue ischemia. To restore blood flow, angiogenesis, an ischemia-driven neovascularization process, is needed. Inhibition of 14q32 microRNAs miR-495-3p and miR-329-3p improves post-ischemic neovascularization. Using SILAC followed by pre-microRNA pulldown and Mass Spectrometry, Cold-inducible RNA-binding protein (CIRBP) was found to regulate these microRNAs. CIRBP expression is induced by hypothermic stress, an important component of PAD. Therefore, we hypothesized that CIRBP inhibition can improve post-ischemic angiogenesis via inhibition of 14q32 microRNA expression.

Methods and results: In this study, we investigated the regulatory mechanisms of CIRBP in relation to 14q32 microRNA expression and angiogenesis *in vitro*. We assessed expression of different CIRBP splice variants (CIRBP-SVs), as well as antisense lncRNA CIRBP-AS1 in hypothermia. We used siRNAs to determine how CIRBP and CIRBP-AS1 regulate each other, 14q32 microRNA expression and angiogenesis. In HUVECs cultured at 32°C for 24h and 48h, CIRBP expression was upregulated, but miR-495-3p and miR-329-3p expression remained unaffected. CIRBP-SV1 and miR-495-3p, but not miR-329-3p or CIRBP-SV2-4, were downregulated in HUVECs after CIRBP knockdown. To assess angiogenesis, scratch-wound healing assays and tube formation assays were performed and both improved migration and tube formation were observed after either CIRBP or CIRBP-AS1 knockdown. CIRBP-AS1 expression increased under hypothermia and decreased after CIRBP knockdown, mimicking the CIRBP-SV1 expression pattern. Similarly, knockdown of CIRBP-AS1, resulted in decreased expression of CIRBP, in particular of CIRBP-SV1, as well as inhibition of miR-329-3p and miR-495-3p expression.

Conclusions: Both CIRBP-SV1 and CIRBP-AS1 were upregulated under hypothermia without affecting miR-495-3p and miR-329-3p expression. However, total CIRBP and CIRBP-SV1 knockdown inhibited miR-495-3p expression and improved *in vitro* angiogenesis. Therefore, we conclude that CIRBP contributes to processing of miR-495-3p, but is not rate-limiting under normothermic conditions. CIRBP-SV1 and CIRBP-AS1 expression patterns closely mimicked each other under all experimental conditions. CIRBP-AS1 knockdown also increased angiogenesis and downregulated both miR-495-3p and miR329-3p. The mechanism of interaction will be studied *in vitro* and *in vivo*. Further exploration of CIRBP's function in post-ischemic neovascularization will be investigated in an *in vivo* hindlimb ischemia model, using $CIRBP^{-/-}$ mice.

Introduction

Peripheral artery disease (PAD) is caused by occlusions of the arterial vasculature in the lower limb, mainly the femoral artery, resulting in deprivation of blood flow, and thus of oxygen and nutrients, to the lower extremities. This shortage in blood supply leads to clinical features of painful and cold extremities (poikilothermia, i.e. inability to maintain core temperature). Other clinical features are pulselessness, pallor, paresthesia, paralysis. Together these symptoms are called the six Ps. Current treatment options include angioplasty procedures with stent placement and bypass surgery. However, these therapies have the risk of restenosis or bypass stenosis, and often they cannot be applied at all, because of anatomical restrictions or advanced stages of the disease. That is why other therapeutic neovascularization approaches are still required. The body has its own mechanism to restore blood flow to ischemic and cold tissues, namely neovascularization, the collective term for angiogenesis and arteriogenesis. In patients with severe PAD, this is insufficient to completely recover blood flow to the leg. Therefore, enhancing neovascularization is an interesting and promising new treatment option for patients with PAD. In this study we explored the role of the Cold-Inducible RNA Binding Protein (CIRBP) as a pro-angiogenic factor and study the potential of modulating CIRBP in order to enhance neovascularization. CIRBP is regulated by differential stress factors including ischemia[1, 2] and, as its name suggests, temperature[1, 3-6]. In fact, CIRBP was described in 1997 as the first cold shock protein that was induced at mild hypothermia[7] and this effect was conserved between humans and mice[8].

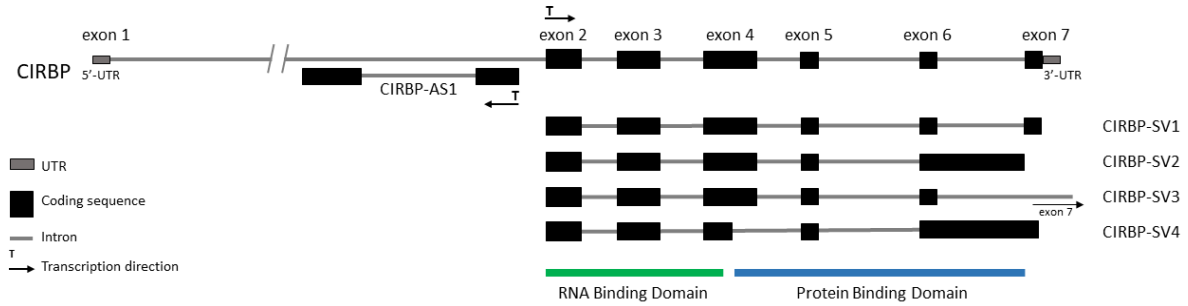

Figure 1 Schematic overview of CIRBP gene with splice variants and CIRBP-AS1. according to UCSC Genome Browser alignment GRCh38/hg38. Only splice variants affecting the protein coding sequence are depicted, however more variants are known that affect 5'- or 3'-UTR composition.

CIRBP is an RNA-binding protein (RBP) that influences post-transcriptional processing of its target RNA[9] and its gene is located at chromosome 19 in humans (Figure 1). CIRBP contains an N-terminal RNA-binding domain and a C-terminal domain that has protein binding properties[7, 10]. There are various splice variants of CIRPB which, in mice, showed altered expression patterns in response to hypothermia[11]. The four main splice variants in humans, CIRBP-SV1, CIRBP-SV2, CIRBP-SV3 and CIRBP-SV4, have the RNA-binding domain in common,

but have different C-termini. Furthermore, the antisense strand of CIRBP contains an antisense long noncoding RNA (CIRBP-AS1). Antisense long noncoding RNAs (lncRNAs) can have several functions. Antisense lncRNAs have been shown to affect transcription and support function of their respective coding sense-strand[12]. For example, lncRNA MALAT1 has an antisense transcript TALAM1 and together they function as a sense-antisense pair[13, 14]. Therefore, it is possible that either sense and antisense strands are co-transcribed and counteract or cooperate in their actions[12] or that one strand affects expression of the other strand.

CIRBP, as an RBP, does not only affect processing of messenger RNAs (mRNAs), but also has the ability to act in microRNA processing. MicroRNAs (miRs) are small noncoding RNA molecules of approximately 22 nucleotides in length. They are transcribed from DNA by RNA polymerase II into primary microRNAs. Next, these primary microRNAs (pri-miRs) are processed by Drosha, a processing complex, into precursor microRNAs (pre-miRs), which in turn are cleaved into two mature microRNA strands by the enzyme Dicer[15, 16]. Mature microRNAs are loaded into an RNA Induced Silencing Complex (RISC), which binds to the 3'-untranslated region of target mRNAs, leading to translational repression. Therefore, microRNAs are negative regulators of protein expression. Because a single microRNA has the ability to bind to a large number of target mRNAs, microRNAs can affect complete physiological and pathophysiological processes. However, the expression of microRNAs themselves can also be regulated, either transcriptionally or post-transctiptionally[17-19].

Previously, we showed that a large microRNA cluster located on chromosome 14 (14q32 locus), plays a regulatory role in different types of vascular remodelling, including atherosclerosis and restenosis, but also in post-ischemic neovascularization[20-23]. This cluster is also known as DLK1-DIO3 cluster and is conserved in mice where it is located at the 12F1 locus. CIRBP was shown to directly bind two precursors of 14q32 microRNAs, namely pre-miR-329 and pre-miR-495[18], thereby inducing the processing into the mature microRNAs miR-329-3p and miR-495-3p. In previous studies, we found that inhibition of 14q32 microRNAs miR-495-3p and miR-329-3p increased post-ischemic neovascularization[20]. At the same time, inhibition of these microRNAs also reduced post-interventional restenosis[21], potentially offering a double advantage for patients with severe PAD. Therefore, we hypothesized that inhibition of CIRBP leads to a decrease in mature miR-495-3p and miR-329-3p and consequently promotes post-ischemic neovascularization.

In this study, we first studied how hypothermic stress affects total CIRBP, its splice variants and its antisense lncRNA, and subsequently, 14q32 microRNA expression. Furthermore, we studied the effect of CIRBP and CIRBP-AS1 inhibition on angiogenesis.

Materials and Methods

Isolation of human umbilical cord arterial fibroblasts (HUAFibs), arterial smooth muscle cells (HUASMCs), venous endothelial cells (HUVECs) and arterial endothelial cells (HUAECs)

Primary human vascular cells were isolated as described earlier by Welten et al[20]. In brief, for HUAFib and HUASMC isolation, the arteries were removed and cleaned from remaining connective tissue. Endothelial cells were removed by gently rolling the artery over a blunted needle. The tunica adventitia and tunica media were separated using surgical forceps. After overnight incubation in HUAFib/HUASMC culture medium, (DMEM GlutaMAX™ (Invitrogen, GIBCO)), 10% heat inactivated fetal calf serum (FCSi) (PAA), 10% heat inactivated human serum, 1% penicillin (10000U/mL) / streptomycin (10000U/mL) and 1% nonessential amino acids (ref 11140-035, GIBCO, Life Technologies), the tunica adventitia and the tunica media separately were cut with scissors in pieces of maximum of 2mm incubated in a 2mg/ml collagenase type II solution (Worthington) at 37°C. Cell suspensions were filtered over a 70µm cell strainer and centrifuged at 400g for 10 minutes. Cell pellet was resuspended and plated in culture medium. Cells isolated from the tunica adventitia were washed with culture medium after 90 minutes to remove slow-adhering non-fibroblast cells. Cells isolated from tunica media were plated in 1% gelatin coated plates with culture medium.

For HUVEC and HUAEC isolation, respectively, the vein and the arteries were inserted with a cannula and was flushed with sterile PBS. The vessel was infused with 0.075% collagenase type II (Worthington) and incubated at 37°C for 20 minutes. The collagenase solution was collected and the vessel was flushed with PBS in order to collect all detached endothelial cells. The cell suspension was centrifuged at 400g for 5 minutes and the pellet was resuspended in HUVEC culture medium (EBM-2 (LONZA) with 2% FBS) HUVECs were cultured in plates coated with fibronectin from bovine plasma (Sigma).

Primary cell culture

HUAFibs and HUASMCs were cultured at 37°C in a humidified 5% CO_2 environment. Culture medium (DMEM GlutaMAX™ (Invitrogen, GIBCO)), 10% FCSi (PAA), 1% penicillin (10.000U/mL) / streptomycin (10.000U/mL)) was refreshed every 2-3 days. Cells were passed using trypsin (Sigma) at 70-80% confluency. HUAFibs were used for scratch-wound healing assay at passage four, HUVECS at passage three. Stock solutions of isolated HUAFibs up to

passage four and murine fibroblasts up to passage five were stored at -180°C in 50% DMEM GlutaMAX™ containing 10% FCSi and 1% Penicillin/Streptomycin, 40% FCSi (PAA) and 10% DMSO (Sigma). HUVECs were stored up to passage three in 90% heat-inactivated New Born Calf Serum (NBSCi) (Sigma) and 10% DMSO (Sigma).

Hypothermic HUVEC cell culture

Primary HUVECs were seeded in 12-well plates coated with fibronectin at 100.000 cells per well in culture medium. After overnight incubation at 37°C, cells were washed with PBS and new medium was applied before putting the plates in the right incubator: normothermic incubator 37°C and hypothermic incubator 32°C, all humidified and 5% CO_2 and 20% O_2. After 24 or 48 hours, cells were washed with PBS and 0.5mL TRIzol/well was added for RNA isolation. Each single condition was performed in triplicate and the hypothermia experiment was performed three independent times.

In vitro CIRBP and CIRBP-AS1 knockdown with siRNA transfection

Primary HUAFIBs were seeded in 12-well plates at 80.000 cells per well in culture medium, for HUVECs 100.000 cells per well. After 24 hours, cells were washed with PBS and each well was incubated with 900µL of Opti-MEM medium with 10% NBSCi for HUVECs and 1% penicillin/streptomycin for both cell types and, after 10 minutes of incubation of transfection medium, 100µL of transfection medium (94µL Opti-MEM with 3µL of Lipofectamine RNAiMax (Life Technologies) and 3µL of siRNA) was added. siRNA concentration used per well was 30nM. siRNAs used were siRNA CIRBP (sasi-172352), siRNA CIRPB-AS1 (sasi-208901) and siRNA NegCtrl: Mission universal Negative Control #1 (all Sigma-Aldrich). After addition of transfection agents, cells were put in the incubator at 37°C for 24 hours.

Migration assay - scratch-wound healing

After incubation of 24 hours, medium was aspired and a scratch-wound was made across the diameter of each well using a p200 pipet tip. Next, cells were washed with PBS and fresh starve medium (EBM-2 (LONZA) containing only 0.2% of FBS and 1% Gentamicin Amphotericin of the provided bulletkit) was added. In order to monitor scratch-wound closure, live phasecontrast microscropy (Axiovert 40C, Carl Zeiss) was used for taking pictures immediately after (0h) and 18 hours (HUVECs) after introducing the scratch-wound. Pictures were taken at two different locations in each well and averaged for analysis. Scratch size was calculated at 0h and 18h using the wound healing tool macro for ImageJ. Finally, cells were washed with PBS and 0.5mL TRIzol/well was added for RNA isolation. Each single scratch assay condition

was performed in triplicate and this scratch-wound healing assay was performed three independent times.

Tube formation assay

Tube formation assay was performed using HUVECs at passage three. At confluency, cells were transfected as described previously with Lipofectamine RNAiMax and siRNA CIRPB or siRNA Negative Control. After 24 hours, cells were counted and seeded on solidified Geltrex™ (ref: A14132-02, Gibco) in a 96-wells plate. Photos were taken using live phasecontrast microscropy at 12 hours after seeding and quantified using ImageJ Angiogenesis Analyzer. Each single tube formation assay was performed in 6 wells per condition and the independent tube formation assay was performed five independent times.

RNA isolation

RNA isolation of cultured cells was performed by standard TRIzol-chloroform extraction, according to the manufacturer's instructions (Thermo Fisher Scientific). RNA concentrations were measured using Nanodrop™ 1000 Spectrophotometer (Thermo Fisher Scientific).

MicroRNA Quantification

For microRNA quantification of miR-329-3p and miR-495-3p, in all samples RNA was reversed transcribed using the Taqman™ MicroRNA Reverse Transcription Kit (Thermo Fisher Scientific) and subsequently quantified using microRNA-specific Taqman™ qPCR kits (Thermo Fisher Scientific) on the VIIa7 (Thermo Fisher Scientific). MicroRNA expression was normalized against U6 small nuclear RNA.

mRNA, pri-microRNA and pre-microRNA quantification

For mRNA quantification of CIRBP, antisense lncRNA, primary microRNAs and precursor microRNAs, RNA was reverse transcribed using 'high-capacity RNA to cDNA kit' (Thermo Fisher Scientific) and quantified by qPCR using SybrGreen reagents (Qiagen) on the VIIa7. mRNA and antisense lncRNA expression was normalized against GAPDH and primary-microRNA and pre-microRNA expression was normalized to U6. Primer sequences are provided in Supplementary Table 1.

Statistical Analysis

Data are presented as mean ± SEM. Indicated differences have the following levels of significance: *p<0.05, **p<0.01, ***p<0.001, ****p<0.0001. All tests were performed with a significance level of α<0.05.

One-sample t-tests were performed to test differences of treated groups that are expressed relative to the negative control treatment, which is set to 100%. This test was used in knockdown experiments, hypothermia experiment and functional assays.

Differences in scratch wound healing van PCNA expression between CIRBP-AS1 siRNA and negative control siRNA treated cells were assessed using independent sample Student's t-tests.

One-way ANOVA test was performed to detect statistical significant differences over multiple groups. Between specific groups, the presence of differences was assessed with independent sample Student's t-tests, corrected for multiple testing. These tests were used in comparison of CIRBP expression in different vascular wall cell layers.

Results

CIRBP expression of in primary vascular cells

First, we determined total CIRBP gene expression in primary vascular cells originating from human umbilical cords. These cells were HUVECs, HUAECs, HUASMCs and HUAFIBs. CIRBP was expressed in cells derived from all layers of the vessel wall and no differences in expression levels were observed (Figure 2). However, as venous or capillary endothelial cells initiate angiogenesis and are thus leading cells in angiogenesis[24], we focused on HUVECs in all further experiments to study the pro-angiogenic potential of targeting CIRBP.

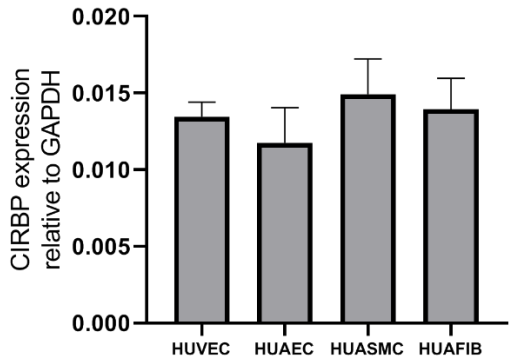

Figure 2 CIRPB expression in primary cells of human umbilical cord cell layers. For each cell type, total CIRBP mRNA expression was measured in three independent samples and did not show differences in expression between different vascular cell layers. Mean expression is indicated and error bars represent SEM. No significant differences were observed with one-way ANOVA (α<0.05).

Total CIRBP and CIRBP splice variants in hypothermia

Previous studies showed upregulated CIRBP expression under cellular stress conditions, including mild hypothermia[3]. Therefore, we measured total CIRBP expression in HUVECs that were subjected to mild hypothermia (32°C) either for 24 or 48 hours. Total CIRBP expression was increased after both 24 and 48 hours compared to the normothermic condition (37°C) with ~200% and ~70%, respectively (Figure 3B+C).

Furthermore, we measured the expression of four different splice variants (SV) of CIRBP shown in Figure 3A. Although not significant, CIRBP-SV1 expression was increased by ~80% at 24 hours (p=0.12) and by ~60% at 48 hours (p=0.14) of hypothermia (Figure 3D+E). The remaining three splice variants were not altered consistently over time under hypothermia, however.

CIRBP-AS1 in hypothermia

As CIRPB expression was induced in HUVECs under hypothermic conditions, we asked what would happen to the expression of the antisense long noncoding RNA of CIRBP (CIRBP-AS1) under hypothermia. CIRBP-AS1, like CIRBP, showed a trend towards increased expression of ~160% under hypothermia after 24 hours (p=0.096, Figure 4A) and we observed even further upregulated expression of ~220% after 48 hours of hypothermia (p=0.097, Figure 4B) compared to normothermia.

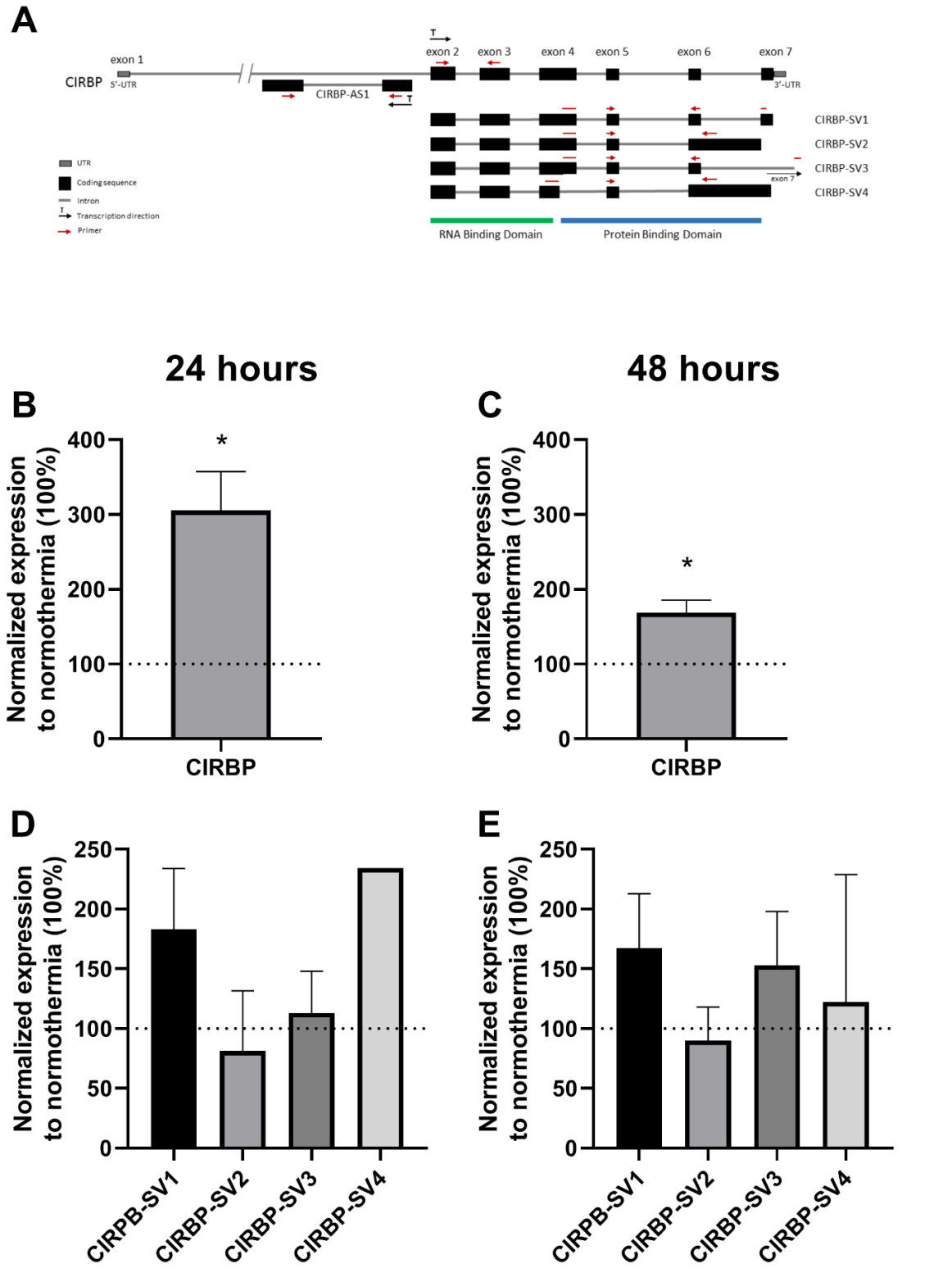

Figure 3A-E Total CIRBP and CIRBP splice variants expression after 24 or 48 hours hypothermia. A – schematic representation of the CIRBP gene and its splice variants with primer binding sites indicated. B+C – total CIRBP expression after 24 and 48 hours of hypothermia was induced compared to normothermic condition (200% increase and 70% increase, respectively). D+E – expression of CIRBP splice variants after 24 and 48 hours of hypothermia, respectively, was not changed significantly for any splice variant. Mean expression relative to GAPDH and normalized to normothermic condition (dotted line). Error bars represent SEM (N=3). One sample t-test is performed with $\alpha < 0.05$. *$p<0.05$.

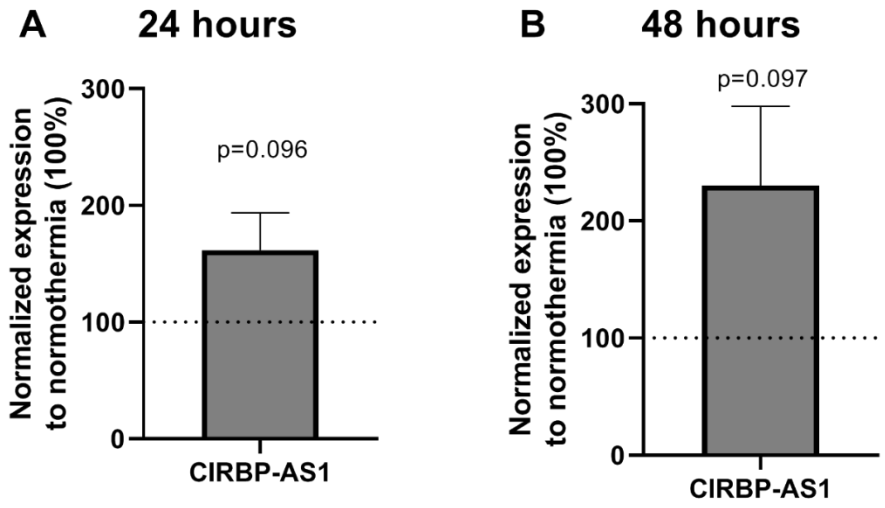

Figure 4A-B CIRBP-AS1 expression under hypothermia in HUVECs. A – CIRBP-AS1 expression after 24 hours of hypothermia showed a trend towards increased expression (p=0.096). B – CIRBP-AS1 expression after 48 hours of hypothermia showed a trend towards increased expression (p=0.097). Mean is indicated relative to GAPDH and normalized to normothermia (dotted line). Error bars represent SEM (N=3). One-sample t-test with a significance level of $\alpha<0.05$ did not show significant changes.

Target microRNAs in hypothermia

As our previous study showed that CIRBP targets 14q32 microRNAs miR-329-3p and miR-495-3p on a post-transcriptional level[18], we determined the levels of all intermediate products of these microRNAs, i.e. primary, precursor and mature microRNA levels. Under hypothermic conditions, no changes in pri-, pre- nor mature microRNA expression of miR-329-3p were observed (Figure 5A-B). Similarly, for miR-495-3p no differences in any stage of microRNA processing was observed (Figure 5C-D).

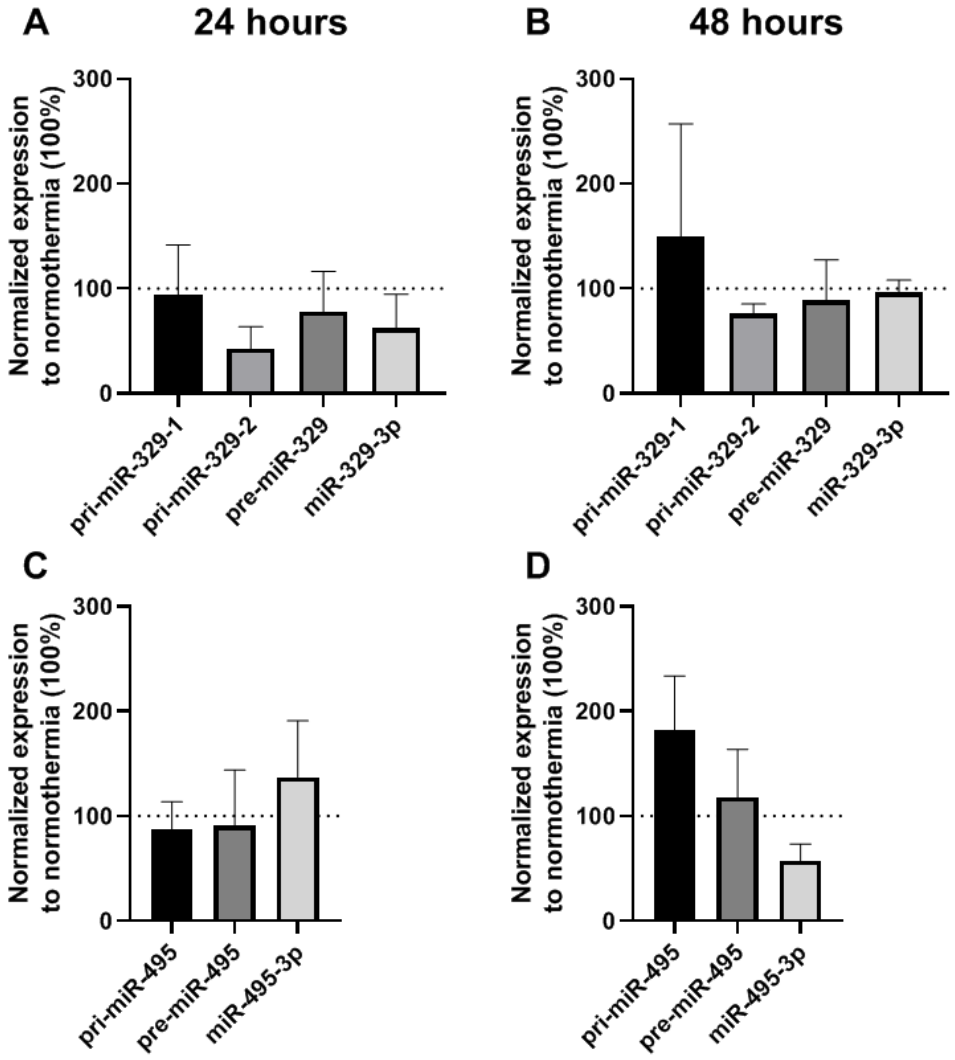

Figure 5A-D 14q32 microRNA expression after 24 or 48 hours hypothermia in HUVECs. A – primary, precursor and mature miR-329-3p expression after 24 hours of hypothermia did not show significant differences compared to normothermia. B – primary, precursor and mature miR-329-3p expression after 48 hours of hypothermia did not show significant differences compared to normothermia. C – primary, precursor and mature miR-495-3p expression after 24 hours of hypothermia did not show significant differences compared to normothermia. D – primary, precursor and mature miR-495-3p expression after 48 hours of hypothermia did not show significant differences compared to normothermia. Mean expression relative to U6 and normalized to normothermic condition (dotted line) is indicated. Error bars represent SEM (N=3). One sample t-test was performed and did not show any significant differences ($\alpha < 0.05$).

CIRBP knockdown with siRNAs

Hypothermic stress induced total CIRBP expression, but it did not affect target microRNA expression. Next, we used an siRNA to silence CIRBP and assessed the expression of total CIRBP and of its splice variants. As shown in Figure 6A, the siRNA was expected to target all splice variants of CIRBP. Total CIRBP expression was indeed knocked down by ~90% (p=0.002). Of the splice variants, especially CIRBP-SV1 was knocked down even further than total CIRBP

(~99% decrease, p=0.002, Figure 6B), whereas other splice variants remained unaffected. When measuring CIRBP-AS1 in CIRBP-silenced cells, we observed a trend towards decreased CIRBP-AS1 expression (40% decrease, p=0.078, Figure 6C).

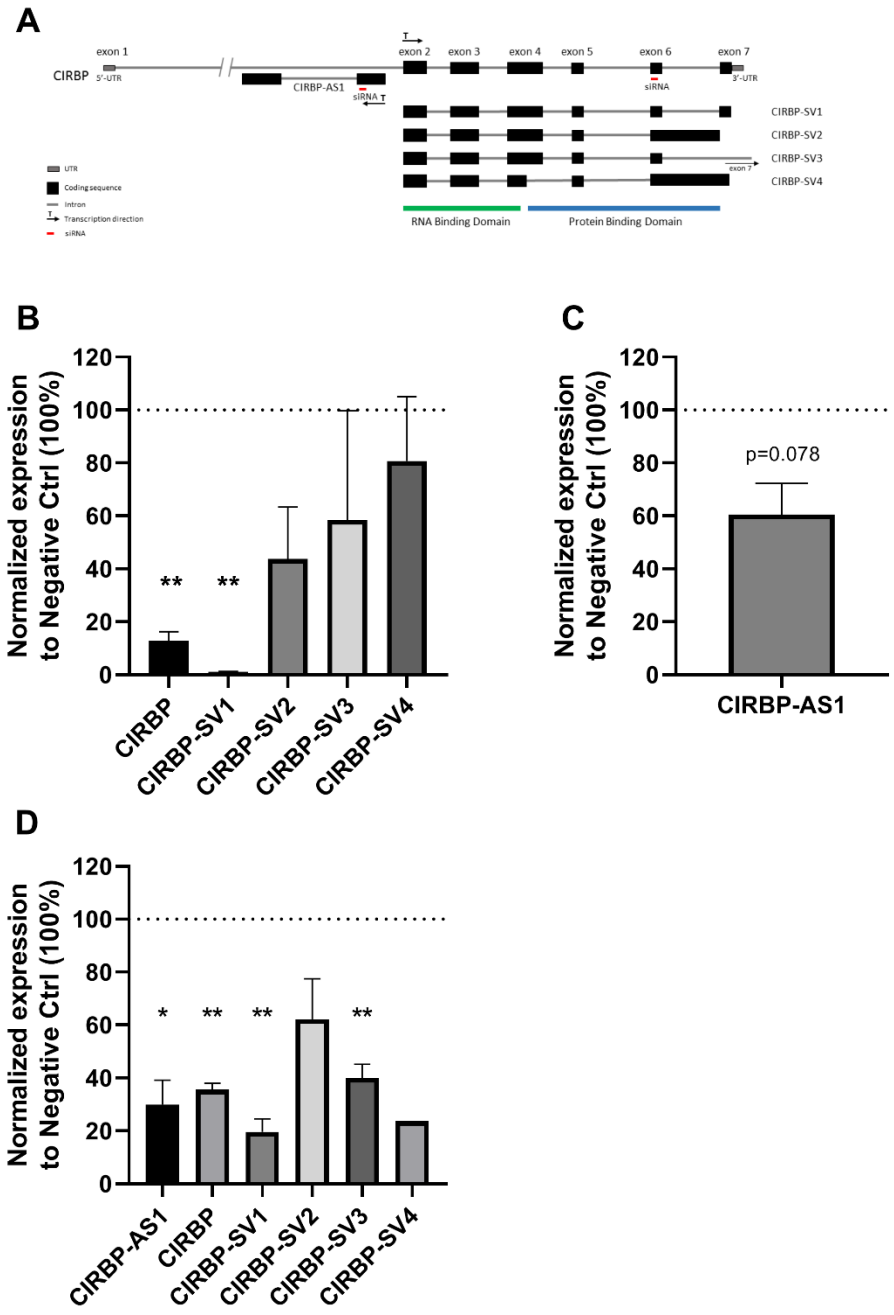

Figure 6A-D CIRBP and CIRBP-AS1 expression after knockdown with siRNAs in HUVECs. A – schematic representation of siRNA target sites along the CIRBP and CIRBP-AS1 genes. B – Expression of total CIRBP and CIRBP splice variants after CIRBP knockdown using siRNA showed a downregulation of total CIRBP by 90% (p=0.002). Of the splice variants, only CIRBP-SV1 showed a knockdown (99%, p=0.002). C – CIRBP-AS1 expression after CIRBP siRNA knockdown showed a trend towards decreased expression (p=0.078). D – CIRBP and CIRBP-AS1 expression after CIRBP-AS1 silencing using siRNA showed effective knockdown of CIRBP-AS1. Total CIRBP was downregulated as well (p=0.017) and of the CIRBP splice variants, only CIRBP-SV1 and CIRBP-SV3 were decreased (p=0.004 and p=0.007 respectively). Mean expression relative to GAPDH is indicated and normalized to negative control siRNA treatment (dotted

line). Error bars represent SEM (N=3). One-sample t-tests were performed with a significance level of $\alpha<0.05$. *$p<0.05$, **$p<0.01$.

CIRBP-AS1 knockdown

After CIRBP knockdown, CIRBP-AS1 changed in a similar direction as total CIRBP, i.e. a ~40% decrease (p=0.078). Next, CIRBP-AS1 was knocked-down using an siRNA (Figure 6A) and expression of CIRBP-AS1, total CIRBP and the CIRBP splice variants was assessed. CIRBP-AS1 knockdown was successful with 70% (p=0.017). In response to CIRBP-AS1 knockdown, total CIRBP was also downregulated by ~65% (p=0.001). When looking at the specific splice variants, CIRBP-SV1 (~80% downregulation, p=0.004) and CIRBP-SV3 (~60% downregulation, p=0.007) were downregulated, whereas the expression of CIRBP-SV2 and CIRBP-SV4 was not affected (Figure 6D).

MicroRNA expression in CIRBP and CIRBP-AS1 knockdown

Then we asked what the effect of CIRBP-silencing was on its target microRNAs. For miR-329-3p no effects on expression levels were observed for either primary and precursor microRNAs or the mature miR-329-3p (Figure 7A). Figure 7B shows that pri-miR-495 and pre-miR-495 also remained unchanged by CIRBP siRNA treatment, compared to Negative Control siRNA. Mature miR-495-3p, however, was affected by CIRBP knockdown and showed a downregulation of ~70% (p=0.02).

Knockdown of CIRBP-AS1 resulted in a ~55% downregulation of mature miR-329-3p (p=0.01), but expression of primary and precursor miR-329 remained unchanged compared to negative control treated HUVECs (Figure 7C). For miR-495-3p, similar results were observed as with siRNA-mediated silencing of CIRBP. Primary and precursor miR-495 expression were not affected, whereas miR-495-3p was significantly downregulated by ~85% (p=0.003) in CIRBP-AS1 knockdown (Figure 7D).

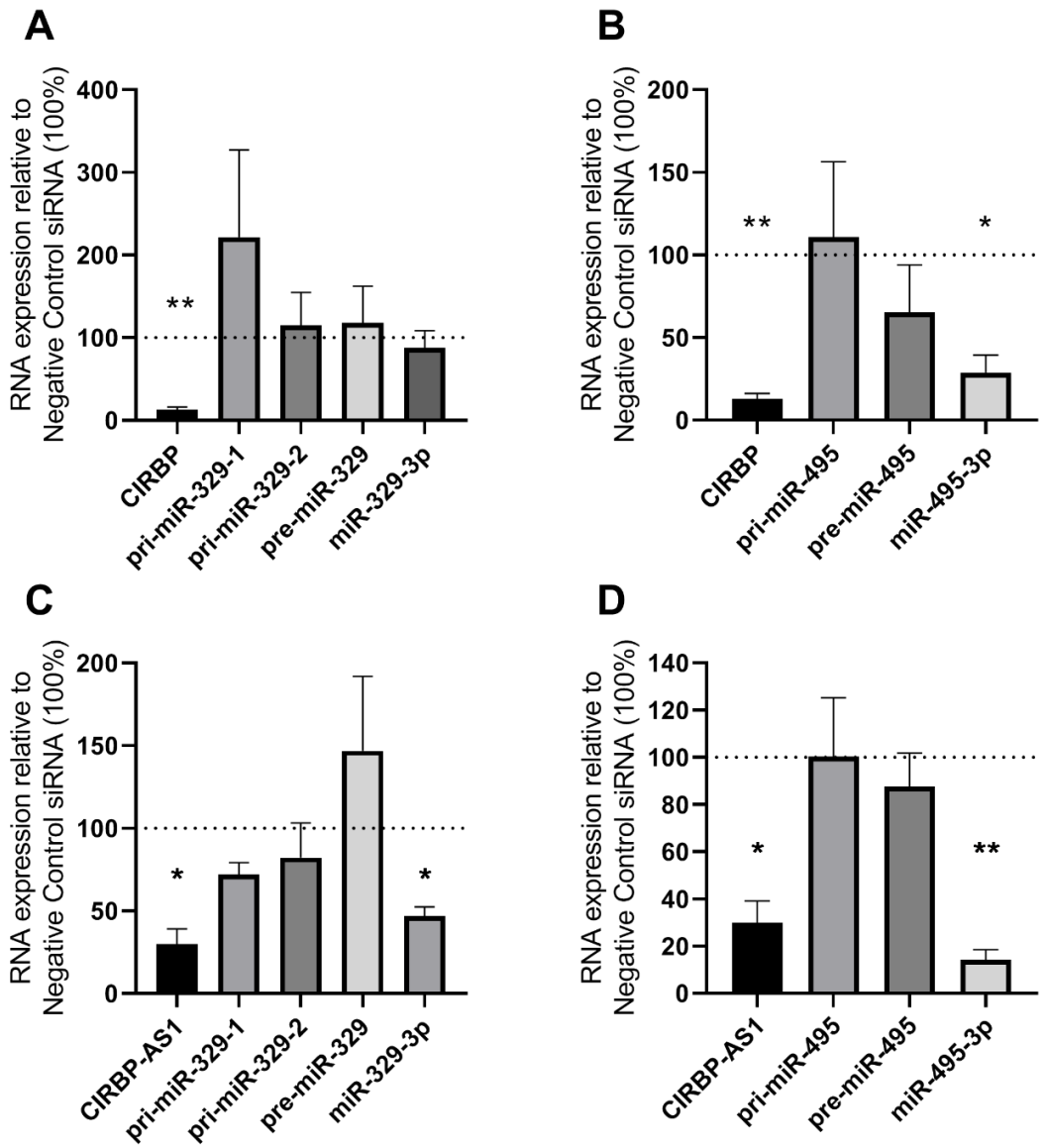

Figure 7A-D MicroRNA expression in HUVECs after CIRBP or CIRBP-AS1 siRNA treatment. A – expression of primary, precursor and mature miR-329-3p after CIRBP knockdown using siRNA did not show differences compared to negative control siRNA treatment. B – expression of primary and precursor miR-495 remained unchanged after knockdown of CIRBP, but mature miR-495-3p was significantly downregulated after CIRBP silencing. C – knockdown of CIRBP-AS1 led to mature miR-329-3p downregulation, but primary and precursor microRNAs remained unchanged. D – expression of primary and precursor miR-495 did not change in CIRBP-AS1 knockdown, but miR-495-3p expression was downregulated. Mean expression relative to U6 (miRs) and GAPDH (CIRBP) is indicated and normalized to negative control siRNA treatment (dotted line). Error bars represent SEM (N=3). One-sample t-tests were performed with a significance level of $\alpha<0.05$. *$p< 0.05$, **$p<0.01$.

Scratch wound healing in HUVECs after CIRBP and CIRBP-AS1 knockdown

Subsequently, the effect on endothelial cell migration as measure of angiogenic potential was assessed, using scratch wound healing assay in siRNA treated endothelial cells. Scratch wound healing in HUVECs after CIRBP knockdown was 4 times higher compared to the negative

control treated cells (p=0.004, Figure 8A+B). Expression of PCNA mRNA in CIRBP knockdown was assessed as a measure of proliferation, but did not show differences compared to negative control treatment (Figure 8C). Furthermore, the angiogenic potential of CIRBP-AS1 knockdown was investigated as well. Knockdown of CIRBP-AS1 resulted in 5-fold increased cell migration compared to negative control treated HUVECs (p=0.0002, Figure 8D+E). PCNA mRNA expression levels were similar in CIRBP-AS1 knockdown and negative control (Figure 8F).

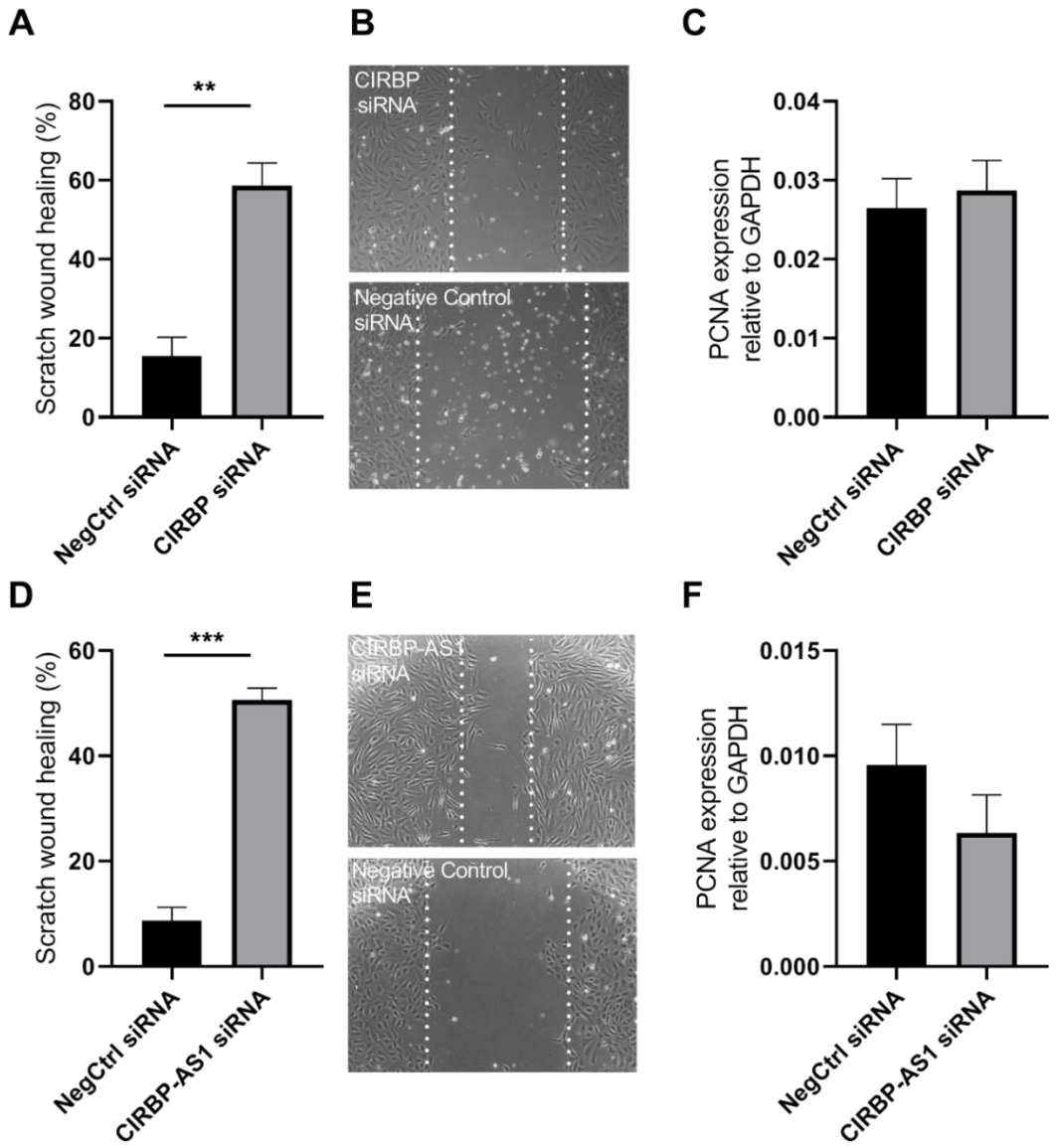

Figure 8A-F Functional assays after CIRBP siRNA treatment in HUVECs. A+B - Scratch wound healing in siRNA CIRBP treatment increased compared to negative control siRNA treatment (p=0.004). C - PCNA expression in HUVECs after CIRBP siRNA treatment did not show differences in expression compared to negative control. D+E – CIRBP-AS1 knockdown resulted in increased cell migration compared to negative control siRNA treated cells (p=0.0002). F - PCNA expression in HUVECs after CIRBP-AS1 siRNA treatment did not show differences in expression compared to negative control. Mean is indicated and error bars represent SEM (N=3). Significant differences were found with independent sample Student's t-test with a significance level of $\alpha<0.05$. **p< 0.01, ***p<0.001.

Tube formation in CIRBP knockdown

Next, we performed Matrigel tube-formation assays with HUVECs treated with siRNAs against CIRBP. As shown in Figure 9, CIRBP siRNA-treated cells showed significantly more segments and branches compared to Negative Control siRNA-treated cells (~100% increase, p=0.046 and ~60% increase p=0.016, respectively). Moreover, the total length of all tubes was increased when CIRBP was knocked down (~25% increase, p=0.014).

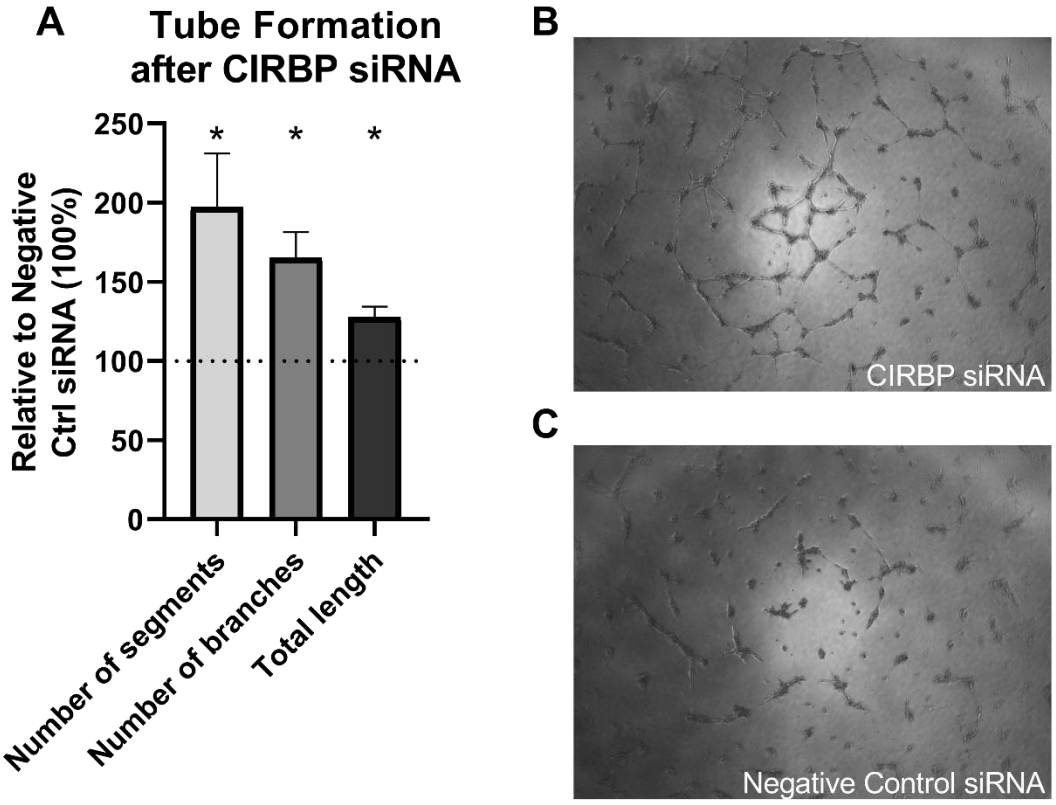

Figure 9A-C Tube formation assay in HUVECs. A – tube formation indicated in number of segments, number of branches and total length of tubes of HUVECs after CIRBP siRNA treatment compared to Negative Control siRNA treatment. Mean is indicated and error bars represent SEM (N=5). Indicated bars show significant change to Negative Control siRNA treated HUVECs (dotted line), found with one-sample t-test. *p< 0.05 with a significance level of $\alpha<0.05$. B+C – pictures of siRNA treated HUVECs at 12 hours after start of tube formation in CIRBP siRNA-treaded and negative control siRNA treated cells, respectively.

Discussion

In this study, we investigated Cold-Inducible RNA Binding Protein (CIRBP) as a potential therapeutic target to stimulate angiogenesis in patients with PAD. We show that CIRBP is upregulated under hypothermic conditions and, when we directly inhibit CIRBP expression, cell migration and tube formation capacity of endothelial cells is promoted. Upon inhibition of CIRBP, miR-495-3p expression is downregulated as well, suggesting that pro-angiogenic properties of CIRBP may act via miR-495.

We confirm that CIRBP is regulated under hypothermic conditions, as was reported previously[1, 3-6]. The novelty of this study, however, is that we showed this in vascular endothelial cells that were subjected to hypothermic conditions, as frequently occurs in PAD. CIRBP has four splice variants that alter the coding sequence. Of these four variants, CIRBP-SV1 specifically showed a trend towards upregulation after 24 and 48 hours of hypothermia. When we knocked-down CIRBP using an siRNA, we again observed specific knockdown of CIRBP-SV1 (as well as of total CIRBP). This was unexpected, as the binding site of the siRNA was predicted to target an mRNA sequence that is present in all four splice variants.

The antisense strand of CIRBP encodes a long noncoding RNA, CIRBP-AS1, of which the function has not yet been elucidated. We observed a trend towards upregulation of CIRBP-AS1 under hypothermic conditions, although the response to hypothermia was slower than that of CIRBP itself. After CIRBP knockdown, CIRBP-AS1 expression decreased and the opposite was also true. Inhibition of CIRBP-AS1 with an siRNA resulted in simultaneous downregulation of total CIRBP and of CIRBP-SV1 and CIRBP-SV3 expression. Potentially, a positive feedback loop supports transcription of the CIRBP locus, where CIRBP and CIRBP-AS1 induce each other's expression.

The expression of 14q32 microRNAs miR-329-3p and miR-495-3p was not increased under hypothermia, even though the expression of their reported post-transcriptional regulator CIRBP was increased. In contrast, silencing of CIRBP using an siRNA did lead to a decrease in miR-495-3p expression. Likely, the processing rate of 14q32 microRNAs is already at an optimum under normothermic conditions, which explains that an increase in CIRBP does not induce more processing of precursor microRNAs. The dramatic decrease in CIRBP expression does result in insufficient processing of miR-495-3p however. Surprisingly though, expression of miR-329-3p was still unaffected. Furthermore, CIRBP-AS1 knockdown resulted in a decreased expression of both mature microRNAs. However, regulation of microRNA

expression is highly complex and involves many RBPs that may compensate for the loss of CIRBP. Processing of miR-329-3p, but not miR-495-3p, for example, is also enhances by the RBP Myocyte Enhancer Factor 2A (MEF2A)[17]. When we speculate what these findings could mean to human PAD, CIRBP expression would likely be increased, as patients suffer from cold extremities. However, induced CIRPB does not affect 14q32 microRNA expression and thus, there would likely be only minor effects on angiogenesis. Therapeutic silencing of CIRBP however, would decrease the expression of mature miR-495-3p, which has profound effects on ischemia-induced neovascularization and thus on perfusion of the affected limb[20].

Therefore, we assessed these potential pro-angiogenic features of CIRBP knockdown. Indeed, both cell migration assays and tube formation assays in HUVECs showed an increase in angiogenic potential following CIRBP and CIRBP-AS1 knockdown. We know that direct inhibition of miR-495-3p promotes angiogenesis[20] and we observed here that CIRBP knockdown leads to decreased expression of miR-495-3p. These findings of course suggest that the increased angiogenic potential induced by CIRBP downregulation is accomplished via the subsequent miR-495-3p decrease. However, it remains to be determined whether CIRBP can also target additional pro-angiogenic factors.

It has been shown in CIRBP$^{-/-}$ mice that the inflammatory response in tissue wound healing is faster than in wildtype mice. More CD31 expression, as marker of endothelial cells and thus angiogenesis, was observed in wounds of CIRBP$^{-/-}$ mice[25], although the exact mechanism of action for CIRBP in wound healing was not elucidated. The inflammatory function of CIRBP in stress conditions was already reported by Qiang et al[26]. Moreover, the authors reported that CIRBP binds TLR4, MD2 and the TLR4/MD2-complex, which is known to stimulate neovascularization. Therefore, the question arises whether CIRBP binding to TLR4 increases or decreases TLR4 availability. If the latter is the case, CIRBP-silencing would increase TLR4 availability and this may therefore be an explanation for increased neovascularization after CIRBP inhibition.

We found that inhibition of CIRBP leads mainly to a decrease in CIRBP-SV1, which then resulted in increased *in vitro* angiogenesis. It would be interesting in future research to target CIRBP-SV2-4 specifically and assess the effect on angiogenesis, and on 14q32 microRNA expression, for these splice variants separately. With this, we could better understand the exact part of the CIRBP sequence that targets microRNA expression and, possibly, link this to the pro-angiogenic potential of CIRBP. Since the RNA binding domain is similar in all splice variants, it is likely that all bind to precursor microRNAs in a similar manner. However, the

splice variants differ in their protein binding domains, which could result in the attraction of different proteins. This may still lead to changes in microRNA processing, but may also influence angiogenesis more directly via these proteins.
Silencing of CIRBP-AS1, like of CIRBP, resulted in increased angiogenesis and decreased mature microRNA expression. Furthermore, downregulation of CIRBP-AS1 decreased CIRBP expression and vice versa. However, we did not yet uncover whether CIRBP or CIRBP-AS1 is the key regulating factor in angiogenesis and thus the main potential therapeutic target in stimulating neovascularization. Moreover, as both CIRBP and CIRBP-AS1 are able to downregulate expression of mature 14q32 microRNAs, it remains to be determined whether CIRBP-AS1 can affect microRNA processing directly and, thereby, play a role in angiogenesis.

We found that hypothermia caused CIRBP expression upregulation and that CIRBP silencing resulted in proangiogenic features. Therefore, one could speculate that hyperthermia leads to decreased CIRBP expression, followed by subsequent increase in angiogenesis. In PAD, this would imply that warming affected cold legs could lead to increased angiogenesis and therefore to improved circulation. A next step in this study could be to assess whether increased temperature causes decreased CIRBP expression in endothelial cells and subsequent miR-495-3p downregulation.

In conclusion, our findings demonstrate that hypothermia induces CIRBP expression, but does not affect 14q32 microRNAs miR-329-3p and miR-495-3p expression. Silencing of CIRBP decreases miR-495-3p expression and promotes *in vitro* angiogenesis. CIRBP-AS1 is affected by CIRBP knockdown and silencing of CIRBP-AS1 also inhibits CIRBP expression. Furthermore CIRBP-AS1 knockdown inhibits both miR-329-3p and miR-495-3p and promotes *in vitro* angiogenesis as well. This makes CIRBP and CIRBP-AS1 promising targets in post-ischemic neovascularization. Future studies will determine whether these targets work in an *in vivo* model as well.

References

1. Liu A, Zhang Z, Li A, Xue J. Effects of hypothermia and cerebral ischemia on cold-inducible RNA-binding protein mRNA expression in rat brain. Brain research 2010;1347:104-110.
2. Wellmann S, Buhrer C, Moderegger E, Zelmer A, Kirschner R, Koehne P, Fujita J, Seeger K. Oxygen-regulated expression of the RNA-binding proteins RBM3 and CIRP by a HIF-1-independent mechanism. Journal of cell science 2004;117:1785-1794.
3. Liao Y, Tong L, Tang L, Wu S. The role of cold-inducible RNA binding protein in cell stress response. International journal of cancer 2017;141:2164-2173.
4. Al-Fageeh MB, Smales CM. Cold-inducible RNA binding protein (CIRP) expression is modulated by alternative mRNAs. RNA (New York, NY) 2009;15:1164-1176.
5. Lleonart ME. A new generation of proto-oncogenes: cold-inducible RNA binding proteins. Biochimica et biophysica acta 2010;1805:43-52.
6. Fujita J. Cold shock response in mammalian cells. Journal of molecular microbiology and biotechnology 1999;1:243-255.
7. Nishiyama H, Itoh K, Kaneko Y, Kishishita M, Yoshida O, Fujita J. A glycine-rich RNA-binding protein mediating cold-inducible suppression of mammalian cell growth. The Journal of cell biology 1997;137:899-908.
8. Nishiyama H, Higashitsuji H, Yokoi H, Itoh K, Danno S, Matsuda T, Fujita J. Cloning and characterization of human CIRP (cold-inducible RNA-binding protein) cDNA and chromosomal assignment of the gene. Gene 1997;204:115-120.
9. Zhu X, Buhrer C, Wellmann S. Cold-inducible proteins CIRP and RBM3, a unique couple with activities far beyond the cold. Cellular and molecular life sciences : CMLS 2016;73:3839-3859.
10. Zhong P, Huang H. Recent progress in the research of cold-inducible RNA-binding protein. Future science OA 2017;3:Fso246.
11. Horii Y, Shiina T, Uehara S, Nomura K, Shimaoka H, Horii K, Shimizu Y. Hypothermia induces changes in the alternative splicing pattern of cold-inducible RNA-binding protein transcripts in a non-hibernator, the mouse. Biomedical research (Tokyo, Japan) 2019;40:153-161.
12. Pelechano V, Steinmetz LM. Gene regulation by antisense transcription. Nature reviews Genetics 2013;14:880-893.
13. Gomes CP, Nobrega-Pereira S, Domingues-Silva B, Rebelo K, Alves-Vale C, Marinho SP, Carvalho T, Dias S, Bernardes de Jesus B. An antisense transcript mediates MALAT1 response in human breast cancer. BMC cancer 2019;19:771.
14. Zong X, Nakagawa S, Freier SM, Fei J, Ha T, Prasanth SG, Prasanth KV. Natural antisense RNA promotes 3' end processing and maturation of MALAT1 lncRNA. Nucleic Acids Res 2016;44:2898-2908.
15. Bernstein E, Caudy AA, Hammond SM, Hannon GJ. Role for a bidentate ribonuclease in the initiation step of RNA interference. Nature 2001;409:363-366.
16. Lee Y, Jeon K, Lee JT, Kim S, Kim VN. MicroRNA maturation: stepwise processing and subcellular localization. Embo j 2002;21:4663-4670.
17. Welten SMJ, de Vries MR, Peters EAB, Agrawal S, Quax PHA, Nossent AY. Inhibition of Mef2a Enhances Neovascularization via Post-transcriptional Regulation of 14q32 MicroRNAs miR-329 and miR-494. Molecular therapy Nucleic acids 2017;7:61-70.
18. Downie Ruiz Velasco A, Welten SMJ, Goossens EAC, Quax PHA, Rappsilber J, Michlewski G, Nossent AY. Posttranscriptional Regulation of 14q32 MicroRNAs by the CIRBP and HADHB during Vascular Regeneration after Ischemia. Molecular therapy Nucleic acids 2019;14:329-338.
19. Treiber T, Treiber N, Plessmann U, Harlander S, Daiss JL, Eichner N, Lehmann G, Schall K, Urlaub H, Meister G. A Compendium of RNA-Binding Proteins that Regulate MicroRNA Biogenesis. Molecular cell 2017;66:270-284.e213.

20. Welten SM, Bastiaansen AJ, de Jong RC, de Vries MR, Peters EA, Boonstra MC, Sheikh SP, Monica NL, Kandimalla ER, Quax PH, Nossent AY. Inhibition of 14q32 MicroRNAs miR-329, miR-487b, miR-494, and miR-495 increases neovascularization and blood flow recovery after ischemia. Circ Res 2014;115:696-708.
21. Welten SMJ, de Jong RCM, Wezel A, de Vries MR, Boonstra MC, Parma L, Jukema JW, van der Sluis TC, Arens R, Bot I, Agrawal S, Quax PHA, Nossent AY. Inhibition of 14q32 microRNA miR-495 reduces lesion formation, intimal hyperplasia and plasma cholesterol levels in experimental restenosis. Atherosclerosis 2017;261:26-36.
22. Wezel A, Welten SM, Razawy W, Lagraauw HM, de Vries MR, Goossens EA, Boonstra MC, Hamming JF, Kandimalla ER, Kuiper J, Quax PH, Nossent AY, Bot I. Inhibition of MicroRNA-494 Reduces Carotid Artery Atherosclerotic Lesion Development and Increases Plaque Stability. Annals of surgery 2015;262:841-847; discussion 847-848.
23. Welten SM, Goossens EA, Quax PH, Nossent AY. The multifactorial nature of microRNAs in vascular remodelling. Cardiovascular research 2016;110:6-22.
24. Risau W. Mechanisms of angiogenesis. Nature 1997;386:671-674.
25. Idrovo JP, Jacob A, Yang WL, Wang Z, Yen HT, Nicastro J, Coppa GF, Wang P. A deficiency in cold-inducible RNA-binding protein accelerates the inflammation phase and improves wound healing. International journal of molecular medicine 2016;37:423-428.
26. Qiang X, Yang WL, Wu R, Zhou M, Jacob A, Dong W, Kuncewitch M, Ji Y, Yang H, Wang H, Fujita J, Nicastro J, Coppa GF, Tracey KJ, Wang P. Cold-inducible RNA-binding protein (CIRP) triggers inflammatory responses in hemorrhagic shock and sepsis. Nature medicine 2013;19:1489-1495.

Supplementary Data

Supplementary Table 1 sequences of primers used for qPCR and of siRNAs used for knockdown

	Forward sequence	Reverse sequence
HSA-CIRBP	TTGACACCAATGAGCAGTCG	GGCATCCTTAGCGTCGTCAA
HSA-splice variant 1	CGTGGGTTCTCTAGAGGAGGA	CTCGTTGTGTGTAGCGTAACTG
HSA-splice variant 2	CGTGGGTTCTCTAGAGGAGGA	CGCCCTCGGAGTGTGACTTA
HSA-splice variant 3	CGTGGGTTCTCTAGAGGAGGA	TCAACCGTAACTGTCATAACTG
HSA-splice variant 4	GTAGACCAGGCAGGAGGAG	CGCCCTCGGAGTGTGACTTA
HSA-CIRBP-AS1	CAATGGGAAAAGGAGGAAACT	CCTTGTAAAGCTGGTTCTCCA
GAPDH	CACCACCATGGAGAAGGC	AGCAGTTGGTGGTGCAGGA
HSA-pri-miR-329-1	TGGGGAAGAATCAGTGGTGT	GACCAGAAGGCCTCCAAGAT
HSA-pri-miR-329-2	TGTCAAGTTTGGGGAAGGAA	GACCAGAAGGCCTCCAAGAT
HSA-pre-miR-329	TGAAGAGAGGTTTTCTGGGTTT	ACCAGGTGTGTTTCGTCCTC
HSA-pri-miR-495	CTGACCCTCAGTGTCCCTTC	ATGGAGGCACTTCAAGGAGA
HSA-pre-miR-495	GCCCATGTTATTTTCGCTTT	CCGAAAAAGAAGTGCACCAT
U6	AGAAGATTAGCATGGCCCCT	ATTTGCGTGTCATCCTTGCG
siRNA CIRPB	GAGUCAGAGUGGUGGCUAC	
siRNA CIRBP-AS1	CAGGACCCUCACUCACUA	

Part III

Chapter 7

General Discussion and Future Perspectives

General discussion

A large noncoding RNA gene cluster located on the 14th chromosome in human includes the largest known microRNA cluster, a snoRNA cluster and three long noncoding RNAs. MicroRNAs and snoRNAs of the 14q32 locus are known to play different roles in cardiovascular disease and vascular remodelling. The aim of this thesis was to elucidate the differential expression of 14q32 microRNAs and snoRNAs in the vasculature and to identify regulators of 14q32 microRNAs in vascular remodelling. It is known that microRNAs can change in vascular remodelling processes. However, it was not uncovered whether expression of 14q32 microRNAs differs between different locations in the vasculature. Moreover, 14q32 microRNAs are regulators of vascular remodelling processes, but can also be regulated. The mechanisms of action of 14q32 microRNA regulators and the possibility to use these regulators in targeting vascular remodelling were investigated in this thesis.

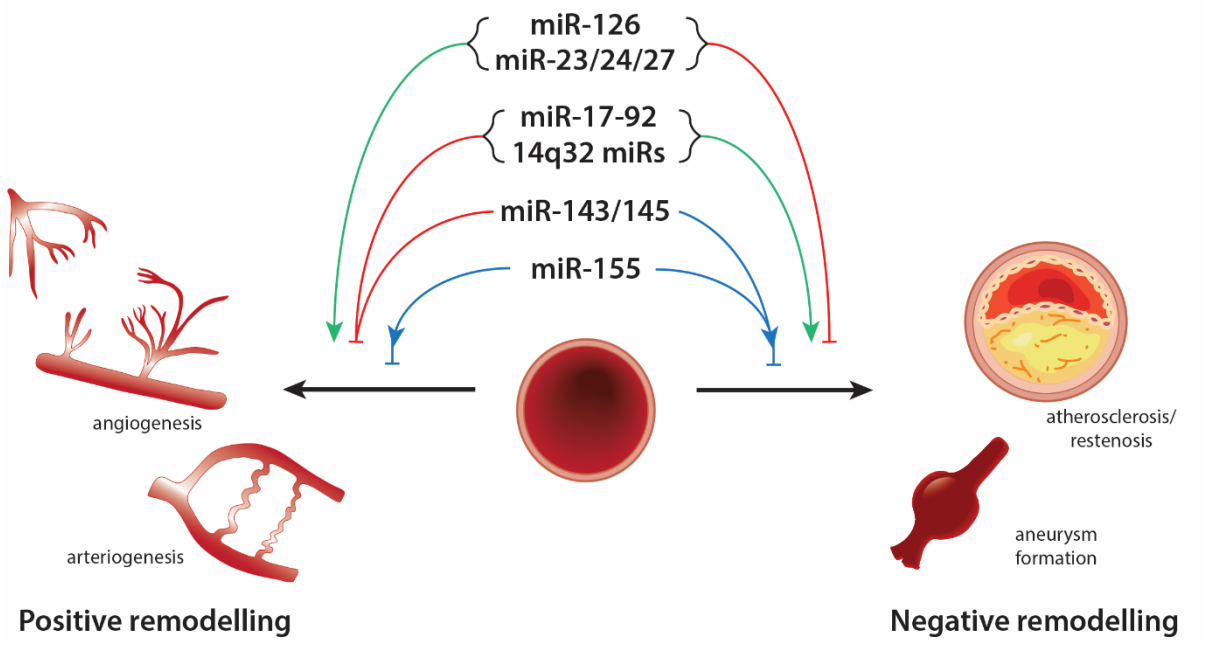

Figure 1 Graphical representation of microRNA clusters in vascular remodelling. MiR-126 and miR-23/24/27 induce positive remodelling and inhibit negative remodelling, whereas miR-17-92 and 14q32 microRNAs inhibit positive remodelling and stimulate negative remodelling. The effect of miR-143/145 and miR-155 on negative remodelling is inconclusive, but miR143/145 inhibits positive remodelling. Figure from *Welten & Goossens et al. Cardiovasc Res. 2016.*

In **Chapter 2**, we focused on microRNAs that are involved in both positive vascular remodelling (neovascularization) and negative vascular remodelling (atherosclerosis, restenosis and aneurysm formation). The individual microRNAs miR-126 and miR-155 as well as microRNA gene clusters miR-17/92, miR-23-24-27, miR-143/145 and 14q32 microRNAs were reviewed. Their multifactorial nature was highlighted as they play a role in

multiple vascular remodelling processes. MiR-126 and the miR-23/24/27 family was shown to stimulate positive vascular remodelling and inhibit negative remodelling at the same time. MiR-17/92, miR-143/145 and the 14q32 microRNA cluster, on the other hand, inhibit positive remodelling and induce negative remodelling. MiR-155 was described to play a role in all vascular remodelling processes, but could not be determined as specific inhibitor or inducer of remodelling processes. As different microRNAs or microRNA families affect vascular remodelling similarly or oppositely, it could be suggested that they reinforce each other, however, this needs to be studied further. This chapter provides openings for new therapeutic opportunities and more research is needed to identify the efficacy of promising microRNAs or microRNA clusters in treatment of cardiovascular disease. Findings of **Chapter 2** are summarized in Figure 1.

14q32 ncRNA expression

The human 14q32 ncRNA cluster is known to include 41 snoRNAs. In mice, the number of snoRNAs has not yet been established. The function of snoRNAs in general in cardiovascular disease[1, 2] and the function of 14q32 microRNAs in cardiovascular disease[3-6] was studied. However, the role of 14q32 snoRNAs in cardiovascular disease had not yet been elucidated. In **Chapter 3**, several lines of evidence are found to support 14q32 snoRNAs to be highly important regulators in cardiovascular disease. Firstly, single nucleotide polymorphisms (SNPs) that are present in genes encoding for 14q32 snoRNAs, were associated with heart failure, independently of microRNAs and long noncoding RNAs. Furthermore, in human blood vessel samples, both healthy and diseased, 14q32 snoRNAs were measured and showed higher expression in the head and neck area than in the lower limbs. Moreover, five out of seven measured 14q32 snoRNAs were upregulated in failed human vein grafts compared to the naïve vein grafts. In mice a similar upregulation of snoRNA expression was observed in vein graft disease. Next, in the STEMI cohort blood samples collected during ST-Elevation Myocardial Infarction (STEMI). After STEMI, SNORD113-2 in peripheral blood was changed 4 days after the myocardial infarct compared to 30 days after the event. This implies that 14q32 snoRNAs are affected in various forms of cardiovascular disease. Additionally, functional *in vitro* assays showed that upregulation of snoRNAs in murine cells led to a decreased cell migration in two of five measured snoRNAs and Fibrillarin, a methyltransferase that acts as a snoRNA-guided 2'O-ribose-methylation agent of target ncRNAs, was bound to 14q32 snoRNAs. Taken together, this study demonstrates the importance of 14q32 snoRNAs in cardiovascular disease and vascular remodelling. Further studies into finding snoRNA targets and mechanistic pathways of 14q32 snoRNAs are required to fully understand the role of snoRNAs in vascular processes.

More was already known about 14q32 microRNAs in cardiovascular disease. Inhibition of 14q32 microRNAs decreases negative vascular remodelling processes and improves positive vascular remodelling[3-6]. As it was not known what 'normal' expression of these microRNAs is, how they change under pathophysiological conditions and whether 14q32 microRNAs have vascular location-specific expression patterns, we aimed to make a vascular map of microRNA expression. This study is described in **Chapter 4** for which a biobank was compiled of vascular tissue samples originating from most location in the vasculature. Surplus vascular tissue samples were discarded during surgery and microRNA expression levels were measured. As for 14q32 snoRNAs, microRNA expression was shown to be highly vascular location specific. We could therefore conclude that microRNA expression really shows vascular fingerprints. Highest expression was present in the lower limb vessels, whereas vessels in the neck area that could suffer from the same vascular disease, namely atherosclerosis, showed lowest expression for all microRNAs. Furthermore, all 14q32 microRNAs showed higher expression in arteries than in veins. Within a blood vessel wall, highest microRNA expression was present in the smooth muscle cell layer. This is a layer that is prominently present in the arterial wall, but smooth muscle cells are less abundant in the venous vessel wall. Endothelial cells had lowest expression for all microRNAs. 14q32 microRNA expression did not correlate with age, nor with sex, but showed inverse expression of target genes that were known to play a role in cardiovascular disease. Malignancies tended to increase vascular microRNA expression which was already shown within tumor cells itself. While compiling the miRMap biobank, even though we succeeded in including many different vessels, we realized that parts of the vasculature are missing to complete the atlas. For example, lung vessels, heart tissue, intracranial vessels and caval vein are not included as these tissues are not taken out during surgery of living patients. However, it would be interesting to include these samples as cardiovascular disease like thromboembolic events occur in the brain and lung vessels.

Interestingly, expression in atheroprone locations as the lower limb vessels and the neck vessels is opposing for 14q32 snoRNAs (**Chapter 3**) and microRNAs (**Chapter 4**). Whereas both ncRNAs showed increased cell migration upon downregulation. Given these differences in expression patterns, the question remains what the association is between microRNAs and snoRNAs encoded in the same locus. Both ncRNAs could antagonize each other, like was seen between lncRNAs and other ncRNAs as microRNAs and snoRNAs[7]. Another possibility is that, for example, in a healthy vessel microRNAs are residing and, therefore, not active during low expression in the neck vessels, whereas the snoRNAs are

highly expressed and actively repressing vascular remodelling. In that way, they cooperate in maintaining integrity of the vessel wall. The exact mechanism of interaction between 14q32 microRNAs and snoRNAs has to be investigated. Summarizing, the first part of this thesis emphasizes that expression is regulated individually for each 14q32 ncRNA and is highly vascular disease and location specific.

Expression regulation

DNA methylation along the 14q32 locus was proposed as a possible gene expression regulator and, therefore, a regulator of 14q32 microRNA expression. In **Chapter 4** 14q32 DNA methylation was measured throughout the human vasculature. In comparison of arteries and veins of patients with either PAD or CAD, differences between naïve VSMs harvested before implantation as coronary bypass, lower limb veins of patients with PAD and critically ischemic lower limb veins were observed. Especially in patients with severe ischemia, for which lower limb amputation was indicated, 14q32 DNA methylation was extremely high in the IG-DMR-CG4-2, MEG3-DMR-1B and MEG8-DMR-1H. Furthermore, in a murine ischemia model and a vein graft disease model, we observed remodelling-specific 14q32 DNA methylation changes. In vein graft remodelling, during active remodelling at two weeks after grafting[8, 9], DNA methylation was changed. At four weeks this process is more or less stabilized and 14q32 DNA methylation level returned to the native status. This was observed for DNMTs as well. In hindlimb ischemia, DNA methylation increased over time within the different DMRs between ischemic and control hindlimbs. However, as microRNAs and DNA methylation vary between vascular remodelling statuses, it was assessed whether these two correlate directly. This was not the case for any microRNA or DMR along the 14q32 locus nor for primary microRNAs and DNA methylation and not for (primary) microRNAs and DNMT expression. Therefore, 14q32 DNA methylation is not directly linked to 14q32 microRNA expression throughout the human vasculature. This was previously claimed by Aavik et al.[10] for atherosclerotic plaques. This difference could be explained by the fact that we looked at individual methylation site changes using restriction enzyme digestion followed by qPCR and not looked at a more global level, using bisulfite sequencing. DNA methylation is not only known as a gene expression regulator, but was also described as a regulator of alternative splicing[11]. However, the extend in which 14q32 DNA methylation acts in this process in cardiovascular disease, has to be investigated. Taken together, 14q32 DNA methylation cannot be considered as regulator of 14q32 microRNA expression in cardiovascular disease, but is associated with vascular remodelling status independently of 14q32 microRNAs.

Another possible 14q32 microRNA regulator discussed in this thesis is myostatin. As described in **Chapter 5**, myostatin is a negative regulator of muscle cell proliferation and of 14q32 microRNA expression. This is due to the ability of myostatin to bind the callipyge locus, another name for the 14q32 locus, and thereby affects microRNA expression. Therefore, we decided to study the effects of inhibiting 14q32 microRNA expression by myostatin administration. It is interesting that previous studies found that microRNA expression of the whole locus was affected by myostatin, because we observed in **Chapter 4** that expression of the 14q32 microRNAs along the locus differs from microRNA to microRNA. We observed indeed a downregulation of 14q32 microRNA expression upon myostatin administration in a dose-specific way. Next to the effect of myostatin on microRNA expression, the functional hypothesis was that myostatin, as negative muscle cell regulator, could inhibit vascular smooth muscle cell proliferation, one of the main features of post-interventional restenosis. Proliferation was indeed inhibited both *in vitro* and *in vivo*. However, myostatin did not have a clear consistent effect on the other cell type that is involved in restenosis, i.e. macrophages. Moreover, 14q32 microRNA expression in macrophages was not consistently changed either. As myostatin only has an effect on VSMCs, but not on macrophages, no clinical effect was found. This emphasizes that for targeting restenosis, compounds are needed that target both inflammation and VSMC proliferation. Findings of **Chapter 5** are summarized in Figure 2.

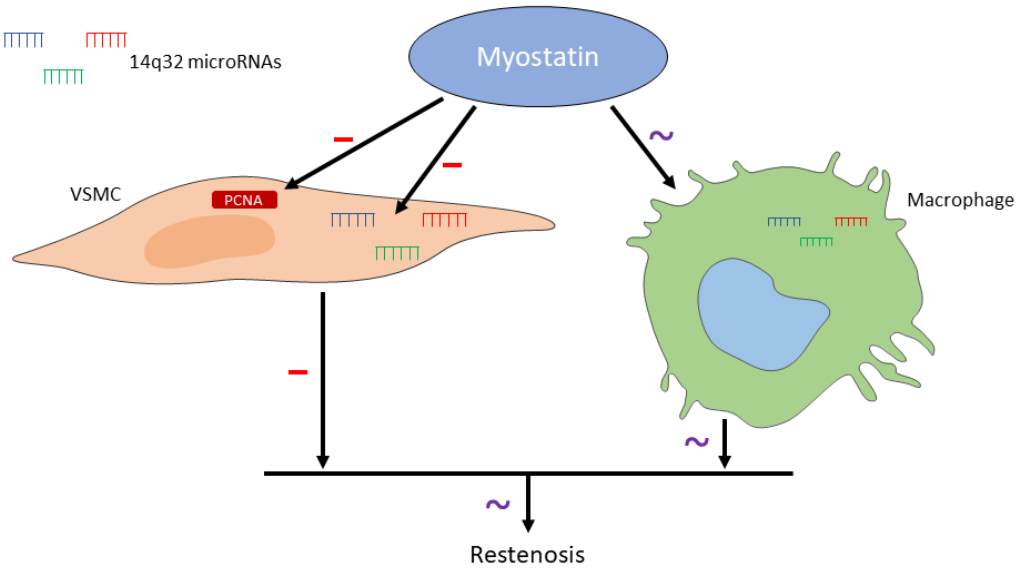

Figure 2 Graphical representation of the function of myostatin in restenosis.

The last possible regulator of 14q32 microRNA expression that is discussed in this thesis, is on RNA binding protein (RBP). We investigated cold-inducible RNA binding protein (CIRBP) in detail. It was shown previously that this RBP is able to bind 14q32 precursor microRNAs of

miR-329 and miR-495 to enhance processing into mature microRNAs[12]. **Chapter 6** investigates the *in vitro* effects of hypothermia and knockdown of CIRBP on total CIRPB, its splice variants, antisense long noncoding RNA and the target microRNAs. The target microRNAs of CIRBP, miR-495 but not miR-329, were downregulated in CIRBP knockdown. They were not altered in CIRBP overexpression, suggesting that CIRBP is needed for processing, but is not a rate limiting factor under normothermic conditions. Furthermore, the proangiogenic features of CIRBP knockdown, especially splice variant 1 of CIRBP, CIRBP-SV1, were assessed and it was shown that this condition had better migration and tube formation capabilities. Moreover, the antisense long noncoding RNA of CIRBP, CIRBP-AS1, seemed to react similarly to hypothermia and CIRBP knockdown as CIRBP itself. Therefore, CIRBP-AS1 was knocked down and this showed a knockdown of CIRBP as well. Again, CIRBP-SV1 was most prominently affected. Furthermore, endothelial cell migration increased upon CIRBP-AS1 knockdown. However, it remains unclear whether CIRBP affects CIRBP-AS1 or vice versa and whether they collaborate or reinforce each other in angiogenesis. This still needs to be elucidated. Taken together, CIRBP is a promising target to stimulate post-ischemic neovascularization, like another RBP, MEF2A, was shown to act on 14q32 microRNAs to stimulate neovascularization[5]. HADHB in a previous study was shown to have the same 14q32 microRNA targets as CIRBP[12] and it is interesting to assess the effect of HADHB knockdown on angiogenesis and its target microRNAs. Moreover, other RBPs that target microRNAs[13] have to be investigated for binding to 14q32 microRNAs to link them to specific vascular remodelling processes. Given this, it is interesting to target RBPs to affect microRNAs and thus regulating vascular remodelling processes. Thereby, off target effects of direct microRNA manipulation are avoided, as microRNAs have specific expression patterns for each vessel type. This was shown in **Chapter 4**. However, it remains to be investigated whether RBPs only bind microRNAs under specific conditions or stress factors or that this binding and affecting process is always present. Findings of **Chapter 6** are summarized in Figure 3.

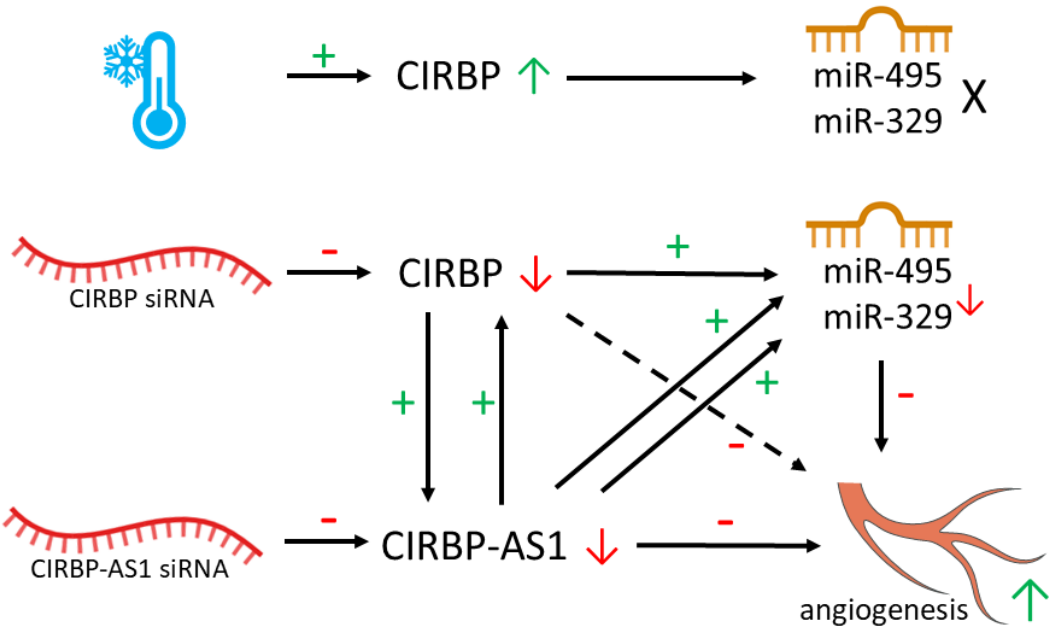

Figure 3 Graphical representation of CIRBP in angiogenesis.

Future perspectives

This thesis has uncovered that 14q32 noncoding RNA expression differs highly throughout the human vasculature. Moreover, we have discussed several potential 14q32 microRNA regulators. However, still numerous hurdles have to be taken before this knowledge can be applied in clinical practice.

As we now know that 14q32 noncoding RNAs have location-specific expression fingerprints, it would be interesting to investigate the possibility to target these noncoding RNAs locally. Systemic side effects of noncoding RNAs are avoided in this strategy. In future clinical practice it would be ideal to treat patients suffering from cardiovascular disease by targeting, for example, a microRNA or snoRNA that is only present in the diseased vessel. It would even be more interesting to use microRNAs or snoRNAs as guide RNAs to bring a specific substance to particular cells and once it is in the cell, release a DNA methylation changing substance to affect methylation that is specific for the remodelling process, as DNA methylation is vascular remodelling process-specific. Thereby, systemic DNA methylation treatments that are mostly toxic and used in the field of oncology, are avoided. Steps that have to be taken, are investigation of off-target effects of noncoding RNA treatment in different cell types and vascular locations. Identifying these effects, results in finding an optimal therapeutic window.

In this thesis, restenosis is emphasized to involve both VSMC migration and -proliferation and inflammatory reactions, mainly by macrophage influx. These factors are equally important to be targeted in restenosis prevention or treatment. Therefore, to overcome post-interventional vascular remodelling, both VSMCs and macrophages should be targeted. Myostatin acts on local VSMCs and local microRNAs in VSMCs, but a regulator of macrophages should be added to decrease restenosis. Preferably, again only local anti-inflammatory compounds should be considered, as systemic immune suppressing agents are not favorable.

CIRBP is a promising target for increasing angiogenesis and it is even more interesting as downregulation of CIRBP-AS1 also targets CIRBP and angiogenesis. It has to be elucidated in further research what the actual interaction is between CIRBP and CIRBP-AS1. Furthermore, future research will point out whether CIRBP knockout *in vivo* results in increased blood flow recovery in hindlimb ischemia. Does CIRBP knockout increase neovessel formation around the occluded vessel in this model and ultimately in PAD? The final aim is to target CIRBP in human PAD or CAD. Moreover, in this thesis, we found that miR-495 is affected by CIRBP knockdown, but it remains to be determined whether this is the key factor in promoting angiogenesis or that CIRBP has another main target in stimulating neovascularization. A remaining question is whether CIRPB-AS1 knockdown affects angiogenesis via 14q32 microRNA expression or via which other pathway CIRBP-AS1 knockdown stimulates neovascularization. In finding answers to these questions CIRBP will turn out as potential clinical target or not.

The ultimate goal in noncoding RNA research in vascular remodelling is to find a therapeutic option to prevent, stop or even diminish cardiovascular disease and the subsequent burden on patients. This aim could either be accomplished by direct or indirect targeting of noncoding RNAs.

In conclusion, this thesis provides novel insights in the differential expression of 14q32 noncoding RNAs in the human vasculature. Experimental studies have identified possible regulators of 14q32 microRNA expression in vascular remodelling processes as restenosis and neovascularization. With many steps to take, ncRNA therapies in cardiovascular disease are still far away, but hopefully in the future it is possible to prescribe these therapies to patients that are currently not treated optimally.

References

1. Brandis KA, Gale S, Jinn S, Langmade SJ, Dudley-Rucker N, Jiang H, Sidhu R, Ren A, Goldberg A, Schaffer JE, Ory DS. Box C/D small nucleolar RNA (snoRNA) U60 regulates intracellular cholesterol trafficking. The Journal of biological chemistry 2013;288:35703-35713.
2. Michel CI, Holley CL, Scruggs BS, Sidhu R, Brookheart RT, Listenberger LL, Behlke MA, Ory DS, Schaffer JE. Small nucleolar RNAs U32a, U33, and U35a are critical mediators of metabolic stress. Cell metabolism 2011;14:33-44.
3. Nossent AY, Eskildsen TV, Andersen LB, Bie P, Bronnum H, Schneider M, Andersen DC, Welten SM, Jeppesen PL, Hamming JF, Hansen JL, Quax PH, Sheikh SP. The 14q32 MicroRNA-487b Targets the Antiapoptotic Insulin Receptor Substrate 1 in Hypertension-Induced Remodeling of the Aorta. Ann Surg 2013;258:743-753.
4. Welten SMJ, de Jong RCM, Wezel A, de Vries MR, Boonstra MC, Parma L, Jukema JW, van der Sluis TC, Arens R, Bot I, Agrawal S, Quax PHA, Nossent AY. Inhibition of 14q32 microRNA miR-495 reduces lesion formation, intimal hyperplasia and plasma cholesterol levels in experimental restenosis. Atherosclerosis 2017;261:26-36.
5. Welten SMJ, de Vries MR, Peters EAB, Agrawal S, Quax PHA, Nossent AY. Inhibition of Mef2a Enhances Neovascularization via Post-transcriptional Regulation of 14q32 MicroRNAs miR-329 and miR-494. Molecular therapy Nucleic acids 2017;7:61-70.
6. Wezel A, Welten SM, Razawy W, Lagraauw HM, de Vries MR, Goossens EA, Boonstra MC, Hamming JF, Kandimalla ER, Kuiper J, Quax PH, Nossent AY, Bot I. Inhibition of MicroRNA-494 Reduces Carotid Artery Atherosclerotic Lesion Development and Increases Plaque Stability. Annals of surgery 2015;262:841-847; discussion 847-848.
7. Yamamura S, Imai-Sumida M, Tanaka Y, Dahiya R. Interaction and cross-talk between non-coding RNAs. Cellular and molecular life sciences : CMLS 2018;75:467-484.
8. de Vries MR, Parma L, Peters HAB, Schepers A, Hamming JF, Jukema JW, Goumans M, Guo L, Finn AV, Virmani R, Ozaki CK, Quax PHA. Blockade of vascular endothelial growth factor receptor 2 inhibits intraplaque haemorrhage by normalization of plaque neovessels. Journal of internal medicine 2019;285:59-74.
9. Lardenoye JH, de Vries MR, Lowik CW, Xu Q, Dhore CR, Cleutjens JP, van Hinsbergh VW, van Bockel JH, Quax PH. Accelerated atherosclerosis and calcification in vein grafts: a study in APOE*3 Leiden transgenic mice. Circulation research 2002;91:577-584.
10. Aavik E, Lumivuori H, Leppanen O, Wirth T, Hakkinen SK, Brasen JH, Beschorner U, Zeller T, Braspenning M, van CW, Makinen K, Yla-Herttuala S. Global DNA methylation analysis of human atherosclerotic plaques reveals extensive genomic hypomethylation and reactivation at imprinted locus 14q32 involving induction of a miRNA cluster. Eur Heart J 2015;36:993-1000.
11. Shayevitch R, Askayo D, Keydar I, Ast G. The importance of DNA methylation of exons on alternative splicing. RNA (New York, NY) 2018;24:1351-1362.
12. Downie Ruiz Velasco A, Welten SMJ, Goossens EAC, Quax PHA, Rappsilber J, Michlewski G, Nossent AY. Posttranscriptional Regulation of 14q32 MicroRNAs by the CIRBP and HADHB during Vascular Regeneration after Ischemia. Molecular therapy Nucleic acids 2019;14:329-338.
13. Treiber T, Treiber N, Plessmann U, Harlander S, Daiss JL, Eichner N, Lehmann G, Schall K, Urlaub H, Meister G. A Compendium of RNA-Binding Proteins that Regulate MicroRNA Biogenesis. Molecular cell 2017;66:270-284.e213.

Nederlandse Samenvatting

Introductie

Cardiovasculaire ziekten

Cardiovasculaire ziekten zijn vandaag de dag nog steeds de meest voorkomende oorzaak van mortaliteit en morbiditeit in de westerse wereld. Dit komt met name doordat risicofactoren voor het krijgen van cardiovasculaire ziekten, zoals inname van te veel vet en zout, een zittende leefstijl en te weinig fysieke activiteiten, in de hedendaagse maatschappij niet meer weg te denken zijn.

Bij hart- en vaatziekten is er een gemeenschappelijke factor, namelijk dat er in de bloedvatwand vasculaire remodellering plaatsvindt. Deze vasculaire remodellering kan onderverdeeld worden in positieve remodellering en negatieve remodellering. Onder negatieve remodellering vallen atherosclerose, restenose en de vorming van aneurysmata, allemaal processen die nadelig zijn voor gezondheid van vaten. Positieve remodellering omvat de vorming van nieuwe bloedvaten, bijvoorbeeld als natuurlijke bypass om een geoccludeerd bloedvat heen, en is in hart- en vaatziekten dus een gunstig proces.

Momenteel zijn preventie- en behandelopties voorhanden, maar deze zijn nog steeds ontoereikend om de ziektelast te verlagen. Daarom is verder onderzoek nodig naar nieuwe strategieën om positieve remodellering te stimuleren en negatieve remodellering te remmen. De laatste decennia is veel onderzoek gedaan naar de genetische componenten van vasculaire remodellering. Een van deze genetische componenten is het gebied van niet-coderende RNA's, maar ondanks het feit dat al vele studies op dit gebied zijn verricht, is nog veel onbekend.

Niet-coderende RNA's

Een klein deel van het genoom codeert voor messenger RNA (mRNA) dat vervolgens wordt getransleerd tot proteïnen. Het grootste deel van het genomische materiaal (>95%) codeert niet voor eiwitten, maar heeft wel degelijk een functie. Deze RNA's worden niet-coderende RNA's genoemd. Nadat DNA is afgelezen, en het dus RNA wordt genoemd, hebben de gevormde moleculen een sturende functie op andere RNA's, waaronder mRNA. Hiermee kunnen niet-coderende RNA's dus de expressie van eiwitten reguleren. Een niet-coderend RNA kan meerdere target RNA's hebben en daarmee is een niet-coderend RNA dus in staat om complexe fysiologische processen te reguleren. Er bestaan heel veel verschillende niet-coderend RNA's, die onderverdeeld kunnen worden in grote- en kleine niet-coderende RNA's. MicroRNA's en small nucleolar RNAs (snoRNA's) die in dit proefschrift worden besproken vallen onder de kleine niet-coderende RNA's.

Niet-coderende RNA's, met name microRNA's, komen vaak voor in clusters of families. Het 14q32 niet-coderende RNA cluster is een voorbeeld hiervan. Het is gelegen op de lange arm

van het 14e chromosoom in de mens en bestaat uit 54 microRNA's, 41 snoRNA's en 3 lange niet-coderende RNA's. In de muis is het equivalent gelegen op het 12e chromosoom (12F1 locus) en bevat 61 microRNA's. Van enkele microRNA's van het 14q32 cluster is aangetoond dat remming hiervan positieve remodellering stimuleert en negatieve remodellering remt. Daarom zijn dit en mogelijk andere clusterleden ideale kandidaten om toekomstige therapeutische interventies op te baseren.

Regulatie van microRNA's

MicroRNA's reguleren niet alleen andere RNA's, maar kunnen ook zelf gereguleerd worden. Dit betekent dat hiermee indirect de targetgenen van microRNA's gereguleerd worden. Regulatie kan op meerdere manieren plaatsvinden en de meest voorkomende vormen van regulatie zijn transcriptionele regulatie en posttranscriptionele regulatie. Bij de eerstgenoemde vorm van regulatie kunnen transcripten die coderen voor microRNA's, beter of juist minder goed afgelezen worden van het DNA. Bij posttranscriptionele regulatie van microRNA's is transcriptie onveranderd, maar grijpt de regulator aan tijdens de ontwikkeling van primair- naar precursor- en/of naar volwassen microRNA. Ook hierbij kan de regulator deze processen remmen of juist stimuleren.

Proefschrift

Het doel van dit proefschrift is om de expressie van 14q32 niet-coderende RNA's in het menselijke vaatbed te onderzoeken. Tevens worden mogelijke regulatoren van 14q32 microRNA expressie besproken en onderzocht in diverse vormen van vaatremodellering.

In **Hoofdstuk 2** is een overzicht gegeven van diverse microRNA's en microRNA clusters die in verschillende vormen van vasculaire remodellering (i.e. positieve en negatieve remodellering) een rol spelen. Hierbij wordt de multifactoriële aard van deze microRNA's benadrukt. De individuele microRNA's miR-126 en miR-155 en de microRNA clusters miR-17/92, miR-23-24-27 en 14q32 microRNA's werden besproken. In eerdere studies is gevonden dat miR-126 en de miR-23-24-27 familie positieve remodellering stimuleren en negatieve remodellering tegelijkertijd remmen. Deze microRNA's zouden daarom ideale targets zijn om te stimuleren in de strijd tegen cardiovasculaire ziekten. Het miR-17/92 cluster, het miR-143/145 cluster en het 14q32 microRNA cluster hebben tegenovergestelde effecten. Zij remmen juist positieve remodellering en stimuleren negatieve remodellering. Door het remmen van deze microRNA's is aangetoond dat neovascularisatie gestimuleerd kan worden, maar ook dat atherosclerose en restenose geremd kunnen worden. Juist de mogelijkheid om beide processen tegelijk te beïnvloeden in een gunstige richting, biedt

interessante therapeutische mogelijkheden. In het verleden is namelijk gebleken dat door andere targets te beïnvloeden, neovascularisatie werd gestimuleerd, maar atherosclerose tegelijk ook werd gestimuleerd. Dit is geen positieve ontwikkeling en daarom zijn de beschreven microRNA's en microRNA clusters idealere kandidaten in toekomstige behandelingen voor cardiovasculaire ziekten.

Differentiële expressie van 14q32 niet-coderende RNA's

Zoals hierboven beschreven, hebben de 14q32 microRNA's diverse functies in vasculaire remodellering. De 14q32 locus in de mens bevat naast deze 54 microRNA's ook 41 snoRNA's. Echter, over snoRNA's is nog weinig bekend. Enkele eerdere studies hebben beschreven dat snoRNA's een functie kunnen hebben in vasculaire remodellering, maar van de 14q32 snoRNA's is nog niet bekend of zij een rol spelen in cardiovasculaire ziekten en, indien dit het geval is, hoe dit precies werkt. In **Hoofdstuk 3** worden meerdere onafhankelijke bewijzen gegeven die allemaal ondersteunen dat 14q32 snoRNA's belangrijke regulatoren zijn van cardiovasculaire ziekten. Als eerste is aangetoond dat Single Nucleotide Polymorphisms (SNP's) in het 14q32 snoRNA cluster significant geassocieerd zijn met hartfalen, onafhankelijk van SNP's in het microRNA cluster of MEG3, een lang niet-coderend RNA op de 14q32 locus. Daarnaast is gevonden dat 14q32 snoRNA expressie in de bloedvatwand erg bloedvat specifieke patronen laat zien. Hoge expressie is gemeten in hoofd-halsvaten en lage expressie was aanwezig in bloedvaten uit de onderste extremiteiten. Tevens werden snoRNA expressie levels van naïeve venen die erna gebruikt zouden worden als bypass, vergeleken met geoccludeerde, en dus gefaalde, bypass venen. De expressie van SNORD113.2 was significant hoger bij geoccludeerde vaten. Expressie van dit snoRNA was ook tweemaal zo hoog in het bloed direct na ST-elevatie myocard infarct (STEMI) vergeleken met 30 dagen na behandeling, maar de hoogste 14q32 snoRNA expressie werd gezien in hartsamples van patiënten met hartfalen. Al deze associaties laten dus zien dat snoRNA's daadwerkelijk een rol moeten spelen in cardiovasculaire ziekten, maar hoe snoRNA's precies een functie hebben of worden beinvloedt in cardiovasculaire ziekten, is nog niet bekend. Veranderen zij als gevolg van de ziekte of treedt de ziekte op als gevolg van snoRNA veranderingen, zijn vragen die nog beantwoord moeten worden. Hiervoor is het nodig de exacte aangrijpingspunten van snoRNA's te achterhalen. Daarom zijn in deze studie reeds enkele functionele experimenten uitgevoerd die aantoonden dat opregulatie van twee snoRNA's in de muis leidde tot verbeterde cel migratie en dat methyltransferase Fibrillarine, dat niet-coderende RNA's kan methyleren als het is aangestuurd door snoRNA's, ook gebonden kan zijn aan 14q32 snoRNA's.

Samenvattend laat deze studie zien dat 14q32 snoRNA's een belangrijke rol spelen in cardiovasculaire ziekten en mogelijke werkingsmechanismen zijn onderzocht. Echter, hoe dit exact werkt, via welke mechanistische route en welke targets 14q32 snoRNA's precies hebben, zal moeten worden onderzocht in vervolgstudies.

Mechanistische werking van microRNA's is al veel meer bestudeerd. MicroRNA's worden afgeschreven van het DNA tot primair microRNA. Vervolgens wordt het omgezet tot precursor microRNA door het enzym Drosha. Als het precursor microRNA vanuit de nucleus naar het cytoplasma wordt getransporteerd komt het enzym Dicer dat zorgt voor de omzetting naar volwassen microRNA. De volwassen vorm wordt geladen in een zogenoemd RISC complex (RNA-Induced Silencing Complex) waarmee het de uiteindelijke functie kan gaan uitoefenen. Daarmee bindt het microRNA aan het 3'uiteinde (3'UTR) van zijn target mRNA en reguleert zo de expressie van zijn targetgenen. Omdat is aangetoond dat 14q32 microRNA's in diverse vormen van vasculaire remodellering een rol kunnen spelen en dat cardiovasculaire ziekten vaak op specifieke locaties in het menselijk lichaam voorkomen, kwam de vraag op of 14q32 microRNA's specifieke expressiepatronen hebben in de vaatboom. Daarom is het doel gesteld om de expressie van 14q32 microRNAs in de menselijke vasculatuur in kaart te brengen. **Hoofdstuk 4** beschrijft de resultaten van deze studie waarin vaatweefsel samples vanuit zoveel mogelijk verschillende locaties in de menselijke vaatboom zijn verzameld. In deze samples is de microRNA expressie van 17 van de 54 14q32 microRNA's gemeten. Deze microRNA's liggen verspreid over de locus en zij zijn in eerdere studies beschreven belangrijke functies te hebben in vasculaire remodellering. In deze studie zijn inderdaad bloedvat specifieke microRNA expressiepatronen gevonden. De bloedvaten in de benen lieten hoge expressie levels zien, waar de bloedvaten uit het hoofdhalsgebied een lage 14q32 microRNA expressie hadden. Dit was een interessante bevinding, omdat in beide bloedvaten atherosclerose kan voorkomen, maar de microRNA expressie dus duidelijk verschilt. Ook is gevonden dat voor elk microRNA de expressie in arteriële bloedvaten hoger is dan in veneuze bloedvaten. Daarnaast correleerde 14q32 microRNA expressie niet met leeftijd of geslacht, maar werd wel gezien dat de targetgenen lager tot expressie kwamen wanneer er hoge microRNA expressie was, en vice versa. Dit laatste werd ook verwacht op basis van het eerder beschreven werkingsmechanisme van microRNA's en dit impliceert dat de 14q32 microRNA's die aanwezig zijn ook daadwerkelijk een functie uitoefenen.

Samenvattend benadrukt het eerste deel van dit proefschrift dat 14q32 niet-coderend RNA expressie individueel gereguleerd is voor elk niet-coderend RNA en dat bloedvatlocatie- en vasculaire ziekte specifieke expressie aanwezig zijn.

Regulatoren van 14q32 microRNA expressie

14q32 microRNA's komen differentieel tot expressie in de menselijke bloedvatwand en dit verschil uit zich in locatie en ziekte specifieke expressiepatronen. De vraag die hierbij opkomt is hoe deze regulatie precies verloopt en op welke verschillende manieren 14q32 microRNA expressie gereguleerd kan worden. Dit wordt in het tweede deel van dit proefschrift besproken.

Allereerst is in **Hoofdstuk 4** DNA methylatie besproken als mogelijke microRNA expressie regulator. DNA methylatie is de additie van een methylgroep aan een cytosine-guanosine dinucleotide, zogenoemde CpG's. Op het DNA zijn regio's waarin veel CpG's gelegen zijn en er dus veel methylatie plaats kan vinden. Deze regio's worden Differentially Methylated Regions (DMR's) genoemd. Ook op het 14q32 cluster zijn drie DMR's gelegen. Methylatie is niet een statisch proces, maar kan veranderen tijdens ziekte. Het is bekend dat DNA methylatie status verandert tijdens oncogene processen en enkele cytostatica grijpen dus aan op methylgroepen. In fysiologische omstandigheden veranderd DNA methylatie niet zomaar. Dit gebeurt onder invloed van enzymen die DNA MethylTransferases (DNMT's) heten. In eerdere studies was aangetoond dat DNA methylatie omgekeerd evenredig is met de expressie van nabijgelegen genen. Dit kan verklaard worden doordat de methylgroep het onmogelijk maakt voor RNA polymerase om te binden en dus het DNA te transcriberen. In deze studie hebben wij echter gevonden dat op de 14q32 locus DNA methylatie levels en microRNA expressie levels niet correleren in de bloedvatweefsel. Ook DNA methylatie status en primair microRNA expressie of DNMT expressie en (primair) microRNA expressie tonen geen relatie in bloedvaten. Wel is aangetoond dat 14q32 DNA methylatie direct gerelateerd kan worden aan status van het bloedvat in vasculaire remodellering. Ook DNMT expressie liet dit zien. Deze bevindingen werden in menselijke zieke en gezonde bloedvaten gedaan, maar zijn ook in diverse diermodellen bevestigd. 14q32 DNA methylatie is dus geen 14q32 microRNA expressie regulator, maar een onafhankelijke factor die geassocieerd is met vasculaire remodellering. Hoe deze associatie precies werkt en of dit mogelijkheden biedt tot nieuwe therapeutische interventies, zal verder onderzocht moeten worden.

In **Hoofdstuk 5** is een andere 14q32 microRNA regulator bestudeerd, namelijk myostatine. Myostatine was reeds bekend als regulator van skeletspiercelgroei en -proliferatie. De

afwezigheid van myostatine leidt tot overmatige spiermassa in zowel mensen als dieren. In de veehouderij is dit een positief verschijnsel, maar in mensen veroorzaakt het ook overmatige groei van hartspiercellen. Dit kan leiden tot een verslechterde pompfunctie van het hart met ziekte en mogelijk de dood tot gevolg. Niet alleen skeletspiercellen en hartspiercellen, maar ook gladde spiercellen kunnen van fenotype veranderen door myostatine. Juist deze gladde spiercellen spelen in post-interventionele restenose een belangrijke rol. Normaal gesproken verblijven gladde spiercellen in de mediale laag van een bloedvat. Zij dragen bij aan de elasticiteit en compliantie van een bloedvat en daarmee kan een bloedvat hoge systolische drukken weerstaan, maar tegelijk ook rekbaar zijn. Als een bloedvat (kransslagader of beenslagader) occludeert door het ontstaan van een atherosclerotische plaque, moet deze met spoed behandeld worden om de bloedstroom door het vat te herstellen. Dit gebeurt door middel van een dotterprocedure. Ter plaatse van de vernauwing wordt een ballonnetje opgeblazen waardoor de plaque naar buiten geduwd wordt en het lumen weer groot genoeg is om voldoende bloed door te laten. Om snelle re-occlusie te voorkomen, wordt vaak een stent achtergelaten. Meest gebruikte stents geven ook medicijnen af die re-occlusie vertragen. Ondanks de medicijnen uit de stent en het feit dat de patiënt levenslang medicijnen moet slikken, komt het vaak voor dat er toch ter plaatse van de stent restenose optreedt. Dit komt doordat het opblazen van de ballon en het achterlaten van de stent reacties triggert in de bloedvatwand. Gladde spiercellen reageren door extra te prolifereren en van de media naar de intima te migreren. Daarbij vormen ze een dikke intima en dit wordt de neointima genoemd. Daarnaast wordt een ontstekingsreactie uitgelokt waarbij met name macrofagen geactiveerd worden en in de laesie migreren. Met het feit dat myostatine afwezigheid leidt tot verhoogde spiercel proliferatie, werd in deze studie verwacht dat de toediening van myostatine zou leiden tot minder gladde spiercelproliferatie, wat een gunstig effect zou hebben op post-interventionele restenose.

Daarnaast is in eerdere studies beschreven dat myostatine de callipyge locus, een andere naam voor de 14q32 locus, beïnvloedt en microRNA expressie van de locus verandert. Myostatine knock-out muizen hebben naast grote spiermassa ook een verhoogde 14q32 microRNA expressie. Andersom wordt dus verwacht dat myostatine aanwezigheid leidt tot een verlaging van 14q32 microRNA expressie. Ook dit zou een positieve invloed moeten hebben op post-interventionele restenose, omdat eerder onderzoek heeft aangetoond dat directe remming van 14q32 microRNA miR-495 restenose vermindert en ook de macrofageninflux verlaagd. Dit effect op macrofagen door myostatine is ook onderzocht.

Zowel *in vitro* als in een *in vivo* model voor post-interventionele restenose werd de functie van myostatine op restenose en 14q32 microRNA's onderzocht. De resultaten van deze

studie lieten zien dat myostatine inderdaad gladde spiercel proliferatie remt en microRNA's in gladde spiercellen lager tot expressie brengt. We zagen echter niet dat myostatine een effect had op macrofaagactivatie of de microRNA's in macrofagen. Dit verklaart ook waarom restenose niet afnam in de myostatine behandelde groepen vergeleken met de controle groep. Myostatine alleen zal dus niet de nieuwe remedie zijn tegen restenose, ondanks dat het een sterke 14q32 microRNA regulator is in gladde spiercellen. Deze bevindingen benadrukken dat voor de behandeling van post-interventionele restenose niet slechts een component getarget moet worden, maar dat therapieën zowel gladde spiercelproliferatie als macrofaagactivatie moeten kunnen remmen om succesvol te zijn in de strijd tegen restenose.

De laatste regulator van 14q32 microRNA's die in dit proefschrift (**Hoofdstuk 6**) besproken wordt, is CIRBP. Dit is de afkorting van Cold-Inducible RNA Binding Protein. Zoals de naam suggereert, staat dit proteïne bekend om de eigenschappen om RNA te binden, en dus te beïnvloeden, en om geïnduceerd te worden door kou. Dit zijn twee interessante eigenschappen. Allereerst kan CIRBP diverse soorten RNA binden, zowel mRNA's als niet-coderende RNA's. Onder deze niet-coderende RNA's die target zijn van CIRBP vallen ook twee 14q32 microRNA's. In een eerdere studie is aangetoond dat CIRBP de omzetting van precursor microRNA naar volwassen microRNA beïnvloedt voor 14q32 microRNA's miR-329 en miR-495. Daarnaast wordt CIRBP geïnduceerd door lage temperatuur. Juist dit is een belangrijk kenmerk van perifeer vaatlijden. Wanneer in het been door een arteriële occlusie de bloedstroom naar lager gelegen weefsels wordt afgesloten, zullen verschijnselen als polsloosheid, pijn, paresthesie, pallor (bleekheid), paralyse en poikilothermie (onmogelijkheid om lichaamstemperatuur te behouden) optreden, samen de 6 P's. Door het tekort aan bloedtoevoer, en dus zuurstof en voedingsstoffen, naar de perifere weefsels, worden deze ischemisch en sterven af. Daarom moet een arteriële occlusie behandeld worden. Dit kan, zoals ook in **Hoofdstuk 5** beschreven is, door middel van een dotterprocedure met of zonder plaatsing van een stent, maar ook door middel van een bypass. Deze omleiding om de occlusie heen kan chirurgisch worden aangelegd met behulp van een ander lichaamseigen bloedvat, maar het lichaam heeft ook zelf een manier om een bypass te vormen. Dit heet neovascularisatie en omvat de vorming van nieuwe bloedvaten ófwel uit bestaande onrijpe bloedvaten door toename in druk en shear stress (arteriogenese) ófwel de vorming van volledig nieuwe bloedvaten naar ischemisch weefsel (angiogenese). Hoewel het lichaam zelf in staat is tot neovascularisatie, is dit in omstandigheden zoals perifeer arterieel vaatlijden niet voldoende om de bloedstroom naar lager gelegen gebieden volledig te herstellen. Daarom moeten strategieën gevonden

worden waarbij neovascularisatie ondersteund en versterkt wordt. In eerdere studies is gevonden dat directe remming van 14q32 microRNA's, waaronder miR-329 en miR-495, leidt tot betere neovascularisatie in een diermodel voor achterpootischemie. Tevens is gevonden dat remming van een ander RNA bindingsproteïne, MEF2A, leidt tot lagere 14q32 microRNA expressie met als gevolg betere post-ischemische neovascularisatie. Voortbordurend op deze studies, is in **Hoofdstuk 6** onderzocht of door het targetten van CIRBP 14q32 microRNA's gereguleerd worden en dus neovascularisatie gestimuleerd wordt. Daarnaast is gekeken naar het effect van hypothermie op CIRBP, verschillende splice varianten van CIRBP en het antisense long noncoding RNA CIRBP-AS1. Ook is het effect van CIRBP op 14q32 microRNA expressie onderzocht. Vervolgens is gekeken naar het effect van CIRBP- en CIRBP-AS1 remming op de 14q32 microRNA's en ook is onderzocht of dit angiogenese stimuleert *in vitro*. CIRBP werd in endotheelcellen geïnduceerd door koude stress, met name CIRBP-SV1, maar een duidelijk effect op CIRBP-AS1 en de 14q32 target microRNA's bleef uit. CIRBP remming leidde tot downregulatie van volwassen miR-495, maar niet van miR-329, en zorgde voor verbeterde *in vitro* angiogenese. Ook bewerkstelligde deze CIRBP remming een lagere CIRBP-AS1 expressie. Andersom zorgde CIRBP-AS1 remming ook voor een lagere CIRBP expressie en tevens een verbetering van *in vitro* angiogenese. Hoe deze interactie tussen CIRBP en CIRBP-AS1 precies werkt en welke van de twee de hoofdverantwoordelijke factor is van de proangiogene eigenschappen, moet nog onderzocht worden.
Deze bevindingen samen impliceren dat CIRBP en CIRBP-AS1 zeer interessante mogelijke targets zijn in neovascularisatie en verder onderzoek zal moeten uitwijzen of dit daadwerkelijk in een levend organisme ook werkzaam is. Daartoe is de volgende stap om in CIRBP knock-out muizen een achterpootischemie model te verrichten. Hierbij wordt de arteria femoralis geligeerd en vervolgens gekeken naar het herstel in de bloedtoevoer naar de poot via neovascularisatie. Normaal gesproken zal dit in 7-10 dagen hersteld zijn, maar de verwachting is dat in muizen die geen CIRBP hebben, 14q32 microRNA's veel lager tot expressie komen en er dus meer en snellere neovascularisatie plaatsvindt.

Samenvattend bespreekt het tweede deel van dit proefschrift drie verschillende mogelijke regulatoren van 14q32 microRNA expressie. 14q32 DNA methylatie bleek geen regulator van 14q32 microRNA expressie te zijn, maar is een onafhankelijke factor die geassocieerd is met vasculaire remodellerings status. Myostatine daarentegen is wel een duidelijke regulator van 14q32 microRNA expressie, maar alleen in spiercellen, dus in VSMCs in de bloedvatwand. Myostatine heeft geen duidelijk effect op andere cellen in restenose zoals macrofagen. Daarom is het geen potente regulator van post-interventionele vasculaire

remodellering, omdat dit een proces is waarin meerdere factoren tegelijk getarget moeten worden om een klinisch effect te bereiken. De laatste regulator van 14q32 microRNA expressie die in dit proefschrift is besproken, is CIRBP. Bij remming van CIRBP in endotheelcellen wordt miR-495 eveneens geremd zoals verwacht. MiR-329 werd niet beïnvloed. Tevens liet remming van CIRBP een duidelijk positief effect zien op *in vitro* angiogenese. Of deze effecten *in vivo* ook aanwezig zijn, zal onderzocht moeten worden, maar *in vitro* data zijn zeer veelbelovend.

Conclusie

Dit proefschrift geeft nieuwe inzichten in de differentiële expressie van 14q32 niet-coderende RNA's in het menselijke vaatbed. Experimentele studies hebben enkele mogelijke regulatoren van 14q32 microRNA expressie in vasculaire remodelleringsprocessen, zoals post-interventionele restenose en post-ischemische neovascularisatie. Veel stappen moeten nog gezet worden en therapieën met 14q32 niet-coderende RNA's of regulatoren van 14q32 microRNA's zijn nog ver weg, maar hopelijk is het in de toekomst mogelijk om deze therapieën aan patiënten voor te schrijven die vandaag de dag nog suboptimaal behandeld worden.

List of Publications

1. A Wezel, SMJ Welten, W Razawy, HM Lagraauw, MR de Vries, **EAC Goossens**, MC Boonstra, JF Hamming, ER Kandimalla, J Kuiper, PHA Quax, AY Nossent, I Bot. Inhibition of microRNA-494 reduces atherosclerotic lesion development and increases plaque stability. *Annals of Surgery* 2015 Nov; 262 (5): 841-8.

2. **EAC Goossens***, SMJ Welten*, PHA Quax^, AY Nossent^. The multifactorial nature of microRNAs in vascular remodeling. *Cardiovascular Research* 2016 May 1;110(1):6-22.
   * authors contributed equally

3. A Downie Ruiz Velasco, SMJ Welten, **EAC Goossens**, PHA Quax, J Rappsilber, G Michlewski, AY Nossent. Posttranscriptional Regulation of 14q32 MicroRNAs by the CIRBP and HADHB during Vascular Regeneration after Ischemia. *Molecular Therapy Nucleic Acids* 2018 Dec; 14: 329-338.

4. **EAC Goossens***, KEJ Hakansson*, S Trompet*, E van Ingen, MR de Vries, RVCT van der Kwast, RS Ripa, J Kastrup, PJ Hohensinner, C Kaun, J Wojta, S Böhringer, S Le Cessie, JW Jukema, PHA Quax, AY Nossent. Genetic associations and regulation of expression indicate an independent role for 14q32 snoRNAs in human cardiovascular disease. *Cardiovascular Research* 2019 Aug 1;115(10):1519-1532.
   * authors contributed equally

5. **EAC Goossens**, MR de Vries, KH Simons, H Putter, PHA Quax, AY Nossent. miRMap: profiling 14q32 microRNA expression and DNA methylation throughout the human vasculature. *Frontiers in Cardiovascular Medicine* 2019 Aug 8;6:113.

6. **EAC Goossens**, MR de Vries, JW Jukema, PHA Quax, AY Nossent. Myostatin inhibits vascular smooth muscle cell proliferation and local 14q32 microRNA expression, but not systemic inflammation or restenosis. *Submitted to International Journal of Molecular Sciences.*

7. RVCT van der Kwast, L Parma, E van Ingen, F Baganha, HAB Peters, **EAC Goossens**, KH Simons, M Palmen, MR de Vries, PHA Quax and AY Nossent. Adenosine-to-Inosine editing of vasoactive microRNAs alters their targetome and function in ischemia. *Under review at Molecular Therapy.*

8. **EAC Goossens**, L Zhang, PHA Quax, AY Nossent. Inhibition of Cold-Inducible RNA-Binding Protein decreases 14q32 microRNA miR-495 expression and enhances *in vitro* angiogenesis. *Manuscript in preparation.*

Curriculum Vitae

Eveline Albertine Cornelia Goossens werd geboren op 8 januari 1993 te Leiderdorp. In 2011 behaalde zij cum laude haar diploma aan het Stedelijk Gymnasium in Leiden, waar zij tijdens de laatste twee jaren het Pre-University College volgde. In 2011 begon Eveline aan haar studie geneeskunde aan de Universiteit Leiden. In het tweede studiejaar van haar bachelor werd ze toegelaten tot het MD/PhD-traject van het Honours College waarbij zij begon aan onderzoek naar 14q32 microRNA's onder leiding van prof. dr. Quax en dr. Nossent op de afdeling vaatchirurgie in het Leids Universitair Medisch Centrum. Dit resulteerde in haar eerste publicatie en een grote biobank van bloedvatmateriaal welke de basis vormde voor haar tweede en derde publicatie. Na de coschappen tijdens de wetenschapsstage in 2017 heeft Eveline de MD/PhD-beurs toegewezen gekregen. Hiermee kon zij twee jaar als promovenda aan de slag om het gestarte onderzoek naar 14q32 noncoding RNAs in vascular remodelling te vervolgen. Het resultaat hiervan ligt voor u. In november 2019 is zij gestart als arts-assistent niet in opleiding tot specialist (ANIOS) op de afdeling cardiologie in het Elizabeth-Twee Steden Ziekenhuis in Tilburg.

Dankwoord

Graag wil ik iedereen bedanken die heeft bijgedragen aan de totstandkoming van dit proefschrift.

Allereerst **professor Quax,** beste **Paul**, wil ik je bedanken voor alle jaren in de onderzoeksgroep. Ons eerste gesprek in 2013 zorgde ervoor dat ik direct geïnteresseerd werd voor het onderzoek naar microRNA's in de vasculatuur, mede door jouw en Yaëls enthousiasme. Het basale karakter van het onderzoek waarbij altijd het oog op de kliniek gehouden wordt, bleef me er continu aan herinneren waarvoor we het allemaal doen. Een hoogtepunt buiten het onderzoek was in 2017 waarbij jij mij toesprak tijdens mijn afstuderen. Je was een fantastische begeleider.

Yaël, jouw al genoemde onuitputtelijke enthousiasme, werkt aanstekelijk. Ik heb veel van je geleerd en jouw talent om van ieder resultaat een positieve kant te zien, bewonder ik. Jouw directe manier van begeleiden was wennen in het begin, maar ik had geen betere copromotor kunnen bedenken. Dankjewel!

Eva, vanaf het begin, in 2017, waren we maatjes in het lab en ook nog op D6. Ik ben blij dat je vandaag naast me staat als paranimf. We hebben veel gelachen, ook gehuild en nog veel meer gekletst. Je was onmisbaar tijdens mijn promotie. Dank voor alle momenten aan de RNA-bench en in de celkweek, maar natuurlijk ook voor alle andere momenten!

Erna, dank voor alle hulp in het lab, het luisterende oor, de onuitputtelijke zoete stimulansen tussen experimenten door en je altijd behulpzame kritische blik. De vraag "en wat vind jij van dit experiment dat je moet gaan doen?" heeft me meermaals tot extra nadenken aangezet en het onderzoek verder gebracht. Dankjewel dat ook jij mijn paranimf wilde zijn!

Verder wil ik uit de Quax-groep iedereen bedanken. **Margreet**, dank voor jouw expertise met de *in vivo* experimenten en de samenwerkingen die geleid hebben tot mooie publicaties. **Regi**, jij wist altijd oplossingen voor technische vragen over mijn RNA-experimenten. **Laura**, Queen B herself in the lab, thanks for your HUVEC expertise and making me laugh every day! Ook **Fabiana**, **Licheng, Alwin, Leontien**, **Valérie**, **Karin**, **Sabine** en **Rob** wil ik graag heel hartelijk bedanken.

Daarnaast mag D6 niet ontbreken. **Annelieke**, **Michèle**, **Fenna** en **Ruth**, jullie zijn fantastisch. Niets helpt beter tijdens een promotie dan jullie mentale steun. Heel veel dank en ik weet zeker dat jullie GraphPad aankunnen!

Meike, dank voor je hulp in het lab. Je hebt een goede stage gedaan en ik wens je heel veel succes met de afronding van je studie.

Tot slot wil ik **papa** en **mama** heel erg bedanken. Jullie waren er altijd voor me en jullie support was geweldig. **Roderik**, je zei wat ik niet altijd wilde horen, maar misschien heb je soms wel gelijk en gaf jouw kijk op de zaak me nieuwe inzichten. Dankjewel! **Merijn**, je bent altijd geïnteresseerd en denkt met alles mee. Ook al waren de microRNA's inhoudelijk abacadabra voor jou, dank voor je steun!